4ᵗʰ IEEE International Symposium on
Exploitation of Renewable Energy Sources

Subotica, Serbia   March 09-10, 2012

EXPRES 2012

Final Program

4ᵗʰ IEEE International Symposium on
Exploitation of Renewable Energy Sources

EXPRES 2012

4th International Symposium on Exploitation of Renewable Energy Sources

March 9-10, 2012

Subotica, Serbia

---

http://conf.uni-obuda.hu/expres2012

IEEE requirements were respected when writing and reviews papers

EXPRES 2012

4th International Symposium on Exploitation of Renewable Energy Sources

Subotica, Serbia

March 9-10, 2012

Proceedings

Table of Contents

EXPRES 2012 Papers

Committees

HONORARY COMMITTEE
Imre J. Rudas, Óbuda University
Branislav Todorović, University of Beograd

GENERAL CHAIR
József Nyers, Subotica Tech

INTERNATIONAL ADVISORY COMMITTEE
Sándor Horváth, Óbuda University
István Patkó, Óbuda University

ORGANIZING COMMITTEE CHAIR
László Karai, Subotica City Government
Erika Kudlik, Subotica City Government
László Veréb, V3ME

ORGANIZING COMITTEE
József Gáti, Óbuda University
Orsolya Hölvényi, Óbuda University
Gyula Kártyás, Óbuda University
Ilona Reha, Óbuda University

TECHNICAL PROGRAM COMMITTE CHAIRS
Péter Kádár, Óbuda University
Péter Odry, Subotica Tech

TECHNICAL PROGRAM COMMITTE
Milorad Bojić, Univ. Kragujevac
Stevan Firstner, Subotica Tech
László Garbai, BME, Budapest
Dušan Gvozdenac, Univ. Novi Sad
Jenő Kontra, BME, Budapest
Kornél Kovács, Univ. Szeged
Marija Todorović
László Tóth, Univ. Gödöllő

SECRETARY GENERAL
Anikó Szakál, Óbuda University
szakal@uni-obuda.hu

PROCEEDINGS EDITOR
Anikó Szakál, Óbuda University

http://conf.uni-obuda.hu/expres2012

Buildings Envelopes Controlling Solar Radiation Gains

Branislav Todorovic,
Professor at University Belgrade,
Permanent visiting professor at South-East University in Nanjing, China,
Editor of International Elsevier's journal Energy&Buildings
todorob@EUnet.rs

Abstract- In seasons with low outside temperatures in the continental climates zones, toward hot periods in summer, there are two extremely different approaches to solar thermal influence. In the first case, there is a need to use the heat solar radiation for heating of inside buildings volume. In the hot periods, to minimize solar influence and reduce solar heat gains as much as possible. The way to achieve these opposite goals could be building with double façade, with some additional technical solutions concerning application of wetted building's envelope with water evaporation effect. And, of course, combinations with different option of screens protecting of solar radiation effects through glass elements of building's facades.
New technologies are bringing some more new ideas, like use of evaporation cooling effect

*Key words- **Buildings, energy, envelope, evaporative cooling, double facades,***

I. INTRODUCTION

If we would learn from examples of nature, a building envelope could be compared with human skin behavior, and its reaction to different thermal conditions. There are some typical characteristics of human reactions noticeable in buildings: double facades as a copy of wearing coats, various constructional structures throwing a partly shadow on a building as use of umbrella or having a hut, or sitting in a shadow, etc. However, human reaction to very high temperatures is perspiration, producing the evaporation effect for cooling; the application of human perspiration effects on facades was found on several buildings, in the world, with water flowing above facades.

The world's energy requirements show permanent growth. In last 50 years the energy needs increased 200%, with the average annual increase of 3, 3%. The population growth, as well as the economic development, where the industrialized countries of the worlds (OECD) and the central Europe are accounted for 61% of the world's total energy consumption.The population growth is especially remarkable in developing countries, where it was doubled from 1965 to 2000, with stagnation in developed countries, and in countries of central and Eastern Europe.

In such a situation, with energy crisis becoming more serious and critical every day, because of the consequences of the emission of the green house gases and need for their elimination, the global energy consumption has to be decreased and very seriously controlled. There are constant efforts to reduce use of classical energy sources and stop the emission, and force use of renewable sources, primary, direct solar radiation.

Knowing that there is the greatest energy demand in the building sector, engineers of HVAC, together with architects and building specialists, have to build efficient energy buildings what should be the first step to Zero energy buildings. In respect to the fact that wind, geothermal, and especially solar energy are becoming the mostly used energy resources, new buildings have to be projected and constructed adopting the application of these energy resources. That is why is important to study and simulate the new forms for each location, each specific climatic condition, and used materials, as well as building envelope's thermal properties.

Following the EU directive, energy losses are limited, and till end of this decade all buildings have to be built as zero energy buildings.

II. OLD FACADES

The old buildings' thermal properties, based on buildings in Belgrade erected in the first half of the 19th century, have very thick brick walls (0.9m) with an overall coefficient of heat transfer 0.8 W/m2K, and relatively small windows participation of about U=4W/m2K. The mean U factor of the building built in this period is approximately 1,9 W/m2K. Such buildings were during the summer period nearly the entire day under the shadow of façade construction and did not need summer cooling. The buildings built till 1918 were made of similar material, but with very high rooms, even more than 4 m. For such buildings, it was estimated that they had design heating capacity of 232 W/m2 or 50W/m3.

The houses erected between 1918 and 1942 were 3.5m high, and had 200W/m2 or 57W/m3 specific heat, what was caused by relatively thinner walls and bigger windows. The thickness of brick walls was 0.56m and 0.38m, while windows had wooden frames, and were single, or mostly double framed. Immediately after the Second World War, specific heating power was 185W/m2 or 60-70W/m3, decreasing later to 50-60W/m3. Windows were wood framed, height of floors 2,4m in dwelling houses.

Today, when district heating systems are introduced in most cities, with new standards caused by critical situation regarding the energy, needs for sustainability,

environmental protection and global warming, the energy demands of buildings must be much lower. The specific heating power should be under 25 W/m3.

III. MODERN FACADES

The advances of High Tech in the building sector, intelligent buildings, air-conditioning systems, new materials and building's technologies, including glass technologies, have opened great possibilities in realising the importance of and expressing architectural vision, imagination, new ideas, but have also limiting energy aspects, ecological situation, environment protection, sustainability or Green Building directions. The new architectural era, with computer modelling and building simulation have enabled us to analyse a building in its real life, predicting its dynamic behaviour and estimating it's energy consumption, indoor air quality, lighting, even in the projecting period, when building's design is in it's initial phase.

IV. GREEN BUILDING CONCEPT AS THE FIRST STEP TO ZERO ENERGY BUILDINGS

As it is underlined in the ASHRAE Green Guide, the broad characteristics of good building design, encompassing both the engineering and non engineering disciplines, might be briefly outlined as follows: It meets the purpose and needs of the building's owners/managers and occupants, meets the requirements of health, safety and environmental impact as prescribed and by codes and recommended by consensus standards Achieves good indoor environment quality which in turn encompasses high quality in the following dimensions: thermal comfort, indoor air quality, acoustical and visual comfort. They are compatible with and respectful of the characteristics, history, and culture of the closest surroundings, and create the intended emotional impact on the building's occupants and beholders.

A green design proponent might be add to the above list of the items concerning energy conservation, environmental impact, low impact emissions, and waste disposal – those very characteristics that are incorporated in the foregoing definition of green design. While this may be true someday, we are not there yet. There are plenty of designs being built today in our region that exhibit few or no green design characteristics. Many of these are still characterized as well-designed buildings - largely because the generally accepted characteristics of good design do not (at least do not yet) incorporate those of green design. In summary, there are a lot of well designed buildings, but not exactly with all green buildings characteristics.

The green building concept towards building envelope is based on the fact that envelopes are protecting occupants from the outside weather's influence, and when it is feasible, letting its good aspects in. Its design is a key factor that defines how well a building and its occupants perform. Access to outdoor views and natural light has positive psychological and physiological effects upon the building's occupants. Analysis of the building envelope utilizing day-lighting simulations programs can help an optimization of building geometry, define glazing characteristics and provide information needed in performing an energy analysis of the facility (ASHRAE Green Guide).

V. DOUBLE BUILDIG'S FACADES

From a "static mass" the architecture produces "adaptive" building structure, with an envelope as a skin moderating heat flows. A building presents a fully integrated, intelligent adaptable structure, both in terms of the used material's, their fabric, locations, information technologies and all building operation systems. With the central control system, building's intelligence and with defaulted values concerning energy systems, buildings are getting characteristic of a human body, at least in regard to the reaction to thermal conditions - but in which degree? .

In a cold environment, a human body reacts by lowering blood an additional protective cover circulation toward the skin surface by the blood vessels tightening, thus conserving body's heat and controlling it's heat losses. That is an instinctive reaction, default attribute, without any conscious possibility to influence it. But a man can improve the condition by dressings, adding thus over his body, above his skin, and acquiring thus better insulation. This human way of additional protection can be applied on buildings. Why can't they be covered with movable covers, in winter to protect them from the wind and low outside temperature, and in summer from the sun, in order to reduce heat gains from the solar radiation, and so reduce the necessary energy for its air conditioning. Maybe a kind of automatic lowered shades? Or covering a building with a second façade?

There are buildings today with such doubled protection, mostly static, like a "pullover" or a "winter coat" on a man. Those are the double-facade buildings – additional cover is added to the main façade, usually made of glass. A double façade in the summer could be protection from the sun.

A winter coat or a pullover is changed by a light material blouse of the bigger size, roomy over the body, so that the air may circulate next to the body and cool it, enabling the body to transfer a heat out of a body.

In the double façade, various forms of shades, curtains, or similar devices, are put in the inter-space for the sun-protection, though a passage must be provided for the outside air circulation, so that the inter-space temperatures may be as close as possible, if not identical, with the outside temperature.

From the constructional point of view, a double-façade outer envelope may be continuously extended by covering the total height of a building, or discontinued with breaks at each floor level. Disregarding the height, the inter-space is opened both at the bottom and at the top, thus providing the outdoor

air circulation in the summer, when the temperature of inter-space should be as low as possible, in principle equal to the outside temperature. Or the openings may be closed, which is the case during the winter, in order to trap the air in the inter-space, which will act as insulation layer, with the temperature above the outside temperature, producing lower heat losses of a building (Fig. 1.)
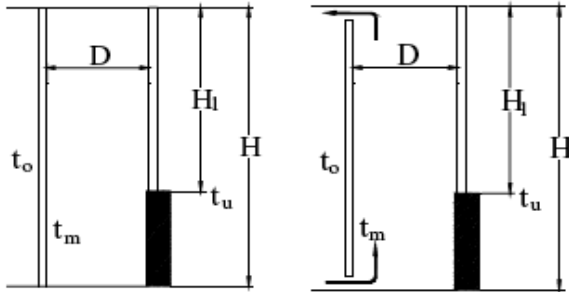
Figure 1. Different double-facade constructions: continues (left) and discontinued (right)
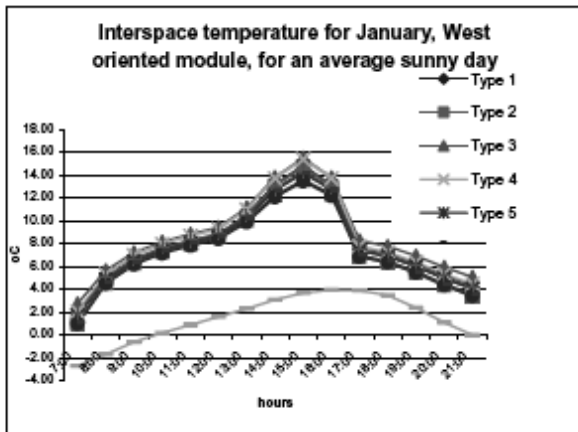
Figure 2. The temperatures during the sunny day in January

Figure 2. Shows the course of temperatures in the inter-space on an average sunny day in January, for the South-turned double facade, in Belgrade (45NL). And the figure 3. the cavity temperature in July summer day
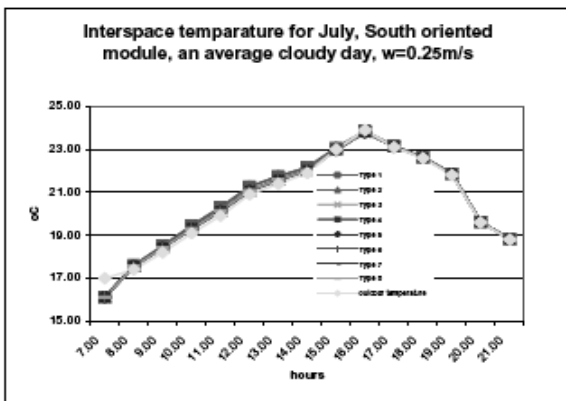
Figure 3. The cavity temperature in July summer day

It is evident that during the heating period, cavity temperature of a building with a double-façade is above the outside one, and will have lower heat losses and decreased needs for heating. In the summer, during the cooling period, the temperature between the two facades could be equal or very close to the outside temperature, and additionally can have smaller heat gains from solar radiation, depending on glass properties regarding solar transmittance. As a consequence, heat gains will not be above the gains of a single façade buildings. During the summer, one uses his conscious reactions for the additional protection of his body. He may protect himself by hats, or make a shade using a parasol. Similar protection is used in buildings by various curtains, shades, and Venetian blinds on windows, while today copies of caps and parasols are constructed, as immovable elements over roofs, or movable, depending on the sun temporary location. All those protections may be also used on facades.

Examples of building protection from the solar radiation are numerous, especially in the regions of tropical conditions. An illustrative example is a building designed by the English architect Grindshaw in Seville, built for the EXPO 1992. Movable protection on the roof is put according to the momentary sun location, controlled by "building's intelligence" (Fig. 3).

VI. BUILDING'S EVAPORATIVE COOLING

During the summer, heat enters into buildings from the outside through hot air and solar radiation, but there are also heat gains inside (lighting, domestic hot water systems, people, electric appliances and devices). Such heat must be eliminated so that the inside temperature would not be above the planned one, for example 22°C. In conditions when the outside temperature is above the human body temperature, the only way for a man to eliminate his inner heat is by perspiration, through evaporation. A building cannot sweat, so that it has to be cooled mechanically by air conditioning system.
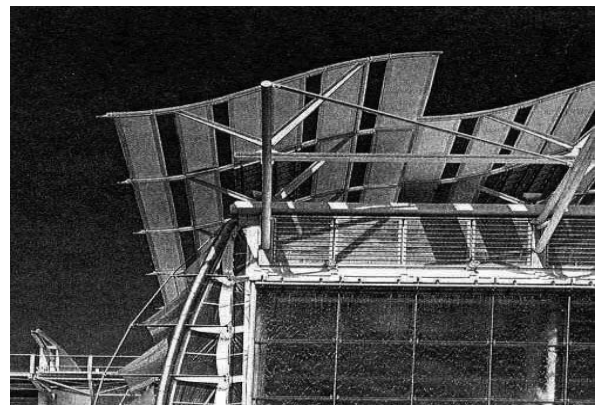
Figure 4. Solar "hats" on the roof of the British pavilion at EXPO 1992.

But can we use the human body sweat evaporation effect on buildings? There are buildings for which it may be said that they use the effect of water evaporation for their cooling, as in the case of a man's sweating.

It is an old practice to put water sprinklers on the roofs of large surfaces, and use them at high outside temperatures, when the sun radiates intensively. The roof is so moistened, and because of the heat absorbed by the outer roof surface and the air layer next to it, water evaporation occurs, and the roof temperature is lowered. Pools are also installed on roofs of multi-storey residential and business buildings.

The idea to let the water flow down a building façade, an imitation of human sweating, is an option in a modern architecture, in case of glass facades as frequently used elements in contemporary buildings, probably more for visual effects, but also as a way to get some kind natural reaction. Flowers, grass, but also water as an especially important element in some cultures becomes a repeatedly used elements in the modern architectural expression -.most often inside the large halls, restaurants, atriums.
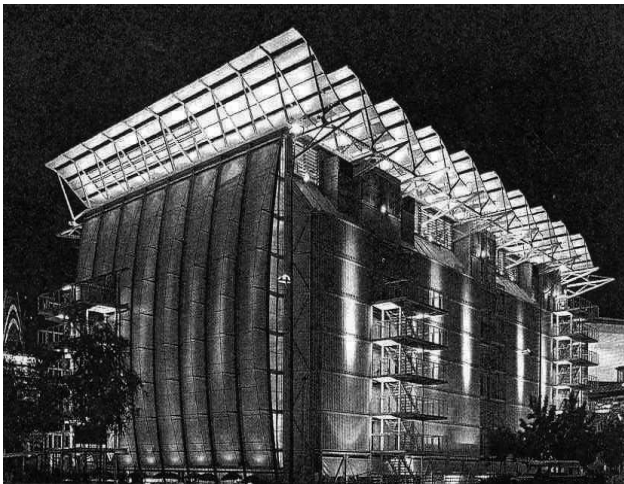
Figure 5. Water down flowing above glass envelope of the British pavilion

There are several buildings around the world with water flowing down the glass vertical or the inclined facade. One of such examples is again the building of the British pavilion in Seville (Figure 4.). Such façade has smaller coefficient of the solar radiation transmission, and with the water layer, due to its evaporation, the temperature next to the façade is significantly lower than the outside one, reducing so the heat gain from the solar radiation, as well as from temperature difference between the outside and the inside.
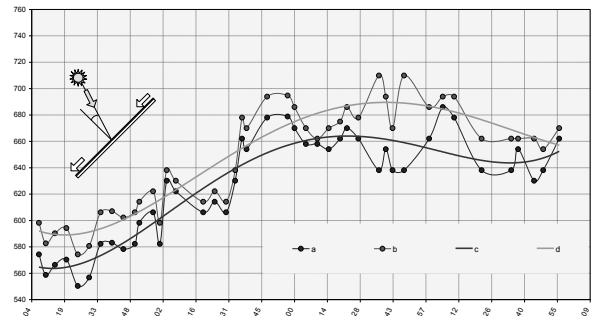
Figure 6. Measurements results of solar radiation transmission effects on dry and wet glass under the angle of 45 deg. . .

. The measurements provided above the glass with an angle of 45 degrees are presented on the Figure 6. showing solar radiation intensity through dry and wet glass. Uniform water flow above glass façade has a lower solar radiation transmittance for 10-15% than an ordinary dry glass. And when the water flow is turbulent and disturbed, even 25-30%, depending on water quantity.

The temperature of a glass under water flow was about 10C lower than the glass without a water above it. The temperature difference on a water inlet and outlet was very small, as the distance between them was 1.5m only.

On the figure 7 is the model of glass above which is lowing water. The thermo-vision made photo is showing temperature differences in a water film. The values of these temperatures are separately given for two horizontal sections and one vertical, with the temperatures of the upper and down horizontal sections as well as through vertical section. The temperature increase was measured 1,5 C.
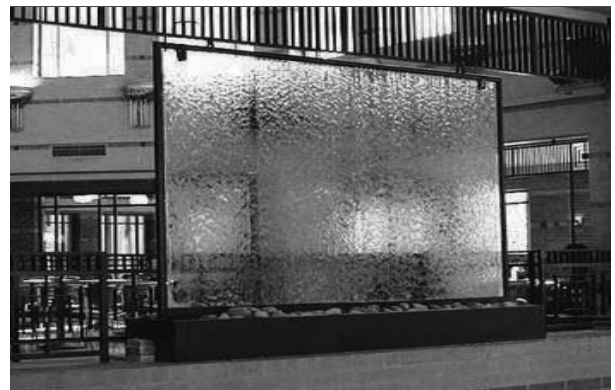
Figure 7. The model of glass façade wall above which is flowing thin layer of water
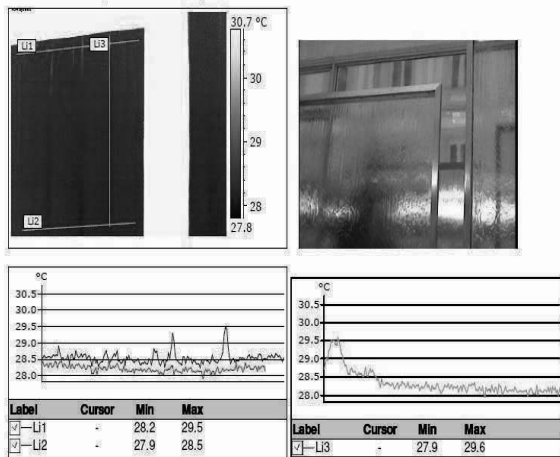
Figure 8.. Thermo vision camera picture of the temperature field in the water film and temperatures along the horizontal and vertical sections above the glass pane

VII. APLICATION OF NEW TECHNOLOFIES

Water cooling system with application of super-hydrophilic of Titanium dioxide TiO_2 coating is developed Japan and described in the paper written by Jiang He and Akira Hoyano (Energy&Buildings 40/ 2008). Water is sprinkled (Figure 8.) From the top of wall or roof flowing down the water. The water is collected in the bottom into water reservoir. This water is pumped up also with collected rainwater and reused for sprinkling the entire cycles. Such technology produces the very thin water layer and water saving and also the uniform distribution of water, as well as water saving what is important in coming future concerning needs of water.

Fig. 1. Diagram of the cooling system.
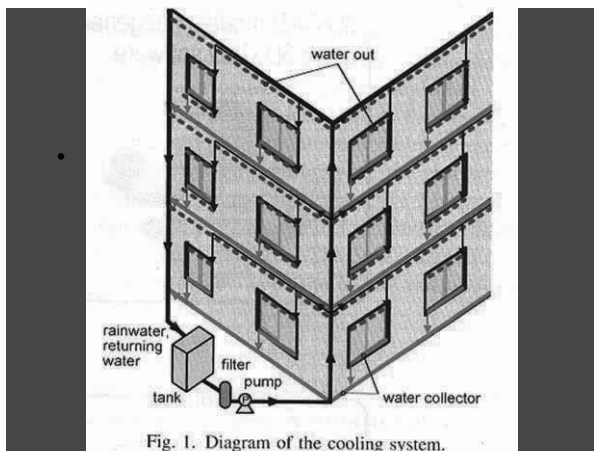
Figure. 9. The view on the new cooling system for buildings

Heating and heat storage of buildings envelopes by sunlight have been found to cause urban heat islands formation. Building envelopes are of materials which have high absorption and thermal capacity and absorbed solar radiation cause during night warmer envelope's surfaces then surrounding air. Reducing the heat absorbed by these surfaces or lowering the surface temperature mitigate influence of heat islands. But as the water layer above wall suface needs a lot of water floing down, new rehnolgy was discovered coating wall surface with TiO_2 developed.

VIII. CONCLUSION

Buildings are protected with insulation which remains unchanged during both the summer and the winter season. It is an advantage for a building, as, opposite to a man, a building uses cooling devices to reduce its temperature. However energy is necessary in such cases, which should be avoided in the present situation, regarding the energy crisis. Perspiration, the only possible effect of a human body cooling in high temperature areas has not been used largely in buildings. A few buildings around the world show it is a possible option. Unfortunately, the impression is that building cooling was not the primary task of the water flow on facades, although it was one of the aims when designing those buildings. The task remains to expand it, but before each such building design, exact calculations, simulations, optimisation should be done, resulting in total energy balance, taking into account water and energy balance.

The building envelopes are the main factor of building energy efficiency, as they represent a skin of a building's body. They should react as real skin as much as possible, defending interior from preheating, conserving it from heat losses in the heating season. That could be achieved relatively easy, but the architects and all factors influencing building design have to be working together in a manner of integral designing.

The energy needs analyze should be implemented in the building technical documentation, as a proof that the building will be a green one - at least from the point of view of energy efficiency and energy conservation. Computer programs that can be easily and quickly used on all locations have defined a meteorological year. For other locations, there are another methods, based on degrees-days, or formulas given in some studies and recommended, as in Germany. The effect of water flowing above glass facades is in lowering the temperature of glass, and in reduced solar radiation transmittance.

IX. REFERENCES

[1] Todorovic B. Cvjetkovic T. 2001. Classical and Double Building Facades-Energy Needs for Heating and Cooling, Proceedings, CLIMA 2000, REHVA, Naples, 2000.

[2] Todorovic B. Past, present and future buildings envelopes-human body thermal behaviour as the final goal, Energy for buildings, Proceedings of 6th International Conference, Vilnius. 2004

[3] Todorovic B Can a building mimic the thermal behaviour of a human body? Presentation at the ASHRAE Chapter in Singapore. 2005

[4] Todorovic B. Building Low energy cooling and advanced ventilation technologies in the 21st century. 2nd PALENC conference, Greece, 2007.

[5] Jiang He, Akira Hoyano, A numerical simulation method for analysing the thermal improvement effect of super-hydrophilic photocatalystic building surfaces...Energy&Buildings, 40, 2008.

[6] Todorovic B. Double skin facades : Types of constructions, air circulation between two facades in winter and summer, basis for estimation of heating and cooling load, ASHRAE winter meeting, Chicago, Published on line, ASHRAE , 2009.

Geothermal Energy in District Heating

DR. KONTRA Jenő Ph.D. – Dr. KÖLLŐ Gábor Ph.D.[*]
University Professor – University Professor
Budapest University of Technology and Economics
Faculty of Architecture
Department of Building Energetics and Building Services
H-1111 Budapest, Műegyetem rkp. 3, Hungary
kontra@egt.bme.hu, www.egt.bme.hu

I. GEOTHERMAL CONDITIONS OF THE PANNONIAN BASIN

A **geothermal system** is a restricted domain of earth crust being in heat transfer connection with its environment.

A geothermal reservoir is that part of the system from where internal energy can be partially brought to the surface by the help of a heat carrying medium. This means that a reservoir is a geological formation with adequate porosity storing thermal water or steam. This is called natural geothermal reservoir.

An artificial reservoir does not contain any aquifer fluid; from there heat can be extracted with a heat carrier injected from the surface. This system is called hot dry rock.

In deep-seated strata, heat is transferred by convection or heat conduction.

Geothermal reservoirs are continuously heated by terrestrial heat flow. Heat coming to the surface is replenished by the conductive heat flow being of relatively lower intensity than the convective heat transfer.

The average value of terrestrial heat flow is 90 mW/m^2 in Hungary. This is much higher than the value of 60 mW/m^2 measured on average in other areas in Europe; therefore, heat energy can be produced from deep economically in Hungary if the other geological circumstances are also favourable:
— present in subsidence and sedimentary basins,
— geothermal gradient is 50-60 °C/km,
— presence of adequate aquifer strata.

In such porous sandy and/or sandstone reservoirs, no convection flows can be generated. Temperature gradient measured in deep is fundamentally linear.

Maximum layer temperature of this type of reservoirs, called reservoirs with low enthalpy, does not surpass 150 °C. The largest reservoir vacuum heated by heat conduction is the Upper-Pannonian sandy reservoir in the sediment complex of the Hungarian Great Plain. Its average thickness is 200 m, its area is about 40 000 km^2, lying in the Carpathian basin disregarding frontiers (towards Romania, from the Small Plain to Slovakia, and also to Serbia).

District heating in Hungary and Romania

A new energy policy seems to develop in both countries with a large number of district heating systems in cities as top priority and being delicate field of economics as operational costs of these systems increase. District heating, established originally in combination with heat production in power stations, is a part of national wealth to be preserved by all means. Later on, many systems have been built exclusively with boilers as heat source, and gas heating has become common. Price increase of fossil energy has led to detachments from district heating systems in a high number, mainly in Romania, thus, there is a mixed heat supply in dwelling houses. Under such circumstances, it is a hard task to define a unified solution for modernization and replacement of natural gas. A large part of Hungary and the western areas of Romania have very good geothermal conditions, however, the available thermal water is not satisfactorily used for district heat supply.

II. THERMAL WATER UTILIZATION IN HEATING

Problem of temperature levels

Earlier when buildings consumed heating thermal energy in a very wasting way (judging by the present standard of energetics), in the case of secondary heating systems designed with a nominal temperature gradient of 90/70 °C, the winter design outgoing temperature was higher than 90 °C on the primary side. Nominal outgoing temperatures of 130-140 °C were common on the primary side.

In the present modern or improved buildings, not only the heating output can be decreased but also the temperature level of heat carrier can be lower.

The fundamental relation for the heat carrier at a heating panel designed for a temperature N (normal) of 90/70°C and the output of new radiators working with lower temperature levels is

---

[*] TECHNICAL UNIVERSITY OF CLUJ, Faculty of Civil Engineering, Department for Railways, Roads and Bridges, 400500 Cluj-Napoca, str. Observatorului nr. 72-74. kollo_g@yahoo.com, http://constructii.utcluj.ro/

$$\frac{Q}{Q_N} = \left(\frac{\Lambda t}{\Lambda t_N} \right)^n$$

where $n =$ is the exponent related to the heating panel.

The figure below shows heating outputs attainable by operation at lower temperature levels at an internal temperature of $t_i = 20°C$.

$$\frac{Q}{Q_N} = \left(\frac{\Delta t}{\Delta t_N} \right)^n$$

Pl.: 50/30°C   n = 1,3 tagos radiátor

$\Delta t_N = 40-20 = 20\,°C$

$\frac{Q}{Q_N} = 0,5 \longrightarrow Q = 0,5\,Q_N$
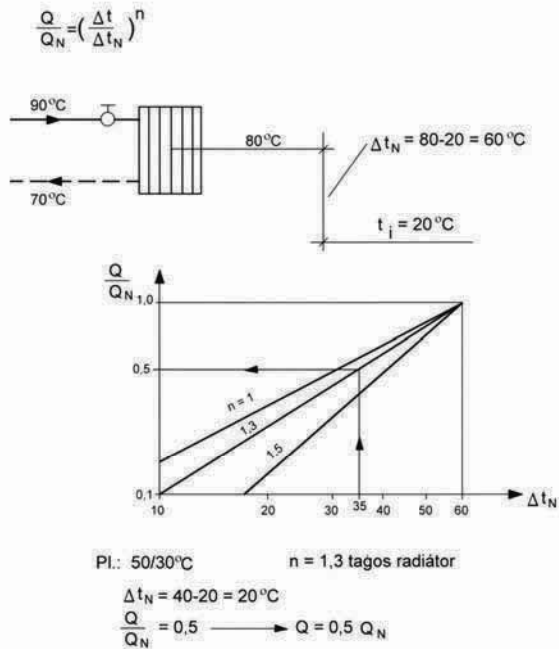
This is of utmost importance when the temperature of thermal water on the heat source side and temperature coming to the surface is lower than usual in heating. Therefore it is important to enable usage of thermal waters for heating buildings within a wider and wider temperature range.

Konvekciós-és padlófűtések
/ több hőfoklépcső /
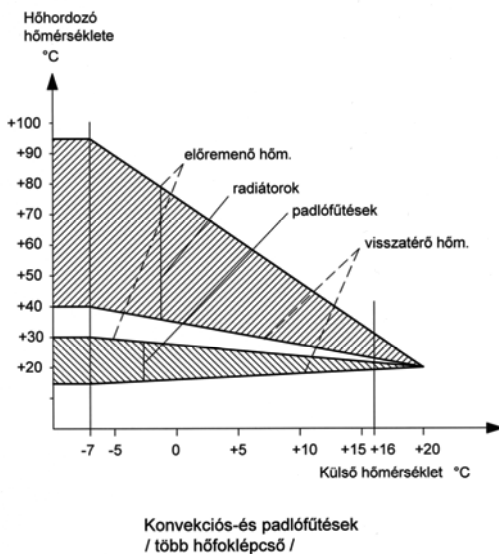
Here we mean various variants of heating in heat pump systems based, e.g., on escaping thermal water already used, escaping water of swimming pools regarded as sewage, escaping water of baths, etc. ...

Usefulness of heat pumps is illustrated by an electricity-driven heat pump connected to the return side of a convection heating, producing heat of 50 °C temperature for .floor heating and wall heating.
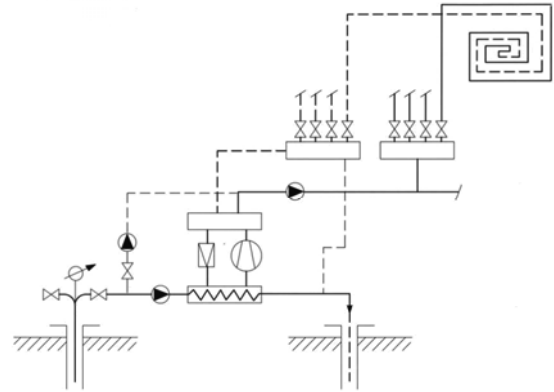
Cascade connection is also a usual solution with two (or more) heat exchangers for heating systems working at continuously diminishing temperature levels.
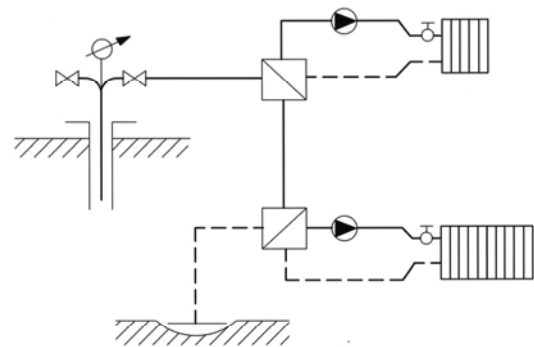
Nyitott kaszkád rendszer

In the case of lower thermal water temperature levels, the same system can be operated with a heat pump and peak boiler plant. At the same time, this peak boiler plant serves as a 100% reserve in the heating season.

III.   DISTRICT HEAT SUPPLY SYSTEMS

The modern district heat systems with re-injection have two major types:

a.) The thermal water heat exchanger transfers heat to the whole district heat network centrally, i.e. soft water circulates in the network.

b.) Thermal water flows in the network to the consumers, and heat transfer occurs through heat exchangers in the receiving thermal centres. This latter type is applicable where thermal water is used also water-technologically (e.g. in thermal baths). Its drawback is gas escape and salting in the whole network which should be treated.

Closed and open thermal water systems

Common feature of the systems with re-injection listed above is that degassing is not allowed in the primary circuit either. This has the advantage that there is no scaling and no gas escape (explosion risk). However, in the case of wells with methane content, it is advisable to burn methane in a boiler or gas engine after demethanization and drying.

This way, through cogeneration, we obtain "green" electricity that can be fed into the network, and waste heat of the engine can be used either for heating or absorption cooling. Lower temperature limit of absorption is 90 °C that can be obtained from a gas engine (like in hospital in Karcag).

Open thermal water systems are degassed just in the degassing storage next to the thermal well. In this case, escort gases (CO_2, CH_4) escape in the air contaminating the atmosphere by their green house effect. As a drawback of open systems, thermal water takes oxygen in the degasser from the ambient air, thus inclining to oxidation when flowing in the system.

IV. USE OF RENEWABLE ENERGY IN DISTRICT HEAT SUPPLY OF HUNGARY

Utilization of renewable energy in district heat supply dates back to a 25-year history in Hungary. It began in the middle of the 80s within energy rationalization when new wells were established by state subsidies resulting in implementation of geothermal energy in district heat supply.

In the field of district heat supply, solar, geothermal and bio-energy can be considered.

In the recent years, intensive development can be observed in utilization of various bio-energy types.

Hungary has very good natural resources in the field of renewable energy carriers applicable at present in district heat supply, offering opportunity to profit from the following advantages:

— significant resources, incoming energy flows,
— aspects of environmental protection,
— decrease of import dependency, replacement of natural gas,
— favourable availability,
— independence from price fluctuation of fossil energy carriers.

Drawbacks and risks connected with renewable energy utilization can be mitigated by far-seeing exploratory surveys.

Publications:

MTA Megújuló energiák hasznosítása; (Utilization of Renewable Energy Carriers) Hungarian Academy of Sciences 2010, Budapest

Magyar Távhőszolgáltatók Évkönyve 2004.; (Almanac of Hungarian District Heat Suppliers), MATÁSzSz, Budapest, 2005.

Komlós Ferenc: Hőszivattyús rendszer, (Heat Pump System), Budapest, ISBN 978-963-06-7574-1

At present, long-term energy data of **geothermal energy utilization** are available for seven cities of Hungary, shown in the table below:

	2002			2010		
	Energy carriers in total [GJ]	Geothermal energy carrier [GJ]	Number of flats	Energy carriers in total [GJ]	Geothermal energy carrier [GJ]	Number of flats.
Csongrád	26,220	19,971	516	29,913	26,949	514
Hódmezővásárhely	167,437	77,075	2,247	109,306	87,940	2,834
Szeged	238,694	67,508	4,477	99,911	21,680	2,349
Szentes	95,207	61,259	1,302	89,896	87,607	1,402
Szigetvár	59,321	12,758	594	30,530	4,829	594
Nagyatád	6,944	4,445	240	10,306	3,320	240
Vasvár	11,341	4,509	40	9,188	2,735	59
In total:	605,164	247,525	9,416	379,050	235,060	7,992

Analysis of the Energy-Optimum of Heating System with Heat Pump using Genetic Algorithm

Jozsef Nyers Dr.Sci.*, **Mirko Ficko** Dr.Sci. ** , **Arpad Nyers** Ph.D student***
* Subotica Tech. Serbia , University Obuda Budapest, Hungary
** University Maribor, Slovenia
*** Subotica Tech. Serbia, Tera Term co. Subotica, Serbia
e-mail : jnyers@vts.su.ac.rs
symposium EXPRES 2012, Subotica-Szabadka

Abstract - This paper analyzes the possibility of obtaining multi variable energy optimum of a heating system with heat pump. The variables are the water mass flow rate from well and the water mass flow rate in the heating circuit. The task is to find the optimal combination of the water mass flow rate in each water circuit. Optimum water mass flow rates provide the maximum COP of the heating system with heat pump by constant mass flow rate of refrigerant. The result can be obtained by using a numerical method based on genetic algorithms.

A mathematical model is formed to the stationary regime with concentrated parameters. The model consists of the mathematical model of the evaporator, centrifugal pump, circulate pump and the compressor. Based on the results it is possible to choose the centrifugal pump and the circulate pump with optimal power consumption.

Keywords- optimum, pump, well, COP, heat pump, stationary mathematical model, genetic algorithm.

I. INTRODUCTION

The heating system based on the heat pump is used for heating residential and commercial buildings. The system consists of a heat source, heat pump and heat sinks. In the present case heat source could be the water from the deep layers of ground or ground it self. Ground heat is transported by water to the same temperature as the temperature of ground. The heat from the ground is collected by vertical ground heat exchangers. In the vertical ground heat exchangers circulates brine or antifreeze. The antifreeze in the vertical ground exchanger is at lower temperature than the water transported directly from ground water layer, because there is a temperature deferens between the ground and the antifreeze. Due to a temperature deferens the overall COP level is lower.

In this case the heat sink is the building. The circulating water in the heating system transports the heat from the heat pump. Heating system has better performance when the heaters has large surface. This criterion is satisfied by heating panels. Form of the heating panels is the piping patterns on the floor, wall or ceiling.

In order to achieve the higher COP of the heating system important is to set the energy relations of the three circuits. There are the refrigeration circuit, cold and hot water circuits. Higher COP can be achieved if the water circuits are energetically optimized.

Water circuits can be optimized through the mass flow rate of water. The optimum mass flow rate of water in the hot and cold water circuits give maximum COP of the system.

To find the exact optimum of the energy system can be an application of mathematical optimization method. A precondition to the optimization is an accurate mathematical description of the system i.e. mathematical model.

Time-varying and stationary mathematical models are known. In the case of energy optimization time-varying mathematical models are not interesting because transient process very short-lived. Transient process occurs only during the switch on the heating system or turning off. The exceptions are systems with air heat pumps due to external air temperature change. In these systems the optimum working point changes in the function of the external air temperature. Recently, the air source heat pump systems equipped with variable speed fans and compressors to keep the optimal level of energy consumption. This provides by a relatively inexpensive frequency speed control of electric motors of fans and compressors.

Water-water heating system with heat pump operates in steady operating mode because of the near constant temperature of the ground. It is not necessary to change the revolution of pumps and compressors. It is important to optimize the mass flow rate of water in the hot and cold water circuit. Based on the optimal mass flow rate of water the circulating pumps can be choosing.

II. DESCRIPTION OF PHYSICAL SYSTEM

The observed system consists of cooling circuit, cold and hot water circuit. Cooling circuit is realized in the heat pump. The heat pump is a refrigeration device based on the left cycle. Considered heat pump is with a compressor. Heat pumps based on absorption give much lower COP than with compressor.

17

Selected heat pump is a classic heat pump, consists of evaporator, compressor, condenser and thermal expansion valve. Cold water circuit carried out of the heat source well or vertical ground heat exchanger, pump, piping, and drains well to absorb the thermal used water. In the center of the optimization procedure are the mass flow rates of the water obtained by the pumps.

Hot water circuit is also the focus of observation. Pipeline and heaters are very important but only provide indirect influence on the COP of the system. The element of the hot water circuit affects the condensation temperature but does not have direct influence on the COP of the system. With increase the surface of the heating panels the degree of COP rising continually without extremes

In this regard pumps provide energy optimum of the system through mass flow rate. For each water-water heating system with heat pump should determine the optimal power of the circulating pumps to reach the maximum COP of the system.

Figure 1. Energy flows and the signs of physical systems

III. GUVERNING STATIONARY EQUATIONS THE MATHEMATICAL MODEL

Heat transfer in the evaporator between the water and the refrigerant, Freon:

Quantity of heat expressed by the convective coefficient of heat $k(\dot{m}_w)$ and the logarithmic temperature-difference $\Delta t_m(\dot{m}_w)$.

$$q_o = k(\dot{m}_w, \dot{m}_f) \cdot F \cdot \Delta t_m \qquad (1.)$$

Heat expressed by caloric equation for the well water.

$$q_o = \dot{m}_w \cdot C_{pw} \cdot \Delta t_w \qquad (2.)$$

Heat expressed by the latent heat of refrigerant vaporization

$$q_o = \dot{m}_f \cdot \Delta i_{fo} \qquad (3.)$$

The power of real compressor

$$P_c \cong \dot{m}_f \cdot \Delta i_{fc} \cdot \eta_s^{-1} \cdot \eta_c^{-1} \qquad (4.)$$

The power of real cintrifugal pump

$$P_{wp} = \left(k_{wp1} \cdot \dot{m}_w^{-0.25} + k_{wp2}\right) \cdot \dot{m}_w^3 \cdot \eta_{wp}^{-1} \quad (5.)$$

The power of real circulation pump

$$P_{cp} = \left(k_{cp1} \cdot \dot{m}_c^{-0.25} + k_{cp2}\right) \cdot \dot{m}_c^3 \cdot \eta_{cp}^{-1} \quad (6.)$$

IV. AUXILIARY STATIONARY EQUATIONS OF THE MATHEMATICAL MODEL

Heat transfer coefficient between water and refrigerant in the evaporator, approksimatry

$$k(\dot{m}_w) \cong \frac{\alpha_w \cdot \alpha_f}{\alpha_w + \alpha_f} \qquad (7.)$$

In studied case evaporator is coaxial, consisting of parallel copper pipe bundle.

The coefficient of convective heat transfer when water or antifreeze flows outside of the copper pipes.

$$\alpha_w(\dot{m}_w) = k_w \cdot \dot{m}_w^{0.6} \qquad (8.)$$

$$\alpha_w(\dot{m}_w) = 7000 \div 3000 \left[W/_{kg°C}\right] \quad (9.)$$

The coefficient of heat transfer when evaporation of refrigerant inside the copper tubes

$$\alpha_f(\dot{m}_f) = \frac{\lambda_{fl}}{d_u} \cdot 0.035 \cdot Re_{ft}^{0.6} \cdot Fr_{ft}^{0.33} \cdot f(x, Re, Fr, P \dots)$$

$$\alpha_f(\dot{m}_f) = 1500 \div 1700 \left[W/_{kg°C}\right]$$

Logarithmic temperature difference between the water and the refrigerant temperature. Approximately

$$\Delta t_m = \frac{\Delta t_{max} + \Delta t_{min}}{ln \frac{\Delta t_{max}}{\Delta t_{min}}} \cong \frac{\Delta t_{max} + \Delta t_{min}}{2}$$

The flow direction of refrigerant and water not important because of the constant evaporation temperature.

$$t_{fu} \cong t_{fi} \cong t_o$$

For the same direction flow the maximum and the minimum temperature difference is

$$\Delta t_{max} = t_{wu} - t_o$$
$$\Delta t_{min} = t_{wi} - t_o$$

Ttemperature difference between input and output of water in the evaporator.

$$\Delta t_w = t_{wu} - t_{wi}$$

The evaporation latent heat of refrigerant R134a depends on evaporation temperature.

$$\Delta i_o(t_o)$$

Increment of Freon vapor enthalpy due adiabatic compression

$$\Delta i_c = i_c(t_c) - i_o(t_o)$$

V. OBJECTIVE FUNCTION

The objective function in analyzed case is the COP of the heating system

$$\eta_{max} == \left\| \frac{q_o(\dot{m}_w, \dot{m}_f) + P_c(\dot{m}_f) + P_{cp}(\dot{m}_c)}{P_k(\dot{m}_f) + P_{wp}(\dot{m}_w) + P_{cp}(\dot{m}_c)} \right\|_{max}$$

In the above function each term depends on the mass flow rate.

Maximum value of COP is obtained optimal combination of mass flow rate of well water, heating water and mass flow rate of Freon.

For optimization is applied numerical procedure, the method of genetic algorithm.

The application of classical optimization procedure using the first derivative at mass flow rates is very complicated and difficult to implement.

VI. MATHEMATICAL OPTIMIZATION PROCEDURE

A. Genetic algorithms

Methods of evolutionary computation are widely used for optimisation of problems [5-7] which can be multi-model, non-differentiable, non-continuous, also in the domain of heating, ventilation and air conditioning [8]. Genetic algorithms proved to be very useful for optimization of multicriteria and multiparameter problems as presented problem of optimization of heating cooling system with heat pump. Evolutionary computation employs the vocabulary taken from the world of genetics itself, and as a result solutions refer to organisms of a population. Each organism represents the code of a potential solution to a problem. A further important characteristic of GAs is that they work by maintaining a set (population) of potential solutions, where as the other search methods process a single point of the search space.

Traditional analytical or numerical based approaches genetic algorithms are based on building of solution. Because this is in the case of optimization of heating system with water-water heat pump impossible we can take different approach. The combination of all independent variables used in the mathematical model for calculation of COP we can designate as solution. And previously stated mathematical formulation for calculation of COP can be designated as target function. The solution is feasible combination of independent variables not only the optimal solution.

Representation of organism is:
$$representation\ of\ organism\ i = \{\dot{m}_{wi}, \dot{m}_{fi}, \dot{m}_{ci}\}$$

Our desire is to advance during evolution of solutions to the optimal solution. In the world of evolutionary computation, solution is called organism. And set of solutions created in one step is called generation. This basically means we are searching for such combination of $\dot{m}_w$, $\dot{m}_f$ and $\dot{m}_c$ that the COP will, be at his maximum. We could check all possible combinations of $\dot{m}_w$, $\dot{m}_f$ and $\dot{m}_c$. Unfortunately this is impossible because of infinite size of search space. An exhaustive search method or an exhaustive search method combined with conventional gradient based methods can be applied to find the optimal solutions, even though it is impractical in real time applications for such a complicated problem due to its time consuming nature.

With genetic algorithms we can manage this problem. Genetic algorithms are effective at search in such large space. It works on set (generation) of possible solution and afterwards it checks the quality of solution (value of COP). The creation of new set of solution (offspring generation) is based on principles of evolution and genetics which takes into account the value of COP. Basic steps of genetic algorithm which repeat for every generation are (
Figure 2):

1. Creation of an initial set of solutions (initial generation of organisms).In our case organism represent combination of mass flows of cooling/heating media. Organism it's a set of numerical values. First generation of solution is created at random from the interval of possible values.

2. Evaluation of organisms by means of a fitness function. This basically means calculation of COP value for all solutions (organism).

3. Execution of evolutionary (reproduction and crossover) and genetic (mutation) operations on solutions (organisms) which solve the problem above average in current generation.

In our model of optimization the tournament selection is used. Tournament selection randomly chooses from the population at least two organisms and the one which represents better solution (COP in our case) is used for creation of new solution by crossover and mutation. It was used simple one point crossover, for example:

$$\{\dot{m}_{w1}, \dot{m}_{f1}, \dot{m}_{c1}\}, \{\dot{m}_{w2}, \dot{m}_{f2}, \dot{m}_{c2}\}$$
$$\xrightarrow{yields} \{\dot{m}_{w1}, \dot{m}_{f2}, \dot{m}_{c2}\}$$

The mutation is based on the randomly insertion of new random value:

$$\{\dot{m}_{w1}, \dot{m}_{f1}, \dot{m}_{c1}\} \xrightarrow{yields} \{\dot{m}_{w1}, \dot{m}_{f1}', \dot{m}_{c1}\}$$

The biggest advantage of search for solution by genetic algorithms is possibility to use mathematical correct definition of COP, without need for simplification. Traditional methods of solving complex real-world problems are based on simplification. At simplification process we have to deal with possibility too simplify too much. With genetic algorithms we can try evolutionary created solutions in the real world, in our case mathematical formulation of COP.
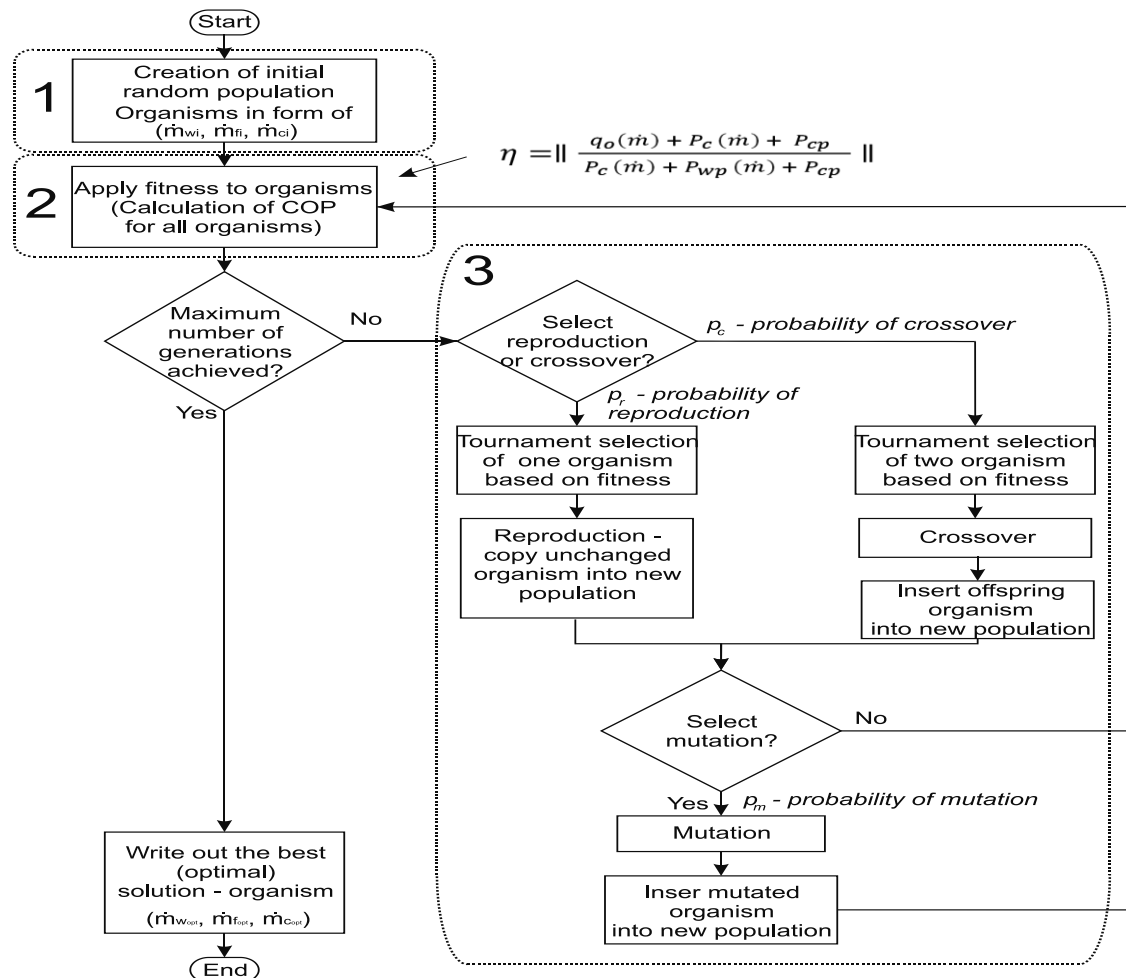
$$\eta = \left\| \frac{q_o(\dot{m}) + P_c(\dot{m}) + P_{cp}}{P_c(\dot{m}) + P_{wp}(\dot{m}) + P_{cp}} \right\|$$

Figure 2. Representation of search for optimal solution by genetic algorithm

VII. CONCLUSION

- To obtain the maximum COP of system is required exact stationary mathematical model of the heating system and an adequate mathematical optimization procedure.
- For energy optimization using the stationary mathematical model, because the system operates 99% of time in stationary regime.
- Mathematical model of the heating system consists of evaporator, compressor, thermo-expansion valve, well pump and circulation pump.
- For the purpose of the completeness, the mathematical model should be extended more with the mathematical description of the condenser.
- For optimization is proposed the numerical procedure, the genetic algorithms.
- The application of classical optimization procedure using the first derivative verydifficult, practically impossible.
- Genetic algorithm provides to obtain the optimum combination of mass flow rate in the system.
- The optimal combination of mass flow rates provide maximum COP of the heating of the system using heat pump.

VIII. REFERENCES

[1] Nyers J. Stoyan G.:" A Dynamical Model Adequate for Controlling the Evaporator of Heat Pump", International Journal of Refrigeration, 1994.

[2] Nyers J.: "Energy optimum of heating system with heat pump"6th international multidisciplinary conference, 545-550,Baia Mare-Nagy Bánya, Romania 2005.

[3] Nyers J.: "Stationary mathematical model of heating system with heat pump" 22 th international conference " science in practice", Schweinfurt, Deutschland 2005.

[4] Nyers J., Nyers A. : "COP of Heating-Cooling System with Heat Pump" International Symposium "EXPRES 2011." Proceedings 17-21 Subotica, Serbia.

[5] Ammeri A., Hachicha W.,Chabchoub H. &Masmoudi, F.A:"Comprehensive Litterature Review of Mono-Objective Simulation Optimization Methods", Advances in Production Engineering & Management, Vol.6, No. 4, 2011.

[6] Ficko M., Klančnik, S., Brezovnik, S., Balič, J., Brezočnik, M. & Lerher, T.. „Intelligent optimization methods for industrial storage systems"In: Manzini, R. (Ed.). Warehousing in the global supply chain : advanced models, tools and applications for storage systems. London: Springer, 2012.

[7] Gen, M. and R. Cheng, Genetic algorithms and engineering design. Wiley series in engineering design and automation. 1997, New York: Wiley. xix, 411 p.

[8] Lu, L., et al., HVAC system optimization—condenser water loop. Energy Conversion and Management, 2004. 45(4): p. 613-630

The Set-Up Geometry of Sun Collectors

István Patkó Prof. Dr, dean*, **András Szeder** instructor**

Óbuda University, Rejtő Sándor Faculty of Light Industry and Environmental Engineering
Doberdó út 6., H-1034 Budapest, Hungary
e-mail: * patko@uni-obuda.hu ** szeder.andras@rkk.uni-obuda.hu

Abstract: In order to efficiently solve the problems created by the deepening energy crisis affecting Europe and the world, governments cannot neglect the opportunities of using the energy produced by sun collectors. In many of the EU countries there are sun collectors producing heat energy, e.g. in Austria more than 3,500,000m² and in Germany more than 12,000,000m² of sun collectors are operated [5]. The energy produced by these sun collectors is utilized at the place of production. In the near future governments will have to focus more on spreading and using sun collectors. Among the complex problems of operating sun collectors, this article deals with determining the optimal tilt angle of sun collectors. The tilt angles which we determined theoretically are confirmed by laboratory measurements. The result of our work will help users and engineers to determine the optimal operation of sun collectors.

Keywords: sun collector, heat energy, optimal tilt angle

I.   SOLAR RADIATION

Sun collectors transform the radiation energy represented by the short wave (λ= 4 μm) beams emitted from the Sun into heat energy. This heat energy may be utilized for terrestrial life. Figure 1 shows the proportion of solar radiation reaching the Earth's surface and the losses of the radiation.
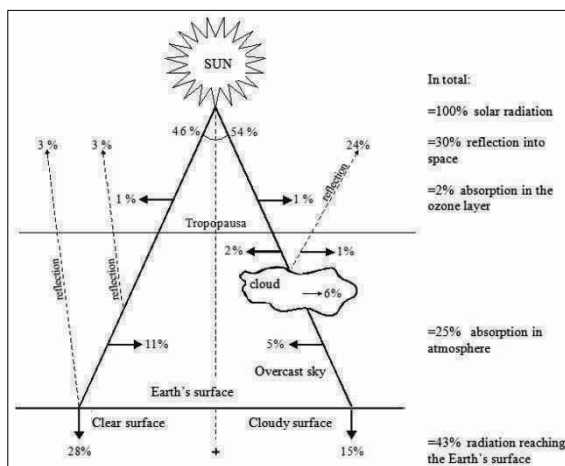

Figure 1
The balance of solar radiation [6]

This figure builds on the assumption that 54% of the Earth's surface opposite the Sun is covered by clouds, while 46% is clear (free of clouds).

A large amount of the radiation leaving the Sun cannot be used on the Earth – for heat production – because they do not reach the Earth's surface or are reflected back from there. These must be considered as losses. The relative values of losses in relation to total radiation, based on Figure 1:

- reflection into space   30 %
- absorption by the ozone layer   2 %
- absorption in the atmosphere   25 %

With these values the total radiation loss amounts to 57% of the radiation of the Sun. This means that 43% of the solar radiation may be utilized on the Earth's surface. These losses occur in the airspace between the lower border of the thermosphere (at a height of ~ 80 km) and the Earth's surface. It is assumed that the losses of solar radiation above the height of 80 km (the lower part of the thermosphere) are negligibly small compared with the total loss. At the lower border of the thermosphere the relative energy of the – loss free – solar radiation, when the Earth is at its mean distance from the Sun, is determined at 1345 W/m2 ± 3 % by the specialist literature. This value is called Solar Constant (N). In this way Id=1345 W/m2 x 0.43 = 582.2 W/m2 relative energy current reaches the Earth's surface represented by the unobstructed part of the radiation coming from the Sun. If we place a surface (e.g. a sun collector) smaller than the Earth's surface irradiated by the Sun in the irradiated area of the Earth's surface, then the solar radiation reaching this surface is shown in Figure 2.
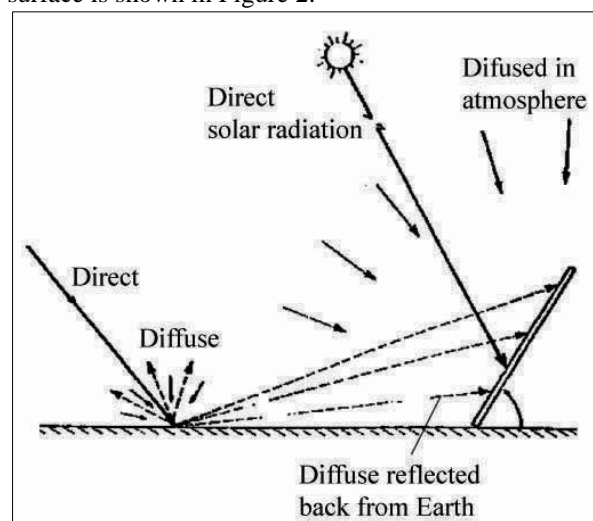

Figure 2
Solar radiation reaching the sun collector [6]

Part of the previously described losses (diffusion) may become utilized on the surface of the sun collector. With these the solar radiation reaching the sun collector is:
- direct: I_d
- diffuse: I_{dif}
  • diffused by the atmosphere: I_{da}
  • diffused by the Earth's surface: I_{dE}

Total radiation reaching the surface of the sun collector (I_{total}):

$$I_{total} = I_d + I_{dif} = I_d + I_{da} + I_{dE} \text{ (W/m}^2) \qquad (1)$$

On the basis of these considerations it is easy to determine the potential of the Earth's surface coming from solar radiation. As an example the situation of Hungary will be presented here. If the area of the country is (rounded) 93,000 km^2, the – specific – energy reaching Hungary's surface through direct solar radiation (I_d):

$$E_{dir.solar\ rad} = 93 \cdot 10^9\ m^2 \cdot 582.2\ W/m^2 = 54.1 TW$$
$$= 54.1\ TJ/s \qquad (2)$$

According to statistical data the hours of sunlight in Hungary are determined at 1,850-2,200 hours/year. Considering these values the energy potential of the country – from solar radiation – is:

$$(360 \cdot 3) \div (428 \cdot 5) \cdot 10^6 TJ \qquad (3)$$

When using sun collectors we must strive to utilize as much as possible from the available energy. For this purpose it is necessary

• to set up the sun collector geometrically optimally on the basis of the position of the Sun and the Earth relative to each other – taking into account the economic considerations,
• to use sun collectors of optimal design from technical and profitability point of view.

II. SUN-EARTH GEOMETRY

In order that the surface of the sun collectors should be able to convert as much as possible from the energy transported by the arriving sun rays we must be familiar with the Sun-Earth movements. When determining the geometry of the Sun-Earth movement we tried to use the simplest formulas possible that engineers and enterprises designing the sun collectors may be able to work with. From the different types of solar radiation discussed in the previous chapter we would like to deal with direct radiation only. Figure 3 shows the geometric relationships of sun collectors placed on the Earth's surface.
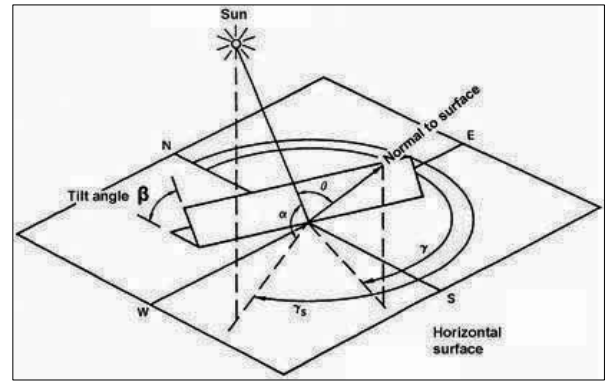
Figure 3
Relationships of the incident beam radiation and a tilted surface [1]
where:
  β: tilt angle of sun collector [°]
  γ: azimuth angle of sun collector [°]
  $γ_s$: azimuth angle of sun's rays [°]
  α: angle of sun's rays [°]
  θ: angle of sun's rays to normal of surface of sun collector [°].

Figure 4 shows the position of direct radiation arriving at the surface of the Earth as a result of the relative position of the Sun and the Earth.
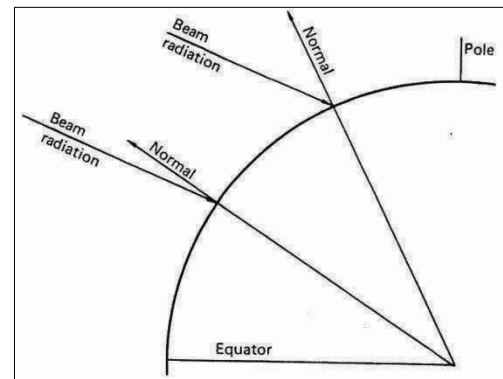
Figure 4
Effect of latitude on sun angle [1]

If we place a sun collector at a tilt angle β, the geometry of the rays reaching the surface is shown in Figure 5. This figure also shows the central angle (ϕ) which belongs to the northern latitude.
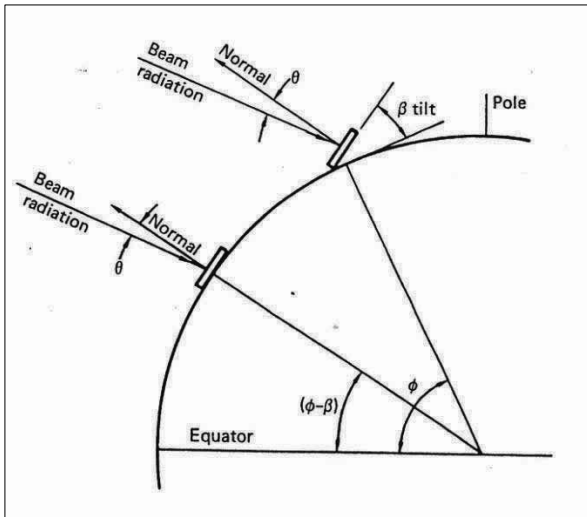
Figure 5
Effect of collector tilt. A collector tilted south at an angle β at a latitude φ has the same sun angle as a horizontal collector at latitude (φ - β) [1]

The amount and intensity of the radiation arriving at the surface of the sun collector also depend on the relative position and movement of the Earth-Sun. Figure 6 depicts the movement of the Sun and Earth in relation to each other, the so-called sun paths at 48˚ north longitude.

Figure 6
Visualization of the sun paths across the sky [1]

At 48˚ latitude of the northern hemisphere the figure shows the sun's movement at the time of the winter and summer solstice and the equinox. If we prepare the top-v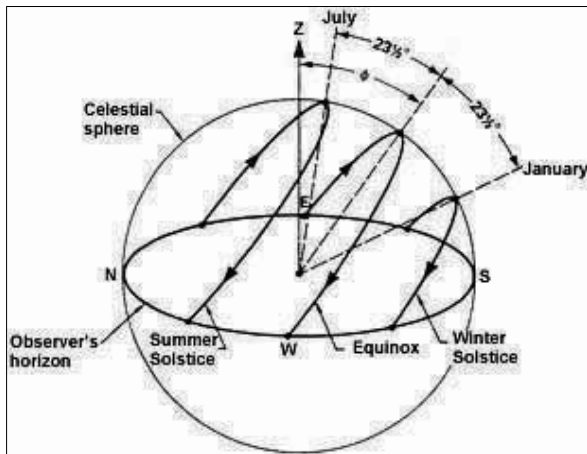iew picture of this figure, we get the sun chart of this northern latitude (Figure 7). According to the sun charts the sun gets the closest to the sun collector placed in the centre of the figure i.e. the observation point, at the time of the summer solstice, i.e. at 12.00 June 21st. It is obvious from this figure that if the sun collector is directed in the true south direction, it gets the largest possible radiation energy. During the day the angle of the sun to the normal of the sun collector (θ) changes according to the passage of time. If we want the sun to reach the surface of the sun collector at the most optimal angle during the day,

continuous east-west sun collector adjustment must be provided. This topic is not dealt with in this work. In our work with change tilt angle β to the horizontal surface and we determine those tilt angles (β) at which, during the year, the collector will be capable of transforming the largest energy deriving from the sun. This means that he tilt angle of the (β) should be modified according to the movement of the sun each day of the year.
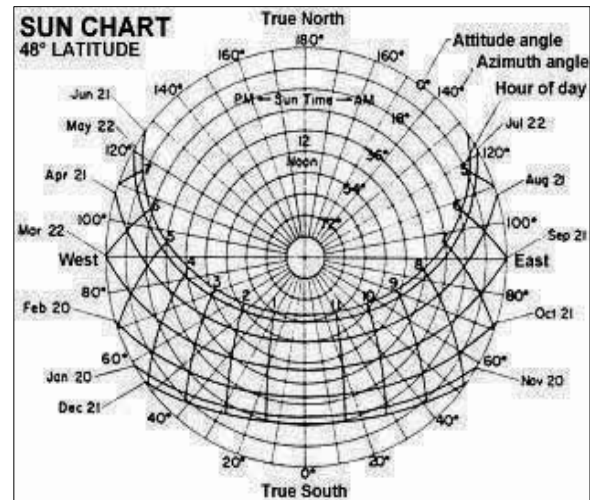
Figure 7
Sun charts [1]

This is technically unimaginable and impracticable, therefore in this section of our article we determine the most optimal tilt angle values at the tested geographical location (N 47.5˚):

- for the whole year
  (the tilt angle of the collector (β_{year}) is not modified during the year),
- seasonally
  (the tilt angle of the collector is modified according to the four seasons. Therefore four tilt angles will be defined (β_{summer}, β_{winter}, β_{autumn}, β_{spring})).

The Earth orbits the Sun in an elliptical orbit with an eccentricity of 3%. The Earth makes a full circle in a year. The Earth does not only go around the Sun but it also rotates around its own axis at a speed of one rotation per day. Its own axis is tilted at δ=23.5˚ from the axis of the orbit around the Sun. In this way during its orbit around the Sun, the northern hemisphere gets closer to the Sun in the summer than the southern hemisphere, and this is changed in winter. In spring and autumn the tilting of the Earth's axis (δ) is such that the distance of the northern hemisphere and the southern hemisphere relative to the Sun is the same. This is shown in Figure 8.

Figure 8
Diagram of the Earth's orbit around the Sun [1]

Figure 9 shows the variation derived from the relative declination of the Earth's axis angle (δ) in relation to the time of year.

Figure 9
Yearly variation of the solar declination [1]

This variation gives a sinusoidal function which shows that on March 20th and September 22nd, i.e. at the time of the summer and winter solstice the incremental distance between the Earth's northern hemisphere and the Sun is zero, while it is the smallest on June 21st and the largest on December 22nd.

On the basis of our theoretical considerations and experience we have accepted that – globally, regarding a whole year – the tilt angle of the sun collector equals the value of the northern latitude, i.e.:
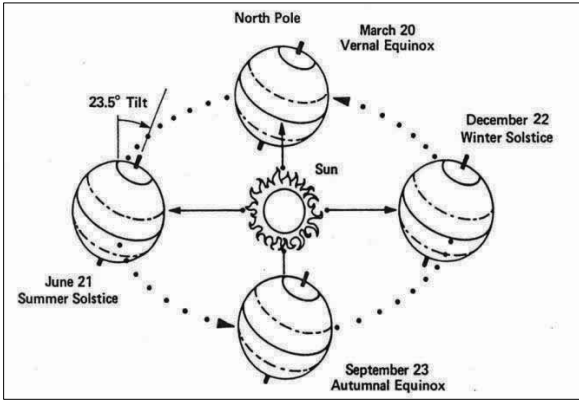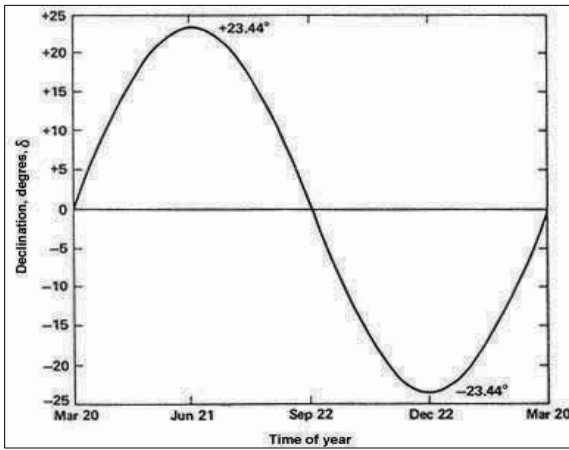
$\beta_{year} = \phi$

so at the test site, in Budapest, (47.5˚ N):

$\beta_{year} = 47.5˚$

According to [1] $\beta_{year} = \phi$ should be modified in the following way:

$\beta_{year} = \phi + (10˚ \div 20˚)$

We disregard this assumption, proposal during our tests.

The – theoretical – values of seasonal tilt angles are the following according to Figure 8.

$\beta_{summer} = \phi - \delta$
$\beta_{winter} = \phi + \delta$
$\beta_{autumn} = \phi$
$\beta_{spring} = \phi$

The tilt angles of the sun collectors at the test site, in Budapest, (47.5˚N):

$\beta_{summer} = 24˚$
$\beta_{winter} = 71˚$
$\beta_{autumn} = 47.5˚$
$\beta_{spring} = 47.5˚$

We made some measurements in order to verify the correctness of the values.

III.   LABORATORY MEASUREMENTS

We made a series of measurements with glass covered flat collectors in order to determine the ideal collector tilt angles (β) in the area of Budapest (47.5˚ N). The main point of the measurement is to determine the optimal tilt angles (β) as a result of comparative series of measurements. We measured the thermal characteristics of two sun collectors parallel, at the same time. We had set the tilt angle of one collector to a value – which we defined – relating to the whole year (β_{year}) and we did not change that during the series of measurements. This collector was later marked collector B. The tilt angle of the other collector marked A was modified according to the seasonal values defined by us (β_{summer}, β_{winter}, β_{autumn}, β_{spring}) during the measurements. Figure 10 depicts the collectors.
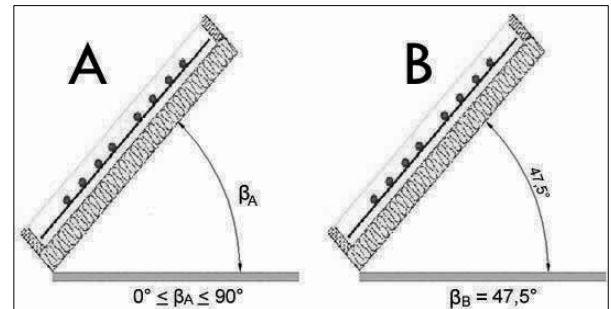
Figure 10
Tilt angles of collectors

During the measurements the thermal characteristics of both collectors were measured and we made our conclusions by comparing these. The measurements were made in the summer, autumn and winter of 2011. In our opinion the autumn and spring measurements – relative to each other – must produce the same result, so we did not make any measurements in spring. This conclusion is supported by Figure 8 as well.

A   Description of the measuring equipment

In order to confirm and support by experiments the sun collector tilt angles (β) determined theoretically in the previous sections, a special measurement station was created at Óbuda University (Hungary, Budapest) and installed on the roof of the building. With the measurement equipment – which is fully automated and controlled by a computer – we were able to

continuously measure the thermal characteristics of the sun collector in summer, autumn and winter. The conceptual layout of the measuring equipment is shown in Figure 11. The equipment incorporates two (1.6 m^2) glass covered flat collectors (marked A and B) witch were developed by us. The system has two loops. The primary loop which consists of the sun collector and the liquid heat exchanger placed in the solar tank, is filled up with antifreeze liquid medium. The secondary loop utilizes the heat content of the water in the solar tank. Measurement points were established in the measuring equipment to measure the water and liquid material temperature, and the mass flow of water and liquids. In order to increase the safety and reliability of the measurements, we measured the amounts by MBUS and PLC systems. The measurements were processed by a monitoring computer and presented them on the screen by VISION system. During the measurements great care was taken to make sure the **temperatures and mass flows of the medium entering the collectors – in the case of both collectors – should be equal**. This was ensured by keeping the secondary loops and the tank temperatures at a constant value. The characteristics of the external atmosphere were measured by a meteorological station located on the roof and equipment measuring solar radiation, and the results were entered into the monitoring computer. Special care had to be taken of the winter measurements. The system had to be protected against freezing in a way that by the beginning of the – daily – measurement the temperature of the solar tank should not be higher than 2÷3˚C. The conceptual layout of the measuring equipment is shown in Figure 11.
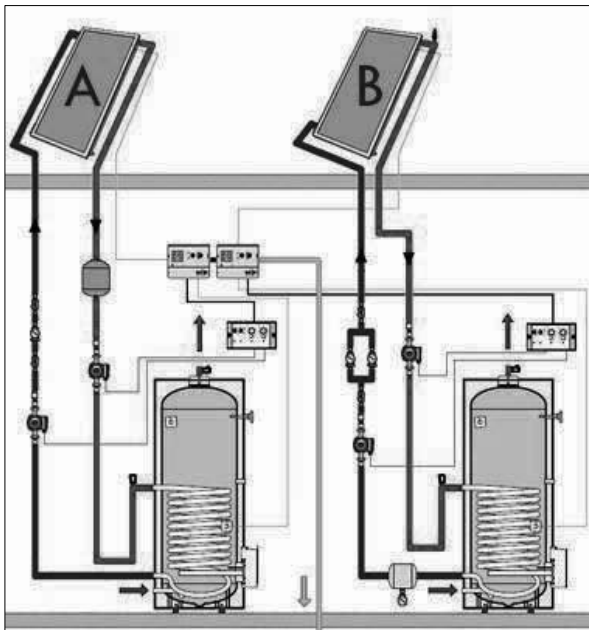
Figure 11
Sun collector measurement system

Parts of the sun collector measurement system:
- sun collectors

- heat exchanger tank (solar tank)
- insulated pipes
- expansion tank
- Drain-back tank
- circulating pump
- control unit
- calorimeters
- temperature sensors
- solar radiation meter
- OPC server
- Vision software

B   Measurements

We set the tilt angle of collector B to β_{year}=47.5˚ and kept it at the same angle during the measurements. We set the tilt angle of collector A to three values in each season. These values are the seasonal values which we determined, i.e.:

$$\beta_{summer} = 24˚$$
$$\beta_{winter} = 71˚$$
$$\beta_{autumn} = 47.5˚$$

During the measurements we measured the temperature and the mass flow of the liquids entering and leaving the sun collectors, the temperature of the solar tank, the amounts of heat carried off the solar tank as well as the data of the external atmosphere and solar radiation. During the measurements it was ensured that the temperatures and mass flows of the medium entering the collectors should be equal (T_{inA}= T_{inB}). As a result when evaluating the measurement results it is sufficient to compare the temperatures of the medium leaving the sun collectors (T_{outA}, T_{outB}). T_{outA}, T_{inA} are the temperatures of the medium exiting collector A, and T_{outB}, T_{inB} are the temperature of the medium exiting collector B. We made conclusions by comparing the exit temperatures. The computer system recorded all the measurement results in diagrams and tables. Figures 12-20 show the – typical – results of the measurements made in the different seasons in diagrams. The exit temperatures of the sun collectors (T_{outA}, T_{outB} i.e. T_{out}) are plotted as the vertical axis, and the measurement time of the measurement results recorded on the measurement day is plotted as the horizontal axis. The descriptions of the diagrams contain the tested tilt angles of the two collectors as: β_B/β_A.
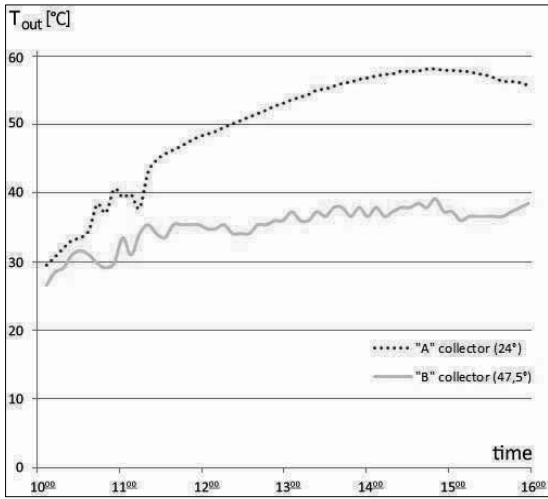
Figure 12
Summer 47.5°/24°
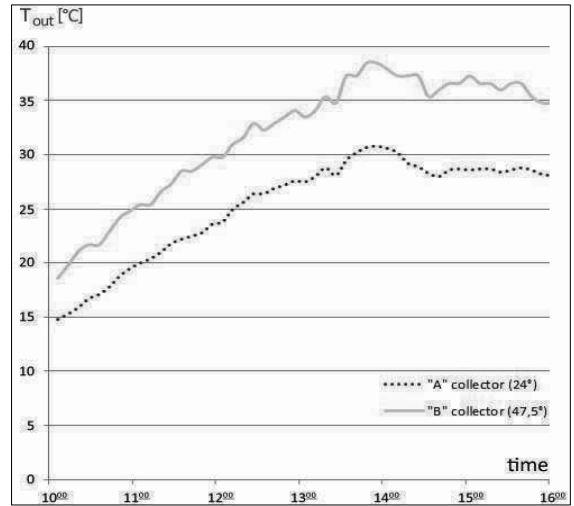
Figure 15
Autumn 47.5°/24°
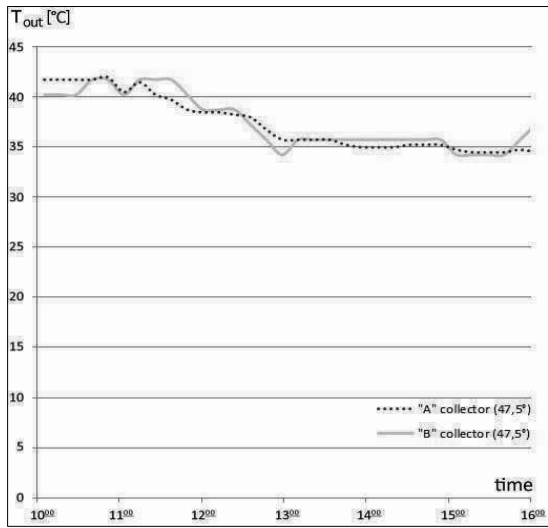
Figure 13
Summer 47.5°/47.5°
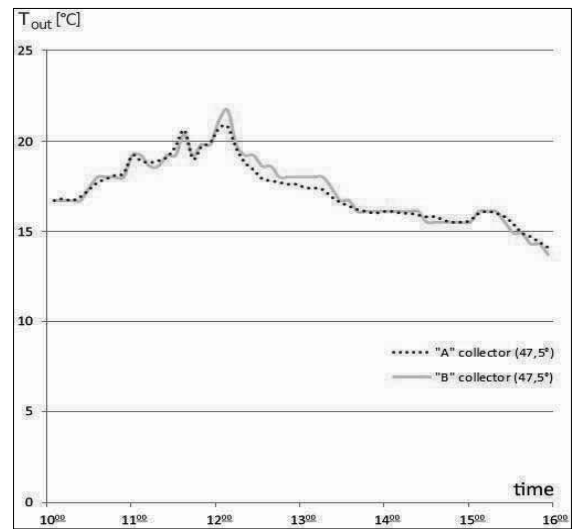
Figure 16
Autumn 47.5°/47.5°
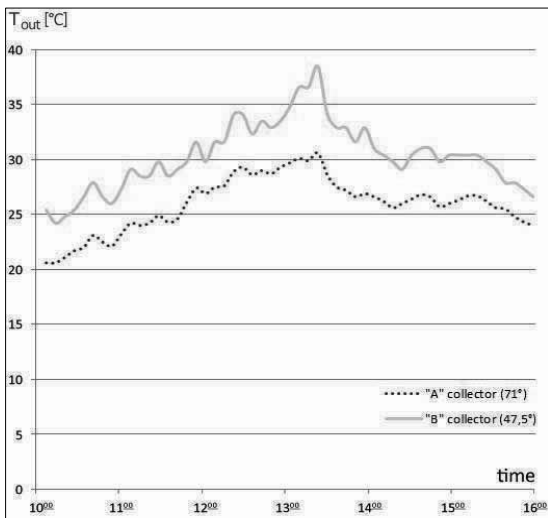
Figure 14
Summer 47.5°/71°
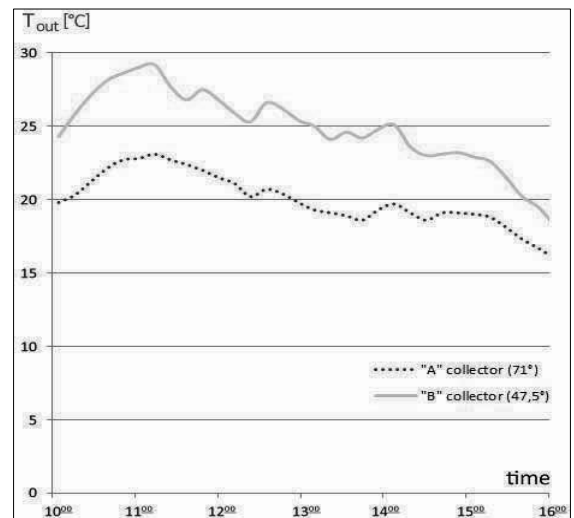
Figure 17
Autumn 47.5°/71°

26
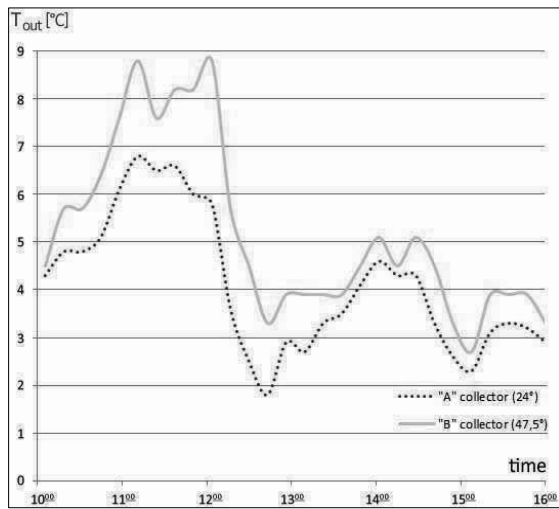
Figure 18
Winter 47.5°/24°
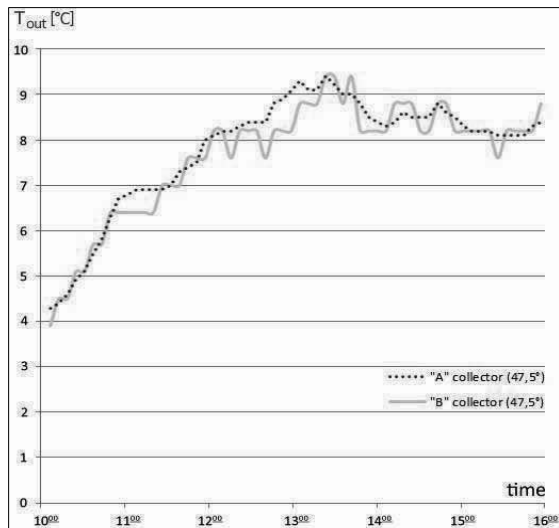
Figure 19
Winter 47.5°/47.5°
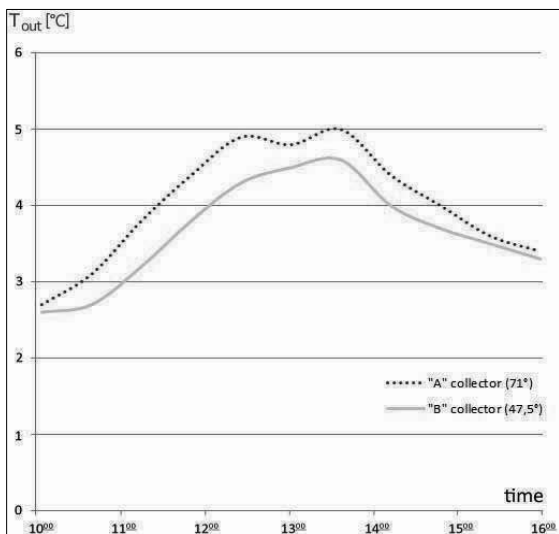
Figure 20
Winter 47.5°/71°

According to the previous chapters the value of entry temperatures of both sun collectors and the value of mass flows of the medium flowing through the collectors were the same during the measurements. In such cases if we want to compare the power of the collectors (P_A, P_B), it is sufficient to compare the temperatures of the medium leaving the sun collector (T_{outA}, T_{outB}) and after this, approximately:

$$\frac{P_A}{P_B} \approx \frac{T_{outA}}{T_{outB}} \tag{4}$$

For each of figures 12-20 we determined the average values of the relation of the exit temperatures (R_{TA}, R_{TB}) with the relevant deviations. The averages were determined with the below equation:

$$\frac{R_{T_A}}{R_{T_B}} = \frac{\sum_{i=1}^{n} \frac{T_{A_i}}{T_{B_i}}}{n} \cdot 100[\%] \tag{5}$$

where $T_A = T_{outA}$, $T_B = T_{outB}$.

If the above described conditions exist, the power relation of the two tested collectors should – approximately - equal the relations of the exit temperatures of the collectors, that is:

$$\frac{R_{P_A}}{R_{P_B}} \approx \frac{R_{T_A}}{R_{T_B}} \tag{6}$$

Where R_{PA}, R_{PB} are the average values of the power of the A and B collectors (P_A, P_B).

The determined power relations, tilt angle β_A of collector A (with modified tilt angle) and the deviation of the calculated temperature relations – according to the seasons – were given in Tables 1-3., where $R_{PA/PB} = R_{PA}/R_{PB}$.

Table 1
Summer, $\beta_B = 47.5°$

β_A [°]	$R_{PA/PB}$ [%]	Deviation
24	141	7,23
47.5	100	2,59
71	86	2,46

Table 2

β_A [°]	$R_{PA/PB}$ [%]	Deviation
24	80	1,55
47.5	100	1,83
71	81	3,37

Autumn, $\beta_B = 47.5°$
Table 3
Winter, $\beta_B = 47.5°$

β_A [°]	$R_{PA/PB}$ [%]	Deviation
24	80	5,54
47.5	102	4,12
71	110	5,49

Figures 21-23 were plotted from figures 12-20 and tables 1-3. These diagrams shows – approximately - the R $_{PA/PB}$ change of the power relation of collectors A and B at angles β_A and β_B=47.5°=constant value per season.
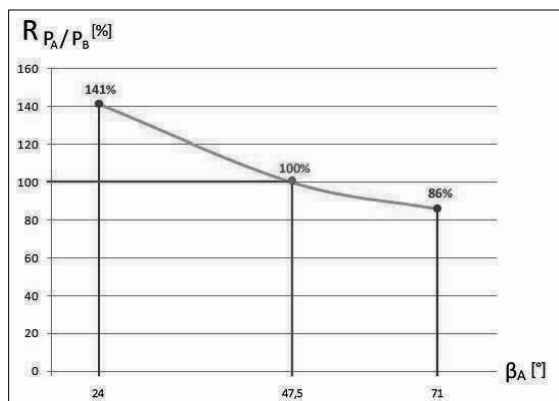
Figure 21
Power relations of collectors in summer, β_B= 47.5°
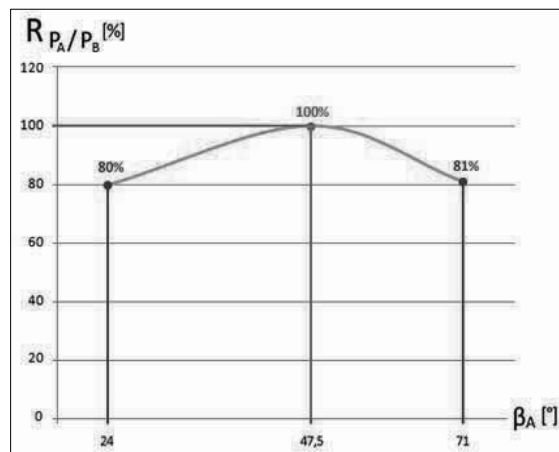
Figure 22
Power relations of collectors in autumn, β_B= 47.5°
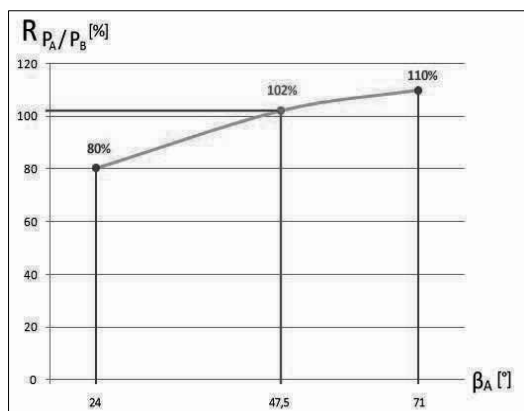
Figure 23
Power relations of collectors in winter, β_B= 47.5°

IV. CONCLUSION

Considering the efficient operation of sun collectors Óbuda University established a special measurement station capable of measuring the thermal characteristics of several sun collectors at the same time. Based on the laws of the Sun – Earth relative movement published in the specialist literature we determined the optimal tilt angle of the sun collectors at which the energy producing capability of the collector is optimal. In this way we determined a set-up angle for a whole year and the collector tilt angles for the four seasons (autumn, winter, spring, summer). Through laboratory measurements we confirmed our conclusions made theoretically. Our measurements made it clear that if the sun collector is not set at the right angle, the power of collector falls by up to 10-20%. Figures 21-23 graphically depict this decrease in power due to improper tilt angles. If the tilt angle of the sun collector is not modified during the year, the power of the collector in summer – when the possibility of energy transformation is the best – is up to 20-30% less than the optimal value. In spring and autumn the operation and energy producing capability of the sun collector is optimal at this tilt angle ($\beta r = \phi = 47.5°$).

For the measurements we used a special sun collector developed by the we, whose construction cost is lower compared to the commercial sun collectors available in Hungary. In the future we find it necessary to repeat our measurements under more precise circumstances, with more tilt angles and at least four collectors in parallel. We hope that those results will give us more accurate information how to modify the tilt angles of sun collectors.

V. REFERENCES

[1] Solar Energy Technology Handbook, New York,1980.
[2] J. Duffie, W. Beckman: Solar Energy Thermal Processes, New York,1980.
[3] A. F. Veneruso: Tracking Angles and Rates for Single Degree of Freedom Solar Collectors, Sandia Labs, March 1976.
[4] Patkó I.: Megújuló energiák integrálása a hazai energiarendszerbe, különös tekintettel a napenergia termikus hasznosítására, MTA előadás, Magyar Műszaki Értelmiség Napja, 2010. 05.
[5] ESTI F.: Statisztikai jelentés, Brüsszel 2009. május
[6] Patkó I.: Környezettechnika I., Egyetemi jegyzet 2004.
[7] Patkó I.: Megújuló energiák, Egyetemi jegyzet Budapest, 2009.
[8] Barótfi I.: Környezettechnikai kézikönyv, Budapest, 2006.
[9] Pikó I.: Thesis
[10] The American Ephemeris and Nautical Almanac, for the year 1978, U.S. Government Printing Office,Washington, D.C., 1976
[11] I.F. Hand, „Charts to Obtain Solar Altitudes and Azimuths," Heating and Ventilating, October 1978m pp. 86-88.
[12] DOE Facilities Solar Design Handbook, U.S. Department of Energy report DOE /AD-0006/1, January 1978.
[13] G. O. G. Lof, „Systems for Space Heating with Solar Energy," Chapter XII. in R. C. Jordan and B. Y. H. Liu, eds., Applications of Solar Energy for Heating and Cooling of Buildings, ASHRAE GRP 170, 1977.

Application of Thermopile Technology in the Automotive Industry

A. Zachár [*], I. Farkas[*], A, Szente[**], M. Kálmán[***] and P. Odry[****]

[*] College of Dunaújváros/Computer Engineering, Dunaújváros, Hungary
[**] Paks Nuklear Power Plant, Paks, Hungary
[***] University of Pécs/Electrical Engineering, Pécs Hungary
[****] Polytechnic of Subotica/Electrical Engineering, Szabadka, Serbia
zachar.andras@gek.szie.hu, imka26@gmail.com, szentea@npp.hu, kalmanmathe@yahoo.com, odry@appl-dsp.com

Abstract— Thermopile technology presents solution for energy reuse in vehicles driven by internal combustion engine. Utilization of this energy reduces consumption of the diesel fuel because it eliminates need for the generator used for battery charging. In this case battery charging is performed with electric energy produced by the thermopile generator. If this technology continues to evolve, in not so distant future it will be possible to reduce fuel consumption up to 10% which would count as significant reduction. This article gives clear overview of the current tendencies in this area.

I.   INTRODUCTION

Thermoelectric generators (TEG) could be used in the near future in many industrial applications ranging from solar energy applications and automotive industry to nuclear power production and several other fields of engineering. Application of thermoelectric generators to recover wasted heat from the exhaust system of an automobile could be a promising utilization of the thermoelectric technology to improve the efficiency of an internal combustion engine. Currently this area is a rapidly evolving segment of the application of TEG technology.

Thermoelectric generators (TEGs) allow direct conversion of heat energy to electricity without any moving parts and have advantages such as durability and maintenance-free and noiseless operation.

The thermoelectric generator is a semiconductor device which is governed by the following physical effects that describe the heat flow inside a thermoelectric generator. These are the Seebeck effect, Fourier effect, Joule effect and the Thomson effect. Generally the simplest mathematical description of the energy conservation of a TEG element can be modeled by one dimensional heat transfer and electrical current flow process.

Zorbas *et al.* [1] developed a model for the evaluation of the performance of a thermoelectric generator. The developed model takes into account the thermal contact resistant effect and also the thermal resistance of the applied ceramic plates of the TEG. The model has been applied to describe the behavior of a commercial TEG which has been tested in an exhaust system of a gasoline engine. Carmo *et al.* [2] presents a characterization of thermoelectric generators by measuring the load

dependent behavior. The investigation has been carried out for modest temperature differences ($\Delta T <= 51$). Waste heat recovery of a low cost thermoelectric generator for a stove investigated by Nuwayhid *et al.* [3]. They have studied an alternative electric power supply from a wood or petroleum heated stove in regions where the constant electric power supply cannot be achieved. F. Meng *et al.* [4] developed a complete numerical model with inner and external multi-irreversibilities of commercial thermoelectric generator in which physical properties, geometric dimensions, and flow parameters are all considered. It has been concluded that the main loss among the losses caused by inner effects is the Fourier heat leakage. The impact of the Thomson effect has been investigated by Chen *et al.* [5]. The thermal behavior and cooling power of three different TECMs have been investigated numerically with the aim to recognize the performance of miniature TEC in the presence\absence of Thomson effect.

Currently the following semiconductor material pairs have been investigated most widely, these are the BiTe, PbTe and SiGe semiconductor materials which can be operated efficiently in different temperature range. Higher the temperature more efficient the TEG device to produce electricity but there is an upper temperature limit where the materials melt. Table I. contains the approximate upper limit temperature and the thermal efficiency of the semiconductor material pairs by Schaevitz [10].

TABLE I.

TEMPERATURE UPPER LIMIT AND THE THERMAL EFFICIENCY OF THE SEMICONDUCTOR MATERIAL PAIRS [10]

Material pair	Temperature limit [ºC]	Efficiency [%]
BiTe	300	6
PbTe	600	9
SiGe	1100	11.5

In addition to this the approximate temperature distribution of an exhaust system of automobiles are needed to calculate a good estimation of the electrical power harvested by thermoelectric generators. Temperature of the different location of the exhaust system has been measured by Gonzales [6] to test the ignition capability of different diesel engine driven

vehicles for forest fuels. Characteristic temperatures have been measured at different locations of the exhaust system which is significantly differs from a common gasoline engine driven vehicle.

The aim of this study is to present a comparison of the efficiency of different commercially available TEG modules applying in the exhaust system of different diesel or gasoline engine automobile.

Table II contains the studied thermoelectric modules. These modules are commercially available with modest price. Table II shows the geometric dimension of the TEG modules, the maximum tested temperature differences between the cold and hot side of the TEG, and the produced maximum electrical power.

TABLE II.
THERMOELECTRIC MODULES OF THEM COMMERCIAL USE
[1, 2, 3]

Module name	Dimensions	ΔT [^{o}C]	P_{max} [W]
TEC1-12707	40 mm x 40 mm	51	0.5
TEC1-12708	40 mm x 40 mm	68	0.85
Melcor HT9-3-25 Bi2Te3 N=31	25 mm x 25 mm	190	2.5
		61	0.4
Melcor HT6-12-40 Bi2Te3	40 mm x 40 mm	68	0.75

II. TEMPERATURE DISTRIBUTION OF TYPICAL EXHAUST SYSTEMS

Recent progress in thermoelectric device technology has revealed the possibility of practical large-scale TEGs and various applications such as vehicles and microelectronic devices.

This is especially interesting with the vehicles on diesel drive like cars and boats. Application of the thermopile technology reduces overall diesel consumption. By applying the thermopile technology it is possible to cover energy costs for eg light and computer systems etc. This way it isn't necessary to use the diesel generator because dissipated thermo energy can be converted to electricity.

The four following potential sources are recoverable by a thermoelectric generator on a long-haul truck Diesel engine [7]:

– Coolant water (between 90_C and 110_C);
– Exhaust gases (between 250_C and 350_C, Fig. 1b);
– Exhaust gas recirculation (EGR) gases (between 400_C and 500_C, Fig. 1a);
– Charge air cooler outlet gases (CAC) (usually around 150_C).

Exergy calculations show that the most energy can be extracted from exhaust gases. Despite the lower exhaust gas temperature (due to temperature loss in the turbocompressor) compared with the EGR temperature, exhaust gases exhibit a higher mass flow rate, which increases their exergy (available recovery).

Figure 1 shows the structure of the Exhaust system in one diesel drive car, with marked points of the thermo energy dissipation area like Diesel Oxidizing Catalyst, Diesel Particulate Filter and Exhaust Cooler.

This construction allows effective application of the thermopile technology on larger surface.

Thermoelectric generators utilizing as a source of heat the exhaust gas from internal combustion engines mounted in vehicles, primarily automobiles, are well known. It should be noted, however, that the requirements imposed on such generators are rather complex and diverse. They must be compact, lightweight, and able to endure heavy vibration during transport. Furthermore, thermoelectric generators for such applications must operate efficiently in different engine operating modes, which entails additional difficulties.

The use of thermoelectric materials in vehicular engines for wasted heat recovery, can help considerably in the world need for energy saving and reduction of pollutants.

The allocated power and the temperatures that prevail in the exhaust pipe of an intermediate size car are satisfactory enough for the efficient application of a thermoelectric device. The most advisable place appears to be precisely after the catalyst, where high temperatures prevail. The output power and the efficiency of the device depend on the operational situation of the engine and on the effective designing of the heat exchanger.

Each TE element experiences a small temperature difference, so that greater surface area will improve performance. As the system is fully scalable and modular, different layouts can be designed for specific needs such as optimized electrical output, power density, and size. Heat pipes are one solution for carriage of heat to TEMs, providing a large heating area that can support many modules.

Figure 1. An approximate temperature distribution of a gasoline fueled automobile (BMW 318i) with two different operating modes

The temperature distribution of the exhaust system of the automobiles depends on the engine type. An approximate temperature distribution of a gasoline fueled automobile (BMW 318i) with two different operating modes (full and a usual or averaged load) can be seen in Figure 2 from qualitative point of view the temperature of the exhaust system is monotonically decreasing along the exhaust pipe from the engine toward the tail of the pipe.
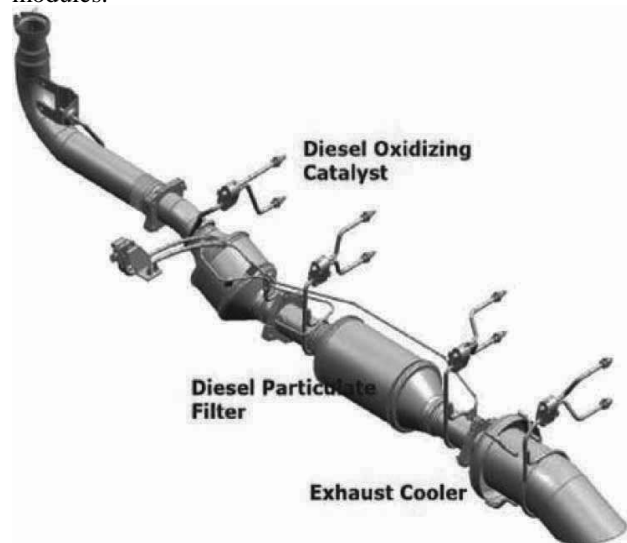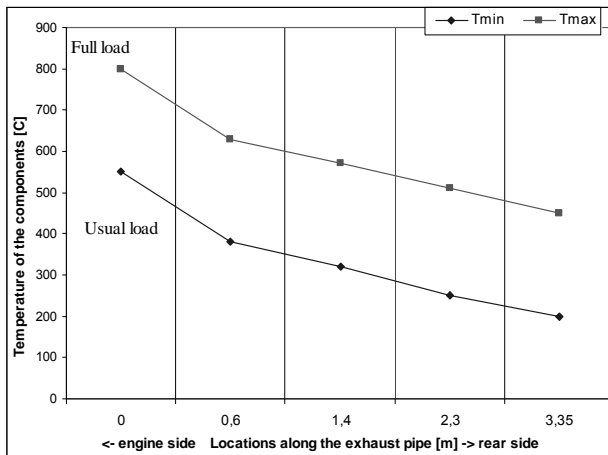
Figure 2. An approximate temperature distribution of a gasoline fueled automobile (BMW 318i) with two different operating modes

The temperature distribution of a diesel engine automobile is different compared to a gasoline fueled automobile because of the additional equipments (Diesel Particulate Filter DPF, Diesel Oxidizing Catalyst DOC). On smaller vehicles the DPF should be active (additionally fueled) equipment which further increases the temperature of the exhaust system around and after the DPF. Generally the highest temperatures occurred after the DPF [6]. This information is important to designers to specify the best location of the TEG modules to convert as much wasted heat as possible to electricity. Table III shows the typical surface temperature [°C] of the components of an exhaust system of smaller sized diesel engine trucks and the assumed average contact surface area [m²] to transfer heat from the different components of the exhaust system toward the TEG modules.

TABLE III.
TEMPERATURE DISTRIBUTION OF THE EXHAUST SYSTEM [6]

Location	Ford	Dodge	Sterling	GMC	Area
Diesel Particulate Filter DPF	295	168	196	307	0.3
After DPF	375	300	293	446	0.1
Before DOC	231	193	241	435	0.1
Diesel Oxidizing Catalyst DOC	356	218	228	308	0.2

It can be clearly seen from Figure 3 that the generated electrical power is strongly depend on the location of the thermocouples because the temperature of the exhaust system is varying along the different components.

In the same operating environment the TEG modules give a slightly better performance in case of electrical power production than the other modules. But the reliability of the modules have not been tested which is also an important factor of the practical applications.

III. CONCLUSION

In the same operating environment the Melcor modules give a slightly better performance in case of electrical power production than the other modules. But

the reliability of the modules have not been tested which is also an important factor of the practical applications.

The data presented in the tables clearly indicates that even with today's thermopile technology we have means to cover part of the electrical consumption in automobiles. On the other hand, at present it is only justified to use the thermopile technology in the vehicles with greater fuel consumption. With further development of the new types of the TEG converters it will became more and more economical to install the thermopile technology in the vehicles with small diesel consumption.
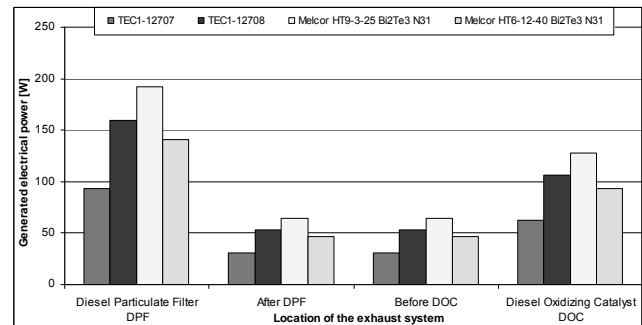
Figure 3. The influence of the position TEG generator on the amount of the generated electrical power

REFERENCES

[1] 1. K. T. Zorbas, E. Hatzikraniotis, K. M. Paraskevopoulos, Power and efficiency calculation in commercial TEG and application in wasted heat recovery in automobile.

[2] 2. J.P. Carmo, J. Antunes, M.F. Silva, J.F. Riberio, L.M. Goncalves, J.H. Correia, Characterization of thermoelectric generators by measuring the load-dependence behavior, *Measurement* 44, (2011), 2194-2199.

[3] 3. R.Y. Nuwayhid, D.M. Rowe, G. Min, Low cost stove-top thermoelectric generator for regions with unreliable electricity supply, Renewable Energy 28, (2003), 205-222.

[4] 4. Fankai Meng, Lingen Chen, Fengrui Sun, Numerical model and comparative investigation of a thermoelectric generator with multi-irreversibilities, *Energy*, 36, (2011) 3513-3522.

[5] 5. Wei-Hsin Chen, Chen-Yeh Liao, Chen-I Hung, A numerical study on the performance of miniature thermoelectric cooler affected by Thomson effect, Applied Energy, 89, (2012) 464-473.

[6] 6. Ralph H. Gonzales, Diesel exhaust emission system temperature test, San Dimas Technology & Development Center, San Dimas, California, December 2008.

[7] N.ESPINOSA, M.LAZARD, L.AIXALA, H.SCHERRER: "Modeling a Thermoelectric Generator Applied to Diesel Automotive Heat Recovery" Journal of ELECTRONIC MATERIALS, Vol. 39, No. 9, 2010 pp: 1446-1455

[8] MOLAN LI, SHAOHUI XU, QIANG CHEN, LI-RONG ZHENG: "Thermoelectric-Generator-Based DC–DC Conversion Networks for Automotive Applications" Journal of ELECTRONIC MATERIALS, Vol. 40, No. 5, 2011, pp: 1136-1143

[9] HIROSHI NAGAYOSHI, TATSUYA NAKABAYASHI, HIROSHI MAIWA, TAKENOBU KAJIKAWA: "Development of 100-W High-Efficiency MPPT Power Conditioner and Evaluation of TEG System with Battery Load" Journal of ELECTRONIC MATERIALS, Vol. 40, No. 5, 2011 pp: 657-661

[10] S. B. Schaevitz, A MEMS Thermoelectric generators, Master Thesis, MIT, September 2000.

AMTEC Solar Space/Terrestrial Power Generation and Wireless Energy Transmission – How Far Is The Realization?

M.S. Todorović[*], Z. Civrić[**] and O. E. Djurić[***]

[*] University of Belgrade, Serbia and Southeast University, Nanjing China
[**]Museum of Science and Technology, Belgrade, Serbia
[***] University of Belgrade, Serbia
deresmt@eunet.rs, zorica.civric@gmail.com, nera@agrif.bg.ac.rs

Abstract— In this paper hybridization and cogeneration with concentrated solar radiation (CSR) technology coupled a) with alkali metal thermoelectric conversion (AMTEC) and b) with combined AMTEC-steam power cycles (AMTEC/SPC) has been studied. Thermodynamic models of combined CSR - AMTEC system and CSR - AMTEC/SPC for the cogeneration of electric and thermal energy, using hybridization of solar and fossil fuels, has been analyzed. Parametric system analysis has been performed taking in account radiative - reflective losses and thermal energy losses by thermal radiation, convection and conduction. Finally, a program, defined to evaluate the commercial applications of these emerging hybrid solar technologies is presented. Program includes the evaluation of case studies as possible sites for commercial hybrid solar energy utilization.

I. INTRODUCTION

Victor Hugo's famous sentence "*There is nothing more powerful than an idea whose time has come*" may challenge the question "*Solar Space/Terrestrial Power Generation and Wireless Energy Transmission – How far is the realization; and is the Earth energy sustainability really reachable*? Paper entitled "Elements of the Concept of Sustainability in the Works of Nikola Tesla" /10/ examines practical results and theoretical issues that Tesla dealt with and that could be attributed to the concept of sustainability more than 100 years ago.

Tesla`s patents and most important articles related to energy were analyzed in search for ideas on sustainability: technology – energy transformation and transmission, renewable sources, coal technologies, metal processing, electric vehicles, turbines, environment – the integrated "whole" of planetary and human systems, forests and fresh water, production of ozone, society – human needs, behavior and health /10/.

The role of Tesla's scientific contribution becomes more important from the perspective of contemporary energy standpoint, in the context of the need for sustainable development, as well as in the context of sustainable science /10/. For Tesla the Sun is the main source that drives everything, it follows that we should promote ways of getting more energy from the Sun. Tesla distinguishes a form of Sun energy obtained from burning materials like coal, wood, oil, from a form of Sun energy that is contained in the water, wind and ambient.

Today, in the world substantial natural renewable energy comes from hydropower sources, and a much smaller amount from geothermal power; however, these are still only a modest fraction of the total. In addition, a wide variety of Sun's energy technologies – including photovoltaic arrays, fuel cells, and wind turbines – have been applied on Earth during the past several decades in newer renewable energy systems. Expectations is that full commercialization and spreading of use of these renewable "green" energy technologies can make substantial contributions to meeting long-term energy challenges faced by the global economy. However, these technologies can not provide the huge amounts of new and sustainable energy that will be needed in the coming decades of 21st century. Similar technologies applied in extraterrestrial space exposed to the extraterrestrial solar radiation, may be, could provide quantitatively and qualitatively (exergetic higher) more sustainable energy to Earth.

Hence, it is crucial for the world to research, develop, demonstrate, commercialize and deploy more affordable and more sustainable Sun's energy utilization technology – solar space power generation. Notwithstanding optimistic claims to the contrary, it does not appear that there is at present a solution to these concurrent challenges. AMTEC Solar Space/Terrestrial Power Generation and Wireless Energy Transmission could be a solution. Thus, we came to the crucial statement Nikola Tesla made more than 100 years ago: "Besides progress toward discovering different ways of solar energy transformation, the next progress in history was the discovery of ways to transfer energy from one place to another without transmitting the material which is source of energy." Tesla suggested that the transfer of power over long distances as we know, based on his invention, are to be replaced by wireless transmission whose principles and methods he had also developed more than 100 years ago.

In the late 1960s, Dr. Peter Glaser of Arthur D. Little invented technically a fundamentally new solar approach to global energy /11/: the Solar Power Satellite (SPS). The basic concept of the SPS is as follows: a large platform, positioned in space in a high Earth orbit continuously collects and converts solar energy into electricity. This power is then used to drive a wireless power transmission (WPT) system that transmits the solar energy to receivers on Earth. Because of its immunity to

nighttime, to weather or to the changing seasons, the SPS concept has the potential to achieve much greater energy efficiency than ground based solar power systems (in terms of utilization of fixed capacity) /12/.

II. PRESTIGIOUS CONCENTRATED SOLAR RADIATION TECHNOLOGY

Solar technologies are maturing and new opportunities are emerging due to continuing improvements in designs. Concentrated solar radiation (CSR) technologies, combining less-expensive optical components with small area, highly efficient, and somewhat more expensive devices to achieve low cost, in general, are on the threshold of significant development

The stretched membrane concentrator cluster and innovative cavity - heart type high temperature receiver focally positioned present attractive solution for thermal power and photo-thermal applications – second award at the DOE and Southern California Edison Solar Two Challenge Design competition 1994 KU Lawrence team (/4/, Fig.1). Concentrated solar radiation transmitted by the receiver's cover and adjacent liquid is absorbed by the absorber which has a black nonselective coating and is with its integrated liquid passages immersed directly inside the circulating stream of liquid /4/. Highly specularlly reflective internal skin of receiver walls reduces the complex of radiative, conductive and convective heat losses and results in a more efficient alternative to highly insulated receiver enclosures.

Figure 1. Stretched membrane concentrator cluster and focally positioned high temperature receiver.

The receiver's instantaneous thermal efficiency is equal to the ratio of heat supplied to the receiver's working fluid and used for the sodium evaporation and its isothermal expansion q_{krf} versus the incident concentrated solar radiation flux q:

$$\eta = \frac{q_{krf}}{q} = 1 - \sum_{k=1}^{m} q_g / q \tag{1}$$

where q_g presents receiver's total heat losses - reflective, radiative, convective and conductive. The concentrated solar radiation energy flux incident in the receiver's plane is a function of the concentrator field area A_g covered by heliostats $A_h = \phi \cdot A_g = \phi \cdot CR \cdot A_p$, is given as:

$$q = I_b \cdot \phi \cdot CR_e \cdot A_p \cdot \rho \cdot r \quad (W) \tag{2}$$

where I_b, CR_e, ρ and r intensity of incident direct solar radiation, effective concentration factor, heliostats field efficiency and its mirror reflectance, respectively.

Steady-state energy flux losses can be expressed as a sum of reflective radiation losses and heat-transfer losses:

$$q_g = q_r + q_{tg} \tag{3}$$

Radiative losses are given as.

$$q_z = \varepsilon \cdot \sigma \cdot A_p \cdot \left(T_z^4 - T_a^4\right) \quad (W) \tag{4}$$

Convective q_{kon} and conductive losses q_{pr} are::

$$q_{kon} + q_{pr} = A_z \, (h + k_z / \delta_z) \cdot (T_z - T_a) \tag{5}$$

where the receiver's wall temperature, ambient temperature, receiver wall surface area, wall thickness, thermal conductivity and convective heat transfer coefficient are denoted by T_a, T_z, , A_z, δ_z, , k_z, and h respectively. Thus total heat transfer losses are

$$q_g = q_z + q_{kon} + q_{pr} = \varepsilon \cdot \sigma \cdot A_p \cdot \left(T_z^4 - T_a^4\right) + A_z \left(h + k_z / \delta_z\right) \cdot \left(T_z - T_a\right) \tag{6}$$

a)

b)
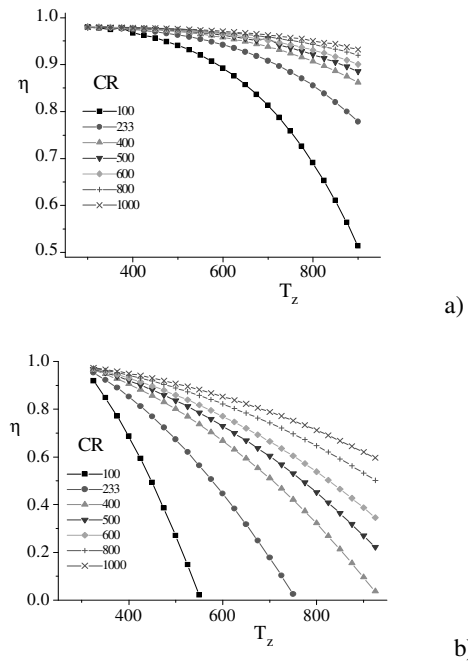
Figure. 2. Receiver's heat losses (a - radiative losses, b - total heat losses) dependence on solar radiation concentration factor and the receiver's temperature.

Solar radiation concentration factor and temperature influence on receiver's simultaneous short and long wave radiative, convective and conductive heat transfer losses are presented on diagrams in Figure 2.
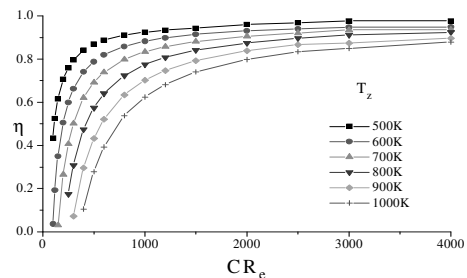
Fig. 3 Dependence of the instantaneous thermal efficiency on the effective concentration factor and receivers wall surface temperature.

33

More directly, the kind of efficiency dependence on the solar radiation concentration factor illustrates the diagram given in the Figure 3.

III ALKALI METAL THERMOELECTRIC CONVERSION

The Alkali Metal Thermo-Electric Conversion (AMTEC) (1, 6) a very prospective (2-5) solution for a high performance power generation became recently a subject of our interest (4, 5). The key element of an AMTEC device is the β alumina solid electrolytte (BASE) which conducts positive sodium ions much better than sodium atoms or electrons (Figure 4).
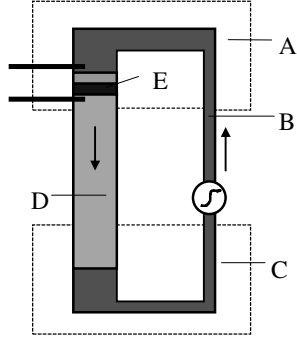
Figure 4 Scheme of alkali-metal-thermo-electric conversion system: A - Heat source T_2, B - Liquid sodium, C - Heat sink, D - Sodium vapor, E - Beta-alumina solid electrolyte

A sodium pressure difference across a thin BASE sheet drives sodium ions from the high pressure side to the low pressure side. Thus positive sodium ions accumulate on the low pressure side, and electrons collect on the high pressure side, resulting in an electrical potential. By the appropriate electrode use, this electrical potential can be utilized and an electrical current can be driven through a load.

Liquid sodium in upper part is maintained at the temperature T_2 (900 to 1300K) by the heat supply from an external heat source (concentrated solar radiation). The lower part containing condensing sodium vapor and liquid sodium, is in contact with heat sink at the temperature T_1 (400 to 800K). The thermodynamic cycle equivalent to an the reversible AMTEC process is given in Figure 5.
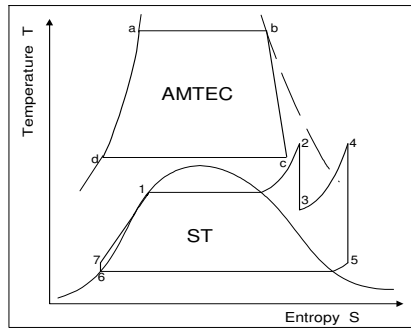
Figure 5. The thermodynamic cycle equivalent to the reversible AMTEC process and binary AMTEC/SPC.cycle.

Thus, BASE presents a mean of converting mechanical energy, related to the established pressure difference, into electrical energy - equivalent to the chemical potential conversion in an electrical potential difference. More accurate study shows that the AMTEC process is more complex interaction of a variety of irreversible transport processes, kinetically governed at the electrode interfaces by the BASE material's specific features. The BASE process described as an isothermal expansion of sodium from pressure p_2 to p_1 at the temperature T_2.

Mechanically AMTEC can be described as a simple system without moving parts, except a liquid sodium pump. Assuming that the sodium vapor can be represented as an ideal gas and employing the Clausius-Clapeyron equation, the instantaneous efficiency of the reversible AMTEC process can be expresses as follows:

$$\zeta = \frac{W_A}{q_{krf}} = \frac{W_1 - W_2}{L_2 + q_2 + q_3} = \frac{(T_2 - T_1)/T_2}{(T_2 - T_1)/T_2 [1 + C_p T_1 / L] + T_1/T_2}$$

(7)

where is W_1 is the maximum work obtained by isothermal expansion of gas from pressure p_2 to p_1 at temperature T_2, L_2 is the heat of vaporization at T_2, q_2 is the heat absorbed during isothermal expansion, and by q_3 is denoted the enthalpy difference of liquid between T_2 and T_1.

IV CONCENTRATED SOLAR RADIATION TECHNOLOGY - AMTEC AND BINARY CSR - AMTEC CYCLE

The combined CSR-AMTEC system thermal efficiency can be expressed by the product of CSR receivers thermal efficiency and the reversible AMTEC process efficiency ($\eta_u = \eta \cdot \zeta$) by the equation:

$$\eta_u = \eta \cdot \zeta = \left(1 - \frac{q_r + q_z + q_{kon} + q_{pr}}{I_b \cdot \phi \cdot CR \cdot A_p \cdot r}\right) \cdot \frac{(T_2 T_1)/T_2}{(T_2 - T_1)/T_2 [1 + C_p T_1 / L] + T_1/T_2}$$

(8)

The instantaneous thermal efficiency of the binary CSR - AMTEC/SPC cycle, which has been defined as the combination of the CSR - AMTEC cycle and the steam power cycle can be determined as below:

$$\eta_{BC_u} = \eta \cdot \eta_{BC}$$

(9)

$$\eta_{RCC} = \frac{W_{RCC}}{q_{RCC}} \quad ; \quad q_{RCC} = q_{AO}$$

(10)

$$\eta_{BC} = \frac{W_A + W_{RCC}}{q_{krf}} = \frac{\xi \cdot q_{krf} + \eta_{RCC} \cdot q_{AO}}{q_{krf}} = \xi + \eta_{RCC} \cdot \frac{q_{AO}}{q_{krf}}$$

where the steam power cycle efficiency, steam power cycle technical work, AMTEC cycle technical work, and the heat rejected by AMTEC are respectively denoted by η_{RCC}, W_{RCC}, q_{AO}.

The results of conducted thermodynamic analysis are very impressive. The obtained values of the relevant thermal efficiencies of CSR - AMTEC and CSR - AMTEC/SPC (Figure 7) processes given in Figures 6 and 8 are significantly higher than the corresponding values of any conventional power plant in existence today (calculated for the steam power reheat cycle - superheated vapor temperature of 450^0C, condensation temperature of 150^0C, and with the SPRC efficiency of 36%).

This fact clearly justifies R&D efforts to be increased in the field of relevant fundamental, applied and engineering areas.

Figure 6. The dependence *of* the combined CSR - AMTEC cycle thermal efficiency on the effective solar radiation concentration factor, vapor temperatures and condenser temperature.
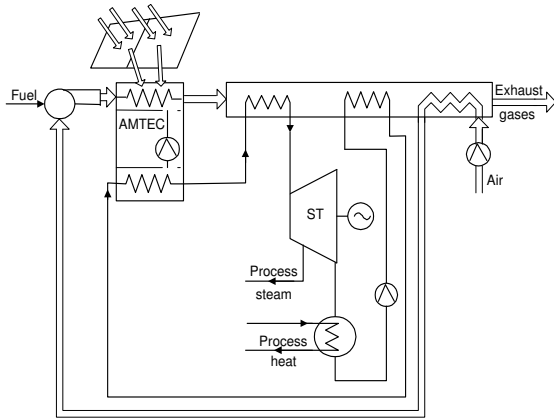
Figure 7. Scheme of the hybrid binary CSR - AMTEC/SPC system for the cogeneration of electrical and thermal energy.
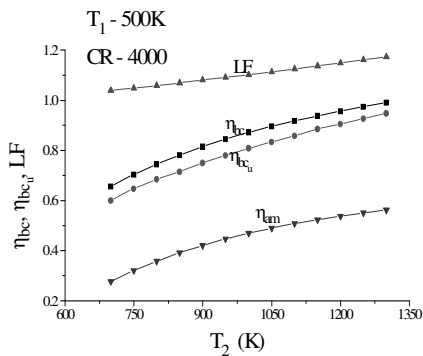
Figure 8. The dependence of the thermal efficiencies of CSR - AMTEC and CSR - AMTEC/SPC processes on the temperature T_2

V HYBRIDIZATION AND SOLAR SPACE/TERRESTRIAL AMTEC TECHNOLOGY DEVELOPMENT

For spreading the use of solar energy today is mandatory to have fully dispatch-able systems. The best way to do this nowadays is by hybridization with natural gas or oil. In particular both near- and mid-term applications are foreseen for different hybrid solar systems. Such systems, especially those based on concentrated solar radiation conversion technologies are much more competitive and better suited for many diverse applications and emerging international markets than mono-type technologies. Scheme of the hybrid combined. CSR - AMTEC/SPC system given on Figure 7 is ideal for the cogeneration of electrical and thermal energy. For example the binary cycle efficiencies given in Figure 8 are obtained for the steam power cycle condenser temperature of 150^0C - the temperature level which can be utilized even as process heat or in district heating systems.

A review of current local conditions confirms that the technical expertise is appropriate and partly necessary technologies (including concentrated radiation technologies and PV) are available but financial situation and economy status present serious barriers and do not favor promotion of new programs neither in manufacturing and energy engineering nor investment generally. However demand side managed decentralized energy production and integration of RES in local energy structure shall be seen as an option which can contribute to improve basic energy supply and living conditions coupled with the creation of small-scale industry providing labor and hindering migration to urban centers. In addition to the possible impact on decentralized energy production development, combined hybrid solar CSR - AMTEC systems applications include as very prospective generally autonomous systems (for example electricity for the self powered convective solar dryers - Figure 9).
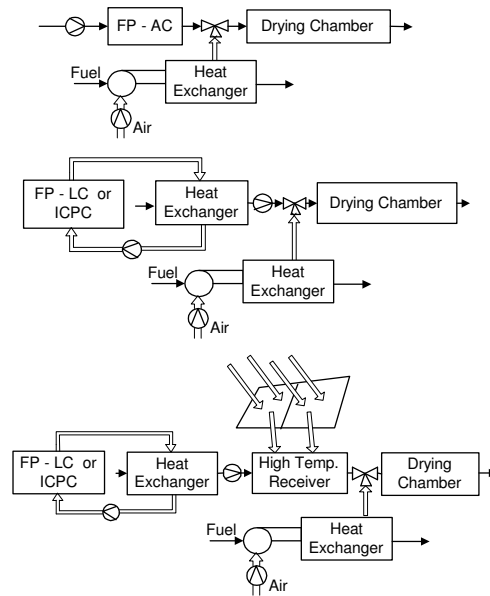
Figure 9. Schemes of convective solar dryers which become self powered and controlled - by the addition of CSR - AMTEC units.

Solar space AMTEC power system concept integrated with advanced global positioning system satellites was

developed by Johnson *et al.* /23/. Its main component were two symmetric generators which contain parabolic concentrator/reflector units and solar receivers which were designed to produce sufficient electric power from the absorbed solar radiation, and the advanced multi-tube vapor anode AMTEC cell with 24% conversion efficiency.

The system integration and performance analysis result showed that the solar AMTEC power system can be a very good option for space energy generation and that the size of the solar AMTEC system was much smaller than that of a solar-PV array and its mass also could be competitive with that of the PV/battery power system /23/. In addition, the solar AMTEC system could be more robust and stable. Therefore, a solar AMTEC power system could be very attractive for space energy generation. However study /23/ did address space power production and space vehicle energy supply, and not generating energy transmission to the Earth.

Theoretical design optimization of a radial AMTEC cell design parameter was analyzed by Hendricks and Huang, /24/ with an aim to establish optimum design parameters and achieve better cell performance for high-power space mission requirements. The design parameter analysis showed that cell efficiency could increase dramatically, with strictly controlled parasitic losses and introduced larger area BASE tubes, concluding that a much higher system power could be achieved from the optimum efficiency designs than the maximum power-per-BASE-area designs, and in the same time could reduce cell cost and complexity /24/.

Apart from independent direct solar thermal power generation methods, cascade systems which combine several power generation methods to obtain higher power output were also widely studied./19/. Cascade systems can have significantly higher efficiency and consequently much higher electric power output. However, different stages must match well, especially their temperature levels, what is important to be considered for the system design optimization.

For example, as the thermionic converter has a very high reject temperature which is very near the input temperature for an AMTEC, it is appropriate to achieve higher power output by cascading these two types of converters. In paper /19/ has been shown that the efficiency of the Cs–Ba thermionic-AMTEC system could be 7%–8% higher than that of the Cs–Ba thermionic-thermoelectric cascade system. Hence, a high temperature Cs–Ba thermionic-AMTEC cascade system can be very attractive for solar thermal power generation and would allow the development of a highly efficient, compact power system

For the solar AMTEC program further development and its effective technical feasibility - reliable and cost-effective solutions have to be searched encompassing as more as possible accurate investigation of demand diversity and storage capacities focusing on modular units from small to medium size engine capacities, around 1 – 20 MW capacity.

As the conclusions concerning solar-AMTEC technology following R&D needs can be outlined:

a. Thermodynamic study of innovative combined and cascade cycles/systems.

b. Fundamental heat transfer research on different AMTEC systems, relevant materials and structures.

c. Engineering investigation, development and standardization of related technical systems and components.

d. Case studies: loads profiles, storage, cogeneration and hybridization related dynamics.

e. Optimization under various policy/rate scenarios including the dispatch optimization and related generalized procedure.

In addition, concluding the solar AMTEC development R&D needs is to be stated, that the detailed analysis of all known direct solar thermal power generation technologies, conducted by Yue-Guang Deng and Jing /19/ determined solar AMTEC as the most advantageous comparing it with thermoelectric, magnetohydrodynamic, and thermionic. In order to materialize its enormous potential, and to make full use of its advantages, according to /19/ considered are to be aspects which are essentially more precise definitions of specific research tasks of the above given items *b*. and *c*. as follows:

- "Optimizing structure design and reducing system heat radiation and conductive loss as much as possible;

- Seeking for excellent electrode materials and better fabrication techniques for porous metal electrode, so as to improve the output current density and reduce the polarization effect of electrodes;

- Substituting sodium with kalium as the working fluid under certain conditions however, proper system design and suitable working conditions are very important because some problems, such as dryout in the evaporator wick, could more easily happen for kalium-based AMTEC; and

- Raising the temperature of the AMTEC high-temperature side however, the temperature should not be too high since the degradation of the electrode material would happen under a high temperature".

VI SPACE SOLAR POWER GENERATION AND TRANSMISSION

The most recent document on the status of space solar power generation and transmission is presented in August 2011 entitled "**T**he first international assessment of space solar power opportunities, issues and potential pathways forward" by the International Academy of Astronautics /12/.

Solar Power Satellite (SPS) was described by American scientist Peter Glaser in his inventive US patent in 1973. His method was based on transmitting power over long distances (from space to Earth's surface) using microwaves from a very large antenna (up to one square kilometer) on the satellite to a much larger one, now known as a rectenna on the ground. (Illustration shown in Fig. 10). Because of its immunity to nighttime, to weather or to the changing seasons, the SPS concept has the potential to achieve much greater energy efficiency than ground based solar power systems (in terms of utilization of fixed capacity).
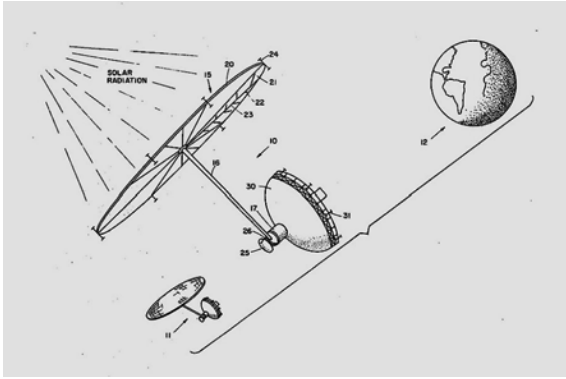
Figure 10. . SPS Concept illustration - 1973 US Patent No. 5019768.

The SPS concept has been the subject of numerous national systems studies and technology development efforts from 1970 to 2010 (included efforts in the US, Canada and Europe, as well as steady technology R&D in Japan, and more recent activities in China and India /12/. Because significant advances in space solar power could have profound benefits for human and robotic space exploration capabilities as well as other space applications, the study /12/ also identified such opportunities and evaluated the potential for synergies between these benefits for space missions and space solar power for terrestrial markets /12/.

Three highly promising SPS platform concepts were examined by the IAA study /12/. All three examined cases were geostationary Earth orbit-based SPS concepts; these were /12/:

- An updated version of the microwave wireless power transmission (WPT) 1979 SPS Reference System concept, involving large discrete structures (e.g., solar array, transmitter, etc.) assembled by a separate facility in space;

- Modular electric/diode array laser WPT SPS concept, involving self assembling solar power-laser-thermal modules of intermediate scale; and

- Extremely modular microwave WPT SPS "sandwich structure" concept, involving a large number of very small solar power-microwave-thermal modules that would be robotically assembled on orbit.

A few alternative space solar power (SSP) concepts were also identified but not analyzed /12/ (low Earth orbit-based "Sun Tower" SPS concept, lunar solar power, etc).

Papers (/16/-/22/) present insight in, and development overview of the advanced space/terrestrial power generation device: AMTEC.

An AMTEC converter was under development for use in the AMTEC Radioisotope Power System (ARPS) program (collaboration between DOE and NASA) /22/. Program goal was to develop the new generation of thermal to electric power conversion systems for use in deep space probes. The advantageous AMTEC feature for space operation is that it has no moving parts. By the radioisotope powered AMTEC produces electric energy through the interaction of its two main components: the radioactive heat source (fuel and containment) and the thermoelectric generator. Radioactive material used for fuel spontaneously disintegrates into a different atomic form dissipating - producing heat, which AMTEC converts into electricity. The prime system contractor was Lockheed Martin Corporation, with Advanced Modular Power Systems, Inc. (AMPS) responsible for the development of the AMTEC converter /22/.

The most recent development of space solar power technologies reviews Japanese paper /13/, and earlier reviews of all relevant known technologies present papers (/17/, /19/-/21/). Particularly important papers relevant for the wireless transmission of space "produced energy" to Earth are those treating broad spectral range of energy-waves transmission methods and technologies as /14/, /15/, /16/ and /18/.

Recognizing the spin-off impact of new technologies, especially those space-based as solar power, China recently unveiled a plan to build and orbit a solar power station for commercial use by 2040 /19/. The Chinese plan drawn by one of its space pioneers Wang Xiji is an ambitious one and aims to look at various aspects of space-based solar power applications, designs and key technologies which could make the option economically feasible in the first instance and sustainable by 2020.

Detailing the research conducted by the China Academy of Sciences, Wang said /19/ at the fourth China Energy Environment Summit Forum:"The development of solar power station in space will fundamentally change the way in which people exploit and obtain power. Whoever takes the lead in the development and utilization of clean and renewable energy and the space and aviation industry will be the world leader."

While China's lead in the SBSP could provide for a co-operative framework in Asia, there lies a strong imperative also for India and other particularly growing economies endangered with energy shortages to come together and realize the SBSP utilization dream.

Other countries like Japan have also done considerable research in this field. Japan's Aerospace Exploration Agency has done decade-long research on SBSP in collaboration with high-end technological companies such as Mitsubishi. Collaboration among these countries would also facilitate funding for this ambitious project.

The actual beginning of the realization of the SBSP is associated with the further development of the existing space and wireless industry, development of related new branches that will emerge from current SBSP research and that must support the continuing survival of SBSP and corresponding issues of energy and environmental security.

VII WIRELESS ENERGY TRANSISSION STATUS

Approaching concluding remarks of this study, we reviewed conclusions of the study /12/ relevant to the wireless energy transmission (WET) technology.

The report /12/ is the most recent comprehensive document presenting status of the WET or WPT (wireless power transmission) technology. Prepared implementing readiness and risk assessment methodology it used as the relevant indicators on the technology maturity and risk following quantities:

- Technology Readiness Levels (TRLs), and

- Research and Development Degree of Difficult (R&D3) Scale.

Key technologies for the primary WET or WPT system options identified are:

- Electron tube RF generating devices (such as magnetrons, gyrotrons, TWTs, etc.);
- Solid state radio frequency (RF) generating devices (such as FET amplifiers); and
- Solid state laser generative devices (such as laser diode arrays).

Key technologies involved in solar power generation for future solar power satellite (SPS) platforms, in addition to different PV cell types include solar dynamic power conversion options (e.g., Sterling engines, Rankine Cycle engines, Brayton Cycle engines, etc.), However, presented study confirms the solar AMTEC highly advantageous features with the reference to the listed dynamic system as shown in /12/.

The major technology areas in the category of power management and distribution (PMAD) include: high voltage power cabling, modular/intelligent power conversion, and advanced power management options (e.g., superconductors).

Excluding the discussion of generic SPS or SES system architectures, final and after the WET the most crucial for the focused theme/question of this study are the Ground Energy and Interface Systems some of which are based on the primary WPT system options including: RF conversion via a rectenna, including both panel and mesh type rectennas; high-efficiency grid integration transformers, rolling energy storage systems, etc.

Proceeding, the summarized study /12/ results, we can agree with comment given, referring to it in "News, Views and Contacts from the global power industry" which was stating *"Giant leap for space-based solar - Solar power is entering into a space age thanks to the rocketing speed of technology development"* and further *"It' has been a mere 30 years since the first commercial solar plants were built on Earth - a short stint compared to the length of time fossil fuels have been meeting our global electricity needs - yet, the speed of technological development has allowed us to think realistically about orbiting these renewable energy structures in space, in the not too distant future /12/"*.

Yes, we can "think realistically about orbiting these renewable energy structures in space" but still there is a way to go to reach the whole and fully operational WET between Earth and Space as it had been searched and in a certain way visionary foreseen by Nikola Tesla.

To shorten that way, may be crucial would be to merge current R& D approaches more directly with the core of Tesla's intrinsic inventive ideas. Investigations in the field of high frequency alternating currents and wireless energy transmission Tesla started 120 years ago in 1890-1891. Proceeding unexpected behavior of these currents in comparison to low frequency alternating currents, supported by many experiments, Tesla gradually increased his conviction that these currents can be used for efficient illumination, in medicine and in wireless transmission of electrical energy. Later, discussing about the nature of electricity he said: *"I adhere to the idea that there is a thing which we have been in the habit of calling electricity. The question is ,What is that thing? Or, What, of all things, the existence of which we know, have we the best reason to call electricity? We know that it acts like an incompressible fluid; that there must be a constant quantity of it in nature; that it can be neither produced nor destroyed; ..."*

Finally, a partial answer to this paper title "AMTEC Solar Space/Terrestrial Power Generation and Wireless Energy Transmission – How Far Is The Realization?" referring its WET part could be "might be it would be closer if we would put efforts to activate reading of tens of thousands of Nikola Tesla's no yet read manuscripts stored in the cellar of the Nikola Tesla Museum in Belgrade."

REFERENCES

[1] Cole:"Thermoelectric Energy Conversion with Solid Electrolytes" Science, Vol. 221, No 4614, pp. 915-920, 1983.

[2] Sasakawa, M. Kanzaka, A. Yamada, H Tsukuda: "Perfomance of the Terrestrial Power Generation Plant Using the Alkali Metal Thermo-Electric Conversion (AMTEC)", Proceedings of the 25th Intersociety Conversion Engineering Conference, Vol 3, pp 143-149, 1992.

[3] Sievers, F.J. Ivanenok and K.T. Hunt: "Alkali Metal Thermal to Electric Conversion", Mech. Engineering, Vol. 117, No 10, pp. 70-76, 1995.

[4] Todorovic M., F. Kosi: "Ekoenergo-tehnologije - novi sistemi pretvaranja energije za termoenergetiku i termotehniku", KGH, Vol. SMEITS 1996.

[5] Todorovic M., S. Mentus, O. Ecim and Lj. Simic: "Thermodynamic Analysis of Alkali Metal Thermoelectric Converters of Solar Radiation", Proceedinings of the Fifth International Conference Tesla - III Millennium, pp. IV-87-94., Belgrade, 1996.

[6] Weber: A Thermoelectric Device Based on Beta-Alumina Solid Electrolyte", Energy Convers. 14, No. 1, pp.1-8, 1974.

[7] Dan McCue: Japan continues to pursue dream of solar power harvested from space, http://www.renewableenergymagazine.com /energias/renovables/index/pag/pv_solar/colleft/colright/pv_solar/t ip/articulo/pagid/16323/botid/71/, July 2011.

[8] Aristeidis Karalis a,*, J.D. Joannopoulos b, Marin Soljacˇic, Efficient wireless non-radiative mid-range energy transfer, Annals of Physics 323, 2008.

[9] Mclinko, Ryan M., and Basant V. Sagar: Space-based solar power generation using a distributed network of satellites and methods for efficient space power transmission, International Conference on Space Information Technology 2009

[10] Zorica Civric: Elements of the Concept of Sustainability in the Works of Nikola Tesla, Proceedings ECOS Conference, Novi Sad, 2011.

[11] Glaser, Peter, Ph.D.; "Method and Apparatus for Converting Solar Radiation to Electrical Power." (US Patent No. 3,781,647; U.S. Patent and Trademark Office; Washington, D.C.) 25 December 1973.

[12] John C. Mankins, Nobuyuki Kaya: Space Solar Power - The first international assessment of space solar power opportunities, issues and potential pathways forward, Int. Academy of Astronautics., http://iaaweb.org/iaa/Studies/sg311_finalreport_solarpower.pdf., August, 2011.

[13] T. Narita, T. Kamiya, K. Suzuki, K. Anma, M. Niitsu and N. Fukuda: The Development of Space Solar Power System Technologies, Mitsubishi Heavy Industries Technical Review Vol. 48 No. 4, December 2011.

[14] A.Marinčić1, Z. Civrić, B. Milovanović: Nikola Tesla's Contributions to Radio Developments, Serbian Journal of Electrical Engineering, Vol. 3, No. 2, pp. 131-148, November 2006.

[15] Karalis, J.D. Joannopoulos b, M. Soljacic: Efficient wireless non-radiative mid-range energy transfer, Annals of Physics 323, pp. 34–48, 2008.

[16] Zoya B. Popović**:** Wireless Powering for Low-Power Distributed Sensors, Serbian Journal of Electrical Engineering, Vol. 3, No. 2, pp. 149-162, November 2006.

[17] Space-Based Solar Power As an Opportunity for Strategic Security, Phase 0 Architecture Feasibility Study Report to the Director, National Security Space Office Interim Assessment, Release 0.1, 2007, www.nss.org/settlement/ssp/library/nsso.htm

[18] Barathwaj. G1, Srinag. K: Wireless power Transmission of Space Based Solar Power, 2011 2nd International Conference on Environmental Science and Technology, IPCBEE vol.6 (2011) IACSIT Press, Singapore.

[19] Yue-Guang Deng and Jing Liu: Recent advances in direct solar thermal power generation, Journal of Renewable and Sustainable Energy **1**, 052701, 2009.

[20] Noam Lior: Power from Space, Energy Conversion and Management, pp. 1769-1805, 2001.

[21] M.A.K. Lodhi, P. Vijayaraghavan, A. Daloglu: An overview of advanced space/terrestrial power generation device: AMTEC, Journal of Power Sources 103, pp. 25-33, 2001.

[22] Joseph C. Giglio, Robert K. Sievers, Edward F. Mussi: Update of the Design of the AMTEC Converter for Use in AMTEC Radioisotope Power Systems, AIP Conf. Proc. 552, pp. 1047-1054, 2001.

[23] G. Johnson, M. E. Hunt, W. R. Determan, P. A. HoSang, J. Ivanenok, and M. Schuller, IEEE Aerosp. Electron. Syst., Mag. 12, 33 1997.

[24] T. J. Hendricks and C. D. Huang, J. Sol. Energy Eng. 122, 49, 2000.

Testing Heat Recovery Ventilation Units for Residential Buildings in Combination with Ground Heat Recovery

Mihály Baumann[*], **Dr.LászlóFülöp*, László Budulski*, Roland Schneider** student **

[*] PTE - Pollack Mihály Faculty of Engineering and Information Technology, University of Pécs, Hungary
** PTE - Pollack Mihály Faculty of Engineering and Information Technology
E-mail: baumann@pmmik.pte.hu, fulop@pmmik.pte.hu, budulskil@pmmik.pte.hu

The objective of the test is to carry out research regarding the possibilities of reducing energy consumption for ventilation with heat recovery and ground heat utilisation. The following operating modes of the residential building ventilationhave been tested: (1) ventilationunit operated in a direct fresh air mode, (2) ventilation unitoperated in combination with ground-air heat exchanger system, (3) ventilation unitand indirect ground-air heat exchanger system operated withwater ground collector and (4) with a ground probe. The comparison of the four ground heat utilising systems shows that thewater ground collector mode provides less heat gain than the air modes do, but its overall efficiency is the best among them. In addition we should note thatground heat recovery compared to pure heat recovery did not lead to significant energy savings in wintertime, but it played an important rolein summertime in terms of thermal comfort.

I. READINGS

The test roomis a single air space of 66m^{2}area with a volume of 175 m^3, in which the ventilation system described below was installed. Testing energy savings really makes sense at bigger differences in indoor and outdoor temperatures, so we performedour tests insuch a period.

We conducted measurements by NI FieldPoint measuring devices. The ventilation machine was HELIOS KWL EC 300.. R and HELIOS SEWT-W fitted with a heat exchanger module for the indirect ground-air heat exchange. The ground-air collector was a REHAUAwaductThermo system.

Hereby we present the results of the four modes of operation. The measurements were made and analysed in a 24-hour period. During the measurements there was no movement or any other factor that may have influenced the results.

01	room intake air	A	HELIOS KWL EC 300R
02	room extract air	B	HELIOS SEWT-W heater
03	extract air	C	HELIOS SEWT hydraulic unit
04	fresh air intake	D	Rehau ground-air system
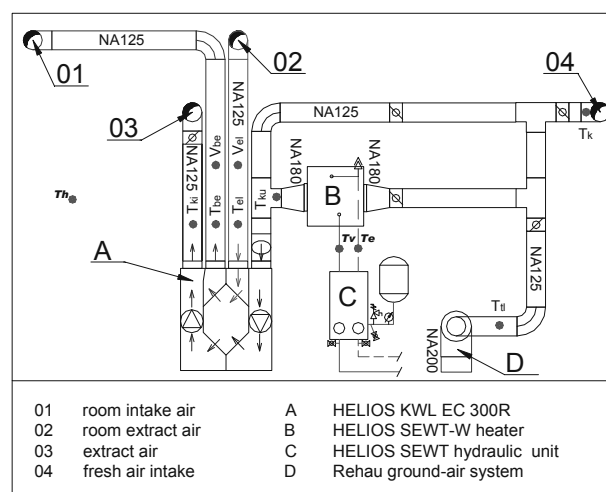
Figure 1. Block diagram of the system

A. Ventilationunit operated in a direct fresh air mode

Under this mode fresh air at its external temperature enters directly the ventilation device. Table I. shows such temperatures. The temperatures measured in the test room are graphically illustratedin Figure 2. asa functionof time.

TABLE I.
FRESH AIR OPERATION

	Minimum (05.12.2010 20:36)	Maximum (06.12.2010 10:47)	Average (05.12.2010 15:00 – 06.12.2010 15:00)
$t_{extract\ air}$	21.46°C	21.78°C	21.56°C
t_{room}	19.61°C	20.85°C	19.85°C
$t_{intake\ air}$	18.36°C	19.84°C	18.89°C
$t_{outgoing}$	10.99°C	15.43°C	12.60°C
$t_{external}$	0.60°C	10.93°C	3.87°C
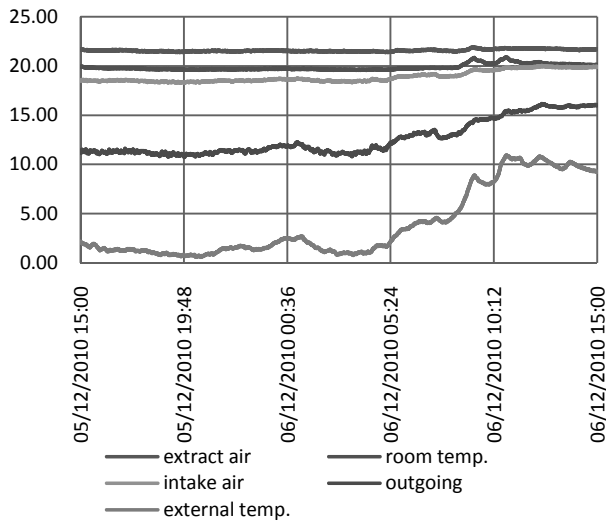
Figure 2. Changes in temperature under fresh air operation mode

Figure 3. Changes in temperature under ground-air collector operation mode

B. Operation of ventilation unit in combination with ground-air collector system

In this case the external air first flows through the ground-air collector. This ensures a certain degree of preheating, the values of which areshown in Table II.

TABLE II.
MODE OF OPERATION COMBINED WITH GROUND-AIR COLLECTOR

	Minimum (02.12.2010 5:11)	Maximum (02.12.2010 11:47)	Average (01.12.2010 16:00-02.12.2010 16:00)
$t_{extract\ air}$	21.44°C	22.27°C	21.67°C
t_{room}	19.93°C	21.06°C	20.06°C
$t_{outgoing}$	19.60°C	20.33°C	19.91°C
$t_{intake\ air}$	18.91°C	19.66°C	19.20°C
$t_{ground-air}$	11.17°C	12.32°C	12.03°C
$t_{external}$	2.05°C	7.56°C	3.93°C

C. Operation of ventilation unitrun by an indirect ground-air heat exchanger system, complemented by water ground collector

In this case a heat exchanger helps the water ground collector to indirectly pass on heat to incoming external fresh air. (Table III.)

TABLE III.
INDIRECT, WATER GROUND COLLECTOR OPERATION

	Minimum (11.12.2010 7:27)	Maximum (10.12.2010 14:35)	Average (10.12.2010 14:00-11.12.2010 14:00)
$t_{extract\ air}$	21.46°C	21.76°C	21.61°C
t_{room}	19.68°C	20.83°C	20.25°C
$t_{intake\ air}$	19.53°C	20.11°C	19.82°C
$t_{outgoing}$	14.71°C	16.09°C	15.40°C
t_{flow}	9.62°C	10.83°C	10.22°C
t_{return}	8.56°C	10.29°C	9.42°C
$t_{post\ heat\ exchanger}$	7.05°C	9.01°C	8.03°C
$t_{external}$	-2.26°C	4.50°C	1.12°C

41
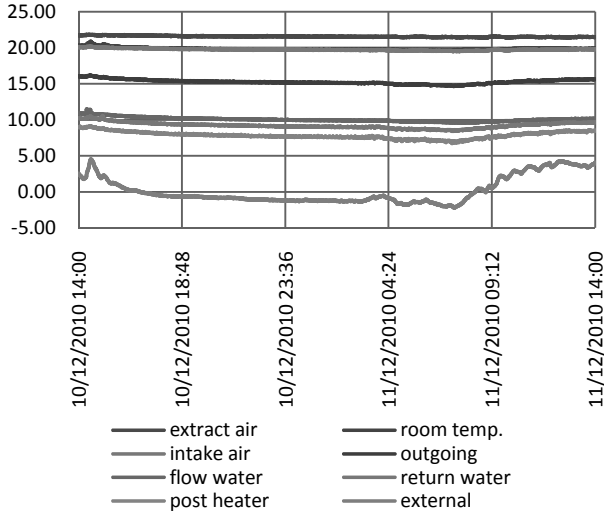
Figure 4. Changes in temperature under indirect, waterground collector operation

Figure 5. Changes in temperature under indirect, ground probe operation

D. Operation of ventilation unitrun by an indirect ground-air heat exchanger system, complemented by ground probe

In this casea ground probe helps the heat exchanger to indirectly pass on heat to incoming external fresh air. (Table IV.)

TABLE IV.
INDIRECT, GROUND PROBE OPERATION

	Minimum (04.12.2010 2:57)	Maximum (04.12.2010 13:05)	Average (03.12.2010 17:29-04.12.2010 17:29)
$t_{extract\ air}$	21.34°C	22.13°C	21.49°C
t_{room}	19.66°C	21.36°C	20.07°C
$t_{outgoing}$	19.40°C	20.32°C	19.62°C
$t_{intake\ air}$	18.60°C	19.50°C	18.82°C
t_{flow}	14.17°C	14.85°C	14.26°C
t_{return}	12.63°C	13.52°C	12.89°C
$t_{post\ heat\ exchanger}$	11.38°C	12.34°C	11.65°C
$t_{external}$	0.51°C	9.66°C	3.17°C

II. ANALYSIS OF READINGS

A. Ventilationunit operated in a direct fresh air mode

Efficiency calculated in line with mean readings:

$$\eta_{total\ average} = \frac{t_{intake\ av.} - t_{outgoing\ av.}}{t_{extract\ av.} - t_{external\ av.}}$$

$$\eta_{total\ av.} = \frac{18.89 - 3.87}{21.56 - 3.87} = 84.9\%$$

Heat saved:

$$v_{extract} = 6.4\frac{m}{s}$$

$$v_{intake} = 6.0\frac{m}{s}$$

$$A_{duct} = \frac{d^2 \cdot \pi}{4} = \frac{0.125^2 \cdot \pi}{4} = 0.0123 m^2$$

$$\rho_0 = 1.293\left[\frac{kg}{m^3}\right]$$

$$c_{air} = 1.012\frac{kJ}{kg \cdot K}$$

$$\dot{V}_{intake} = A_{duct} \cdot v_{intake} = 0.0123 m^2 \cdot 6.0\frac{m}{s}$$

$$= 0.0738\frac{m^3}{s} = 265.7\frac{m^3}{h}$$

$$\rho_{19°C} = \rho_0 \cdot \frac{T_0}{T} = 1.293\frac{kg}{m^3} \cdot \frac{273K}{292K} = 1.209\frac{kg}{m^3}$$

$$\dot{m}_{intake} = \dot{V}_{intake} \cdot \rho_{19°C} = 0.0738 \frac{m^3}{s} \cdot 1.209 \frac{kg}{m^3}$$

$$= 0.0892 \frac{kg}{s}$$

$$Q_{total\ heat-up} = \dot{m}_{intake} \cdot c_p \cdot (t_{extract\ av.} - t_{external\ av.})$$

$$=$$

$$= 0.0892 \frac{kg}{s} \cdot 1.012 \frac{kJ}{kg \cdot K} \cdot (21.56°C - 3.87°C) =$$

$$= 1.597 \frac{kJ}{s} = 1.597 kW$$

$$Q_{total} = Q_{total\ heat-up} \cdot \eta_{total\ av.} = 1.597 kW \cdot 84.9\% =$$

$$= 1.356 kW$$

B. Operation of ventilation unit in combination with ground-air collector system

Efficiency calculated in line with mean readings:

$$\eta_{total\ av.} = \frac{t_{intake\ av.} - t_{external\ av.}}{t_{extract\ av.} - t_{external\ av.}} =$$

$$= \frac{19.20 - 3.93}{21.67 - 3.93} = 86.1\%$$

Distribution of total efficiency between ground collector and heat recovery unit:

$$ground\ collector = \frac{t_{ground-air\ av.} - t_{external\ av.}}{t_{extract\ av.} - t_{external\ av..}} =$$
$$= \frac{12.03 - 3.93}{21.67 - 3.93} = 45.7\%$$

$$heat\ recovery\ unit = \frac{t_{intake\ av.} - t_{ground-air\ av.}}{t_{extract\ av.} - t_{external\ av.}} =$$
$$= \frac{19.20 - 12.03}{21.67 - 3.93} = 40.4\%$$

$$\Bigg\} =$$

$$= 86.1\%$$

Efficiency of heat recovery unit:

$$\eta_{heat\ recovery} = \frac{t_{intake\ av.} - t_{ground-air\ av.}}{t_{extract\ av.} - t_{ground-air\ av.}} =$$

$$= \frac{19.20 - 12.03}{21.67 - 12.03} = 74.4\%$$

Heat saved:

$$v_{extract} = 5.8 \frac{m}{s}$$

$$v_{intake} = 5.8 \frac{m}{s}$$

$$\dot{V}_{intake} = A_{duct} \cdot v = 0.0123 m^2 \cdot 6.0 \frac{m}{s} = 0.0713 \frac{m^3}{s}$$

$$\rho_{19°C} = \rho_0 \cdot \frac{T_0}{T} = 1.293 \frac{kg}{m^3} \cdot \frac{273K}{292K} = 1.209 \frac{kg}{m^3}$$

$$\dot{m}_{intake} = \dot{V}_{intake} \cdot \rho_{19°C} = 0.0713 \frac{m^3}{s} \cdot 1.209 \frac{kg}{m^3}$$

$$= 0.0862 \frac{kg}{s}$$

$$Q_{total\ heat-up} = \dot{m}_{intake} \cdot c_p \cdot (t_{extract\ av.} - t_{external\ av.})$$

$$=$$

$$= 0.0862 \frac{kg}{s} \cdot 1.012 \frac{kJ}{kg \cdot K} \cdot (21.67°C - 3.93°C) =$$

$$= 1.548 \frac{kJ}{s} = 1.548 kW$$

$$Q_{total} = Q_{total\ heat-up} \cdot \eta_{total\ av.} = 1.548 kW \cdot 86.1\% =$$

$$= 1.333 kW$$

C. Operation of ventilation unit run by an indirect ground-air heat exchanger system, complemented by water ground collector

Efficiency calculated in line with mean readings:

$$\eta_{total\ av.} = \frac{t_{intake\ av.} - t_{external\ av.}}{t_{extract\ av.} - t_{external\ av.}} = \frac{19.82 - 1.12}{21.61 - 1.12}$$
$$= 91.3\%$$

Distribution of total efficiency between ground collector and heat recovery unit:

$$ground\ collector = \frac{t_{post\ heat\ exchanger\ av.} - t_{external\ av.}}{t_{extract\ av.} - t_{external\ av.}} =$$
$$= \frac{8.03 - 1.12}{21.61 - 1.12} = 33.7\%$$

$$heat\ recovery\ unit = \frac{t_{intake\ av.} - t_{post\ heat\ exchanger\ av.}}{t_{extract\ av.} - t_{external\ av.}} =$$
$$= \frac{19.82 - 8.03}{21.61 - 1.12} = 57.6\%$$

$$\Bigg\}$$

$$=$$

$$= 91.3\%$$

Efficiency of heat recovery unit:

$$\eta_{heat\ recovery} = \frac{t_{intake\ av.} - t_{post\ heat\ exchanger\ av.}}{t_{extract\ av.} - t_{post\ heat\ exchanger\ av.}} =$$

$$= \frac{19.82 - 8.03}{21.61 - 8.03} = 86.8\ \%$$

$$v_{extract} = 6.3 \frac{m}{s}$$

$$v_{intake} = 5.6 \frac{m}{s}$$

Heat saved:

$$\dot{V}_{intake} = A_{duct} \cdot v = 0.0123 m^2 \cdot 5.6 \frac{m}{s} = 0.0688 \frac{m^3}{s}$$

$$\rho_{20°C} = \rho_0 \cdot \frac{T_0}{T} = 1.293 \frac{kg}{m^3} \cdot \frac{273K}{293K} = 1.205 \frac{kg}{m^3}$$

$$\dot{m}_{intake} = \dot{V}_{intake} \cdot \rho_{20°C} = 0.0688 \frac{m^3}{s} \cdot 1.205 \frac{kg}{m^3}$$

$$= 0.0829 \frac{kg}{s}$$

$$Q_{total\ heat-up} = \dot{m}_{intake} \cdot c_p \cdot (t_{extract\ av.} - t_{external\ av.})$$
$$=$$
$$= 0.0829 \frac{kg}{s} \cdot 1.012 \frac{kJ}{kg \cdot K} \cdot (21.61°C - 1.12°C) =$$

$$= 1.719 \frac{kJ}{s} = 1.719 kW$$

$$Q_{total} = Q_{total\ heat-up} \cdot \eta_{total\ av.} = 1.719 kW \cdot 91.3\% =$$

$$= 1.569 kW$$

D. Operation of ventilation unitrun by an indirect ground-air heat exchanger system, complemented by ground probe

Efficiency calculated in line with mean readings:

$$\left.\begin{array}{l} ground\ probe = 46.3\% \\ heat\ recovery\ unit = 39.1\% \end{array}\right\} = 85.4\%$$

$$\eta_{heat\ recovery}\ 72.9\%$$

Heat saved:

$$Q_{total\ heat-up} = 1.542 kW$$

$$Q_{total} = 1.317 kW$$

III. MEASUREMENT RESULTS

Measurements cannot be considered exact as the timing of the measurements made under the four different modes of operation was not simultaneous. Measurements were conducted in wintertime. The difference in external and internal temperatures was the biggest in case D, when the ventilation unit was run by an indirect ground-air heat exchanger system complemented by ground probe, and this was the case when the highest efficiency was achieved.

The summary of operation modes reveals that no matter what heat recovery system is applied in combination with

the ventilation unit, the input energy saving is minimal.Consequently, if we only use the inner heat exchanger of the ventilation unit, we can practically save the same amount of energy as in the cases of combining it with the above-mentioned heat recovery systems. From an energy saving point of view thus it makes no sense combining it with complementary systems in wintertime. (Figure 6.)

It may be an advantage though that in order to prevent the heat exchanger from freezing, such complementary systems can perform the function of preheating, without any additional energy need.

TABLE V.
SUMMARY

	average external temp. (°C)	Total efficiency (%)	preheating/ efficiency of heat recovery(%)
fresh air	3.87	84.9	00.0 / 84.9
air-ground collector	3.93	86.1	45.7 / 40.4
water ground collector	1.12	91.3	33.7 / 57.6
ground probe	3.17	85.4	46.3 / 39.1

- heat loss
- heat gain of preheating
- heat gain of heat recovery
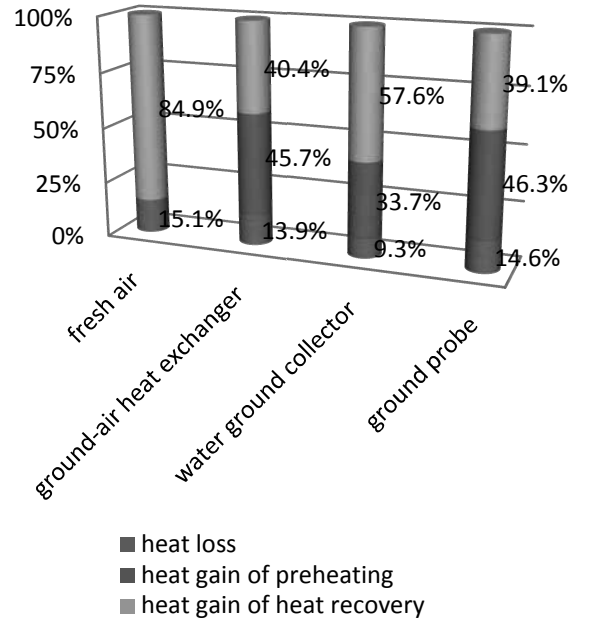
Figure 6. Comparison of systems

IV. CHARACTERISTICS OF GROUND-AIR HEAT EXCHANGER

During our measurements we examined the ground-air heat exchanger mode, as one of the possible solutions. Its

44

use may be advantageous not only in wintertime preheating, but also in summertime cooling. Figure 7.illustrates performance changes of a ground heat exchanger: it well depicts changes in performance as a function of external temperature. When external temperature is higher than the desired room temperature, the system cools the air flow, i.e.it simultaneously heats ground structure. Conversely, when the external air temperature is lower than that of the room, then the air flowis warmed up and the ground structure is regenerated, cooled.
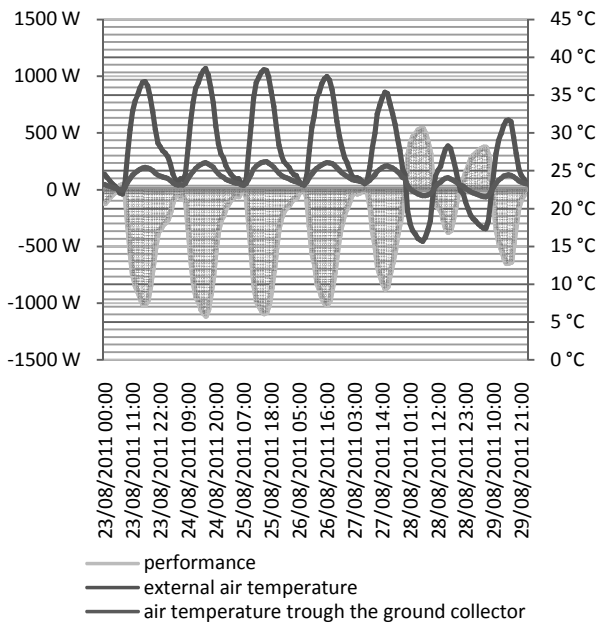
Figure 7. Performance of ground-air heat exchanger in relation to changes in external air temperature

Our measurements also revealed it that within 1.5…2weeks overheating sets in, which can be regenerated in the casedepicted in Figure 7., though it rarely occurs in summertime.

Another artificial regeneration method is illustrated in Figure 8. In this case the ventilation unit directly intakes cooler external air at night. During this period the ground-air collector is artificially ventilatedregardless of the ventilation unit, i.e. it is not involved in the ventilation of the room. In the daytime operation then, somewhat regenerated, it can again to some extent perform its pre-cooling function to a certain extent.
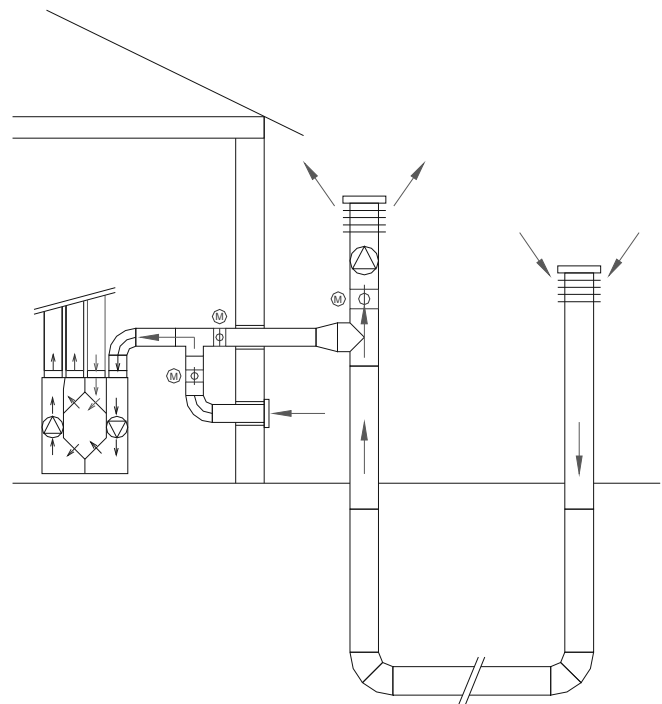
Figure 8. The artificial regeneration of the ground-air heat exchanger and the operation of the ventilation unit at night time

REFERENCES

[1] Roland Schneider, "Helios lakásszellőztetőmérése"thesis, PTE-PMMIK,*Pécs*, 2011.

[2] Gábor Loch, " Lakóépületekkontrolláltszellőzése" thesis, PTE-PMMIK, *Pécs*, 2012.

[3] "Helios KWL® rendszerek" catalogue, Kamleithner Budapest Kft., Budapest 2011.

[4] LászlóGarbaiDr., LászlóBánhidiDr., "Hőátvitel - Azépületgépészeiésipariberendezésekben",MűegyetemiKiadó, *Budapest*, 2001.

[5] "Energiatudatoslakásszellőztetés", Magyar Épületgépészet 2010/1-2.

Evaluation of a Wind Turbine with Savonius-Type Rotor

N. Burány* and A. Zachár**

* Subotica Tech, Subotica, Serbia; burany.nandor@gmail.com,
** College of Dunaújváros, Dunaújváros, Hungary; Zachar.Andras@gek.szie.hu

Abstract—**A wind turbine with a patented Savonius-type rotor is built and tested under different loading conditions and wind velocities. The turbine is modeled and simulated in a computational fluid dynamics software. Measurement and simulation results are discussed. Turbine modifications for achieving higher torque and power coefficient are suggested and analyzed.**

I. INTRODUCTION

Wind and sun are the most promising renewable energy sources concerning availability and concentration [1]. In urban areas solar energy is preferred, in other areas wind energy conversion is more suitable. Even, significant efforts are made to use the lower velocity and turbulent wind, typical in urban areas. There are many patent documents [2] describing wind turbines applicable in turbulent winds as they do not require re-orienting the turbine according to the wind direction. Mainly these turbines are some derivatives of the well known Savonius rotor [3]. Unfortunately the patent files usually do not report about the torque and power coefficients of these constructions or the reports are not based on thorough measurements and calculations. Sometimes it is purely believed that the preferred embodiment of the patent gives optimum results.

The aim of this paper is to propagate the evaluation of different turbine shapes by use of computational fluid dynamic (CFD) modeling and analysis. Analytical modeling of turbines is difficult even in 2D cases. Fortunately, today there are sophisticated software tools which can analyze the turbine operation with much less effort. This way numerous constructions could be evaluated and optimized in a short time. Even some new ideas can be tested.

II. MODEL OVERVIEW

The turbine construction reported in US patent 5,494,407 [2] by Benesh is modeled and analyzed through this research. The horizontal cross sectional drawing of the turbine is shown in Fig. 1. It is stated by the patent holder that the turbine will generate maximum power for some special ratios of the diameter to other dimensions of the rotor, given in the patent document.

The construction built by the authors shown in Figure 2. includes two turbines on the same axis, rotated relative to one another for 90°, to achieve less pulsation of torque. The blade height for both turbines is the same, 0.9 m, the diameter is $D_1=1.3$ m, so the effective vertical cross section area of the turbine is $A=2.34\ m^2$.
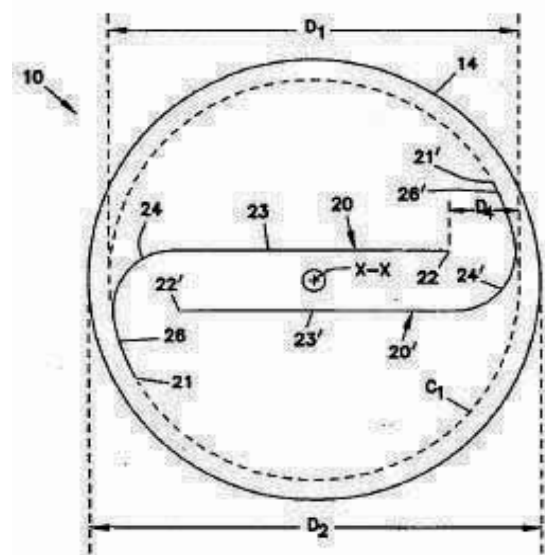
Figure 1. Cross sectional drawing of the patented Savonius-type wind turbine [2].

The total power of the wind [4] with velocity v on cross section A is given by formula:

$$P_W = \frac{1}{2}\rho A v^3$$

where: $\rho=1.29\ kg/m^3$ is the air density.

For given size of wind turbine at wind velocity $v=10$ m/s, the total wind power is $P_W=1510\ W$.

Power coefficient value of $C_P=0.37$ is reported in the patent document. Accepting this value, the power extractable from the turbine for the same wind speed, neglecting bearing losses is:

$$P = C_P \cdot P_W \approx 560\ W.$$

Measurements on the built turbine shown for about ten times lower power for the given wind speed. The great disagreement can not be explained by losses in the mechanical construction or deviations from the preferred embodiment in the patent document. Bearing losses are minimized by use of quality ball bearings. The turbine elements are manufactured on CNC cutting machines, controlled by files prepared in CAD software.

To find the reasons for this disagreement, CFD analysis of the turbine is done. Commercially available CFD analysis software is used to evaluate the static torque dependence on wind direction and the speed-torque characteristic of the turbine.

Static analysis is much easier to do, even it is useful to find near to optimum turbine geometry. During this research it is found that some modifications on the original turbine blades described in the patent documents can increase the peak static moment. This gives a hope that a somewhat larger power can be achieved from the given size of the turbine than it was possible in the first approach.

Using a dynamic analysis, the speed-torque characteristic can be derived. The maximum power point for a given wind velocity can be found and wind power converted to shaft power can be evaluated.

Figure 2. The wind turbine built by the authors.

III. MATHEMATICAL FORMULATION

A. Conservation equations

This section provides a short summary to the applied mathematical models to describe the velocity field and the pressure distribution around and on the surface of the Savonius rotor blades. The physical problem currently studied is a steady, three dimensional flow configuration. The momentum equation of the fluid is based on the three dimensional Navier-Stokes equations. The applied turbulence model is the SST $k\text{-}\omega$ model which can be used to model correctly the turbulent flow state. A SIMPLE like method is applied to solve the momentum, continuity, and the turbulent transport equations. The conservation equations are formulated in the Cartesian coordinate system because the applied flow solver (Ansys CFX 11.0) uses the Cartesian system to formulate the

conservation equations for all (vector U_i and scalar P, k, ω) quantities. Description of the entire geometry of the studied flow problems is incorporated into the generated unstructured numerical grid which was created by the Workbench built in grid generator.

B. Domain of discretization

The applied grid can be seen in Figure 4. is strongly non-uniform near the blades of the studied Savonius rotor. The presented grid has been created for a static flow simulation. A careful check for the grid-independence of the numerical solution has been made to ensure the accuracy and validity of the numerical scheme. The generated grids contain 498 542, 747 398, 1 784 285 finite volumes respectively. The induced torque around the vertical axis (z axis) has been used to compare the results on the different grids.
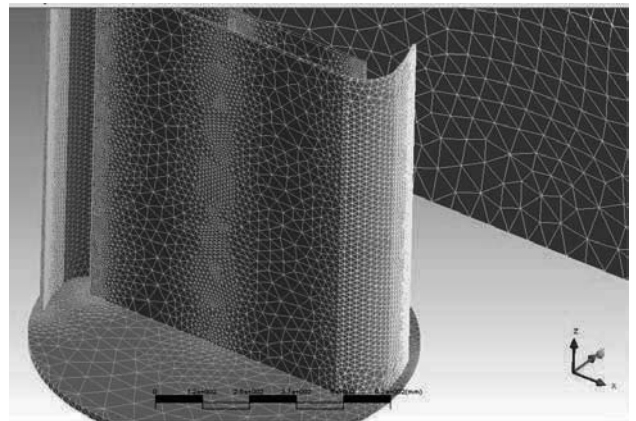
Figure 3. Details of the generated grid for CFD analysis: surface mesh on the blade

C. Initial and boundary conditions

The initial velocity field is zero everywhere in the calculation domain. Constant inflow velocity has been assumed at the inlet surface of the calculation domain. The gradient of the velocity profile and of the pressure field normal to the outlet surface of the downstream region of the rotor is assumed to be zero.

D. Numerical solution of the transport equations

The corresponding transport equations with the appropriate boundary conditions have been solved a commercially available CFD code (Ansys CFX 11.0). A "High Resolution Up-Wind like" scheme is used to discretize the convection term in the transport equations. The resulting large linear set of equations is solved with an algebraic multi-grid solver.

IV. MODEL GEOMETRY

The 3D model of the turbine is constructed in CFX module of Ansys software. The 3D geometry is shown in Fig. 4. The original mechanical drawings are prepared in Solid Edge ST4 software and imported to the Ansys WorkBench as IGES files.
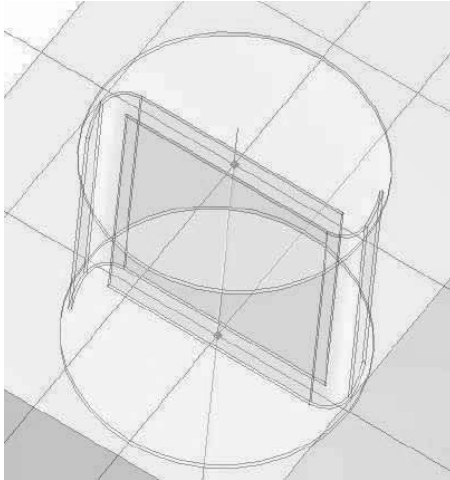
Figure 4. CFX model of the Savonius-type wind turbine.

V. ANALYSIS RESULTS AND DISCUSSION

A. Static Analysis

The turbine performances under fixed rotor conditions are explored. The torque generated for fixed wind velocity is analyzed. As the torque depends on the rotor angular position, the analysis is repeated for successive positions. Analysis from 0 to 180 degree (half turn) is sufficient due to the symmetry of the rotor. The analyses are time consuming: with the available computer the analysis time for one position was about ten hours. The results are given by diagram in Fig. 5. The wind velocity profile for the horizontal cross section, near the maximum torque case, is given in Fig. 6.
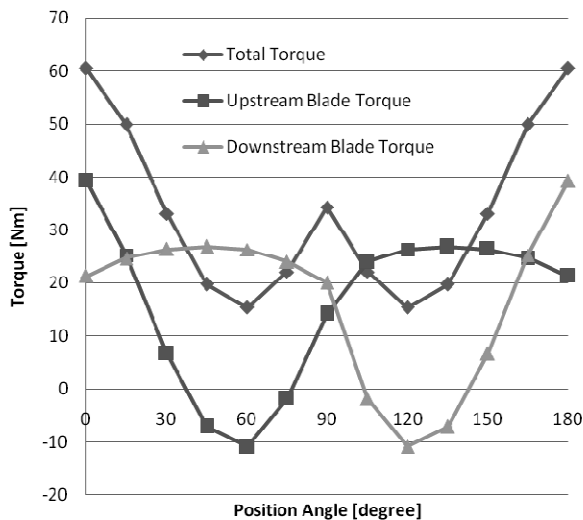
Figure 5. Static torque dependence on rotor angular position and wind velocity.

Figure 5. shows separately the torques acting on the upstream blade (the blade closer to the wind inlet surface) and the downstream blade (closer to the wind outlet surface) and the resulting torque. For a traditional Savonius turbine the torque acting on the blade with its concave side turned to the inlet surface is the opposite of the blade with its convex side turned to the inlet surface. This way the resulting torque is the difference of the two torques. The geometry described in the patent document has the advantage that for almost all angles the torques on the two blades are of same polarity, so the torques are summed up.
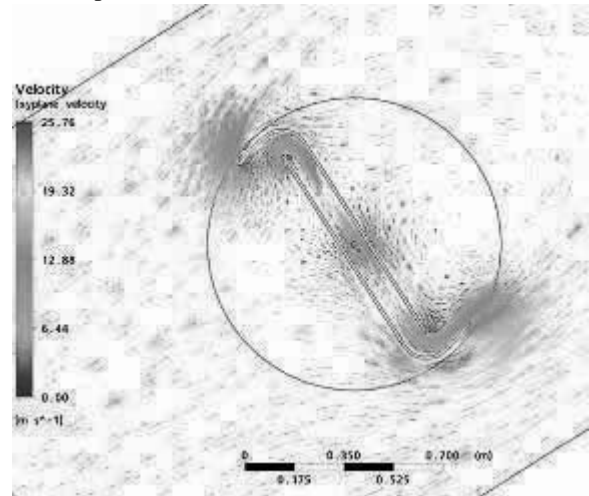
Figure 6. The wind velocity profile in the horizontal cross section for the maximal torque case.

Calculation of the static torque for zero angle position have shown that shortening straight ends of the blades increase the torque in this position. Further analyses are necessary to find the average value of the torque for a complete revolution and justify that the original geometry is not optimal.

B. Dynamic Analysis

The dynamic analysis of the turbine requires a different CFD modeling approach which needs further research work. Based on experiments, for wind speed 10 m/s, the optimal angular velocity of the turbine was about 5 rad/s. The dynamic torque is not evaluated until now, but supposing that it is not much smaller than the average static torque, values from 20 Nm to 30 Nm can be supposed. Multiplying the angular velocity with the average torque, the estimated turbine power is from 100 W to 150W. This gives power coefficients far below the value reported in the patent document and below the achievable values for vertical axis wind turbines. The authors suppose that it is possible to optimize the geometry which will be done in further work.

REFERENCES

[1] S. Carcangiu, A. Fanni and A. Montisci, "Computational Fluid Dynamics Simulations of an Innovative System of Wind Power Generation," Proceedings of the 2011 COMSOL Conference in Stuttgart.

[2] A. H. Benesh, "Wind Turbine with Savonius-type Rotor", US Patent Number 5,494,407, Feb. 27, 1996.

[3] S. J. Savonius, "Rotor", Österreichisches Patentschrift Nr. 103819, July 10, 1925.

[4] L. Tóth, G. Horváth, "Alternatív energia, Szélmotorok, szélgenerátorok", Szaktudás Kiadó Ház, Budapest, 2003.

Toward Future: Positive Net-Energy Buildings

M. Bojic* J. Skerlic* D. Nikolic* D. Cvetkovic* M. Miletic*

* University of Kragujevac /Faculty of Engineering, Kragujevac, Serbia
bojic@kg.ac.rs, jskerlic@kg.ac.rs, danijelan@kg.ac.rs, dragan_cw8202@yahoo.com, marko.m.miletic@hotmail.com

Abstract—**For a positive net energy building (PNEB), the paper presents its need, definition and elements. The most important is that the PNEB should provide the maximum thermal comfort with a minimum of energy, primary energy, and exergy consumption, and a minimum of CO_2 emission throughout its life. Then, the paper presents the software for a energy simulation and optimization of PNEB. After that, the paper describes the five examples connected to the PNEB. The first example is a simulation of a residential PNEB, second the optimization of the photovoltaics in the residential PNEB, third the description of an the building as a power plant initiative, fourth the description of an office PNEB, fifth description of an archive PNEB and finally a description of a headquarter PNEB.**

INTRODUCTION

Daniel M. Kammen, Director of the Renewable and Appropriate Energy Laboratory, University of California, Berkeley wrote the following in Nature[1]. "By 2020. humankind needs to be solidly on to the path of a low-carbon society — one dominated by efficient and clean energy technologies. Several renewable technologies are ready for explosive growth. Energy-efficiency targets could help to reduce demand by encouraging innovations such as PNEBs and electric vehicles. Research into solar energy — in particular how to store and distribute it efficiently— can address needs in rich and poor communities alike. Deployed widely, these kinds of solutions and the development of a smart grid would mean that by 2020 the world would be on the way to an energy system in which solar, wind, nuclear, geothermal and hydroelectric power will supply more than 80% of electricity."

Globally, the drive for PNEB is necessity and urgency to decrease carbon emission, and relive energy shortage.

Several worldwide targets are established. First, the Energy Performance of Buildings Directive of EU states that all buildings built after 31 December 2018 will have to produce their own energy onsite [2]. Second, from beginning of 2020 in USA, all new Federal buildings will be designed to consume zero-net-energy and be zero-net-energy buildings (ZNEBs) by 2030 [3]. Third, to progress with the development and adoption of high performance buildings in USA, there is the Net Zero Energy Commercial Building Initiative. The initiative aims to achieve marketable net-zero energy buildings by 2025 through public and private partnerships [4]. Finally, UK Government sets out improvements to energy requirements in Building Regulations to include that all new homes has to be 'zero carbon' by 2016[5].

The objective of this paper is to introduce definitions and general characteristics of PNEB that go beyond ZNEB, show software for their design and give their several examples.

DEFINITIONS

The schematic of a PNEB is shown in Fig.1.
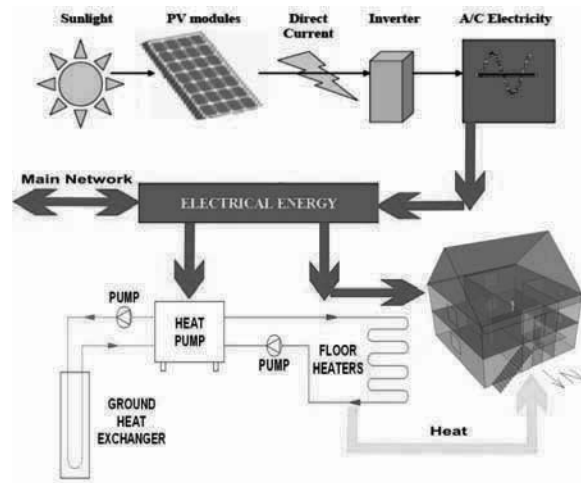
Fig.1 Schematic of a PNEB

A. Ordinary Definitions [6]

Positive-Zero Site Energy — PNEB generates more energy than it consumes. It usually produces electrical energy through PV modules and is connected to the grid. The building may either consume electrical energy from the PV modules or from the grid. The generated electrical energy may either feed the building or the grid. The electric energy supplies the grid when there is the electrical energy surplus. When there is electrical energy shortage the grid supplies electrical energy to the building. The ''positive-net'' concept means that yearly the excess electrical energy sent to the grid is larger than the amount received from the grid. The PNEB uses the power grid as an electrical storage battery.

Positive-Zero Source Energy — A building that produces and exports more energy as the total energy it imports and uses in a year, when accounted for at the source. "Source energy" refers to the primary energy required to generate and deliver the energy to the site. To calculate a building's total source energy, imported and exported energy is multiplied by the appropriate site-to-source conversion multipliers.

Positive-Zero Energy Costs — A building where the amount of money a utility pays the building's owner for the renewable energy the building exports to the grid is

49

larger than that the owner pays the utility for the energy services and energy used over the year.

Positive-Zero Energy Emissions — A building that produces and exports more emissions-free renewable energy as it imports and uses from emission-producing energy sources annually. Carbon dioxide, nitrogen oxides, and sulfur oxides are common emissions that PNEBs offset.

B.   Embodied energy [7]

Life positive net energy building (L-PEB) is defined that during entire life it produces more energy than it spends for the embodied energy of building components and its energy use [6].The net energy ratio (NER) is a as the ratio of the decrease on annual energy use to the increase in annualized embodied energy. The higher NER better more effective is move toward L-ZEB.

II.   ENERGY

A.   Energy consumption

In ZNEHs, energy may be used for space heating, space cooling, DHW heating, lighting, and appliances, etc.

Technologies for lighting and appliances should be energy efficient to minimize use of electrical energy that has to be generated by the building.

In future buildings, space heating should be efficient. In this direction, technologies for space heating are usually ground coupled heat pumps (GCHP) as they give around 3 times greater amount of heat energy than that of electrical energy with which it was run. The heat pumps may be used for heating and cooling when the direction of refrigeration fluid is reversed. The most often it is a GCHP with hydronic floor heating or air space heating.

B.   Energy generation

Technologies for heat & cold generation from geothermal energy use electrical energy to operate. These devices are called heat pumps. They should be energy efficient and have the highest COP (to use as low amount of electrical energy as possible).

Technology used for DHW heating may be heat used by solar collectors and electrical energy produced by the PV modules, or the heat pump driven by electrical energy. The most efficient heating may be performed by either solar collector with electric backup.

Technologies that are used for energy generation should be energy efficient and to use as low surface area as this is possible. These technologies are generation of heat energy by solar collectors, and electrical energy by the PV modules and wind power. When there are energy generation with the PV panels and solar collectors, one should determine the ratio between areas of the PV modules and of solar collectors. However, there is also simultaneous generation of heat and electricity by hybrid PVT panels.

C.   Building envelope

In future buildings, a building envelope should minimize heat transfer. In cold climate, the building envelope has to be super insulated and air tight. Special double glazed windows are used at the south wall that are filled with argon and have low heat emissivity film coating.

D.   Rule of thumb

However, the amount of energy generated by the PV modules and solar collectors located on the building roof is limited as there is shortage in surface (space) needed for energy generation. Consequently, the rule of thumb of design of ZNEH is to minimize energy consumption in the building. This would minimize required energy generation and surfaces required for this energy generation.

E.   Cost effectiveness

Energy saving and producing technologies should be cost effective. That means minimum construction costs for these houses and their fastest penetration into practice. The highest cost is the cost of its GCHP heating system and the PV modules. To minimize these costs, the designer has to minimize heating and cooling loads to these homes. For designer, the most interesting questions are that of area of the PV modules and financial attractiveness of their installation. As these technologies are still relatively expensive, the government should enhance financial attractiveness of the investment in such devices.
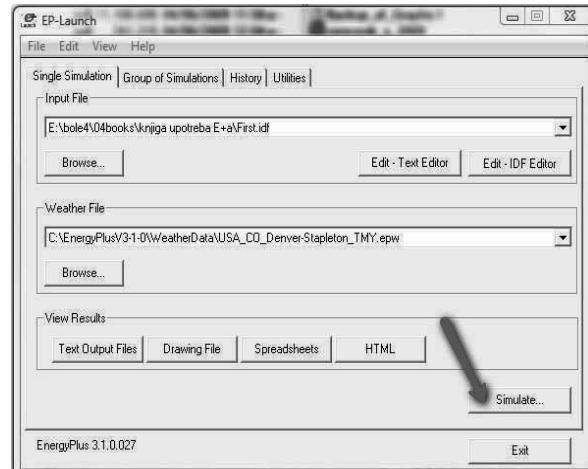
Fig.2 EnergyPlus interface

SIMULATIONS AND OPTIMIZATIONS

A. Simulation software - EnergyPlus

EnergyPlus is made available by the Lawrence Berkley Laboratory in USA [8]. EnergyPlus interface is shown in Fig.2. EnergyPlus development began in 1996 on the basis of two widely used programs: DOE-2 and BLAST. The software serves to simulate building energy behavior and use of renewable energy in buildings. The renewable energy simulation capabilities include solar thermal and photovoltaic simulation. Other simulation features of EnergyPlus include: variable time steps, user-configurable modular systems, and user defined input and output data structures. The software has been tested using the IEA HVAC BESTEST E100-E200 series of tests. To model, the building and renewable energy systems in

EnergyPlus environment, we used models of different components that are embedded in EnergyPlus such as that of PV-array, inverter, flat-plate solar collector, storage tank, tempering valve, and instantaneous water heater. Water in the storage tank was heated by solar energy and water in the instantaneous water heater by electricity.

B. Simulation software - Google SketchUp

Google SketchUp is a free 3D software tool that combines a tool-set with an intelligent drawing system. Building in Google Sketch-up environment is shown in Fig.3. The software enables to place models using real-world coordinates. Most people get rolling with SketchUp in just a few minutes. There are dozens of video tutorials, an extensive Help Centre and a worldwide user community.
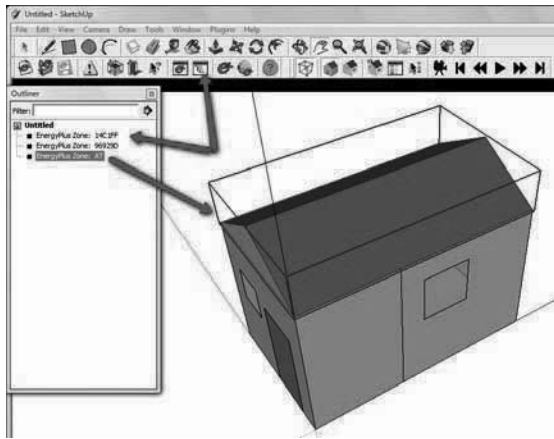
Fig.3 Building in OpenStudio environment

C. Simulation software - OpenStudio

The OpenStudio is free plug-in that adds the building energy simulation capabilities of EnergyPlus to the 3D SketchUp environment. A house in OpenStudio environment is shown in Fig.3. The software allows you to create, edit and view EnergyPlus input files within SketchUp. The plug-in uses the standard tools provided by SketchUp. The software adds as much extra detail as you need to zones and surfaces. The plug-in allows you easy to create a building geometry from scratch: add zones, draw heat transfer surfaces, draw windows and doors, draw shading surfaces, etc. You can save what you have drawn as an EnergyPlus input file. The plug-in also allows users to launch EnergyPlus simulations and view the results from within SketchUp.

D. Optimization software - GenOpt

GenOpt is an optimization program for the minimization of a cost function evaluated by an external simulation program [9]. Optimization and simulation data flow paths by using Genopt are shown in Fig.4. GenOpt serves for optimization problems where the cost function is computationally expensive and its derivatives are not available or may not even exist. GenOpt can be coupled to any simulation program that reads its input from text files and writes its output to text files. The independent variables can be continuous variables (possibly with lower and upper bounds), discrete variables, or both, continuous and discrete variables. Constraints on dependent variables can be implemented using penalty or barrier functions. GenOpt is written in Java so that it is platform independent. GenOpt is applicable to a wide range of optimization problems. GenOpt has a library with adaptive Hooke-Jeeves algorithm.
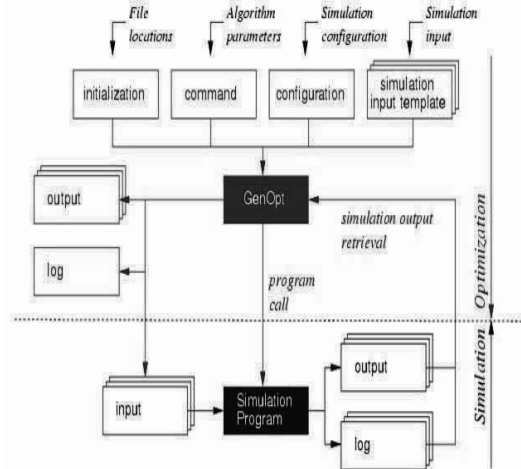
Fig.4 Optimization by using Genopt

4. EXAMPLES

A. Residential PNEB in Serbian conditions [11]

This article reports investigations of a residential building in Serbian conditions energized by electricity from photovoltaics (PVs), and the electricity grid. The building uses electricity to run its space heating system, lighting and appliances, and to heat domestic hot water (DHW). The space heating system comprises floor heaters, a water-to-water heat pump, and a ground heat exchanger. The schematic of this PNEB is shown in Fig.1. The PV system generates electricity that either may be consumed by the building or may be fed-in the electricity grid. The electricity grid is used as electricity storage. Three residential buildings are investigated. The first residential building has PVs that yearly produce smaller amount of electricity than the heating system requires. This is a negative-net energy building (NNEB). The second building has the PVs that produce the exact amount of electricity that the entire building annually needs. This is a zero-net energy building ZNEB. The third building has PVs that entirely cover the south-facing roof of the building. This is a PNEB. These buildings are presented by a mathematical model, partially in an EnergyPlus environment. For all buildings, simulations by using EnergyPlus software would give the generated, consumed, and purchased energy with time step, and monthly and yearly values. For sure, these buildings would decrease demand for electricity during summer, however they will increase this demand during winter when there is no sun and start of space heating is required. Depending on the size of PV array this building will be either NNEB, or ZNEB, or PNEB. However it is crucial for such a building to be connected to the electricity grid. The smaller payback for investment in the PV array is obtained for buildings with larger size of PV array. The feed-in tariff for the generation of electricity in

Serbia should be under the constant watch to be corrected accordingly for larger penetration of this technology in the Serbian market.

B. Optimizing performances of photovoltaics in Reunion Island – tilt angle [12]

As in Reunion Island, France, around 61% of electricity is produced by using coal and fuel oil with high greenhouse emissions. It is beneficial to the environment to produce electricity from solar energy. Therefore, there is a large push to generate electricity from solar energy by use of photovoltaic (PV) arrays. However, it is important to have high efficiency of electricity generation, that is, to locate PV arrays in an optimal direction. The investigated PV systems may take 1, 2, 4, and 12 tilts per year. For the PV arrays facing the north–south direction, this paper reports investigations of their optimum tilts and the maximum amounts of generated electricity. The investigated PV arrays are located in the towns of Saint-Benoit, Les Avirons, Piton Saint-Leu, and Petite-France in Reunion Island. To obtain optimal tilt of the PV arrays for electricity production from solar energy, EnergyPlus software and GenOpt software are used with Hooke–Jeeves optimization routine. For the investigated PV arrays, the percentage gains in energy, exergy, avoided fossil energy, and the percentage decrease in CO_2 emission are around 5% when compared with that of the PV array that takes only one optimum tilt per year.
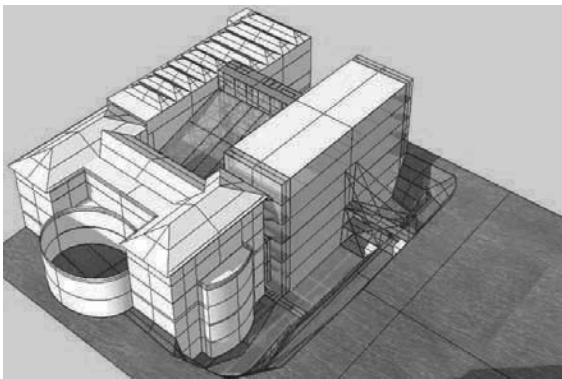
Fig.5 BAPP initiative object

C. The building as Power Plant initiative[13]

The Building as Power Plant (BAPP) initiative seeks to integrate advanced energy-effective building technologies (ascending strategies) with innovative distributed energy generation systems (cascading strategies), such that most or all of the building's energy needs for heating, cooling, ventilating, and lighting are met on-site, under the premise of fulfilling all requirements concerning user comfort and control (visual, thermal, acoustic, spatial, and air quality). BAPP is shown in Fig.5. This will be pursued by integrating a "passive approach" with the use of renewable energies. BAPP is designed as a 6-story building, located in Pittsburgh (a cold climate with a moderate solar potential), with a total area of about 6000 m2 which houses classrooms, studios, laboratories, and administrative offices. At present, the combined cooling, heating, and power generation option that is being

considered for the demonstration building is a Siemens Westinghouse 250-kW solid oxide fuel cell (SOFC).

D. The office project (commercial building) [14]

In the green office project (commercial building) in Meudon outside Paris, FRANCE, by Bouygues Immobilier, energy consumption is reduced to the strict minimum with the bioclimatic design of the building and a high-performance natural ventilation system (shown in Fig.6). The building has a north-south building orientation; its outer walls have enhanced external insulation, with wood and aluminum joinery for improved performance, and motor-controlled vents for natural ventilation; the open-plan office space is 13.50 metres deep, making it easier to make full use of natural lighting and ventilation; air circulating fans enhance comfort levels in summer; the motor-controlled external blinds provide good solar protection. The thermal inertia of the floor slabs is made more readily accessible by dispensing with false ceilings and raised floors. Lighting in the building has been designed to contribute to energy savings while still providing maximum comfort levels. Control of lighting has been optimised to reduce power consumption by automatically turning lights off when the office is not occupied. Energy balance says that this building produces more energy than it consumes.

Fig.6 The Green Office in Meudon

Green office will reduce power consumption by 60% compared to a standard building constructed to the RT 2005 thermal regulations, and by 30% relative to the most energy-efficient buildings on the market today. More than 5,000 sq. metres of solar panels produces energy for the building. They are installed on walls; and as "car ports" in outdoor parking areas. The building also uses a biomass combined heat and power system fuelled by wood or oil. The produced heat covers the building's entire heating requirement, and the electricity produced covers power needs above and beyond the capacity of the solar panels. The project is carbon-neutral. In addition, the special attention is given to reducing its carbon footprint by limiting carbon emissions during construction.

E. An archives building [15]

The archives building for the Nord administrative district is built by Bouygues Construction, in Lille, northern France (Fig.7). In addition to archives rooms, The building has the total floor space of more than 13,000 sq. metres that include extensive work areas.

52

To keep future energy consumption down, the building has enhanced insulation (walls, roof, glazing), superior air and water tightness, and the innovative, energy-efficient equipment and technologies. Since its overall priority is to store archives under the optimum temperature and humidity conditions, a special innovative, high-performance air-conditioning system (desiccant-based) is applied. The applied systems achieve a record low level of primary energy consumption, at 12.9 kWh/sq. metre/year compared to the average consumption of 105 kWh/sq. metre/year for a conventional building of the same type.

Fig.7 An archives building

Heat and electricity will be produced by a combined heat and power plant running on plant oil and by 350 sq. metres of solar cells.

F. The Masdar Headquarters, Abu Dhabi [16]

In Chicago, architecture firm Adrian Smith + Gordon Gill is chosen to design a positive energy, mixed-use building for the world's first zero-carbon, zero-waste, car-free city called Masdar (Fig.8). As a "positive energy" building, the design aims to generate more energy each day than it consumes. The 130 thousand m^2 ($300 million) headquarters will serve as the centre of Masdar City, which will end up being about a $22 billion development in Abu Dhabi. The headquarters are the lowest energy consumer per square meter for a modern class A office building in an extremely hot and humid climate. They feature one of the world's largest building-integrated photovoltaic arrays. They employ the largest solar thermal driven cooling and dehumidification system.

FIG.8 MASDAR HEADQUARTERS, ABU DHABI

CONCLUSIONS

The paper shows that PNEBs are in strong need worldwide. The most important fact is that throughout their life, the PNEBs should provide the maximum thermal comfort with the minimum of energy, primary energy, and exergy consumption, and the minimum of CO2 emission. The different definitions of the PNEBs are present. They can account for the site energy, source energy, CO_2 emissions, costs, and embodied energy. The PNEBs require up-to-date technologies for efficient energy consumption and energy generation from solar and geothermal energy. The PNEBs may be designed by using software for energy simulation and optimization. The PNEBs would be successfully used for residence, research, office, archive, and business.

REFERENCES

[1] "2020 visions, Opinion", *Nature* Vol. 463, 2010, pp.26-32 (7 January) doi:10.1038/463026a;

[2] J. Kammer, All new buildings to be zero energy from 2019, Press Service Directorate for the Media, European Parliament, 2009.

[3] White house, Federal leadership in environmental, energy, and economic performance (executive order), The white house office of the press secretary, October 5, 2009.

[4] US Department of Energy, NetZero Energy Commercial Building Initiative, Building Technologies Program Energy Efficiency and Renewable Energy.

[5] UK Green Building Council, Zero Carbon Task Group Report, WWF-UK, 2008

[6] P. Torcellini, S. Pless, M. Deru, and D. Crawley, Zero Energy Buildings: A Critical Look At The Definition, Preprint, Aceee Summer Study, Pacific Grove, California, August 14−18, 2006.

[7] P. Hernandez, and P. Kenny, "From net energy to zero energy buildings: Defining life cycle zero energy buildings (LC-ZEB)", *Energy and Buildings*, 42, 2010, pp.815–821

[8] Lawrence Berkeley National Laboratory. EnergyPlus input output reference: the encyclopedic reference to EnergyPlus input and output. Berkely: LBL; 2001.

[9] M. Wetter 2004. GenOpt, Generic Optimization Program. User Manual, Lawrence Berkeley National Laboratory, Technical Report LBNL- 54199, p. 109.

[10] R. Hooke, and TA. Jeeves, "Direct search solution of numerical and statistical problems", *Journal of the Association for Computing Machinery* 1961; 8: pp.212–229.

[11] M. Bojic, N. Nikolic, D. Nikolic, J. Skerlic, and I. Miletic, "Toward a positive-net-energy residential building in Serbian conditions", *Applied Energy* 88, 2011, pp. 2407–2419.

[12] M. Bojić, D. Bigot, F. Miranville, A. Parvedy-Patou, and J. Radulović, „Optimizing performances of photovoltaics in Reunion Island – tilt angle", *Progress in Photovoltaics: Research and Applications*, DOI: 10.1002/pip.1159 (2011) Online ISSN: 1099-159X.

[13] V. Hartkopf, "Building as Power Plant—BAPP", *Cogeneration & distributed generation journal*, Vol. 19, No. 2, 2004, pp. 60-73, DOI: 10.1080/15453660409509039

[14] Immobilier Bouygues. The Green Office project in Meudon; 2007. <http://www.bouygues-immobilier.com/jahia /Jahia/lang/en/aboutus/espace_de_presse/pid/2407> [retrieved 02.09.10].

[15] Bouygues-construction, First positive-energy building; 2009. <http://www.bouygues-construction. com /667i/sustainable-development/news/firstpositive-energy-building.html> [retrieved 02.09.10].

[16] Anonymous, Planning a Sustainable City in the Desert, *The New York Times*, Art & Design, published: September 25, 2010.

A New Calculation Method to Analyse the Energy Consumption of Air Handling Units

László Kajár Dr. Ph.D.*, **Miklós Kassai** Dr. Ph.D. *

* Budapest University of Technology and Economics, Hungary
e-mail : kas.miklos@gmail.com

Abstract: According to the 2002/91/EC, the Directive on the energy performance of buildings it is important to determine the expected energy consumption of the building in the step of the designing. There are imperfections in the actual available national and international regulations as for the methotds to calculate the energy consumption of the air handling units. The actual calculation methods are fairly inexact approximations while they characterise the monthly energy consumption only with the average temperature or average enthalpy which takes into account the changing of the ambient air state only approximately. The most actual calculation procedures also not consider the systems that operate not continuously (only at night or in daytime). Based on the calculation procedure that uses the ambient temperature and enthalpy duration curves these problems can be solved. A new calculation method was worked out that takes into consideration the air handling energy consumption with the ambient temperature and enthalpy duration curves.The research work was supported by "Sustainable Energy Program" of BUTE Research University.

I. INTRODUCTION

The population and residential buildings represent almost 40% of the total energy consumption in Hungary. Their share is similar in the EU countries and if the buildings used in the industrial and transport sector are also taken into consideration, this figure even reaches 50% [1]. The major part of this 50% is used for air conditioning. From the point of view of sustainable development and international agreements (Kyoto protocol) the reduction of carbon dioxide emissions and energy consumption is an important issue. The energy consumption of air handling units can be calculated in two ways. In the case of working air handling units the actual consumption data can be exactly determined by measurement. But according to Directive 2002/91/EC on the energy performance of buildings (EPBD) it is also important to determine the expected energy consumption of buildings in the designing phase. The directive was implemented by the Decree of no. 7/2006 of the Minister Without Portfolio [2]. The decree provides information and methods to calculate the energy consumption of building services but for instance the calculation of the energy consumption of air handling units is still problematic. Effective since 2008, Government Decree 264/2008. (XI. 6.) gives guidelines for the energy audit of boilers and air conditioning systems.

Making a study of the international scientific literature, Erik Reichert worked out a calculation procedure in his Ph.D. thesis at the University of Applied Sciences Stuttgart, with which the net energy consumption of the air handling unit can be calculated. The method sepatares the Mollier h-x chart into 4 parts in accordance with the main changing processes of the air state (air humidification, cooling). With this procedure the energy consumption of the air handling units can be calculated with the help of statistical, meteorological database suitable for the geographic area of the analysed space.

Similarly in Germany with the leading of Professor Bert Oschatz a calculation method was developed to determine the energy consumption of the air-conditioning systems. This method uses specific values [Wh/m^{3}h] to calculate the heating and cooling energy consumption of the air handling units also in monthly period.

Claude-Alain Roulet has also developed a calculation procedure to determine the annual energy consumption of the air handling systems.

From the developed methods also standards were made: VDI 2067 (Blatt 21) based on the research work of Erik Reichert, DIN V 18599-7/3/5/10 based on the research work of Professor Bert Oschatz and EN ISO 13790 based on the research work of Claude-Alain Roulet. The timeliness of this research theme shows that the current available calculation procedures enable the only the rough estimate of the energy consumption of air handling units. The mentioned methods do not take into account of the heat and moisture load of the air handled space.

During our research our objective was to work out a calculation procedure which is suitable for the analysis of the energy consumption of air handling units taking into account the different and complex air handling processes and the above mentioned inadequacies.

II. THE PHYSICAL MODEL

Calculation of heating and cooling energy consumption it is necessary to take account of variation of ambient air parameters (temperature, humidity and enthalpy) that vary in daily and season period [3]. The developed calculation procedure is introduced in the article by a fresh air supply air handling unit (AHU). The connection diagram can be seen of fresh supply air handling system on Fig. 1. The signs of the figure are the following:

PH: Pre-heater,
AH: Adiabatic humidifier,
C: Cooler,
RH: Re-heater,
V: Ventilator,
F: Filter,
SH: Shutter against the rain.
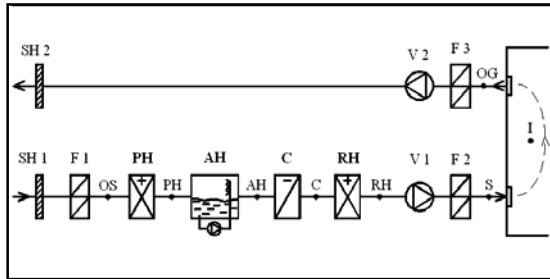
Fig. 1. The connection diagram of the AHU

During the energy calculations it is important to take into consideration the order of the air handling elements and the air handling processes. During the operation of the air handling units the air handling processes can be best demonstrated by the Mollier h-x chart [4]. Some parameters are given such as the temperature and relative humidity of ambient air in the dimensioning phase (t_{OS} ; φ_{OS}), the supply air that enters the room (t_S ; φ_S) and the outgoing air that leaves the room (t_{OG} ; φ_{OG}). To perform the energy calculations it is necessary to know the supply air volume flow and the density of the supply air.

The values of indoor air parameters depend on the air distribution of the room and are shown between the supply air and outgoing parameters. The energy analysis is not influenced by the indoor air parameters.

One of the most popular ways for humidifying is the operation of the adiabatic humidifier. In winter the relative humidity of air coming from the adiabatic humidifier is usually 95 %, although this value depends on the intensity of the vaporization. The Mollier h-x chart is available for further data needed to complete the energy analysis. Fig. 2. shows the process of pre-heating („OS-PH" section), the adiabatic humidifier („PH-AH" section) and the re-heating („AH-RH" section) in the dimensioning phase in winter time.
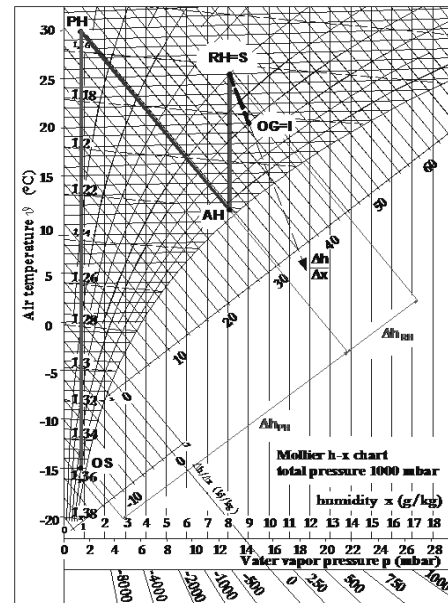
Fig. 2. Air handling processes on the Mollier h-x chart in the dimensioning state in winter time

During the change of the ambient air state the pre-heater heats up the air up to the constant enthalpy line that is determined by the adiabatic humidifier, therefore the ambient enthalpy duration curve has to be used to define the energy consumption of heating.

On the ambient enthalpy duration curve (Fig. 3.) the above mentioned air state parameters in the dimensioning phase are also shown as well as their changes as the ambient air enthalpy varies during the heating season. The areas of the ambient enthalpy duration curve that represent the energy consumption of the pre-heater and the re-heater can be accordingly drawn. Throughout the calculation of the energy consumption of heating the supply and outgoing air parameters were assumed to be constant during the heating season. This approximation was also applied for the supply and outgoing parameters in the dimensioning phase for the cooling season in the summer.
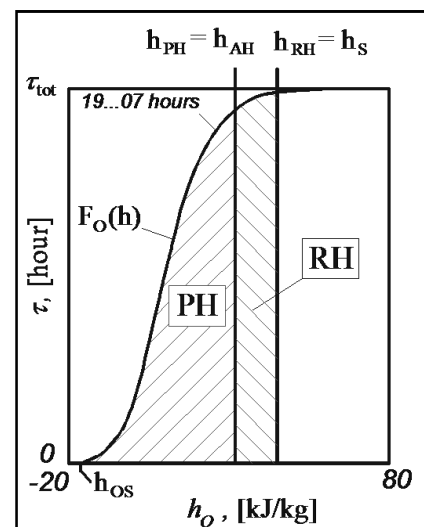
Fig. 3. The areas on the ambient enthalpy duration curve that represent the energy consumption of the pre-heater and re-heater

On Fig. 3. can be seen the areas that proportional to the daytime heating energy consumption of the air handling unit (07-19 hours). In compliance with it the physical and mathematical equations were determined to calculate the energy consumption of the heaters in the fresh air supply air handling unit.

The energy consumption of the pre-heater:

$$Q_{PH} = \rho \cdot \dot{V} \cdot \int_{h_{OS}}^{h_{PH}} F_O(h)dh \qquad \text{[kJ/year]}$$

where:

ρ [kg/m^3]   the air density,

$\dot{V}$ [m^3/h]   air volume flow,

$F_O(h)$ [-]   the ambient enthalpy duration curve (07-19 hours),

h_{OS} [kJ/kg]   the ambient enthalpy in sizing state in the winter time,

h_{PH} [kJ/kg]   the enthalpy of the air after the pre-heater, which is equal with the enthalpy by the adiabatic humidifier.

The energy consumption of the re-heater:

$$Q_{RH} = \rho \cdot \dot{V} \cdot \int_{h_{PH}}^{h_{RH}} F_O(h)dh \qquad \text{[kJ/year]}$$

where:

h_{RH} [kJ/kg]   enthalpy of the air after the re-heater, which is equal with the enthalpy of supply air (h_S).

Analyzing the cooling energy consumption the calculation procedure is similar in the summer time. The dimensioning phase for the summer period is specified by the regulations (Fig. 4.). The average temperature of the surface of cooling coil (t_{SA}) is about 11-12°C when the cooling water temperature is 7/12°C.
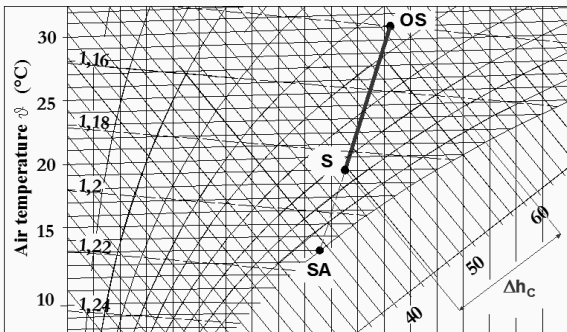
Fig. 4. Cooling process on the Mollier h-x chart in the dimensioning phase in summer time

In light of the above mentioned data the area proportional to the energy consumption of the cooling coil can be drawn in the ambient enthalpy duration curve.

In consideration of the fact that there is condensation on the surface of the cooling coil, the ambient enthalpy duration curve was used to determine the annual energy consumption of the cooling coil (Fig. 5.).
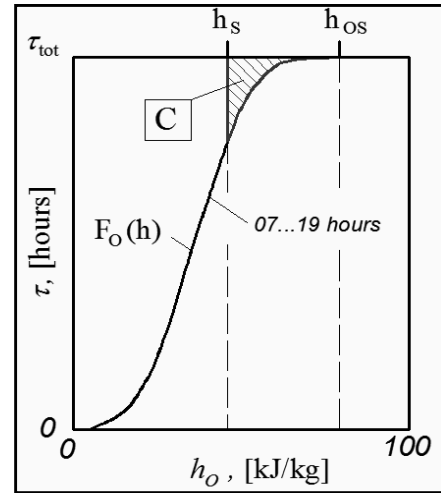
Fig. 5. The area on the ambient enthalpy duration curve that represents the energy consumption of the cooling coil

The energy consumption of the cooling coil: (1)

$$Q_C = \rho \cdot \dot{V}_C \cdot \int_{h_S}^{h_{OS}} [1 - F_O(h)]dh \qquad \text{[kJ/year]}$$

where:

$\dot{V}_C$ [m^3/h]   the air volume flow in the cooling coil,

h_S [kJ/kg]   the enthalpy of the supply air.

In light of the energy consumption of the cooling coil the electricity consumption of the compressor can be calculated as follows [5]:   (2)

$$W_C = Q_C / (SEER \cdot 3600) \qquad \text{[kWh/year]}$$

where:

SEER [-]   Seasonal Energy Efficiency Ratio.

By this manner energy consumption of other constructed air handling units were also determined.

II.   THE MATHEMATICAL MODEL

The ambient temperature (Fig. 6.) and enthalpy duration curves are not known analytically, in this manner the integral values that we developed were determined with appreciative numerical computing.
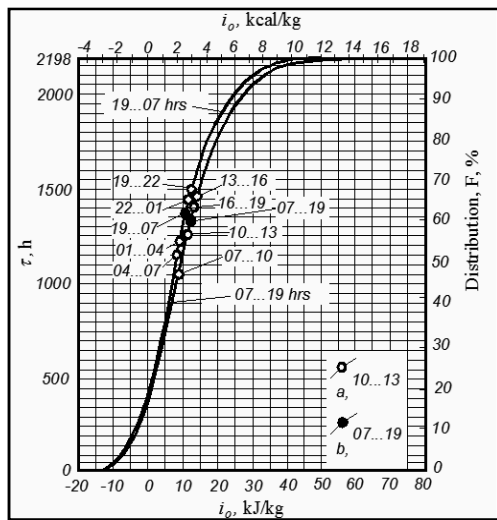
Fig. 6. The ambient enthalpy duration curve from October until March (Budapest, measured temperatures between 1964-1972) [6]

We digitalised the duration curves from the scientific literature, that were fixed in three hours period during the meteorological monitoring, then we placed points to the functions (Fig. 7.). For this task Autodesk AutoCAD 2006 program was right. Wittingly the scale of the duration curves the areas (the values of the integrals) could be computable numerical.
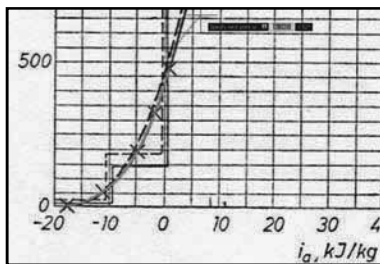
Fig. 7. Application of spline interpolation with Autodesk AutoCAD 2006 program

In the mathematical sciences the spline is a special function that consists from more polynomial. Autodesk AutoCAD 2006 uses rational B-spline curbes (NURBS).

III. RESULTS

In our research work a comparative analysis was made between the new calculation procedure we had developed and the existing international calculation methods. During our analysis the net energy consumption of three air handling units for heating and cooling was determined and the volume flow rate of the air was 3000 m^3/h. The energy analysis was performed using meteorological data for Budapest. The elements of the AHUs are presented in Table 1. The symbols are the following:

HR: Heat recovery unit,
ER: Energy recovery unit,
PH: Pre-heater,
C: Cooling coil,
AH: Adiabatic humidifier,
SH: Steam humidifier,

RH: Re-heater.

	HR	ER	PH	C	AH	SH	RH
AHU 1.	X		X	X		X	X
AHU 2.		X	X	X	X		X
AHU 3.			X	X		X	X

Tab. 1. Elements of the AHUs

The annual net energy consumption of the analysed air handling units for heating and cooling can be seen in Tables 2-3.

Q_H [kWh/year]				
	New method	Erik R.	Bert O.	Claude-A. R.
1.	15 667	15 080	8 514	26 899
2.	28 158	17 150	12 435	-
3.	38 865	24 927	34 264	42 648

Tab. 2 Annual net energy consumption of the AHUs for heating

Q_C [kWh/year]				
	New method	Erik R.	Bert O.	Claude-A. R.
1.	4 773	4 900	5 726	5 832
2.	4 344	4 900	5 412	-
3.	5 873	6 022	5 785	6 374

Tab. 3 Annual net energy consumption of the AHUs for cooling

IV. CONCLUSION

The tables show that the results of the energy consumption different if calculated using the new procedure or the method by Erik Reichert, Bert Oschatz, Calude-Alain Roulet. But in each examined case (AHU 1-3.) the result of the international calculation methods is almost the same as the figures obtained through the new calculation procedure. In the case of AHU 2 equipped with an adiabatic humidifier there is a larger difference with regard to energy consumption for heating. In our view the present international methods do not take into consideration the higher energy consumption of the re-heater, caused by the adiabatic humidifier. Another reason for the different results is that effective regulations define the monthly energy consumption by a single figure only, e.g. average temperature or average enthalpy which only approximately takes into account the changing of the ambient state of the air .

V. REFERENCES

[1] Bánhidi László: Korszerű gyakorlati épületgépészet, Verlag Dashöfer Kiadó, Budapest, 7. rész 2.2. fejezet, 1. o. (2010).
[2] Decree of no. 7/2006 of the Hungarian Minister Without Portfolio, complying the European Directive 2002/91/EC on the energy performance of buildings, 2006.
[3] Jens Pfafferott, Sebastian Herkel, Matthias Wambsganß: Design, monitoring and evaluation of a low energy office building with passive cooling by night ventilation, Energy and Buildings, ISSN 0378-7788, (2004), p. 458.
[4] Heinz Eickenhorst: Einführung in die Klimatechnik, Erläuterungen zum h-x Diagramm, ISBN 3 8027 2371 6, (1998) p.10.
[5] Carson Dunlop: Air conditioning & Heat Pumps, IL 60606-7481, (2003) p. 126.
[6] Róbert Kiss: Légtechnikai adatok, Műszaki Könyvkiadó, Budapest, ISBN 963 10 3152 7, (1980), p. 207-208.

Present and Future of Geothermal Energy in Heat Supply in Hungary

Gyné, Halász Mrs.

Institute of Environmental Systems
Faculty of Mechanical Engineering
Szent István University, Gödöllő, Hungary
halaszne@yahoo.com

Abstract—**The paper focuses on advantages of heat utilization of thermal water with or without exploitation contra regular gas boiler supplied heating systems.**

I. INTRODUCTION

Today the most important issue of energy supply is that the fossil primer energy source of the Earth is limited. Substitution of it is indispensable because environmental pressures require reduction of CO_2 emission. Towards next generations one of the main aims of the researches is to create energy systems that operate with less and less primer energy source thus insure the sustainable development and meet the environmental protection criteria.

The geothermal energy orientated international professional literature claims geothermal heat as the most pure energy source.

Hungary's geothermal production goes back almost a century, and has won a prestige in the World's geothermal energy sector. It is well known that Hungary's geothermal potential is among the world's best territories (not counting the active volcanic areas). Heat flow density is high and can reach up to 100 mW/m^2 value and the geothermal gradient maximum values are close to 60 °C/km^2, but there are no large enthalpy geothermal fields in Hungary [2]. Because of the increased need towards environmental friendly technology, a significant increase of national geothermal heat production is expected in the medium and long term.

II. GEOTHERMAL PERSPECTIVE OF HUNGARY UNTIL 2020

Hungary's primer energy consumption in 2010 according to statistic data by Hungarian Energy Office was 1086.7 PJ. Close to 58 % of the primer energy was imported. 74.7 % of the consumed primer energy was fossil fuel, 7.6 % (82.1 PJ) was renewable energy and 17.8 % was primer electric power. 64.3 % (698.7 PJ) of the primer energy has reached the end-user. The main end-users are households with 22.1 % (240.6 PJ). 6.3 % (49.1 PJ) of the gross final energy consumption were renewable sources, of which nearly 9 % is geothermal energy.

The most important document that determines the future of the geothermal energy is Hungarian National Renewable Energy Action Plan (hereinafter referred as to: NREAP) [6]. NREAP's indicators help us to conclude the development of the coming years. NREAP determines

four times increase regarding the thermal water based heat supply. Table I. shows the growth of the main segments.

The plans are ambitious, but they are in accordance with the technology possibilities of Hungary's geothermal potential and correspond to the major European development appropriations [5].

TABLE I.
PLANNED GROWTH OF THREE MAIN SEGMENTS OF GEOTHERMAL HEAT PRODUCTION [6]

	2010	2020	Growth	(2020/ 2010)
Heat pumps, Supplied heat/year	0.250 PJ	5.99 PJ	5.740 PJ	23.96
Within heat pumps: Ground source heat pumps, Supplied heat/year	0.208 PJ	4.48 PJ	4.272 PJ	21.54
Thermal water based direct heat supply Supplied heat/year	4.23 PJ	16.43 PJ	12.2 PJ	3.88
Geothermal based electric power production, Power	0 MW	57 MW	57 MW	-
Geothermal based electric power production, Energy/year	0 GWh	410 GWh	410 GWh	-

Due to the development of the renewable energy industry, NREAP appropriates 70–80 thousand permanent work places in this sector in 2020. If this occurs, then it significantly helps to decrease the negative effects of the economic crisis.

III. ENERGY AND EXERGY ANALYSIS OF SYSTEMS SUPPLIED WITH DIFFERENT HEAT PRODUCERS

Energy and thermodynamic analysis of heat supply systems supplied with different heat producers (electric power energy, regular and condensation gas boilers, electric power operated heat pumps and thermal water) proved that the heat utilization of thermal water (for heating, cooling with heat, and domestic hot water production) is the most favorable technical solution regarding energy and exergy efficiency. This has a simple explanation: fossil fuel used for space heating and domestic hot water production as low exergy functions is

'wastage'. It is more favorable to use thermal water for heating, DHW production - and cooling if the temperature is above 65 °C – as thermal water is a thermally less valuable heat source [1] [7] [8].

In Hungary's numerous cities, settlements and local government buildings there are decentralized heat supply systems with obsolete gas fired regular wall mounted or standing gas boilers. These systems can be potential consumers for geothermal systems to be built in the future. In this article focusing on this prospect three of the numerous different calculation results are described. Type 'A' is a regular gas boiler supplied radiator heating system, type 'B' is a compressor equipped ground source heat pump system and type 'C' is heat exchanger equipped thermal water supplied system. We assumed at all three calculations that the temperature of heating fluid is controlled according to the outside temperature. We have calculated the energy and exergy efficiency for three different operating statuses.
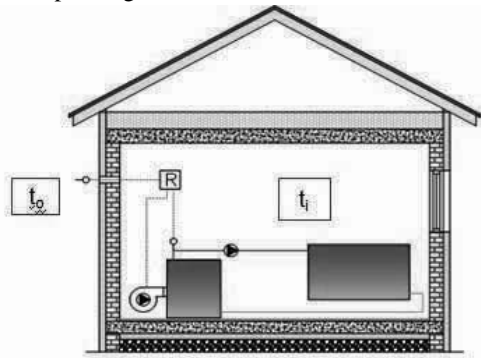
Figure 1. Type 'A' regular gas boiler operated radiator system
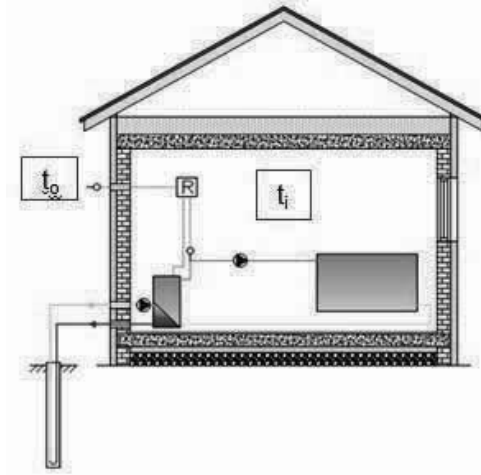
Figure 2. Type 'B' geothermal heat pump supplied radiator system

A complex system's resulting energy efficiency:

$$\eta = \prod_{i=1}^{n} \eta_i \qquad (1)$$

A complex system's resulting exergy efficiency:

$$\eta_{X,FUN} = \prod_{i=1}^{n} \eta_{X,FUN,i} \qquad (2)$$

Exergy efficiency basically is divided into two parts:

$\eta_{x,mech/el}$ – includes mechanical and electrical losses

$\eta_{x,th}$ – includes losses caused by temperature drop (irreversible change). Thus the resulting exergy efficiency of an element can be determined with the following formula [1] [8]:

$$\eta_{X,FUN} = \eta_{X,mech/el} \cdot \eta_{X,th} \qquad (3)$$
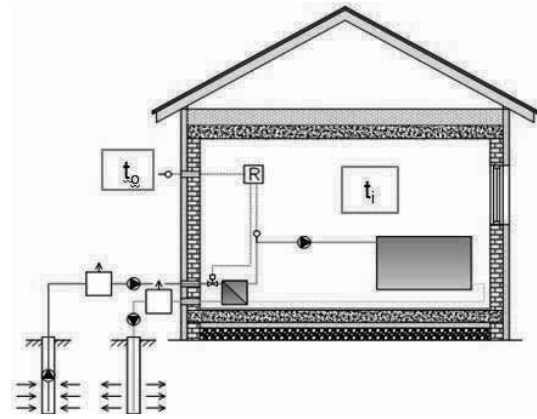
Figure 3. Type 'C' thermal heat supplied system via heat exchanger

Value $\eta_{x,th}$ is calculated from temperature, while value $\eta_{x,mech/el.}$ was taken into account from practical experiences. In the calculations the following values as boundary conditions were assumed [8]:

- The energy efficiency of the regular gas boiler is: 0,9 (which value is considered rather good). The efficiency is assumed to be constant, although it is known that it alters according to fluid and load.
- Electric energy is produced by gas, the assumed efficiency is: 0,5
- Loss factor of heat pump is: 0,6
- Loss of a perfectly insulated heat exchanger is: 0
- The assumed constant medium temperature of thermal water is: 75 °C
- Primer side fluid temperature of the geothermal heat pump is: 10/7 °C
- Electric power used for thermal water exploitation is 5 % of the overall heat exploited (with this assumed value the coefficient of performance is: 20)

TABLE II.
THE TEMPERATURE DATA AND CARNOT EFFICIENCY

Temperatures (°C)	Carnot efficiency of the room	Carnot efficiency of the radiators
T_i = 20 °C T_o = -5 °C T_{fm} = 45 °C	$\eta_{C0i} = (1 - \dfrac{T_0}{T_i}) = 0,0853$	$\eta_{C0fm} = (1 - \dfrac{T_0}{T_{fm}}) = 0,157$
T_i = 20 °C T_o = 0 °C T_{fm} = 40 °C	$\eta_{C0i} = (1 - \dfrac{T_0}{T_i}) = 0,06826$	$\eta_{C0fm} = (1 - \dfrac{T_0}{T_{fm}}) = 0,1278$
T_i = 20 °C T_o = 10 °C T_{fm} = 30 °C	$\eta_{C0i} = (1 - \dfrac{T_0}{T_i}) = 0,03413$	$\eta_{C0fm} = (1 - \dfrac{T_0}{T_{fm}}) = 0,066$

Where:

$T_{fm} - (K)$, $t_{fm} - (°C)$ medium temperature of radiator entering and outgoing fluid

$T_i - (K)$, $t_i - (°C)$ room temperature

$T_o - (K)$, $t_o - (°C)$ exterior (dead state) temperature [8]
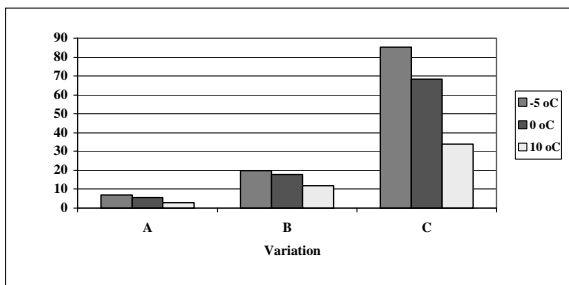
Figure 4.   Exergy efficiency at different systems at three different operation stages
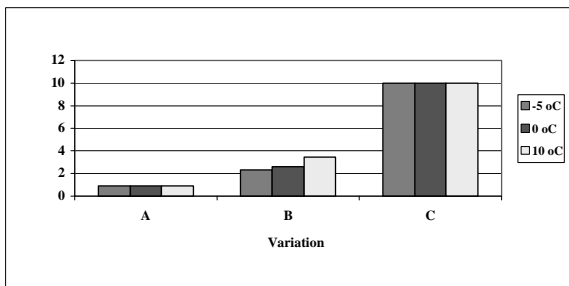
Figure 5.   Energy efficiency, coefficient of performance at three different operating statuses of different systems

The most favorable technical solution regarding the exergy efficiency and the energy efficiency is the thermal water district heat supply system. With the decrease of the capacity demand, exergy efficiency decreases. The amount of the decrease is the smallest regarding the ground heat pump system. According to diagram 'A' and 'C' the energy efficiency and the coefficient of performance are constant, despite the decrease of the capacity need (in reality at existing systems it is known that these factors decrease), while at heat pump system it increases due to the temperature decrease of the heating fluid at condensator side.

IV.   CONCLUSION

In cases of smaller systems exergy analysis is not absolutely necessary; technical sense, energy analysis is sufficient. At larger, complex cases there are many part elements so exergy analysis is necessary to obtain a more realistic picture of the system's thermodynamic efficiency [7].

Some processes cannot be realized without exergy losses to maintain operation of the systems. Avoiding all exergy losses is impossible; decreasing it without limitation is economically unfavorable. However exergy usage of our present systems is multiple of the necessary.

The entering natural gas into combustion system has a great exergy. During the burning process the energy 'suffers' from quality change, it looses significant amount of its working capacity due to irreversibility and exergy losses are great [7].

Today's buildings that fulfill the heat technology requirements have less and less energy demand. Among new buildings especially the passive houses have a low energy demand. Their heating systems are floor, wall, and ceiling heating systems, which are low temperature heating systems with low exergy needs. We proceed correctly if their heat supply is covered with low exergy energy. The great exergy energy sources are more practical to be used to produce great exergy demand electric power, mechanical work, while low exergy demand space heating, DHW production, building cooling should be supplied with low exergy renewable energy sources such as ground heat, thermal water, solar energy, industrial technology's waste energy, or heat energy of sewage.

Our existing energy source management is efficient if quality of supply and consumption match each other. Thereby the amount of consumed fossil primer energy source is decreased as well as the amount of CO_2 emission [7].

V. References:

[1] Müller, H.: Technische Thermodynamik, Wismar, 2000.

[2] Dövényi, P. – Tóth, Gy.: A Kárpát-medence geotermikus és hévízföldtani adottságai, 2008.

[3] Gyné., Halász: Geothermal Energy in Building Energy Supply with Exergy Theory, XIV. Building Services and Mechanical Engineering Professional Days, 2008.

[4] Gyné., Halász: Utility of Geothermal Energy in Building Energy Supply with Exergy Theory, Mechanical Engineering Letters, Selected Collection from the Research Results of Year 2010, Szent István University, 106-120 p. 2011.

[5] Halász Gyné., Kujbus A.: Hazai földhőtermelés és környezettudatosság, 2011.

[6] Magyarország Megújuló Energia Hasznosítási Cselekvési Terve, Nemzeti Fejlesztési Minisztérium, 2010.

[7] (Hungarian National Renewabe Energy Action Plan, Ministry of National Development, 2010.)

[8] Dietrich Schmidt: Methodology for the Modelling of Thermally Activated Building Components in Low Exergy Design, Doctoral Thesis Stockholm, Sweden ISSN 1651-5563, ISRN KTH-BYT/R—04/194-SE, ISBN 91-7283-737-3, 2004.

[9] Halász Gy-né.-Kalmár T.: Különböző hőtermelővel ellátott fűtési rendszerek exergetikai összehasonlítása I.-II. rész, Magyar Épületgépészet, vol. L VI. 12 sz. vol. L VII. 1-2 sz., 2007-2008.

Error in Water Meter Measuring at Water Flow Rate Exceeding Q_{min}

Lajos Hovány*

*PhD, assistant lecturer, Faculty of Civil Engineering, Subotica, Republic of Serbia
e-mail address: hovanyl@gf.uns.ac.rs

Abstract—**The duration of consumption in households is shorter than 1 minute in 95% of consumption cases. The primary aim of this paper is to define the error in measuring consumption shorter than 10 (for Q_{min}=0,03 m³/h), 12,5 (for Q_t=0,12 m³/h) and 4 minutes (for Q_n=1,5 m³/h) for B class water meter with rated diameter of 20 mm, installed in the water supply network of a single household. Error changes in the operation of the water meter were tested by the method of switching off the water meter and by the method without switching off the water meter. During accuracy measurements, water meter readings were as follows: 2,5 centilitres and 1 decilitre. Through testing it has been established: a) that during consumption shorter than the time the meter was calibrated for, the water meter's ranges of measuring error are larger than the ranges of permitted errors, and b) that the biggest errors occur during Q_{min} flow rate.**

Key words: water meter, consumption duration, operation error

I. INTRODUCTION

In line with the Measurement Protocol for Water Meters in the Republic of Serbia, a water meter for water consumption in households is qualified for operation with error below the permitted values, i.e. from ±5% (for Q_{min}) and ±2% (for Q_n and Q_t) from the actual water volume [6]. During calibration, water meter operation errors are checked for the foreseen water volumes. Through this water volume and discharge, the time for which the meter is calibrated was calculated.

TABELE 1.
TIME FOR WHICH THE WATER METER IS CALIBRATED WITH 20 MM RATED DIAMETER, CLASS B (SOURCE:"POTISKI VODOVODI"LTD. FROM HORGOS)

Water discharge	Discharged water volume	Permitted error limit		Time between two readings
m3/h	litres	±%	±litres	minutes
Qmin=0,03	5	5	0,25	10
Qt=0,12	25	2	0,5	12.5
Qn=1,5	100	2	2	4

To eliminate the effects of opening and closing the flow switch to measuring errors during calibration, the standard in force in the Republic of Serbia stipulates the following: „The uncertainty introduced into the volume may be considered negligible if the times of motion of the flow switch in each direction are identical within 5% and if this time is less than 1/50 of the total time of the test" [7]. The same recommendations are given by other standards as well [4, 5]. Based on that, the following is recommended: „Should there be doubts about whether the operation time of the valve affects the results of the tests, it is recommended that the tests should be made longer, and never under 60 seconds" [1]. That is to say, for neglecting the impact of flow switch manipulation on the water meter's measuring errors the standards offer a solution during the calibration of water meter only.

Water consumption in a single household is implemented by the use of taps, washing machine, dishwasher-machine and shower in the bathroom, likewise the flushing cistern of the toilet and the like. Each consumption is characterised by the opening and closing of flow switch and the duration of water discharge from the pipeline in order to satisfy needs. The duration of consumption in households is shorter than 1 minute in 95% of consumption cases [2]. The error in measuring consumption by water meter, due to manipulating the flow switch, practically manifests as an error due to the duration of consumption shorter than the time the meter was calibrated for.

Owing to this fact, the primary aim of this paper is to define measuring errors of consumption shorter than 10 (for Q_{min}), 12,5 (for Q_t) and 4 minutes (for Q_n) of class B water meter with 20 mm rated diameter and flow of Q_n=1,5 m³/hour, installed in the water supply pipeline of a single household.

Water meter operation error depends on water meter reading accuracy [3]. The further aim of this paper is to define water consumption measuring error in households shorter than the time the meter was calibrated for, in the function of water meter reading accuracy.

II. DESCRIPTION OF THE TEST RIG

A water supply pipeline was set up in the Hydraulic Laboratory of the Faculty of Civil Engineering in Subotica, gravitationally supplied from a tank with constant water level, i.e. for 16,25 m higher than the level of the water meter axis. According to both water flow and the water supply pipeline characteristics, the water supply pipeline corresponds to the one of a single household.

For the test rig for a water supply system, new, calibrated multi-jet propeller water meters with wet mechanism were installed for water temperature of 30 °C, and with rated diameter of 20 mm, class B, with the following typical flow rates: Q_{min}=0,03 m³/h, Q_t=0,12 m³/h and Q_n=1,5 m³/h. The water meters were manufactured by Potiski vodovodi Ltd. from Horgos.

During calibration, the reading accuracy of the water meter was 1 decilitre.

A stop valve for starting and stopping water flow was installed at 2,8 m downstream from the water meter.

Water volume flown through the water meter was defined by:

- the difference in reading on the water meter prior and after measuring, and
- measuring water quantity in the vessel (of 15 to 200 litres in volume) and water density.

By measuring time (with stop-watch) between two readings, through the defined water volume in the vessel, the water flow rate Q was calculated.

During accuracy measurements, water meter readings were as follows: 2,5 centilitres and 1 decilitre. Measurement accuracy of water quantity in the vessel was 0,005 kg (for Q_{min}), 0,01 kg (for Q_t) and 0,1 kg (for Q_n).

Under the Measurement Protocol for Water meters of the Republic of Serbia, measuring errors in water meters are:

$$ G = \frac{100\left(Vi - Vc\right)}{Vc}\left(\%\right) (1) $$

where:

Vi – water volume flown through the water meter and registered on the meter's counter, and

Vc – water volume flown through the water meter, measured in the vessel on the scale [6].

Error changes in the operation of the water meter described by equation (1), were tested by applying two methods:

a) by stopping the water meter: according to the valid Protocol of the Republic of Serbia, the status on the water meter and the scale was read prior and after measuring at water meter propeller in stillstand [7], and

b) by a method without stopping the water meter: changes in the status of the water meter and on the scale were monitored with a time interval of 30 seconds without stopping water flow in the installation.
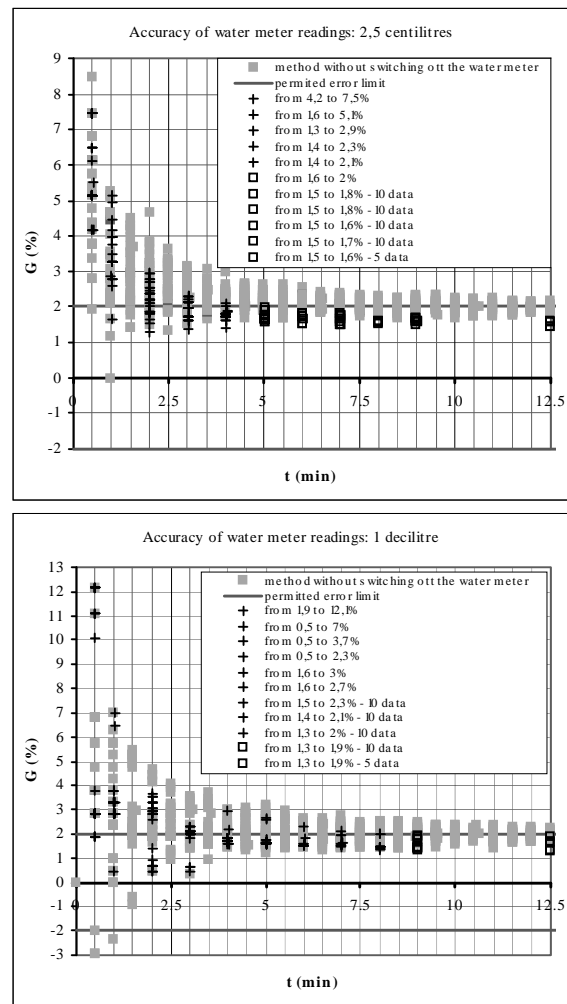
Figure 2. Error in water meter measuring at Q_t flow during water flow shorter than the time for which the meter was calibrated (12,5 min.) in the function of water meter reading accuracy

Figure 1. Error in water meter measuring at Q_{min} flow during water flow shorter than the time for which the meter was calibrated (10 min.) in the function of water meter reading accuracy

The status of the water meter, scale and stop-watch was established by taking photos at the same time during the method without stopping the water meter.

III. RESULTS OF MEASURMENTS

Each measurement was repeated 30 times (There is a remark in the chart key if this number was between 5 and 20).
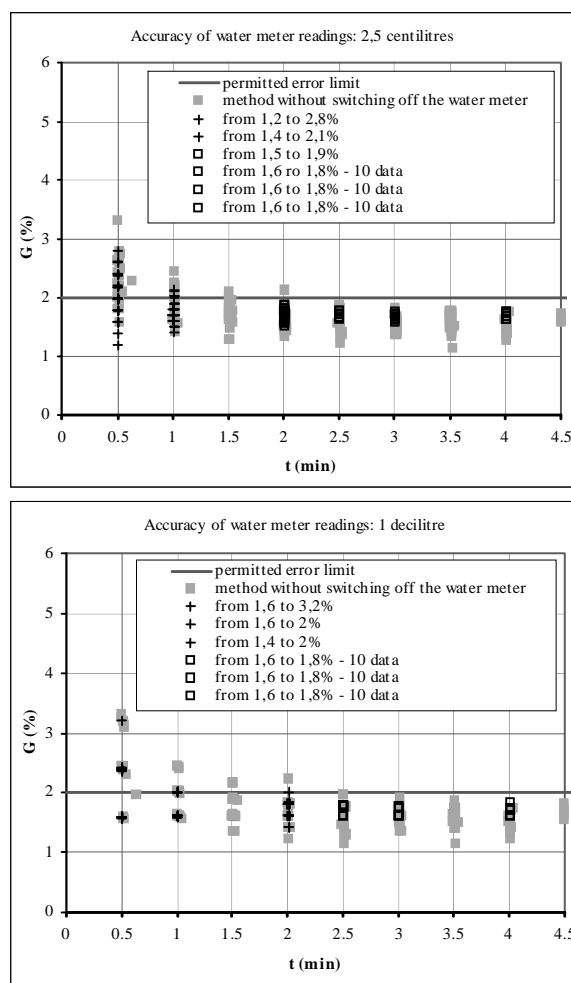
Figure 3. Error in water meter measuring at Q_n flow during water flow shorter than the time for which the meter was calibrated (4 min.) in the function of water meter reading accuracy

IV. DISCUSSION

Both methods of testing provide similar ranges of water meter measuring errors for flows Q_{min} and Q_n. At Q_t flow, the method without stopping the water meter provides larger errors than the method with stopping the meter:

- the most significant allowance (up to 4,7-2,8=1,9%) was registered during the 2 minute long flow, while
- during the time for which the meter was calibrated, the error exceeded (up to 2,2-2=0,2%) the permitted values.

In the case, when consumption time was shorter than the time the meter was calibrated for, the range of the meter measuring error exceeded the range of permitted errors.

ERROR RANGES OF WATER METER MEASURING FOR CALIBRATED DISCHARGES IN THE FUNCTION OF WATER METER READING ACCURACY (CLASS B, RATED DIAMETER OF 20 MM AND DISCHARGE OF $Q_N=1,5$ M3/H),FOR A DURATION OF 0,5 MINUTES FLOW

Reading accuracy	Discharge	Error range (%)	
		For both methods	During calibration
2,5 centilitres	Q_{min}	from -7,4 to 32,1	
	Q_t	from 2 to 8,5	
	Q_n	from 1,2 to 3,3	
1 decilitre	Q_{min}	from -25,9 to 56,9	±5
	Q_t	from -2,9 to 12,1	±2
	Q_n	from 1,6 to 3,2	±2

It means that during consumption shorter than the time the water meter was calibrated for, measuring by the meter is unreliable in 95% of the consumption shorter than 1 minute. During a discharge of 0,5 minutes, the error may be even 56,9%.

V. CONCLUSION

For calibration discharges, foreseen by the Protocol, through the testing of class B flow meter with 20 mm rated diameter and discharge of $Q_n=1,5$ m^3/h, it has been established, that:

- in the case, when consumption time was shorter than the time the meter was calibrated for, at discharges of , the range of the meter measuring error exceeded the range of permitted errors, and
- the biggest errors occur at Q_{min} – for example, at discharge lasting for 0,5 minute, the error may be even 32,1% (for water meter reading accuracy of 2,5 centilitres), or even 56,9% (for water meter reading accuracy of 1 decilitre).

Since it concerns 95% of water consumption measurement, such testings are necessary for all types of water meters used in the supply networks of this country.

REFERENCES

[1] Arregui, Francisco; Cabrera Jr., Enrique; Cobacho, Ricardo 2006 Integrated Water meter Management. IWA Publishing, London.
http://www.iwaponline.com/wio/2007/01/pdf/wio200701RF18433 90345.pdf

[2] Buchberger, Steven G.; Wells, Greg J. 1996 Intensity, Duration, and Frequency of Residential Water Demands. *Journal of Water Resources Planning and Management* **122**(1), 11-19.

[3] Hovanj, Lajoš 2010 Minimalno vreme između dva očitavanja vodomera. *Zbornik radova Građevinskog fakulteta*, Subotica 19, 105-113.

[4] ISO 4064-3:2005(E) Measurement of water flow in fully charged closed conduits – Meters for cold portable water and hot water. Part 3: Test methods and equipment.

[5] OIML R 49-2: 2006 (E) Water meters intended for the metering of cold potable water and hot water. Part 2: Test methods.

[6] Pravilnik 1986 Pravilnik o metrološkim uslovima za vodomere. – Službeni list SFRJ, Beograd 51, 1509-1513.

[7] SRPS EN 14154-3: 2010 (en) Merila protoka vode. Deo 3: Metode ispitivanja i oprema.

Alternative energy source from Earth's core, combined accumulation of solar energy – downhole heat exchangers with heat pump

Dr M. Kekanović [*], Dr D.Šumarac[**] and A. Čeh [***]

[*],[***] Faculty of Civil Engineering, Subotica, Serbia
[**] Faculty of Civil Engineering, Belgrade, Serbia
[*]*kekec@gf.uns.ac.rs*
[**] *sumi@eunet.rs*
[***] *ceh@gf.uns.ac.rs*

Abstract—**The article offers new technical solutions for solar energy accumulation around the vertical downhole heat exchangers (DHE) in the surface of Earth's crust (depth of up to 100 m). In order for the Vertical DHEs to be more efficient and reach surplus thermal energy from the Earth's core in greater quantities, its length should be from 300 to 400 m instead of 120 m. These measures could fully support heat pumps and improve their coefficient of performance (COP) with an excellent value far above 6. Thus granting a rational solution in using a completely renewable ecological energy source and can be applied on bigger scale for heating and cooling large industrial facilities, resorts and even major cities. Dangerous energy sources like nuclear power and fossil fuels can absolutely be avoided from being use. Furthermore, implementing these solutions is exceedingly important reason as to avoid volcanic eruptions, tectonic plate shifts, earthquakes and ravaging tsunamis by reaching and intensively using the so-called "surplus" power of the thermal energy of the Earth's core.**

I. INTRODUCTION

At the beginning of twentieth century, heat pumps have been developed as a technical solution and since then they are in use only individually but never for the whole village or town. Presently, heat pumps had been improved with a coefficient of performance (COP) of even more than 5.

The principle of heat pump consists in the fact that they absorb thermal energy from one place and transfer to another (Fig.1). The thermal energy is taken from the ground (Earth's crust) thus use mostly the downhole heat exchangers (DHE) that is a few tens of meters deep (60-120 m). Another way to use thermal heat from the ground is by burying pipes or from the water in the streams, lakes and the sea. Groundwater-source heat pumps are not environment - friendly and are rarely practiced in EU as well as other developed countries. [6], [7]

Heat pumps are the perfect technical solution, but the quality of thermal energy exploited from the ground thru heat exchangers is a big problem that needs yet to be improved.[2] The difficulty restricts the possibility to use heat pumps for even a small community with less than 10,000 inhabitants.

Earth's crust is composed of materials like clay, stone, sand, water, with their own thermodynamic parameters with different coefficient of thermal conductivity k (Table I.).The overall heat transfer coefficient U (W/m^{2}K) depends on coefficient of thermal conductivity k (W/mK):
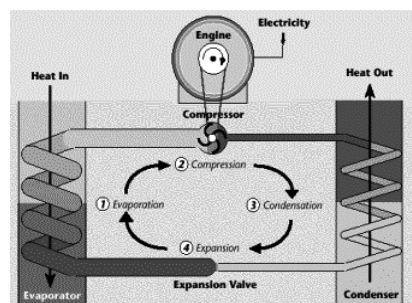
Figure 1. The operating principle of the heat pumps [8]

$$k = \frac{\Delta Q}{\Delta t} \frac{1}{A} \frac{d}{\Delta T} \, , \qquad (1)$$

where:
$\Delta Q/\Delta t$ - rate of heat flow
A - total cross sectional area of conducting surface,
ΔT - temperature difference,
d - thickness of conducting surface separating the two temperatures.

$$U = \frac{1}{\dfrac{d}{k}} . \qquad (2)$$

Since d is the thickness of the layers of soil around the heat exchangers, the expression for the overall heat transfer coefficient U takes on a very small value:

$$d \to \infty \Rightarrow U \to 0 . \qquad (3)$$

Practically this means a large heat transmission resistance R (m^{2}K/W) from the surrounding soil to the heat exchangers.

$$R = \frac{d}{kA} \qquad (3)$$

66

TABLE I.
THE AVERAGE VALUE OF THERMAL CONDUCTIVITY COEFFICIENT FOR MOST FREQUENT MATERIALS IN THE EARTH'S CRUST

Components	Material			
	Clay	Sand	Stone	Water
Coefficient of thermal conductivity (k)	0,8 - 1,3	0,58 - 1,3	1,2 - 3,3	0,83

Based on the thermal conductivity coefficient (k) values for the materials in the Earth's crust, in Table I., it can be concluded that these values are not high and these materials in the Earth's crust – in which immersed the heat exchangers of the heat pump – are heat insulating barrier for the thermal energy of the surrounding environment.

Exploiting the heat from the earth is a particular problem as the geometrical characteristics of DHEs are thin in cross section with a small surface area and are practically one line in the longitudinal section. In recent time DHEs are typically made from materials that are polymer based for better corrosion resistance plus with lower value of thermal conductivity coefficient k and with meager heat conduction.

Thus, during function it often happens that the heat in the ground around the DHEs is not completely recovered. As a result, in this zone, the temperature falls down, which also means a decrease in heat capacity of the heat exchangers (Fig. 2). After a few years it is possible for the DHEs to malfunction.
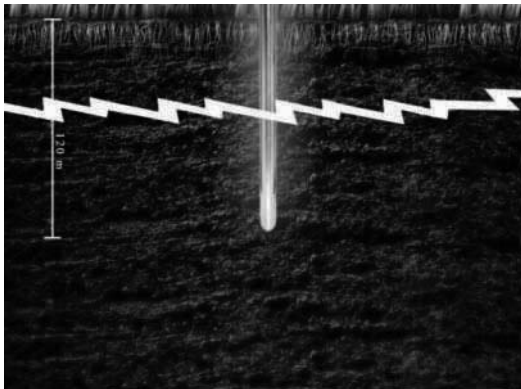
Figure 2.   Cooling of the Earth around the heat exchangers

An event from Sweden is a proof in where the temperature of the soil in the early period of utilization was +8 ℃. [3] After twenty seven years of exploitation, a decrease in heat from +8 ℃ to +1 ℃ was noticed. Every year, due to the inactiveness of the ground, through the insulating properties of the earth manifested by the thermodynamic coefficient of thermal conductivity (k) and the dense installation of DHE, the heat was not restored completely to its previous degree after the heating season. Thus, a fall in the temperature of the Earth of only 0,26 ℃ was noticed each year and increased to 7 ℃ after 27 years.

Another practical evidence for this claim of heat energy accumulation is the possibility in the earth is from distant history. Romans were digging combustion furnace into the ground to a depth of several meters and hot air from the

furnace passes through enclosed areas under floor and inside the walls, after flowed out in the roof – a system known as "hypocaust". At start they had higher heat energy losses, then later on when the heat were already accumulated around the fireplace, with a significantly lesser fuel they could hold the temperature inside the rooms, and afterwards it would be needed in the case when the furnace and the air-flow channels would not be buried. (Fig. 3).
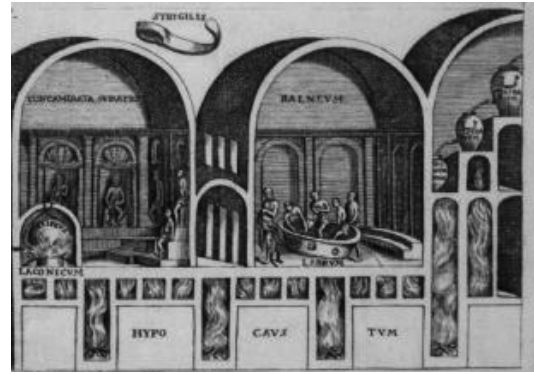
Figure 3. Way of heating at the time of ancient Rome with the aim of accumulation of heat in the ground around the furnace[11]

All of this clearly indicates that the DHEs depth of heat pumps have a number of deficiencies that must be improved so that the solution could be applicable not only individually but also for the largest cities in the world with millions of inhabitants:

1) DHEs length of 120 m is not enough – but rather should be at least 300 m length to be able to take excess energy from the Earth's core.

2) Around DHEs in the surface area of Earth's crust (to depths of 100 m), solar energy should be accumulated using solar collectors.

3) The heat exchangers should be made of metal or a material with a dominant share of metal content in the volume to achieve higher value of coefficient of thermal conductivity (k) and enhanced overall heat transfer coefficient (U)

4) Cementing the boreholes around the DHEs should be done with materials that are hygroscopic and using water (moisture) heat exchange would be faster

II.   A NEW TYPE OF DHEs AS PASSABLY SUPPORTING SOLUTION FOR EXPLOITATION OF THERMAL HEAT WITH HEAT PUMPS

Earth's core temperature is between 4000 and 7000 ^{0}C. Such high temperature is the result of thermonuclear processes initiated during the formation of the Earth itself. Controlled drawing of energy from the Earth's crust could give positive effects as more energy is produce than is released by layers to the surface in the Earth's core. Preventing the release of heat energy from Earth's core creates more pressure inside itself. That pressure is transmitted on the layers around the core, which starts to tighten and that time comes to form new cracks, usually at the place of old ones. This particularly occurs in zones of

tectonic disturbances, which are described as movements of tectonic plates. (Fig. 4).
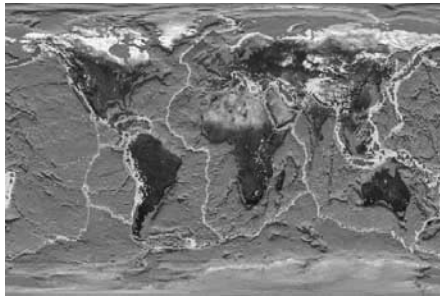
Figure 4. Tectonic plates with fault lines and areas with frequent occurrences of volcanoes and related phenomena - earthquakes and tsunamis [9]

Movements of tectonic plates usually occur because of the existence of volcanoes on the seabed. Another way of releasing energy and pressure within the Earth's core are volcanic eruptions that occur on land. In both cases, especially if we have volcanoes in the sea, a devastating earthquake can evoke tsunamis (Fig. 5). Earth itself naturally regulates the pressure and temperature inside its core. Volcanoes and tectonic plate movements are "safety valves" that Earth itself conditions. Unfortunately, catastrophic consequence happens to humanity itself. If this is true, and the physical logic suggests that it is, then people with artificial interventions should seek solutions in the sense to consume excessive heat from the Earth's core and thus reduce the internal pressure around the core. This would avoid the catastrophic consequences of earthquakes, volcanoes, tsunamis, and at the same time humanity would get the much needed natural renewable energy without burning fossil fuels and CO_2 emissions.

Instead of 120 m, the DHEs should have a length of 300 to 400 m, so that besides the use of solar energy in the upper part (up to 100 m depth), the thermal energy from the Earth's crust can be used more rigorously at the bottom of DHE. The depth from 300 to 400 m, the temperature of the Earth's crust ranges from +40 to +50 °C.
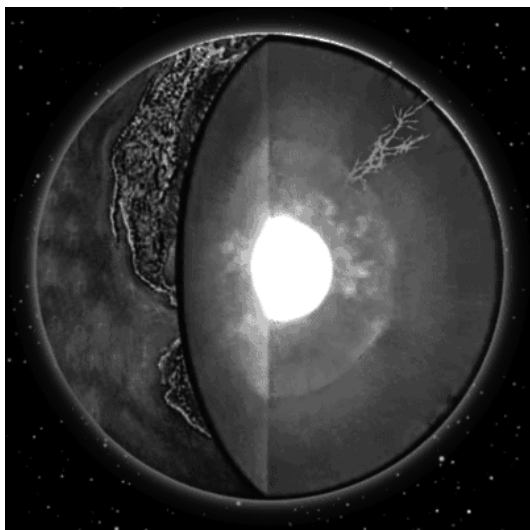
Figure 5. Slice of the Earth from core to cosmic space with spots of Earth´s "valves" - volcanoes and tectonic plate faults

Figure 6. A technical solution to transport solar energy from solar collectors to the vertical DHE

One logical solution in regard to all mentioned problems is to restore the thermal energy in the surface layer of the Earth's crust by constant, intense and renewable solar energy, especially in areas of large consumers such as industrial plants and cities.

Based on the low value of heat transfer coefficient (k) in the ground around the DHE, it can be concluded that the Earth's crust would be a much better accumulator, than a conductor of heat. This leads to the idea that a cheap storage of solar energy could be made, that almost throughout the year, with solar collectors can be transported into the ground, around the DHEs[4].

It is entirely feasible technically in the manner as shown in Figure 6.With solar thermal collectors (flat plate collectors or concentrators) solar energy is transported by liquid medium known as glycol in case of temperatures that is up to +100 °C, or thermal oil if the temperatures are higher than +100 °C. Heat-transport fluid transferring the thermal energy into the ground by thin tubes made from stainless steel (Ø = 15 mm) which are spirally wrapped around the vertical DHE [5].

The heat transfer starts from a lower point (approx. at 1/3 of its length) and so DHE is wrapped with thin stainless steel tubes starting from below (from 100 m depth and up) Fig. 7.

These thin tubes must be made of materials resistant to chemical aggression and simultaneously must have a high coefficient of thermal conductivity (k) in order to deliver energy easier and faster.
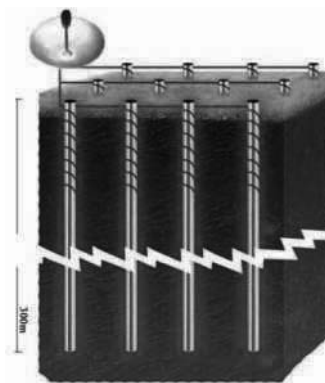
Figure 7. Technical solution of vertical DHE using solar energy accumulated in the surface layer and the excess heat of the Earth's core

If the walls of the DHEs are made of aluminum, or composite materials containing aluminum in its structure, the coefficient of thermal conductivity's value would be k = 200 W/mK or as a composite material with value of k = 50 W/mK and if such is the case, could easily warm and transform the thermal energy to liquid medium (glycol) inside the DHE and finally heat pumps. Under such circumstance might subtract heat from the ground between 10 and 20° C, which is several times more energy than using the current methods of exploitation. It is important to emphasize that DHE system would be stable in terms of heat capacity and it could reach 0,15 to 0,35 kW/m². In other words, a 300 m long DHE could give at least 30 kWh of energy to heat pumps with the assurance that energy will be renewed continuously. The quantity of exploited thermal energy depends on the surface area of the DHE, temperature conditions of the ground, the coefficient of thermal conductivity (k) of the material around the probe, the material from which the probe and the liquid media (water or glycol) are made of. The DHEs depth of up to 15 m can be insulated from the outside and cannot exchange heat with the external environment. During one heating season under above mentioned conditions, temperature around DHE can deliver about 100 MW of thermal energy from ground, which is several times more than today's conventional results.

If the boreholes would be secured with technology of cementing, it should be done with materials that would be hygroscopic. Namely, hygroscopic materials would draw moisture - water and thus the thermal energy would be faster drained in this case, since the c coefficient of thermal conductivity of water is, k = 0.83 W / m K and the specific heat capacity of water is c = 4190 J / kgK. Water is, indeed, the best medium for the transfer of thermal energy and this property can be utilized in the Earth's crust using DHEs.

In order to quickly and easily drill deeper (300 to 400 m), it is necessary to develop an entirely new type of heat exchanger that could be use simultaneously for drilling and later on settle and ensure the borehole itself. Filling of the boreholes could then be omitted if such pipes can take the pressure. Within these probes after the completion of drilling, pipes are lowered with glycol, which transports the heat taken by the heat pump.

III. CONCLUSIONS

This paper offers new technical solution using a combination of two thermal energy sources: the Sun and the Earth's core. (Figure 8.)
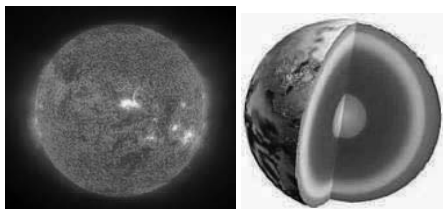
Figure 8. The sun and the Earth´s crust - inexhaustible sources of cheap and environmental-friendly renewable energy for life on Earth [10]

Figure 9. Benefits of changes - no icy roads and sidewalks in large cities

The general belief of physicists for a long time and even until today is that the accumulation of heat in the Earth's crust is not possible because of its large mass and relatively high coefficients of thermal conductivity (k) for material; Earth's crust is built up (Table 1). These presumptions are even more theoretically wrong since these materials have thick layers. Consequently it is not so important that the coefficients of thermal conductivity of these materials in Earth's crust have higher values than usual insulation materials. Heat resistance during heat transfer will definitely be more loaded in view of the large width (d) of layers. After all it can be clearly concluded from (2).

Specifically, this impossibility of fast (equalization) inflow of thermal energy by the thermodynamic laws, in which limits the capacity and service life of heat pumps as well as demonstrating clearly that the Earth's crust could be a better conductor for heat rather than an accumulator. We had also stated 2 evidences for this claim: the example of heat pumps with DHEs from Sweden and the well known Roman system of underfloor heating that had been proven for centuries. All this suggest that it could be possible to accumulate thermal energy in the earth and most likely it can be accomplished easier with solar energy - as with an inexhaustible source.

Accumulation of solar energy around the vertical DHE on the surface of the Earth's crust (depths up to 100 m) is almost possible all year. Furthermore, a DHEs length of 300 to 400 m instead of 120 m is proposed in order to be more efficient and reach the surplus thermal energy from the Earth's core in greater quantities. These measures could fully support heat pumps, and even improved their coefficient of performance (COP) with an excellent value far above 6. Through this a rational solution of using a completely renewable ecological energy source would be granted which is applicable on bigger scale for heating and cooling large industrial facilities, resorts and even major cities (Fig.9.). A high class energy efficiency of A^+ can also be achieved. Buildings in average, the leading consumers of energy in the world, use 50% of the total produced energy. The consumption can enormously be reduced up to 15% using the described solution. Dangerous energy sources like nuclear power as well as fossil fuels can be completely avoided from being use. There is a possibility with deeper boreholes of up to 1500 m and by thermal oil as a medium for heat transfer, and to build electric power plants of few hundred MW. DHEs can even supply steam turbine by taking a part of the Earth's core heat and a fraction from the large solar

collector-concentrator, which would raise the heat around the DHE to a temperature of up to 200 ºC(Fig.10).
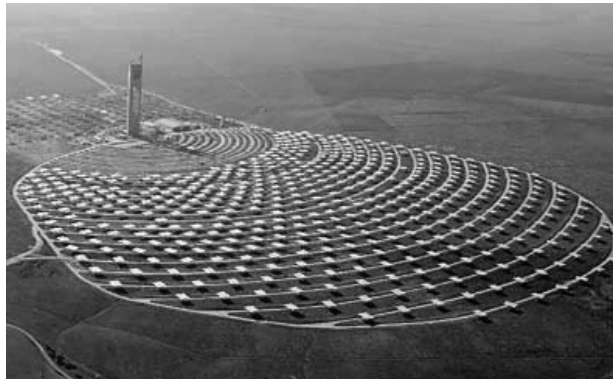
Figure 10. Solar energy captured by solar collector-concentrator of several 10 MW would be transported in the ground around the 1500 m length vertical DHEs[12]

In addition to obtaining cheap and environmentally renewable energy, by implementing these solutions there is a real opportunity to avoid volcanic eruptions, tectonic plate shifts, earthquakes and devastating tsunamis through reaching and intensive use of the Earth's core thermal energy, a so-called "surplus" energy. These surplus energies causes the increase of pressure within the core and stress-tension in the layers of the Earth's crust that crack in places of previous cracks and lines of moving tectonic plates (Fig. 5). And similarly lead to volcanic eruption, which together with dislocation of tectonic plates can cause the onset of devastating earthquakes and tsunamis. Earth on a natural behavior performs the regulation of pressure and temperature inside the core. Instead of Earth itself uncontrollably activating its "safety valves", volcanic eruptions and tectonic plate movements, it is logical for us people to use the surplus of environmental and renewable energy in a natural manner and satisfy humanity, concurrently avoiding catastrophic devastation. The issue of Earth's over-heating and melting of ice at the poles does not only need to be due to the "greenhouse-effects".[1] The reasons for this may exist even in the Earth's crust, where surplus thermal energy "arrives" from the Earth´s core.

REFERENCES

[1] P.Blum, G. Campillo, W. Munch, T. Kölbel, ″CO$_2$ savings of ground source heat pump systems – A regional analysis″, *Renewable Energy*, vol 35, pp.122–127, 2010

[2] G. Hellstrom "Thermal performance of borehole heat exchangers", *The Second Stockton International Geothermal Conference,*1998

[3] F. Karlsson, M. Axell, P. Fahlen, ″Heat Pump System in Sweden″, *Country reports Task 1* – Annex 28, pp. 1-29, 2003

[4] M. Kekanovic, WO/2001/059794 – *Heat Echanger for geothermal heat-or cold*, WIPO,16.08. 2001.

[5] M. Kekanovic, A Ceh, I Hegedis, "Respecting the Thermodynamics Principles of the Heat Transfer – as the Most Important Condition for Achieving High Energy Efficiency in Buildings – Energy of the Ground and Heat Pumps – the Most Reliable Alternative Energy Source", *"3rd IEEE International Symposium on Exploitation of Renewable Energy Sources"*, Subotica, pp.79-84,2011

[6] L. Rybach, B. Sanner, ″Ground-Source Heat Pump Systems the Europian Experience″, *GHC BULLETIN*,pp. 16-26, March 2000,

[7] B. Sanner, C. Karytsas, D. Mendrinos, L. Rybach, ″ Current status of ground source heat pumps and underground thermal energy storage in Europe″, *Geothermics 2003*, vol.32, pp.579–588, 2003

[8] www.filterclean.co.uk/aboutus.htm

[9] www.analogija.com

[10] www.homeofsolarenergy.com/image-files/advanta

[11] http://www.dailymail.co.uk/news/article-1345586

[12] http://www.solarpaces.org/Tasks/Task1/ps10.htm

Environmental External Costs Associated with Airborne Pollution Resulted from the Production Chain of Biodiesel in Serbia

F.E. Kiss[*], Đ.P. Petković[**] and D.M. Radaković[***]

[*] University of Novi Sad/Faculty of Technology, Novi Sad, Serbia
[**] University of Novi Sad/Faculty of Economics, Subotica, Serbia
[***] University of Novi Sad/Faculty of Agriculture, Novi Sad, Serbia
ferenc1980@gmail.com; pegy@ef.uns.ac.rs; radakovic@nscable.net

Abstract—**The Impact Pathway Approach was combined with Life Cycle Assessment method in order to evaluate the external costs caused by airborne emissions released during the production chain of biodiesel in Serbia. The external cost associated with the production of one metric tone of biodiesel was estimated to be 315 EUR. The positive external effects resulting from the absorption of atmospheric CO_2 by rapeseed plant can reduce the overall external cost to 181 EUR per metric tone of biodiesel. The agricultural stage is responsible for 85% of the overall external cost, in particular due to the emissions of N_2O and NH_3 from agricultural soil.**

Keywords: external costs, biodiesel, life-cycle, Serbia

I. INTRODUCTION

An external cost, also known as an externality, arises when the social or economic activities of one group of persons have an impact on another group and when that impact is not fully accounted, or compensated for, by the first group. Bio- and fossil diesel fuelled vehicles are an important source of emissions of many pollutants. The emission of these substances causes considerable damage affecting a wide range of receptors including humans, flora, fauna and materials. For example, a road vehicle that generates emissions of SO_2, causing damage to building materials or human health, imposes an external cost. This is because the impact on the owners of the buildings or on those who suffer damage to their health is not taken into account by the road vehicle operator.

Considerable attention has been focused recently on the assessment of external costs resulted from the tailpipe emissions of bio- and fossil diesel fuelled vehicles (for review see [1]). However, very few studies exist that have attempted to examine the external costs associated with upstream processes, i.e. with the production chain of diesel fuels in Serbia. The goal of this paper is to evaluate the external costs caused by airborne emissions released during the production chain of biodiesel in Serbia. The environmental external costs associated with emissions into water and soil, or depletion of natural resources (e.g. geological reserves of fossil fuels, land use) were not taken into account. Therefore, the estimated external cost represents the lower bound of the potential environmental external costs arising from the production of biodiesel.

In Serbian context the investigation of potential environmental and social effects of biodiesel has become increasingly important after the ratification of the South-East European Energy Community Treaty between EU and Serbia in 2006. By ratifying the Treaty Serbia has accepted the obligation to apply Directive 2003/30/EC which requires the utilization of biodiesel and other fuels from renewable sources in transport [2].

II. METHOD AND MATERIALS

A three-step procedure was adopted to calculate the external costs associated with the production chain of biodiesel.

In the first step the airborne emissions associated with each of the stages in the production chain of biodiesel were quantified using the Life Cycle Inventory (LCI) analysis. The analysis was limited to the following airborne emissions: CO_2, CH_4, N_2O, NH_3, NMVOC (non-methane volatile organic compounds), SO_2, NO_x (nitrous oxides), $PM_{2.5}$ (particles with diameter bellow 2.5 μm) and PM_{co} (particles with diameter bigger than 2.5 μm). The LCI analysis was aided by the use of the SimaPro 7 software.

In the second step appropriate damage cost factor for each of the airborne pollutant investigated was adopted. The damage cost factor represents the environmental external cost caused by the emission of a pollutant.

Finally, the overall external cost is calculated using (1).

$$EC = \sum_{i=1}^{n} EQ_i \cdot C_i \qquad (1)$$

Where:
EC – Total external cost associated with air pollution from the production chain (EUR/mt biodiesel)
EQ_i – Emission quantity of pollutant i in the production chain (kg/mt biodiesel)
C_i – Damage cost factor for the pollutant i (in EUR/kg)
n – Number (type) of airborne pollutant

The process chain for biodiesel production consists of rapeseed cultivation, grain drying, pressing and solvent extraction of rapeseed oil, refining the crude rapeseed oil, transesterification of rapeseed oil into biodiesel, and finally, distribution of biodiesel to final consumers. The main product flow normalized in terms of the production of one metric tone (mt) of biodiesel is presented in Fig. 1. Each stage of the process chain is discussed in more detail in following section.

Process description and input data

Rapeseed production. The method of cultivation and harvesting of oilseed rape modeled in this study as far as possible reflects the usual practice in Vojvodina. It was assumed that the annual yield was 2,305 kg rapeseed per hectare based on average yields of rapeseed in Vojvodina in a five year period (2005-2009). A sowing rate of 5 kg per hectare is assumed. Nitrogenous fertilizer is applied at a rate of 140 kg N/ha, corresponding to 400 kg/ha ammonium nitrate (35% N). Furthermore, the crop was fertilized with 40 kg P_2O_5/ha and 80 kg K_2O/ha, corresponding to 83 kg triple superphosphate fertilizer and 133 kg potassium chloride fertilizer, respectively. As a result of chemical and microbiological processes in the soil during cultivation, it was assumed that the air emissions of NH_3, N_2O and NO were 74 g, 35 g, and 16 g per kg nitrogen supplied, respectively [3]. Regarding pesticides, 1 kg/ha of the herbicides Fusilade forte and BOSS 300 SL were used to control weeds and 0.25 kg/ha of Megatrin 2.5 EC was used as insecticide. The emissions from the process chain of fertilizers and pesticides were calculated after [4].

For the cultivation operations, the total fuel consumption was estimated at 90 l diesel fuel (3,228 MJ) per hectare based on [5]. The air emissions associated

Figure 1.   Main material flows related to the production of 1,000 kg biodiesel in Serbia

with the manufacturing of diesel fuel were calculated with data presented by [6] while the airborne emissions from the combustion process were taken from [7]. The volume of lubrication oil consumed was assumed to be 0.1 l/l of the diesel fuel used based on [8]. Furthermore, it was assumed that manufacturing of lubrication oil results in the same amount of emissions as manufacturing of diesel oil.

After harvesting raw rapeseed grain is transported via diesel truck to the dryer which is located 37.5 km away. Data on air emissions associated with the combustion of diesel fuel in a truck were taken from [9].

Seed drying. In Vojvodina oilseed is harvested with a typical moisture content of 13.5%, which must be reduced to at least 9% as a requirement for the oil extraction facilities, and to ensure stability in storage [10]. It is assumed that the drying process takes place at a vertical gravity dryer Strahl 5000 FR (Officine Minute, Italy) powered by fuel oil and three electric fans of overall installed capacity of 54 kW. According to [10] the heat requirement of the process is 260 MJ/mt of dried grain and electricity is consumed at a rate of 2.7 kWh/mt of dried grain. The data source regarding airborne emissions associated with electricity and heat generation are specified in Table 1. The dried grain is transported via diesel truck to the oil mill plant which is located 37.5 km away.

Solvent extraction and oil refining. After the drying process, typical oilseeds contain 40-44% oil and 54-58% high protein meal [11]. The oil is extracted from the dried rapeseed by solvent extraction which is the most dominant technology in the rapeseed oil industry. The material and energy requirement of the process is based on data presented by [11]. The process involves seed cleaning, cooking and flaking, before the seed is in an appropriate state for mechanical pressing to remove a proportion of the oil. After mechanical pressing, the rape meal still contains a significant amount of oil; counter-current solvent extraction of the meal with hexane is used to reduce this oil content to ca. 2%. The only material used in the solvent extraction is hexane at a rate of 1.19 kg per mt of crude rapeseed oil. The heating requirement of the plant is provided by steam produced from light fuel burned in industrial boiler, using 43 kg (1,797 MJ) light fuel oil/mt crude rapeseed oil produced. Electricity is required at 419 MJ/mt of crude oil produced.

In the refining step the phospholipids from the crude rapeseed oil are removed by the addition of phosphoric acid (H_3PO_4). The remaining free fatty acids are converted to soap by the addition of sodium hydroxide, and removed using a centrifuge. Other impurities are removed via filtration using acid treated natural clay. Data on material and energy requirement of the refining process is available from [11]. Light fuel oil is required at 6.1 kg/mt crude oil to provide the refining plants' heating and electricity is required at 104 MJ/mt of refined oil. The refined oil is transported with diesel truck to the nearby transesterification plant located 1 km away.

Transesterification. The transesterification of refined rapeseed oil into biodiesel takes place at a state of art
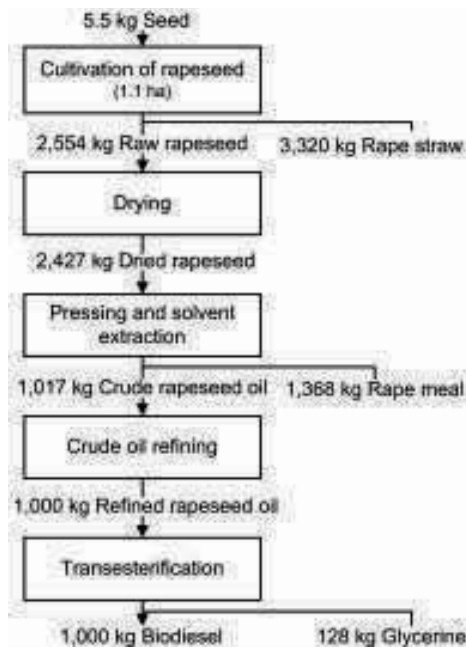
biodiesel production facility with annual production capacity of 100,000 mt of biodiesel. The transesterification process is performed with methanol in the presence of sodium methoxide as an alkali catalyst. The material and energy inputs of the process are described in [12]. The emissions to air during the transesterification process were assumed to be negligible. After the transesterification process biodiesel is transported to the final consumer located 25 km away.

Tab. 1 gives an overview of processes included in the LCI of biodiesel with specification of material and energy inputs and references to data sources used.

LCI assumptions

Allocation procedure. The production of biodiesel generates by-products like rape straw, rape meal and glycerol (Fig. 1). The purpose of allocation is to determine how a particular environmental burden, e.g. CO_2 emission, should be shared amongst the biodiesel and the by-products. The allocation procedure adopted in this study is based on economic allocation, i.e. the overall environmental burden of the system is shared amongst biodiesel and by-products proportionally to their share in the overall revenue of the system. The market prices used to calculate the revenues from biodiesel and co-products

are as follows: 265 EUR/mt of raw rapeseed, 28 EUR/mt of rape straw, 730 EUR/mt of refined oil, 170 EUR/mt of rape meal, 900 EUR/mt of biodiesel, and 80 EUR/mt of glycerol.

Accounting for CO_2 absorbed by the plant. A certain amount of carbon from the air is absorbed by the plant during the process of photosynthesis. This carbon can be accounted for as a positive externality and eventually subtracted from the overall external costs of biodiesel production chain. According to [19] the carbon content of raw rapeseed grain is 58.4% on a mass basis. Under the assumption that all of the carbon is absorbed from the atmosphere it can be calculated that during the production of 2,554 kg raw rapeseed grain 1,491 kg of carbon is absorbed, corresponding to 5,469 kg of CO_2. Of the 1,491 kg of carbon taken up by the rapeseed plants in the agriculture stage, we take credit for only 736 kg of carbon; which equals the biomass-derived carbon content of 1,000 kg biodiesel fuel [3]. This is equivalent to 2,700 kg of CO_2 removed from the atmosphere for every mt of biodiesel produced. The remaining uptake of CO_2 is associated with by-products in the production chain of biodiesel (i.e. rapeseed meal and glycerine). We did not feel it was appropriate to take credit for this carbon.

TABLE I.
MATERIAL AND ENERGY INPUTS IN THE PRODUCTION CHAIN OF BIODIESEL

Stage in the production chain	Source of airborne emission	Inputs of material and energy		Source of data on emissions
		Unit	Quantity	
Rapeseed cultivation and harvesting	Production and use of ammonium nitrate fertilizer	kg N/ha	140	Ref. [4]
	Production of triple superphosphate fertilizer	kg P_2O_5/ha	40	Ref. [4]
	Production of potassium chloride fertilizer	kg K_2O/ha	80	Ref. [4]
	Production of pesticides	kg/ha	1.25	Ref. [4]
	Production of sowing seeds	kg/ha	5	Ref. [4]
	Production and combustion of diesel fuel in agricultural machinery	MJ/ha	3,228	Ref. [6, 7]
	Production of lubrication oil	MJ/ha	322	Ref. [6]
	Transport of rapeseed grain to dryer via diesel truck	tkm/ha	173	Ref. [9]
Drying of the rapeseed grain	Production and combustion of light fuel oil for process heating	MJ/mt of dried seed	260	Ref. [6]
	Production of electricity	kWh/mt of dried seed	2.7	Ref. [13]
	Transport of dried grain to oil mill via diesel truck	tkm/mt of dried seed	75	Ref. [9]
Pressing and solvent extraction	Light fuel oil production and combustion in steam boiler	kg/mt of crude oil	43	Ref. [6]
	Production of electricity	MJ/mt of crude oil	419	Ref. [13]
	Production of hexane	kg/mt of crude oil	1.19	Ref. [14]
Crude oil refining	Production of electricity	MJ/mt of refined oil	104	Ref. [13]
	Light fuel oil production and combustion in steam boiler	kg/mt of refined oil	6.2	Ref. [6]
	Production of phosphoric acid (85% in H2O)	kg/mt of refined oil	0.8	Ref. [15]
	Production of sodium hydroxide (50% in H2O)	kg/mt of refined oil	2.1	Ref. [15]
	Production of sulphuric acid (100%)	kg/mt of refined oil	1.9	Ref. [15]
	Production and consumption of bentonite (clay)	kg/mt of refined oil	9	Ref. [16]
	Transport of refined oil to biodiesel plant via diesel truck	tkm/mt of refined oil	1	Ref. [9]
Transesterification of refined oil into biodiesel	Production of electricity	kWh/mt of biodiesel	12	Ref. [13]
	Natural gas production and combustion in industrial boiler	MJ/mt of biodiesel	1,236	Ref. [17]
	Production of sodium methoxide (100%)	kg/mt of biodiesel	5.0	Ref. [18]
	Production of sodium hydroxide (50% in H2O)	kg/mt of biodiesel	1.5	Ref. [15]
	Production of hydrochloric acid (36% in H2O)	kg/mt of biodiesel	10	Ref. [14]
	Production of methanol	kg/mt of biodiesel	96	Ref. [15]
	Transport of biodiesel to filling station via diesel truck	tkm/mt of biodiesel	50	Ref. [9]

B. External cost resulting from the exposure to airborne pollutants

The external cost associated with a particular airborne pollutant (except greenhouses gases) was estimated using the EcoSenseWeb software [20]. The EcoSenseWeb was developed to support the assessment of impacts on human health, crops, building materials and ecosystems resulting from the exposure to airborne pollutants. The estimation of external costs in EcoSenseWeb is based on the Impact Pathway Approach (IPA) methodology developed in the ExternE Project funded by the European Commission [21]. The IPA starts with the emission of an airborne pollutant at the location of the source into the environment. It models the dispersion and chemical transformation in the different environmental media. Introducing receptor and population date it identifies the exposure of the receptors and calculates the impacts. These impacts are then weighted and aggregated into external costs. The external cost caused by the emission of 1 kg of NH_3, NMVOC, NO_x, PM_{co}, $PM_{2.5}$ and SO_2, was estimated to be 10.21 EUR, 0.76 EUR, 6.95 EUR, 0.64 EUR, 16.31 EUR and 6.95 EUR, respectively.

There is considerable uncertainty attached to the estimation of damage costs of greenhouse gases, given the long-time scales involved, and the lack of consensus on future impacts of climate change itself. The damage cost factors for CO_2 range from 19 EUR [21] to 80 EUR per mt CO_2 [22]. In this study we adopted a central value of 50 EUR/mt of CO_2. The external costs for other greenhouse gases (i.e. CH_4 and N_2O) are calculated by multiplying the damage cost factor of CO_2 with the global warming potential factor of CH_4 and N_2O. According to [23] the global warming potential factors of CH_4 and N_2O are 23 and 296, respectively.

III. RESULTS AND DISCUSSION

Environmental external cost associated with airborne pollution resulted from the production chain of biodiesel was estimated to be 316 EUR per mt of biodiesel produced, corresponding to 0.008 EUR/MJ. Positive external effects resulting from the absorption of atmospheric carbon dioxide by plant can reduce the overall external costs to 181 EUR per mt of biodiesel produced (Tab. 2). The agricultural stage is responsible for 85% of the overall environmental external costs associated with the production of biodiesel. Even if the positive external effects from the absorption of atmospheric carbon dioxide are entirely assigned to the agricultural stage this stage would still have a significant

share (ca. 75%) in the overall environmental cost. Processes associated with the solvent extraction and crude oil refining are causing 8.5%, while the transesterification stage is responsible for 4% of the overall environmental damage caused by the production of biodiesel. The environmental externalities associated with the grain drying stage are less significant.

The relative contributions from different processes which contribute to biodiesel production are illustrated in Fig. 2. In the agricultural stage emissions (N_2O and NH_3) from agricultural soils are causing 54% of the environmental external costs. The remaining part of the environmental external costs in the agricultural stage is associated with airborne emissions from the production of fertilizers (31%) and from the production and combustion of diesel fuel in agricultural machinery (14%).

Airborne emissions associated with the production and combustion of light fuel oil and the production of electricity are responsible for two thirds of the overall environmental external cost caused in the grain drying process. In the oil mill stage the airborne emissions from the production and use of the energy required by the plant are causing 98% of the environmental external costs. Chemicals used during the solvent extraction and the refining process have a minor influence on the results (ca. 2%). Emissions associated with the production of chemicals contribute the most to the overall external cost of the transesterification process, followed by the production and use of the energy required by the plant. The high share of external costs associated with chemicals is mainly due to the significant amount of CO_2 released during the manufacture of methanol.

Fig. 3 shows the relative contribution of each of the investigated airborne pollutant to the overall external costs of the production chain. Greenhouse gases cause around 45% of the overall external cost associated with the production chain of biodiesel. From other pollutants significant share have external costs from the emission of NH_3, which is almost entirely related to the application of nitrogenous fertilizer in the agricultural stage, and NOx and SO_2, mainly released during the combustion of fossil fuels.

IV. CONCLUSIONS

The environmental external costs associated with airborne emissions from biodiesels` production chain are considerable. The agricultural stage is responsible for 85% of negative externalities associated with the

TABLE II.
AIRBORNE EMISSIONS AND ASSOCIATED EXTERNAL COSTS IN THE PRODUCTION CHAIN OF BIODIESEL

Production chain of biodiesel	Airborne emissions released during the production chain of biodiesel (kg per mt biodiesel)									External costs per mt biodiesel
	CO_2	CH_4	N_2O	NH_3	NMVOC	NO_x	SO_2	$PM_{2.5}$	PM_{co}	
Rapeseed production	677.7	1.12	5.57	8.27	0.61	6.41	2.08	0.52	0.52	270 EUR
Grain drying	71.5	0.07	0.00	0.00	0.06	0.21	0.16	0.02	0.02	7 EUR
Solvent extraction and refining	224.1	0.15	0.00	0.00	0.08	0.28	1.52	0.19	0.10	27 EUR
Transesterification	155.3	0.57	0.00	0.00	0.13	0.21	0.31	0.03	0.04	13 EUR
Total	1128.7	1.91	5.57	8.27	0.89	7.12	4.08	0.75	0.68	316 EUR
Total (less the absorbed CO_2)	-1571.2	1.91	5.57	8.27	0.89	7.12	4.08	0.75	0.68	181 EUR
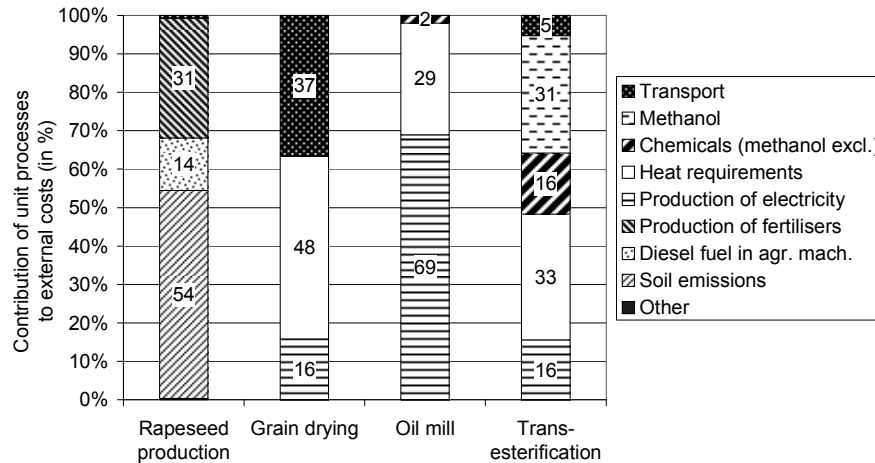
Figure 2. Relative contributions of the unit processes to the external cost of the production chain
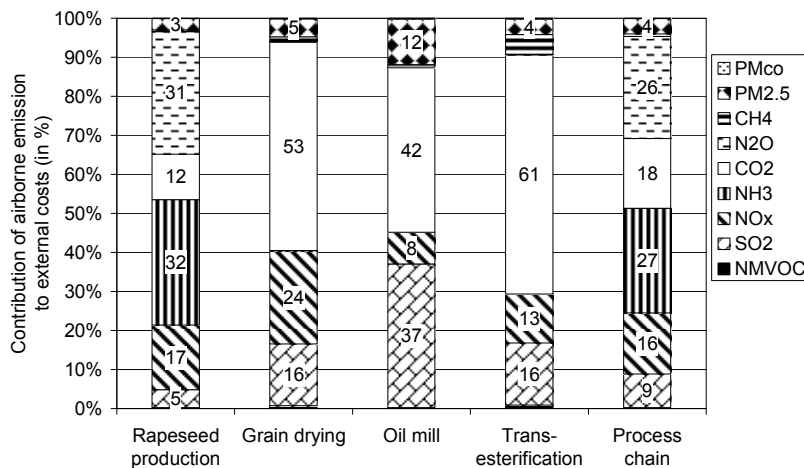
Figure 3. Relative contributions of a particular airborne emission to the overall external cost of the production chain

production chain of biodiesel. It has been shown that field emissions of N_2O and NH_3 have a major contribution to the environmental external cost of the agricultural stage. This result suggests that previous estimates that have not taken into account the impacts of soil emissions have significantly underestimated the environmental impact of biodiesel.

Both converting processes (rapeseed to oil, oil to biodiesel) consume a large volume of energy resulting in significant CO_2 emissions. Since the modeling reflects state-of-art technology it is based on the consumption of fuels of fossil origin. Thus, this step currently contributes significantly to the overall environmental burden but allows replacing with alternative, e.g. renewable energy sources. This may be particularly valid for the replacement of the light fuel oil as a heating source.

An opinion worth of discussion is the possibility of using bioethanol instead of fossil methanol (made from

natural gas prevailingly) in the transesterification of the rapeseed oil.

REFERENCES

[1] F. Kiss, "Assessment of external costs associated with air pollution from the production and usage of biodiesel in Vojvodina," Final project report, The Centre for Strategic Economic Studies "Vojvodina-CESS", Novi Sad, 2010, pp. 21–31.

[2] M. Tešić, F. Kiss, and Z. Zavargo, "Renewable energy policy in the Republic of Serbia," Renew. Sust. Energ. Rev. vol. 15, 2011, pp. 752–758

[3] F. Kiš, "Economic assessment of environmental impacts associated with the usage of biodiesel," PhD thesis. Faculty of Agriculture, University of Novi Sad, Novi Sad, 2011.

[4] T. Nemecek, T. Kägi, and S. Blaser, "Life Cycle Inventories of Agricultural Production Systems," Ecoinvent report version 2.0. Vol. 15. Swiss Centre for LCI, Duebendorf and Zurich, 2007.

[5] R. Nikolić, M. Brkić, I. Klinar, and T. Furman, "Needs for liquid fuels," in *Biodiesel – alternative and ecology liquid fuel,* T. Furman, Eds. Faculty of Agriculture, Novi Sad, 2007, pp. 11 - 40.

[6] N. Jungbluth, "Erdöl. Sachbilanzen von Energiesystemen," Ecoinvent report version 2.0. Vol. 6. Final report No. 6 ecoinvent data v2.0. Swiss Centre for LCI, Duebendorf and Zurich, 2007.

[7] T. Nemecek et al. "Life Cycle Inventories of Agricultural Production Systems," Final report ecoinvent 2000 No. 15. FAL Reckenholz, FAT Tänikon, Swiss Centre for LCI, Dübendorf, 2003.

[8] T. Dalgaard, N. Halberg, and J. Porter, "A model for fossil energy use in Danish agriculture used to compare organic and conventional farming. Agriculture," Ecosyst. Environ. Vol. 87, 2001, pp. 51–65.

[9] M. Spielmann, R. Dones, and C Bauer, "Life Cycle Inventories of Transport Services," Final report ecoinvent Data v2.0. Vol. 14. Swiss Centre for LCI, PSI, Dübendorf and Villigen, 2007.

[10] I. Pavkov, pers. comm. [21/11/2010]. Faculty of Agriculture, Novi Sad

[11] J. Schmidt, "Life assessment of rapeseed oil and palm oil, Part 3: Life cycle inventory of rapeseed oil and palm oil," PhD thesis, Department of Development and Planning, Aalborg University, 2007.

[12] F. Kiss, M. Jovanović, and G. Bošković, "Economic and ecological aspects of biodiesel production over homogeneous and heterogeneous catalysts," Fuel Process. Technol. Vol. 91, 2010, pp. 1316–1320.

[13] R. Frischknecht et al. "Strommix und Stromnetz. Sachbilanzen von Energiesystemen," Final report ecoinvent data v2.0, Vol. 6. Swiss Centre for LCI, PSI, Dübendorf and Villigen, 2007.

[14] N. Jungbluth et al. "Life Cycle Inventories of Bioenergy," Final report ecoinvent data v2.0, Vol. 17, Swiss Centre for LCI, ESU. Duebendorf and Uster, 2007.

[15] H.J. Althaus et al. "Life Cycle Inventories of Chemicals," Final report ecoinvent data v2.0, Vol. 8, Swiss Centre for LCI, Empa - TSL. Dübendorf, 2007.

[16] D. Kellenberger, H.J. Althaus, N. Jungbluth, and T. Künniger, "Life Cycle Inventories of Building Products," Final report ecoinvent data v2.0, Vol. 7. Swiss Centre for LCI, Empa - TSL. Dübendorf, 2007.

[17] M. Faist Emmenegger, T. Heck, and N. Jungbluth, "Erdgas. Sachbilanzen von Energiesystemen," Final report No. 6 ecoinvent data v2.0, Vol. 6. Swiss Centre for LCI, PSI. Dübendorf and Villigen, 2007.

[18] J. Sutter, "Life Cycle Inventories of Highly Pure Chemicals," Final report ecoinvent Data v2.0, Vol. 19, Swiss Centre for LCI, ETHZ. Duebendorf and St. Gallen, 2007.

[19] C. Peterson, and T. Hustrulid, "Carbon cycle for rapeseed oil biodiesel fuels," Biomass Bioenerg. Vol. 14, No. 2, 1998. pp. 91-101.

[20] P. Preiss, R. Friedrich, and V. Klotz, "Report on the procedure and data to generate averaged/aggregated data," NEEDS Project: deliverable No. 1.1 - RS 3a IER, University of Stuttgart, 2008.

[21] European Commission, "ExternE - Externalities of Energy – Methodology 2005 Update," Office for Official Publications of the European Communities, Luxembourg, 2005.

[22] P. Watkiss, T. Downing, C. Handley, and R. Butterfield, "The Impacts and Costs of Climate Change," Final Report to DG Environment. September, 2005.

[23] IPCC 2011, "Climate Change 2001: The Scientific Basis. Contribution of Working Group I to the Third Assessment Report of the Intergovernmental Panel on Climate Change," Cambridge University Press, Cambridge, United Kingdom and New York, NY, USA, 2001.

Heat Pump News in Hungary

Béla Ádám
Hungarian Heat Pump Association, chairman
Email: adam@hgd.hu

I. INTRODUCTION

In Hungary, the heat pump market was not able to exceed the amount of 1.000pc/year sold in the past three years.
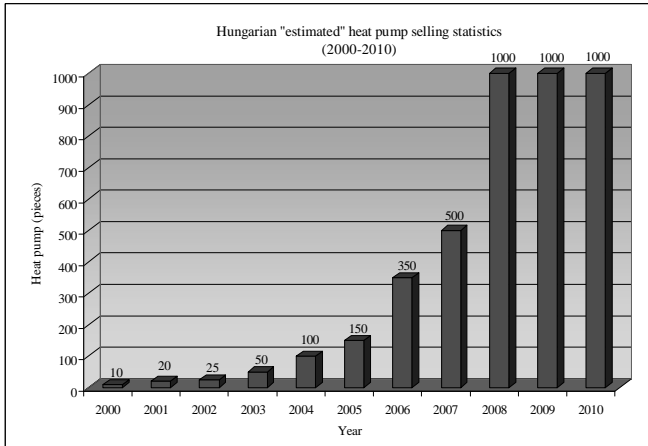
1. Figure: Hungarian estimated heat pump selling statistics

The total number of installed heat pumps is 5.000pc, and the rated output is: 0.25 Peta Joule.
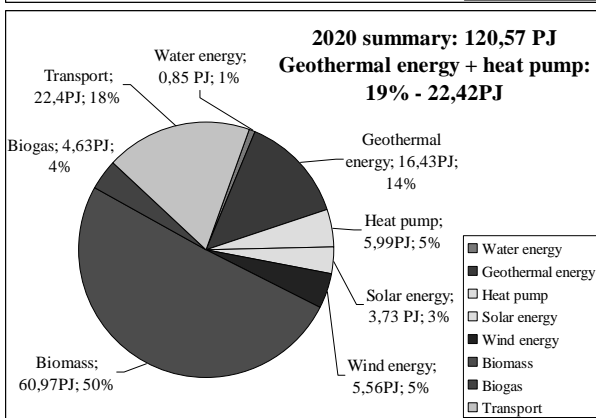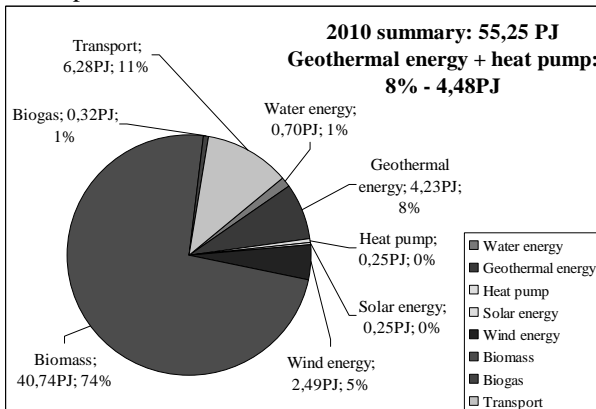
2. Figure: Current situation and the targets in the National Action Plan

II. INTERNATIONAL AND HUNGARIAN INFLUENTIAL FACTORS

If you consider that around the world 69.7% of the use of geothermal energy is utilized by heat pump technology, compared to here in Hungary where we use less than 1% of geothermal energy by heat pump. As we can see in *figure 3*, 3pc heat pumps are sold per 10,000 household in the 2010 EHPA statistics.
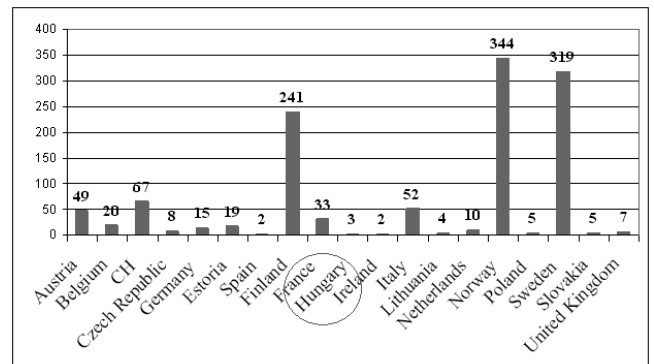
3. Figure: Sales of Heat Pumps per 10.000 households 2010 (EHPA)

If the market situation is compared to the leading EU countries, our fulfilment is 1%. We can ask: what is the reason? The answer is a negatively combination of impact factors:

- The lobby of the fossil energy sector is quite strong, since 90% of Hungary is supplied by natural gas.
- Natural gas prices have been aided by the state depending on the degree of consumption.
- Electricity production efficiency is low (36%), the power loss is 10%, so compared to primary energy, the heat pump technology can not provide a significant primary energy savings even with high COP value.
- In Hungary renewable energy (solar and wind) does not provide a sufficient amount of power to support heat pump technology.
- The heat pump technology can not compensate the share of natural gas and electricity prices. Gas: $0,43€/m^3 \rightarrow 0,046€/kWh$, electrical energy power: $0,16$ €/ kWh $\rightarrow$ in case of COP 4,0: $0,04$ €/ kWh. With GEO tariff: $0,11€/kWh \rightarrow$ in case of COP 4,0: $0,03$ €/ kWh.
- The heat pump manufacturing has not been started in Hungary, and the imported systems and heat pumps are expensive.
  - low-power heat pump system under 20kW: gross approx. 1.333€/kW
  - high-power heat pump system with 20-500kW: gross approx. 733€/kW

- A tender is missing. Occasionally in the last few years small tender amounts were received; because of this the effects were low.
- There is high level of tax: 25%.
- There is high cost of licensing for borehole heat exchangers and water-well systems.

Beside a negative market impact the only positive result from this is that the awareness and acceptance of the heat pumps technology has increased. This activity was helped by the Hungarian Heat Pump Association on the Chamber of Engineers and university training courses. In the last three years, at least 200 engineers learned the basics of heat pump technology design and gained practical experience.

Despite this market situation, we can be proud of some excellent high-performance projects on the high level with the rest of Europe.

1. Table: Several large project in Europe

Europe	Country	City/Project name	No. BHE	Depth BHE	Total BHE length
1.	UK	London Shopping Center	400	150 m	60 000 m
2.	NO	Loerensko, SiA hospital*	ca. 300	150 m	ca. 45 000 m
3.	NO	Oslo, Nydalen district	180	200 m	36 000 m
4.	SE	Lund, IKDC	153	230 m	35 190 m
5.	SE	Stockholm, Vällingby Centr. *	133	200 m	26 600 m
6.	SE	Kista, Kista Galleria*	125	200 m	25 000 m
7.	HU	Budapest Pillangó street, Tesco	150	150 m	22 500 m
8.	HU	Törökbálint, Telenor House	180	100 m	18 000 m
9.	TR	Istambul, Metro market	168	107 m	18 000 m
10.	HU	Törökbálint, School and Sport Centr.*	180	100 m	18 000 m
11.	DE	Golm near Potsdam, MPI	160	100 m	16 000 m
12.	SE	Stockholm, Blackeberg area	90	150 m	13 500 m
13.	HU	Budapest Pesti street, Tesco	130	100 m	13 000 m
14.	HU	Páty, Monicomp Ltd., logistics centr.	120	100 m	12 000 m
15.	SE	Örebo, Musikhögskolan	60	200 m	12 000 m
16.	DE	Langen, DFS	154	70 m	10 780 m
17.	CH	Zürich, Grand Hotel Dolder	70	150 m	10 500 m

BHE: Borehole Heat Exchanger   * under construction

We proved with these examples that there is no lack in the heat pump expertise. Characteristics of these projects is that the investors are foreign multinational companies (Tesco, Telenor), which can show examples of the environmental approach, also using its marketing advantages. Then we can ask what is expected in late 2011 and subsequent years?

Hungary has taken upon itself to achieve 14.64% renewable energy by 2020. In this the heat pump capacity is 5.99 PJ, thus 24-fold growth would be achieved in 9 years. The Hungarian Heat Pump Association prepared the development plans for this purpose. We calculated the opportunity of natural gas substitution, which results 5% reduction and the CO_2 emission mitigation is also significant. What should be implemented?

III. HUNGARIAN MARKET DEVELOPMENT OPPORTUNITIES

Governmental (state) economic and renewable energy development is necessary by development programs and aids from the state. Currently the investments have stopped because of the economic crisis. They must be restarted by EU Structural Funds support, especially the energetically modernization of public institutions and included in this the heat pump technology. The overall energy systems of about 20.000 institutions must be renewed and for a part of this the heat pumps can be used.

Currently, only the solar thermal production is supported in an amount €10 million in case of family and apartment houses. A tender is expected to open in early 2012 for a larger, €133,3 million amount to be used for solar energy, heat pumps, biomass and geothermal energy systems. In this case we can see a possible way out for the development in our sector.

Within the heat pump technology the ground heat source is still the leading primary heat source, but the air heat pumps have had a significant growth in recent years. The sustainability and licensing practice of water-well systems is restricted their development. The following chart shows the distribution.
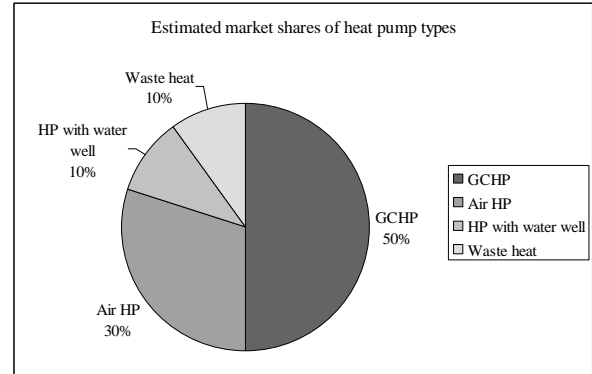
4. Figure: Estimated market shares of heat pump types

In recent years remarkable projects were made according to the EHPA "Future Cities = Cities Heat Pump" program. These include heat pump projects which connected to urban water supply systems, sewage pipeline systems, or thermal wasted water with up to 400-1.200kW power. Some of them are used for industrial or commercial heating and cooling. In one of the pilot projects a heat pump system solves the heating and cooling of 4 objects (schools, social housing, the mayor's office and the sports centre) with the utilization of the water supply system heat.

There are further works in connection with the heat pump licensing. At the end of 2011 the administrative service fee has been significantly increased by 50%, and there is no differentiation between small or large power projects. This is detrimental to the family house projects in the heat pump market. Therefore, we have initiated a legislative amendment.

Professional point of view development is that we participate in the GeoPower heat pump project in cooperation with eight countries. We would like to use this international experience in the Hungarian heat pump market.

IV. CONCLUSION

To sum up the possibilities for 2012, significant advances can be achieved only with increased state aid. With this we can achieve the plan of 2020, but not without it.

Thermal Comfort Measurements In Large Window Offices

L. Kajtár Dr. Ph.D.[*], **J. Szabó** Ph.D student[*]

[*] Budapest University of Technology and Economics, Department of Building Service and Process Engineering, Hungary

kajtar@epgep.bme.hu
szaboj@epgep.bme.hu

Abstract—**A growing number of office buildings have large window surfaces. The architects prefer this solution because of the building's beauty external appearance and because of the natural lighting. The greatly increased incoming direct solar radiation can adversely affect comfort sensation. For these reasons are essential the application of external shading devices. On-site measurements were made in summer in such an office building. We evaluated the thermal comfort under PMV, PPD and air quality based on carbon dioxide concentration. The measurement results were evaluated with scientific research methods, which results we present in this article. The thermal sensation may play important role in especially for office buildings because thermal discomfort deteriorates human productivity. The results of measurements give assistance to planning. Chilled beams were operated in the office building, the measurement results helped improve the regulation of HVAC.**

keywords: thermal sensation, measurement, PMV, PPD, solar radiation, draught

I. INTRODUCTION

In office buildings the thermal comfort and indoor air quality determine the comfort sensation and productivity of people. To be efficient at work needs to be essential to thermal sensation and indoor air quality. It could be possible to evaluate only on objective measurement method. The best indicators of the thermal sensation are the PMV, PPD and these values can definitely be measured in an operating office building. The requirements of CR 1752 were based on the evaluation of comfort.

The results of measurements were evaluated on the base of probability theory. The assumption was that the measurement results followed by distribution of the Gaussian distribution. The daily office work period was interpreted between 7 a.m. and 7 p.m. In every offices we determined by daily measurements the average value and standard deviation of measured data. The CR 1752 comfort categories were determined based on the double average absolute deviation ($\pm$ 2$\times\sigma$) from the mean value (μ) of the measurements and calculations. It is reported corresponding safety because according to the probability theory based on Gaussian distribution the 95.44% of the results located into this range ($\mu \pm 2\times\sigma$).

II. METHODS

The office building contained nine stairs, two of that located underground. In stairs of above-ground were found the offices and meeting rooms. These offices were single and landscaped offices. The total floor area was about 4000 m^2. The building consisted of two longitudinal sides: north and south facing. The window fronts were built without external shading. On the underground stairs were found the garages and technical rooms. The internal environment assessment was carried out according to CR 1752. We were evaluated the temperatures, thermal sensation, draught rates and the carbon dioxide concentration. The measurements results were determined in each compartment the comfort categories and the distribution of categories. Offices were air-conditioned by chilled beams. The total number of operating chilled beams was 562 pieces. The planned cooling water temperature was 15/18°C. The total performance of chilled beams was 660 kW. In the offices were working 750 persons and the planned specific fresh air volume was 45 m^3/h per person.

We were selected typically oriented rooms (9 pieces) to evaluate the comfort in offices. The continuous measures were done from May 10th to September 30th. The measured parameters and sampling frequencies are included in Table I.

The operating characteristics of the climate system is continuously measured, the measured characteristics and the sampling frequencies are shown in the Table II.

The instruments used for measuring temperatures and the thermal parameters were Testo instruments and for measuring the carbon dioxide concentration was Horiba equipment. The daily measured data was processed with an own developed computational program.

TABLE I.
COMFORT PARAMETERS

Measured parameter	Sign	Sampling frequency
Air temperature	t_i	5 min
Mean radiant temperature	t_r	5 min
Relative humidity	φ	5 min
Mean air velocity	w	12 sec
Carbon dioxide concentration	c_{CO2}	5 min

TABLE II.
SYSTEMS OF AIR CONDITIONING

System	Measured parameter	Sign	Sampling frequency
Chilled beam	Entering - cooling water temperature	t_{we}	5 min
	Leaving - cooling water temperature	t_{wl}	5 min
Air handling unit	Supply air temperature	t_{sa}	5 min
	Leaving - cooling water temperature	t_{wl}	5 min

III. RESULTS

The measuring results were registered steady by the data loggers. The data were processed with an own developed computational program and the following parameters were calculated from the data:

Predicted Mean Vote (*PMV*), Predicted Percentage of Dissatisfied (*PPD*), located mean air velocity, (*w*), Turbulence intensity (*Tu*), Draught rating (*DR*). The mean value and dispersion of the calculated and measured values were processed daily and we determined the characteristic of the distribution.

A. Thermal sensation

Figure 1 shows the daily changing of *PMV* values in the case of north and south-east oriented office rooms. The effect of solar radiation the maximum values of *PMV* were greater by 0.36 the case of south-east oriented office rooms. Figure 2 shows *PPD* values for the same day of these represented rooms. The selected diagram illustrates correctly the divergent thermal sensation north and south-east oriented office rooms. The maximum of the *PPD* value was 23.6% in the case of south-east oriented office room and 10.9% by the north oriented office room. The significant divergence caused by the lack of external shading.

B. Draught

The characteristic of the draught was favourable irrespective of the orientation by the case in that office building. The changing of the *w*, *Tu*, *DR* values can be seen on Figure 3 for the same chosen day seen on the previous figures. There was no significant difference in shaded and sunlit offices for *w*, *Tu*, and *DR* values. It is fully visible that the chilled beams supply favourable draught sensation. The maximum of *DR* value was 5.25% and the local mean air velocity was less than 0.1 m/s in the occupied zone.

C. Indoor air quality

Figure 4 shows the daily change of the carbon dioxide concentration in the comfort zone of a represented office room for a chosen day. After the starting of work the carbon dioxide concentration in the comfort zone increased significantly because of the breathing of people. It can be seen the reduction of the carbon dioxide concentration in the lunchtime.
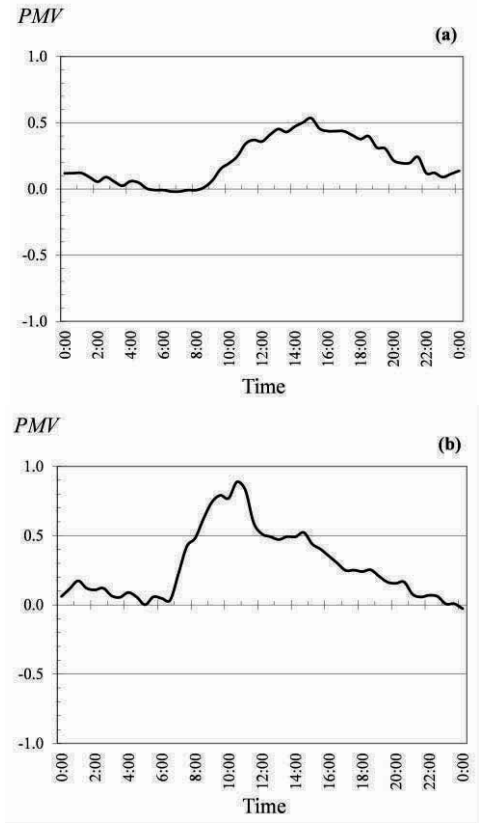
Figure 1. *PMV* values of calculations.
a) North oriented office, b) South-east oriented office
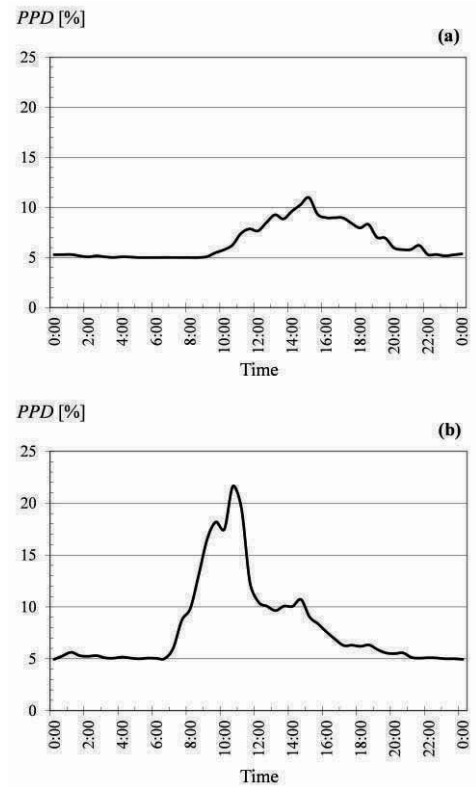
Figure 2. *PPD* values of calculations.
a) North oriented office, b) South-east oriented office
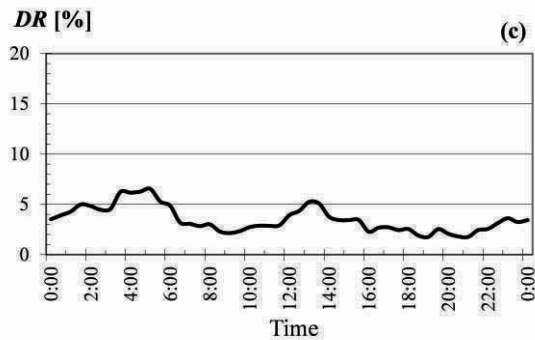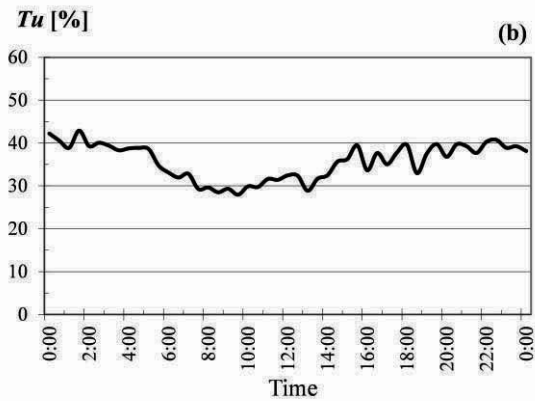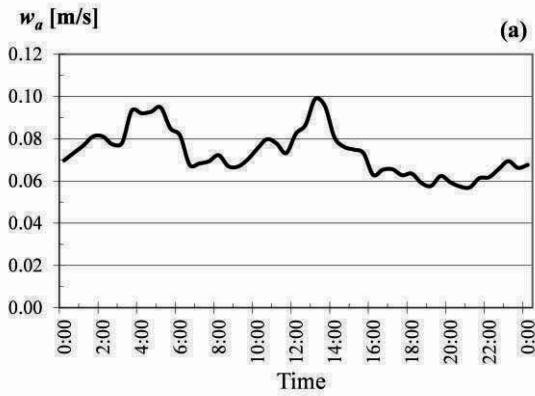
Figure 3. Specifics of draught
a) Local mean air velocity,
b) Turbulence intensity,
c) Draught rating.
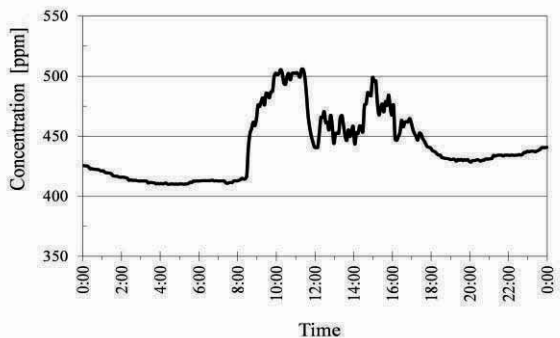
Figure 4. Measurement of the carbon dioxide concentration

IV. Discussion

The sample frequencies and the instruments accuracy made possible the exact calculation and evaluation of the comfort parameters. All measured and calculated parameters were evaluated with the method of probability theory. During the evaluation the Gaussian distribution was taken based on the double average absolute deviation ($\pm 2 \times \sigma$) from the mean value (μ) of the measurements and calculations. With the probability theory we determined the category (CR 1752: "A", "B", "C" and ">C") according to the 95.44% confidential range of the parameter value.

V. Conclusions

During the evaluation we made the distribution of the comfort parameters by comfort categories. Figure 5 shows the significant difference between the distributions of the thermal comfort, air temperature, draught sensation and carbon dioxide concentration. The examined rooms filled the category „A" requirements in the case of the draught sensation with 90.3%, carbon dioxide concentration with 73.7% and air temperature 37.4%. According to thermal comfort there was no result for category "A".

This conclusion of the comfort sensation caused by the lack of shadowing in south oriented rooms. The external shading could improve the thermal comfort and reduced significant the cooling energy consumption. Based on the results of the measurement's evaluation will be built external shading devices on the facade of the office building and the regulation of the HVAC systems will be optimized.
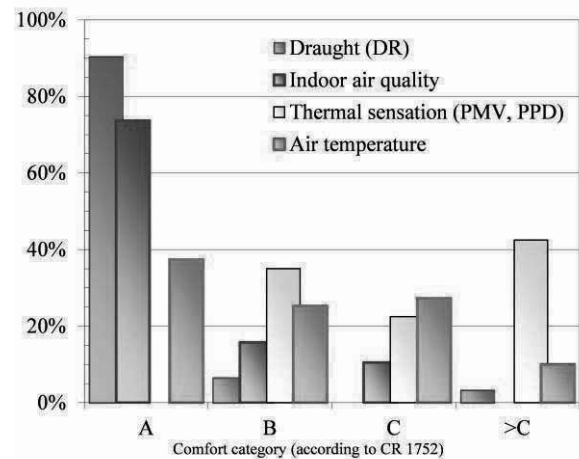
Figure 5. The distribution of measured results by category

REFERENCES

[1] Kajtár L, Herczeg L, et al. 2003. Examination of influence of CO2 concentration by scientific methods in the laboratory. 7th International Conference Healthy Buildings 2003, Singapore, Vol. 3, pp. 176-181.

[2] Kajtár L, Bánhidi L, et al. 2006. Influence of Carbon-Dioxide Pollutant on Human Well-Being and Work Intensity. Proceedings, Healthy Buildings 2006, Lisboa, Vol. 1, pp. 85-90. CD 6p.

[3] Kajtár L, Leitner A, et al. 2007. High Quality Thermal Environment by Chilled Ceiling in Office Building. 9th REHVA World Congress Clima "Well-Being Indoors" 2007, Helsinki, 6 p.

[4] Kajtár L, Hrustinszky T, et al. 2009. Indoor air quality and energy demand of buildings. 9th International Conference Healthy Buildings 2009, Syracuse, 4 p.

[5] Kajtár L and Szabó J. 2010. Effect of window surface on building energy demand (Az üvegfelület hatása az épület energiaigényére) I. Magyar Installateur 2010/5, Budapest, pp. 20-21.

[6] Kajtár L and Szabó J. 2010. Effect of window surface on building energy demand (Az üvegfelület hatása az épület energiaigényére) II. Magyar Installateur 2010/6-7, Budapest, pp. 46-47.

For a Clear View of Traditional and Alternative Energy Sources

Fülöp Bazsó, Ph. D.
SU-TECH College of Applied Sciences, Marka Oreškovića 16, 24000 Subotica, Serbia
e-mail : bf@vts.su.ac.rs

Abstract: We list a number of criteria which have to be considered in order to make meaningful decisions about possible energy sources. At the same time we list pros and cons of some alternative energy sources. One of the reasons for putting down these lines can be traced to the following fact: it is often possible to find statements about practically infinite energy resources, which are inexhaustible and available for almost free, and can be used without any side effects. The intention of these notes are to shed some light on the effects of energy production and consumption on the global climate, the nature of available energy resources, and some of the effects of their exploitation.

Keywords: global climate, energy resources, realistic overview, future prospects

I. INTRODUCTION

Criteria for using one energy source over another, or using a combination of them are manifold. To set the context: Energy consumption has an ever growing, in fact accelerating trend, thus in spite of increase in energy savings and gain in energy efficacy new energy sources need to be found, [2,4,7]. Most, in fact striking 86.4% in 2007 , of the world's energy supply comes from fossil sources, which is unsustainable at the time scale much shorter than the availability of the energy resources would suggest. Because of soaring energy prices, the trend is increasing, as coal regains attention as a primary energy source. As fossil fuels are used in oxidative processes, their consumption results in carbon-dioxide production, most of which is finally released into the atmosphere, resulting in increased carbon footprint. An operational definition of carbon footprint is "A measure of the total amount of carbon dioxide (CO_2) and methane (CH_4) emissions of a defined population, system or activity, considering all relevant sources, sinks and storage within the spatial and temporal boundary of the population, system or activity of interest. Calculated as carbon dioxide equivalent (CO_2e) using the relevant 100-year global warming potential (GWP100)." [23]. The increased amount of carbon-dioxide changes the thermodynamic properties of the atmosphere. Increase of the CO_2 concentration in atmosphere is often depicted in what is known as "Keeling curve", one is depicted in Figure 1, from [22]. Via direct and indirect mechanisms the increased concentration of carbon-dioxide generates the process of global warming, which refers to the rising average temperature of Earth's atmosphere and oceans and its projected continuation [9,13]. Increasing global average temperature trend is known as global temperature anomaly, Figure 2. Spatial variation of the global temperature anomaly is shown in Figure 3., [13]. In fact, carbon-dioxide in only one of greenhouse gases released into the atmosphere, the most important naturally occurring gases being water vapour, which causes 36-70% of the greenhouse effect, methane which causes 4-9%, and ozone, which causes 3-7%. The concentrations of CO_2 and methane have increased by 36% and 148% respectively since 1750, [5]}. These levels are much higher than at any time during the last 800,000 years, the period for which reliable data has been extracted from ice cores.[16,17,11,14] Less direct geological evidence indicates that CO_2 values higher than this were last seen about 20 million years ago, [24]. Ever since the human race exists, Earth had its polar caps. It is right now, at the very beginning of the 21-st century that the possibility of loosing the Arctic ice cap may become a reality. The domino effect on other ice-caps (Greenland, Antarctica, mountain glaciers) can not be excluded.
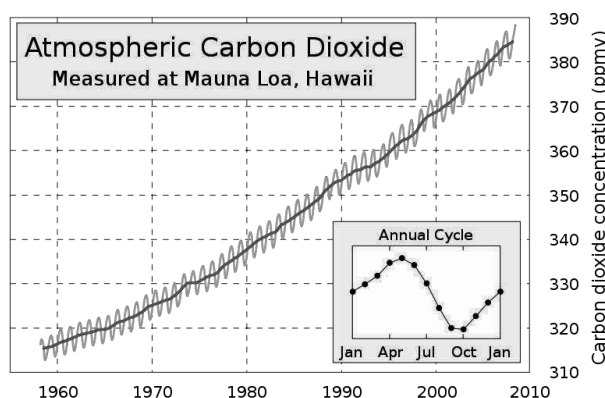
Figure 1. Rise in the atmospheric concentration of CO_2, source of figure [21].
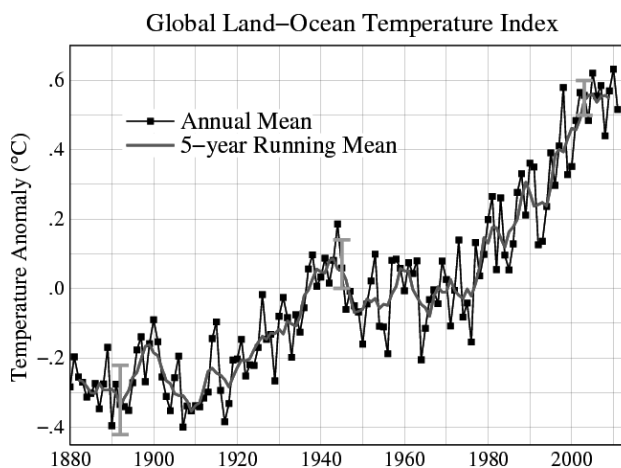
Figure 2. Evolution of global temperature anomaly, [12].
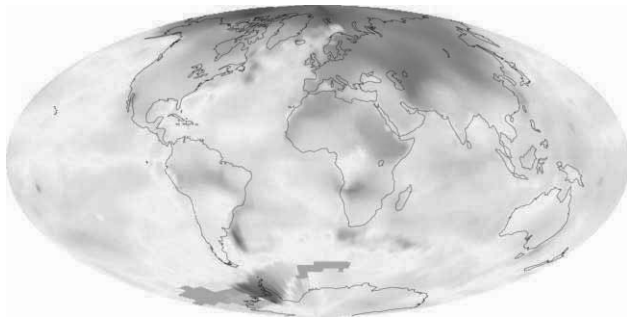
Figure 3. 10-year average (2000–2009) global mean temperature anomaly relative to the 1951–1980 mean. The largest temperature increases are in the Arctic and the Antarctic Peninsula, [13].

Global warming, if no decisive action is taken, will in itself have grave consequences for stability of the climatic patterns worldwide [8,9], e.g. via changing the thermohaline circulation in the world ocean. Predicted temperature rise based on the Hadley Centre Coupled Model, version 3 is shown in Figure 4. Global temperature is a bifurcation parameter in global climate models, so it its variation needs very close monitoring and appropriate actions are needed to conserve stable climatic patterns. Any change, especially human related rise, in global temperature will have far reaching consequences which will materialise in food supply, stability of global economy, social unrest and the future of human civilisation as we know it.
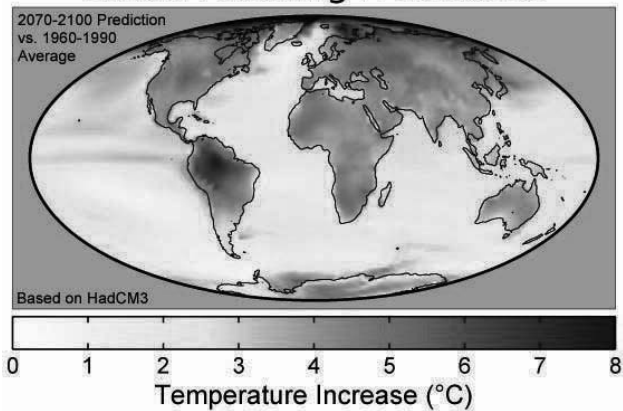
Figure 4. Predicted temperature rise for the 21st century, based on the HadCM3 climate model, figure from [6].

These, and many other facts turned the attention towards so called alternative energy resources.

Before we proceed any further, we have to notice the importance of the nature of energy consumers. Roughly, the energy consumers can be divided into mobile and static. It is much simpler to solve the energy supply in terms of alternative energy resources for static consumers than mobile ones.

Mobile energy consumers can be traced to traffic, which is to a great extent powered by fossil fuels, with the exception of some trains, trolley buses and electric cars, lately. One notable exception being reintroduction of wind energy in a form of combined fossil-fuel wind propulsion of large marine vessels. Mobile consumers

need fuels which have very high energy content, more precisely energy density. None of the alternative sources is such. For the time being, only fossil fuels and their derivatives have sufficient energy densities at affordable prices. Therefore at present, as long as there is no fundamental breakthrough in storing electrical energy and coal chemistry or an industrial scale alternative to some version of photosynthesis is found, alternative energy sources are viable for static energy consumers only.

II. TRADITIONAL VS. ALTERNATIVE ENERGY SOURCES

Traditional energy resources are fossil resources and hydroelectric resources. Because of their long history, to some extent uranium fission power plants can also be considered as traditional energy sources. Out of this list, only hydroelectric resources can be treated as sustainable, though for a variety of causes, in the long-term, they need not be. A point should be made, historically, oil *was* an alternative to coal, say.

Alternative resources cover a wide range of existing, exploitable resources, or resources being developed. An incomplete list would definitely include the following energy sources: wind, sun, geothermal sources, biomass, biofuel, biological hydrogen production, waves, oceanic tides, oceanic currents, oceanic thermal and haline gradients. One immediately notes, that not all the energy sources are always and everywhere available. Use of solar energy is determined with the number of sunny days at each and every location. Windy weather is not guaranteed. Intermittency is an important feature of alternative energy resources. It means, that sufficient backups are needed, in most cases backups are guaranteed from the centralised energy supply system.

At best, ocean can be regarded as energy resource for coastal areas only. Biofuel was meant to be an eco-friendly and seemingly sustainable candidate for a future energy resource, but its overal energy balance turned out to be negative, and its ecological and economical effects, via affecting global food prices, turned out to be devastating.

I will concentrate of alternative energy sources which can be an option in a continental region, without significant wind potential or too big number of sunny days. The alternative options are biogas, and geothermal energy. Biogas, in most cases methane, can be efficiently produced in sewage plants and animal farms to reduce their operational costs via decreased external energy consumption. In spite of some carbon-dioxide release, the net effect from the carbon footprint perspective is positive, as methane is much worse greenhouse gas than carbon-dioxide, not to mention other environmental advantages, such as highly improved quality of processed sewage water. One should note that biogas is used immediately at the production site, because of its scarcity and low energy density. Geothermal energy will have big future in heating technology, though because of transportation costs, this form of energy is also used locally. These two examples illustrate an important feature of alternative energy sources: they are produced and used locally, transport is practically absent. This

results in geographically distributed alternative energy sources, which may have an advantage, and that is fault tolerant property of distributed systems. One should note another feature of the examples, these energy sources need an external energy resource in order to operate. Thus, they can reduce the energy consumption from the external source, but generally, they can not replace it. A further remark has to be made. Geothermal energy is believed to be practically inexhaustible. In fact it is not, as long term exploitation (25 years, say) depletes the amount of thermal energy which can be used from from a well. The lifetime of a well can be greatly prolonged, if during summer the heat is pumped back to the well, i.e. if the well is used for cooling.

III. REALISTIC FUTURE OPTIONS FOR CENTRALISED ENERGY SUPPLY SYSTEMS

Future of centralised energy supply systems will follow a different route. For a centralised energy supply system new, long term, carbon footprint neutral solutions are needed, we just briefly summarise some possible future alternatives. In countries located at the Atlantic coast, wind energy is the source of 20% of all the energy consumption already. Large solar plants in north west Africa can in principle produce enough energy to cover 20-30% of EU's annual energy need [19]. Note, that these sources with current technologies operate intermittently. New solar technologies are already operational, based on salts (60% sodium nitrate and 40% potassium nitrate) for heat storage, which offer constant, or at worst, prolonged energy supply [1] during the whole day-night cycle. Three Andasol plants provide sufficient energy for half a million people in southern Spain. Nevertheless, future of solar energy lies not only in electrical energy production, but to large extent in heating. Combinations of wind and solar plants, in the form solar updraft towers [16] are also being developed with projected 200 MW capacity. This technology uses solar energy to heat large volume of air, which by its upward motion through a large chimney speeds up and propels a wind turbine to produce electrical energy.

I will conclude this section with mentioning two further possibilities, which may be realised within 20-30 years. One being thorium based nuclear fission. Uranium fission results in radioactive waste, which needs costly post-processing and long term storage. Uranium suitable for commercial exploitation can be found only at few sites. On the other hand thorium based fission does not produce long-lived (compared to uranium fission) radioactive waste. The amount of commercially available thorium amount is much larger (thorium is three to four times more abundant than uranium in the Earth's crust, [20]) and its distribution is much more even when compared to uranium, not to mention prices. Countries with largest known thorium reserves are India, Australia and USA. Notably, in case of thorium there is no need of isotope separation. Energy released in thorium reactors is much more suitable for thermal conversion than the energy released in uranium reactors. In fact, thorium reactors can be used to incinerate high-activity nuclear waste and produce energy. Being rich in thorium deposits, India already made advances towards an exploitable thorium reactor.

Nuclear fusion can resolve many problems with energy supply, once the technologies are available. The advantages of nuclear fusion compared to nuclear fission are numerous. The energy yield in fusion is larger than in fission. The amount of radioactive waste is incomparably smaller, in fact, there is no direct waste from the reactor itself, the neutron flux from the fusion reaction activates the reactor's shielding material. The reactor will burn tritium, and in future possibly a light isotope of helium, ^{3}He. For its operation fusion reactor needs lithium. Based on the present estimates, the amount of lithium available is sufficient ensure global energy production. A prototype fusion reactor, ITER (International Thermonuclear Experimental Reactor) [10] is under construction, it is expected to become operational at the end of the decade. Once it is built, it will be a prototype for future commercial fusion reactors. The ITER fusion reactor itself has been designed to produce 500 megawatts of output power for 50 megawatts of input power. It worths mentioning in this context, that the renewed interest in Lunar programmes is related to the fact that the Lunar surface is covered with regolith, which is rich in Helium-3, which is expected to play an important role in future fusion reactors, [3].

IV. CONCLUSION

Energy production and consumption affect the environment, whatever the energy source is. Present energy production and consumption trends are likely to continue in the near future, though they are to change, either because of organised global effort or for another reason. It can not be overemphasised, that the realistic option in future and present energy supply policies is the reduction of energy consumption, and increasing the gain in energy efficacy, whatever the available energy source is. We argue that alternative energy resources have a potential to reduce the strains on centralised energy supply systems, and can increase their fault tolerance. Alternative energy solutions can be applied locally, though their widespread application will have global effects. Large scale energy supply systems will change the primary sources of energy, we hinted some possible future resources. We just note that alternative energetic solutions need consideration of installation, maintenance and operational costs, locally and globally, important issues which we have not discussed. It needs to be stressed, that any solution of future energy supply needs a societal perspective, which neither technology nor economy can bypass.

V. REFERENCES

[1] Andasol 2008
http://www.solarmillennium.de/english/technology/references_and_projects/andasol-spain/andasol_artikel.html

[2] Annual Energy Outlook 2011. U.S. Energy Information Administration (EIA) of the U.S. Department of Energy (DOE) http://www.eia.gov/forecasts/aeo/

[3] F. H. Cocks (2010). "^{3}He in permanently shadowed lunar polar surfaces". *Icarus* **206** (2): 778–779.

[4] Assumptions to the Annual Energy Outlook 2011. U.S. Energy Information Administration of the U.S. Department of Energy.
http://205.254.135.24/forecasts/aeo/assumptions/pdf/0554(2011).pdf

[5] EPA (2007). "Recent Climate Change: Atmosphere Changes". *Climate Change Science Program*. United States Environmental Protection Agency.

[6]http://www.globalwarmingart.com/wiki/File:Global_Warming_Predictions_Map_jpg

[7] International Energy Agency, Worldwide trends in Energy Use and Efficacy, Key Insights from IEA Indicator Analysis,
http://www.iea.org/papers/2008/indicators_2008.pdf

[8] Intergovernmental Panel on Climate Change Fourth Assessment Report, "What is the Greenhouse Effect?" FAQ 1.3 - AR4 WGI Chapter 1: Historical Overview of Climate Change Science

[9] IPCC AR4 SYR 2007. , Section 1.1: Observations of climate change , IPCC, Synthesis Report

[10] ITER http://www.iter.org/

[11] Lüthi, D.; Le Floch, M.; Bereiter, B.; Blunier, T.; Barnola, J. M.; Siegenthaler, U.; Raynaud, D.; Jouzel, J. et al (2008). "High-resolution carbon dioxide concentration record 650,000–800,000 years before present". *Nature* **453** (7193): 379–382.

[12] http://data.giss.nasa.gov/gistemp/

[13] 2009 Ends Warmest Decade on Record. NASA Earth Observatory Image of the Day, 22 January 2010.

[14] Pearson, PN; Palmer, MR (2000). "Atmospheric carbon dioxide concentrations over the past 60 million years". *Nature* **406** (6797): 695–699.

[15] Petit, J. R.; *et al.* (3 June 1999). "Climate and atmospheric history of the past 420,000 years from the Vostok ice core, Antarctica". *Nature* **399** (6735): 429–436.

[16] Schlaich J, Bergermann R, Schiel W, Weinrebe G (2005). Design of Commercial Solar Updraft Tower Systems—Utilization of Solar Induced Convective Flows for Power Generation *Journal of Solar Energy Engineering* **127** (1): 117–124.

[17] Siegenthaler, Urs; *et al.* (November 2005). "Stable Carbon Cycle–Climate Relationship During the Late Pleistocene". *Science* **310** (5752): 1313–1317.

[18] Spahni, Renato; *et al.* (November 2005). "Atmospheric Methane and Nitrous Oxide of the Late Pleistocene from Antarctic Ice Cores". *Science* **310** (5752): 1317–1321.

[19] TREC/Club of Rome White Paper presented in the European Parliament 28 November 2007, http://www.DESERTEC.org/

[20] "The Use of Thorium as Nuclear Fuel" (http://www.ans.org/pi/ps/docs/ps78.pdf). American Nuclear Society. November 2006.

[21] U.S. EIA International Energy Statistics http://tonto.eia.doe.gov/cfapps/ipdbproject/IEDIndex3.cfm

[22]http://en.wikipedia.org/wiki/File:Mauna_Loa_Carbon_Dioxide-en.svg

[23] Wright, L., Kemp, S., Williams, I. (2011). "'Carbon footprinting': towards a universally accepted definition". Carbon Management 2 (1): 61–72.

[24] http://en.wikipedia.org/wiki/Global_warming

Design of a Solar Hybrid System

Marinko Rudić Vranić, ing. Emnel L.T.D., Subotica, Serbia
e-mail:marinko.rudic@gmail.com

Abstract—**This article deals with the fundamentals of solar hybrid systems design. In the first part it deals with the theory of such systems both the thermodynamics and the control logic of the system are discussed. In the second part an actual design of a solar hybrid system is presented.**

I. THEORY

A. Main elements of a solar hybrid system

Solar hybrid systems are heating installations with multiple heat sources and with multiple heat sinks. Common heat sources of a solar hybrid system are:

- Solar collectors
- Gas or coal fired boiler
- Electric boiler
- Heat pump

Common heat sinks of a solar hybrid system are:

- Domestic hot water
- Space heating
- Space cooling with absorption chiller
- Swimming pool heating

The main parts of a solar hybrid system are:

- Solar collector array
- Auxiliary heater
- Heat accumulator
- Automatic energy management system

In solar hybrid systems both flat plate and vacuum tube solar collectors can be used. Both types of collectors have advantages and disadvantages.

Flat plate collectors come with a lower price therefore a larger collector area can be installed. Also flat plate collectors have an advantage over vacuum tube collectors in areas where frequent snowfall occurs, due to relatively larger heat losses through the glassing.

Namely, on flat plate collectors a small amount of sunlight passing through the layer of snow covering the collector heats up the absorber which then heats up the glassing. That way a thin liquid water film forms between the glass and the covering snow which allows the snow to slide down.

The advantage of the vacuum tube collector over the flat plate ones is in the higher output temperature. Higher temperatures allow space cooling to be achieved with supplying the heat to the absorption chiller by the vacuum tube collectors.

Size of the solar collector area in hybrid systems depends on the heat demand of the heated space during the periods of Feb.-March-Apr. and Sept.-Okt.-Nov.

Namely, in solar hybrid systems solar energy provides a part of the total energy needed for heating. Depending on the type of the heating installation and weather conditions this part goes from 10% to 60%.

Picture 1. Solar collector array

The auxiliary heating unit in the solar hybrid systems provides heat for the space heating. The heating capacity of the auxiliary unit matches the peak demand of space heating and domestic hot water preparation combined.

The central unit is the heat accumulator. Its purpose is to store and distribute the heat produced by the solar collector array and the auxiliary heating source.

The energy management unit is an automatic control system for controlling the heat sources and the temperatures of the heat sinks. The control system consists of software embedded in the microprocessor unit with digital and analog inputs and outputs, temperature sensors and actuators.

B. Principles of heat transfer inside the storage tank

The heat accumulator is a vertical cylindrical water tank in which a process of combining the energy from two heat sources with different output temperatures occurs.

The change of density of water due to change of temperature allows stratification of the water stored in the storage tank. Inside the storage, a temperature gradient from bottom to top of the tank is formed, where the lowest temperature is at the bottom of the tank and the hottest water is at the top.
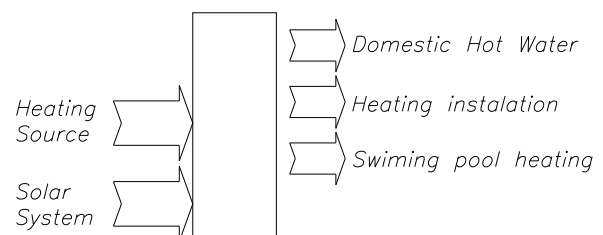
Figure 1. Energy balance of a solar hybrid system

Stratification of the storage tank allows the heat gain from the solar array to be added to the heat produced by the auxiliary heat source. Besides that, stratification allows heat to be drawn at different temperatures from the tank to meet the needs of different heating systems.

During the periods of moderate solar gains, the energy from the solar array is added into the storage tank at the lowest temperature point. The heat from the auxiliary heater is added to the water inside the tank at the medium temperature level. Energy needed for space heating is drawn from the tank at the medium temperature level.

In order to combine the energy from the solar and the auxiliary heat sources to meet the space heating demand the following condition must be met: The difference between the mean temperature of the solar array and the temperature of the return line of the space heating installation must be positive.
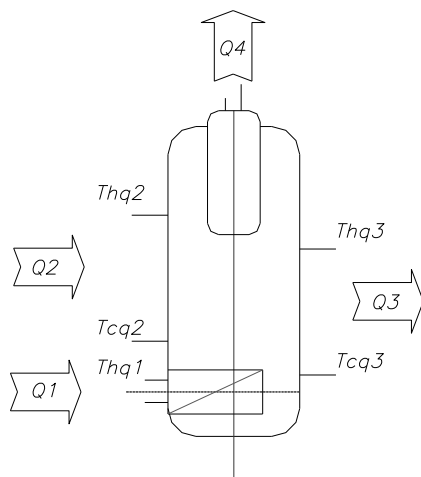
Figure 2.   Temperature layout of the storage tank

Fig 2: Q1- energy input from the solar array, Q2-energy input from the auxiliary heat source, Q3- energy output to the space heating installation, Q4 – energy output to the domestic hot water, Thq1- forward line temperature of the solar collector array, Tcq1-return line temperature of the solar collector array, Thq2- forward line temperature of the auxiliary heat source, Tcq2-return line temperature of the auxiliary heat source, Thq3-forward line temperature of the space heating installation, Tcq3-return line temperature of the space heating installation, Tq4- forward line temperature of the domestic hot water installation.

Heat balance of the storage tank:

$$Q_1 + Q_2 = Q_3 + Q_4 \ldots \ldots \ldots \ldots (1)$$

Let's assume that: $Q_4 = 0$ then:

$$Q_1 + Q_2 > Q_3$$

$$k_1 m_1' \Delta T_1 + k_2 m_2' \Delta T_2 > k_2 m_3' \Delta T_3$$

$$k_2 m_2' = k_2 m_3' > km'$$

$$k_1 m_1' \Delta T_1 + km' \Delta T_2 > km' \Delta T_3$$

$$k_1 m_1' \Delta T_1 + km' (T_{hq2} - T_{cq2}) > km' (T_{hq3} - T_{cq3})$$

$$k_1 m_1' \Delta T_1 + km' (T_{hq2} - T_{cq2}) - km' (T_{hq3} + T_{cq3}) > 0$$

$$T_{hq2} = T_{hq3} = T$$

$$k_1 m_1' \Delta T_1 > km' (T_{cq2} - T_{cq3}) \ldots \ldots \ldots \ldots (2)$$

Where:
k_1- heat capacity of solar working fluid
m_1'-mass flow rate of solar working fluid
k_2-heat capacity of water
m_2'-mass flow rate of water in the auxiliary heating loop
m_3'-mass flow rate of water inside the space heating loop
ΔT_1- temperature difference between the forward line and the return line of the solar array
ΔT_2-temperature difference between the forward line and the return line of the auxiliary heater
ΔT_3-temperature difference between the forward line and the return line of the space heating installation.

The equation (2) shows the amount of energy supplied by the solar array.
$km' (T_{cq2} - T_{cq3})$ Is the heat energy needed to heat up the water from the space heating return line up to the temperature level of the intake of the auxiliary heat source.

This amount of energy is supplied by the solar array. In other words, the energy from the solar array allows the intake temperature of the auxiliary heater to be higher.
This way the auxiliary heater operates with less temperature difference, therefore using less energy.

When the auxiliary heating device is operating part of the energy is used to heat up the domestic hot water. Temperature of the water in DHW systems has to reach 60°C. If this temperature is not reachable by the heating system (in case of panel heating installation) an electric heater is used to match the remaining temperature difference.

In order to prevent mixing and to retain the stratification inside the heat storage tank, a built-in tank is used for storing the DHW. This tank is placed inside at the top of the main tank at the highest temperature level. This prevents heat dissipation from the DHW to the heating water when only the electric heater is switched on.

During summer when there is no demand for space heating, energy output from the solar collector array is greater than the energy needs of the DHW subsystem. Therefore, a heat sink has to be considered to prevent overheating of the system.

An elegant way to cool down the system is to use a swimming pool as a heat sink.

C. Controll Strategy of a Solar Hybrid System

Tasks for the control unit of the solar hybrid system are:

- Maintaining the set point temperature of the heated area.
- Maintaining the set point temperature for the DHW subsystem.
- Maintaining the set point temperature for the swimming pool.
- Maintaining the set point temperature for the auxiliary heat source
- Maintaining the minimal and maximal set temperatures of the storage tank.
- Limiting the maximal temperature of the solar array.
- Managing the energy flow to maximize the usage of solar heat gain.

The control strategy consists of sets of conditions which are implemented into the control algorithm. Some of these conditions are determined by the user, for example the heated space temperature and the DHW temperature.

On the other hand some of these conditions are limited by the equipment and safety, for example the maximal temperatures of the: solar collector array, storage tank and the auxiliary boiler. And third, some temperatures are determined by the control software: for example the set point temperature for the solar array.

Picture 2. Control unit

Inputs of the control unit are:
1. Room thermostat of the heated space.
2. Temperature of the DHW forward line temperature.
3. Swimming pool water temperature
4. Temperature of the forward line of the auxiliary heat source.
5. Solar array forward line temperature
6. Temperature of the lowest temperature layer of the storage tank.

Outputs of the control unit are:
1. Solar array on/off –by means of controlling the circulator pump.
2. Auxiliary boiler on/off
3. Space heating circulator pump
4. DHW circulator pump
5. DHW electric heater
6. Swimming pool heating circulator pump

The heat demand of the heated area is dependent on the outside temperature. Also more solar radiation is available during the months with relatively low heat demand.

In order to collect as much as possible solar energy, the energy management system has to decide where to distribute the collected energy. During low heat demands energy can be stored in the heated area itself.

Meaning, when the output temperature of the solar collector array is high enough, the energy from the solar array can be distributed directly into the heated area.

Energy flow management is also important because the solar flat plate collector can also act as a heat sink. This characteristic of the collectors can be used to cool down the system during nights in summer months to prevent overheating.

However this circumstance is not desirable during winter months. When the outside temperature is low, heat produced by the auxiliary source can be dissipated through the solar collector array to the atmosphere. To prevent this, the control unit must be able to recognize the conditions in which energy dissipation can occur.

Recognizing is done by software subroutines. These are various pre-programmed functions which are automatically activated when certain conditions are met. For example: mean temperature of the solar array drops below preset value – this means that there is no energy gain from the solar array. There are two ways to cope with energy dissipation:
1. The setting up of the kick-in temperature of the solar array higher than the temperature of the medium layer of the storage tank.
2. The ΔT method, solar array starts and remains in operation only when there is a positive temperature difference between the forward flow and the return flow lines. In this case there is a minimal allowed value for ΔT.

The first solution is usable in systems with fixed set point temperatures. An example for this is a solar DHW-only system. However when heating is present the temperature of the auxiliary heat source varies. Therefore it is better to use the second method because that way more solar energy can be collected.

II. DESIGN OF A SOLAR HYBRID SYSTEM

Our company received an order to build a solar system for
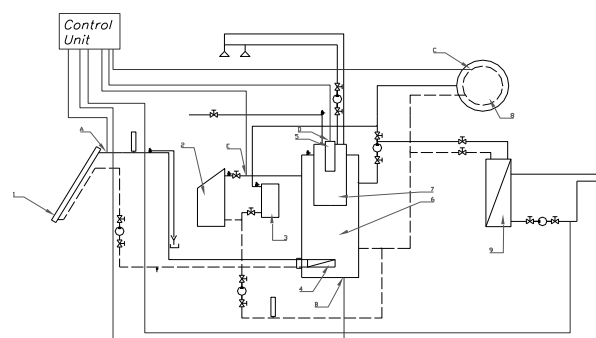
Picture 3. Design layout of a solar hybrid system

heating assistance during winter, and for heating of the swimming pool during summer. The system was to be built in a four person lived house in Subotica. The property has the following characteristics:

Total living area is 240 (m^2) which is pre equipped with a central heating installation with radiators. This installation uses a coal fired 35 (kW) boiler as a primary heat source. Secondary heat source of the heating installation is a 18 (kW) electric boiler. For DHW preparation an 80 (l) electric boiler is used. The house has a good thermal insulation, and a relatively good orientation towards the South. Also the property includes a 40 (m^3) swimming pool located outdoors. For the purposes of the task we have proposed a solar hybrid system with the following characteristics:

- The solar hybrid system will provide heating assistance and DHW to reduce the usage of electrical energy.
- The solar array consists of 5 solar collectors mounted on the roof facing South-West.
- Type of solar collectors is flat plate ES1, produced by our company
- Total net area of installed solar collectors is 9,7 (m^2)
- Combined storage tank with accumulation of heating water and with a built in storage tank for the DHW subsystem. Total volume of the tank is 1000 (l), volume of the DHW sub tank is 90 (l). The storage vessel is produced by our company.
- Automatic control unit is a standard PLC with control software made by our company.
- All the necessary equipment is to be mounted into the existing boiler room

Primary purpose of this system is to reduce the usage of electrical energy for space heating and to provide heating for the swimming pool.

Picture 3. Storage tank during installation

III. CONCLUSION

In this article one possible solution for a design of a solar hybrid system is presented. This system combines two or more energy sources to provide energy for space heating, DHW preparation and for heating of the swimming pool in a family house. This system has the following advantages:

- Adding solar energy into the energy balance of the house results in using less energy that comes from fossil fuels.
- In a solar hybrid system the amount of solar energy that goes into the house is easily controlled – the solar collector array can be switched off when not needed.
- For this particular heating installation it also increases comfort since it reduces temperature oscillations inside the heated space.

Solar hybrid systems can be implemented on any heating system that is using water as a working fluid.

REFERENCES

[1] Rajka Budin and Alka Mihelić-Bogdanović, "Osnove Tehničke Termodinamike", Školska Knjiga, Zagreb 1990.

[2] Dr. Jozsef Nyers, "Grejanje-Termoizolacija,Ventilacija,Klimatizacija", VTŠ Subotica 2005.

[3] Dobrosav Milinčić and Dimitrije Voronjec, "Termodinamika" (Thermodynamics), Mašinski Fakultet Beograd 2000.

[4] Miroslav Lambić, "Priručnik za Solarno Grejanje", Naučna Knjiga, Beograd 1992 (Solar Heating Handbook)

[5] Tomislav Pavlović, "Fizika i Tehnika Solarne Energetike" Građevinska Knjiga Beograd 200

Decision system theory model of operating U-tube source heat pump systems

L. Garbai, Sz. Méhes

Professor at Budapest University of Technology and Economics/Department of Building Services and Process Engineering, Budapest, Hungary
PhD candidate at Budapest University of Technology and Economics/Department of Building Services and Process Engineering, Budapest, Hungary
garbai.laszlo@gmail.com, sz.mehes@gmail.com

Abstract - In this paper we set up a decision system theory model for existing heat pump installations with U-tube heat exchanger. Our models describe the relation and connection between input, output and decision variables of the whole system. For every "stage" of the system we show the expectable return and then we demonstrate the optimal return function. Only the system theory modeling is able to provide an exact definition of the various working points, besides it enables decision-making required to ensure optimal management.

I. INTRODUCTION

U-tube source heat pump systems are complex systems. Their precise energetic and economic analysis can only be conducted with the help of system theory modeling.

The basics of the system theory modeling are demonstrated in our previous papers [3], [4], [5], [6]. In these studies we introduced the "basic" system theory schemes, the decision variables and the transformation equations, which describe the connection between the input and output variables in every stage of the model.

In the development of these models we refer to research and work by G. L. Nemhauser [1] and R. Bellmann [2].

II. DECISION SYSTEM THEORY MODEL'S OF HEAT PUMP SYSTEMS WITH U-TUBES

The energetic U-tube source heat pump systems are complex, consisting of numerous components, each influencing the system's operation.

We are only able to determine the optimal operation of such complex systems and optimal costs of their installation, if we decompose the system to several stages and we define the output accordingly. While describing the decision model we decompose the entire system to a number of sub-systems – stages -; then for certain stages we define input, output and decision variables together with transformation correlations, describing the relationship between inputs and outputs.

In both of the models we consider consumer's heat demand as basis. In existing systems we are looking for those operation conditions, which by certain installation conditions, in case of lower heat demand than the sizing by which parameters can the system's electricity use be minimized. Provided that we deal with systems under design or installation we have to inquire from what kind of elements (accessible on the market) we have to construct our system to achieve high COP value so we can minimize the investment and operation costs.

We performed this task by recursive function equations and optimization theory by Bellman. We decomposed both types of systems to stages, set certain variables and by stages we defined the optimization objective function.

The optimization theory is as follows. We perform optimization from back to the front base on the backward model. We define the optimum of the first stage, which is in our case the stage of consumers. Then we move to the next stage, which comes after the consumers' stage. Hereby we define the optimum of the stage and we add to this value the optimum of the previous stage. We continue this process until we reach the end of the system.

Optimization decision model of the serial mechanical system can be described accordingly "Fig. 1". In this paper we refer to input and output variables in the modeling of exact mechanical systems as Z, to transformation equations as g and result variables (costs) as f.

Objective function of the system [12]:

$$h = f_1(Z_1, U_1) + f_2(Z_2, U_2) + \ldots + f_M(Z_M, U_M) +$$
$$f_{M+1}(Z_{M+1}, U_{M+1}) + \ldots$$
$$+ f_{N-1}(Z_{N-1}, U_{N-1}) + f_N(Z_N, U_N) \rightarrow \text{Extreme.}$$

Function equation of recursive optimization of the system [12]:

$$O(Z_M) = \min_{U_m}\{f_M(Z_M, U_M) + O(Z_{M+1})\}, \qquad (1)$$

We take into consideration the transformational correlation between Z_{M+1} and Z_M state variables (input and output), which can be described as

$$Z_{M+1} = g_M(Z_M, U_M). \qquad (2)$$

If we substitute this to the function equation (1) it is only the function of the stage's Z_M input's as parameter, and of U_M decision variable (3).

$$O(Z_M) = \min_{U_m}\{f_M(Z_M, U_M) + O(g_M(Z_M, U_M))\}. (3)$$
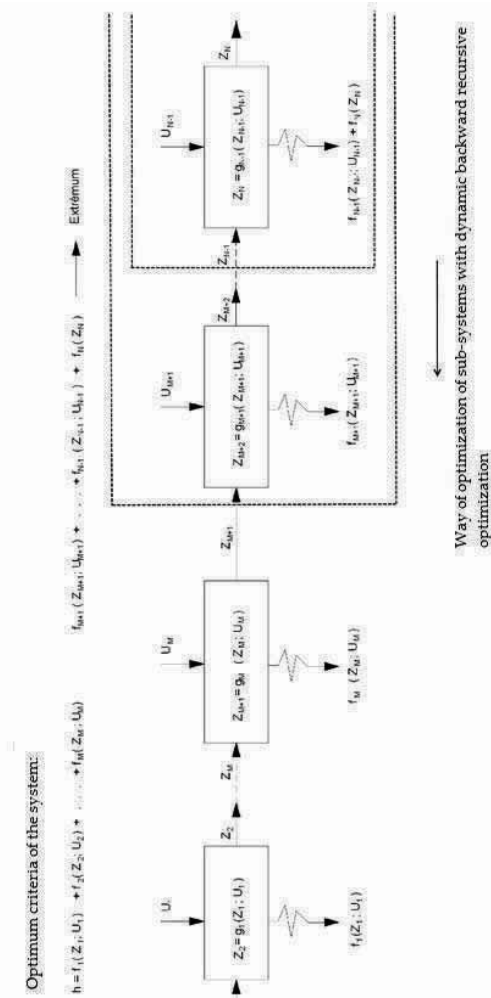
Figure 1. White box model of serial decision system [7]

With the appropriate choice of U_M decision variable in the function of Z_M decision variable we have the optimum of the partial system containing M, M+1,…, N-1 stages, that is the optimal cost of $U_{M,opt}$, $U_{M+1,opt}$, …$U_{N-1,opt}$ optimal decisions. This optimization is called dynamic, backward recursive optimization.

In the first phase of optimization we define the $O_{N-1}((U_{N-1}, Z_{N-1}), Z_N)$ function as follows

$$O_{N-1}(Z_{N-1}) = \min_{U_{N-1}}\{f_{N-1}(Z_{N-1}, Z_N, U_{N-1})\}. \tag{4}$$

As a second step

$$O_{N-2}(Z_{N-2}) = \min_{U_{N-2}}\{f_{N-2}(Z_{N-2}, U_{N-2}) + O_{N-1}(Z_{N-1})\}, \tag{5}$$

but it is observable that

$$Z_{N-1} = g_{N-1}(U_{N-2}, Z_{N-1}), \tag{6}$$

therefore

$$O_{N-2}(Z_{N-2}) = \min_{U_{N-2}}\left\{\begin{array}{l} f_{N-2}(Z_{N-2}, U_{N-2}) + \\ + O_{N-1}(g_{N-1}(U_{N-2}, Z_{N-1})) \end{array}\right\}. \tag{7}$$

By this optimization of the decision variable $O_{N-2}(Z_{N-2})$ for U_{N-2} we can define optimal value of U_{N-2}, which then we substitute to the function $O_{N-2}(Z_{M-2}, U_{N-2})$. Hence, we get to know the optimal (maximal or minimal) costs of the studied stages in the function of Z_{N-2} inputs.

Most frequently the inquiry of the optimal value of the decision variable is done numerically, taking into consideration the discrete character of cost functions and variables.

We discretize the possible value aggregation of the actual status variable – for example Z_M – , and for each exact value we search for the $U_M(Z_M)$ value of decision variable, resulting in optimal minimal value $O(Z_M)$, which we store.

III. DECISION SYSTEM THEORY MODEL OF OPERATING HEAT PUMP SYSTEMS WITH U-TUBE CONSTALLATION

When describing to the optimization of an operating system, we refer to the search of those operating parameters of an installed and operating system – considering heat demand of the consumer - , by which the operating costs of the system are minimal. For this we have to know precisely the type and size of the elements in the system and the demand of the consumer. We demonstrate the system theory scheme of an operating system in "Fig. 2".

Decision variables determining the operation during optimization of an operating system:

- By U-tube heat source: mass flow of primer liquid ($\dot{m}_p$), temperature of primer liquid (forward flow) upcoming from U-tube (T_{pe});

- By evaporator: mass flow ($\dot{m}_h$) of refrigerant applied at cycle;

- By compressor: condensation temperature (T_c) and evaporation temperature (T_o);

- By consumer: mass flow of heating water ($\dot{m}_s$), temperature of the forward heating water (T_{se});

Objective function of the decision system of heat pumps, demonstrated in "Fig 2" is as follows:

$$K(\dot{Q}_{consumer}) = \min \Sigma K_{ii} = \min(K_{consumer} + K_{condensator} + \\ + K_{compressor} + K_{evaporator} + +K_{U-tube}) \tag{8}$$

A. Optimal function by the consumer's stage

The consumer's heat demand is given, which is the known output of the decision stage. The input of the stage is the circulated heating mass flow, which we consider as parameter. We link the optimal function of the stage to this parameter, which is the electric power cost of the heating water's circulation. Mass flow $\dot{m}_s$ of the circulated heating water is parameter and at the same time decision variable.

$$O_1(\dot{m}_s) = k_e \cdot \left| R_s\left(\frac{\dot{m}_s}{\rho_s}\right)^3 \right| \cdot \frac{1}{\eta_e} \cdot \frac{1}{\eta_m}, \tag{9}$$

Whereby R_s is the coefficient of hydraulic resistance of the known pipe system with given geometric parameters, k_e is the unit cost of electric power, η_e is the pump efficiency and η_m is the electric motor efficiency.

The function expresses the utilized electric power efficiency for satisfying consumer's demand with a given

parameter of pump in the function of the parameter, like
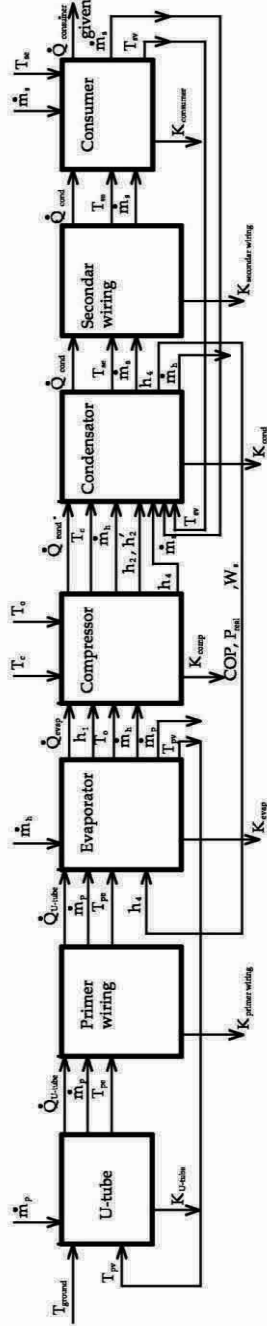
Figure 2. Decision system theory model of an operating heat pump system

the mass flow of the circulated heating water on the secondary side. Provided that we set particular exact values of $\dot{m}_s$ parameter, then correspondingly, we can calculate the secondary forward going and returning water temperature with the help of formulas (10) and (11).

$$T_{sv} = T_{se} - \frac{\dot{Q}_{consumer}}{\dot{m}_s \cdot c_s} = T_b + \frac{\dot{Q}_{consumer}}{k_{rad} \cdot A_{rad}} -$$

$$- \frac{\dot{Q}_{consumer}}{2 \cdot \dot{m}_s \cdot c_s}, \tag{10}$$

$$T_{se} = T_{sv} + \frac{\dot{Q}_{consumer}}{\dot{m}_s \cdot c_s} = T_b + \frac{\dot{Q}_{consumer}}{k_{rad} \cdot A_{rad}} +$$

$$+ \frac{\dot{Q}_{consumer}}{2 \cdot \dot{m}_s \cdot c_s}. \tag{11}$$

B. The optimal function for the partial system with a condensator

While in operation, new operating costs do not emerge by the decision stage of the condensator. Therefore,

$$O_{21}(T_c) = O_1(\dot{m}_s). \tag{12}$$

In case of an operating system mass flow of the operating system on the secondary side by the stage of the condensator remains as parameter. Optimum of the stage equals with the optimum of the previous level. We do not perform optimization. Condensation temperature is determined. It is known from former stages that

$$T_c = T_b + \left(\frac{\dot{Q}_{consumer}}{k_{rad} \cdot A_{rad}} + \frac{\dot{Q}_{cond}}{k_{cond} \cdot A_{cond}} \right), \tag{13}$$

by which

$$O_{21}(T_c(\dot{Q}_{consumer})) = O_1(\dot{m}_s). \tag{14}$$

For the production of $O_1(\dot{m}_s)$ we search for the lowest allowed (lower than nominal) circulate able heating mass flow $\dot{m}_s$.

C. The optimal function for the partial system supplemented by compressor stage

A new cost element enters, namely the electric power utilization of the compressor. In the optimization function we place this electric power utilization of the compressor next to the $O_{21}(\dot{m}_s)$ taken from the previous decision stage. To the optimal function of the newly supplemented 321 system we involve the evaporation temperature as parameter, given that electric power use and COP value of the compressor is determined by condensation and evaporation temperature.

$$O_{321}(T_o) = \left\{ \begin{array}{c} E(T_o, T_c(\dot{Q}_{consumer})) + \\ + O_{21}(T_c(\dot{Q}_{consumer})) \end{array} \right\}. \tag{15}$$

Hereby $E[T_0, T_c(\dot{Q}_{consumer})]$ is the electric power utilization of the compressor, and its cost. The $T_c(\dot{Q}_{consumer})$ and T_o determines the value of COP and the value of $\dot{Q}_{evap}$ as well, whereby $COP = \dfrac{\dot{Q}_{evap} + P_{real}}{P_{real}}$.

The values of ____ are calculated by equations (16) and (17), while P_{real} can be calculated by equation (18). equals with heat quantity extractable by U-tube.

$$\dot{Q}_{evap} = \dot{m}_p \cdot c_p \cdot \left(T_{pe} - T_o \right) \cdot \left(1 - e^{-\frac{k_{evap} \cdot A_{evap}}{\dot{m}_p \cdot c_p}} \right), \tag{16}$$

$$\dot{Q}_{evap} = \dot{m}_p \cdot c_p \cdot \left(T_{pe} - T_0\right) \cdot \left(\frac{2 \cdot k_{evap} \cdot A_{evap}}{k_{evap} \cdot A_{evap} + 2 \cdot \dot{m}_p \cdot c_p}\right), \quad (17)$$

$$P_{real} = \dot{m}_h \cdot W \cdot \frac{1}{\eta_i} \cdot \frac{1}{\eta_m}. \quad (18)$$

D. The optimal function of the partial system supplemented by evaporation stage

A new cost emerges.

$$O_{4321}\left(T_o, \dot{Q}_{evap}\right) = \left\{O_{321}(T_o)\right\}, \quad (19)$$

Whereby $\dot{Q}_{evap}$ is the known value added to T_0.

Heat quantity provided by evaporator

$$\dot{Q}_{evap} = \dot{Q}_{consumer} - P_{real} = COP \cdot P_{real} - $$
$$- P_{real} = P_{real} \cdot (COP - 1) \quad . \quad (20)$$

The stage's optimum is expressed by function $O_{4321}(T_0, \dot{Q}_{evap})$ in the function of evaporation temperature and the heat output of the evaporator.

E. Optimal function for the partial system supplemented by U-tube stage

The new cost is the electronic power use of the circulated fluid in the U-tube's hydraulic system.

$$O_{54321}\left(\dot{m}_p, T_o\right) = \min_{\dot{m}_p, T_{pv}} \left\{ \begin{array}{l} k_e \cdot \left[R_p \left(\dfrac{\dot{m}_p}{\rho_p}\right)^3\right] \cdot \\ \cdot \dfrac{1}{\eta_e} \cdot \dfrac{1}{\eta_m} + O_{4321}(T_o) \end{array} \right\}, \quad (21)$$

Whereby R_p is hydraulic resistance coefficient of the U-tube's hydraulic system, k_e is the unit cost of electric power, η_e is the pump efficiency and η_m is the motor efficiency. The function equation (21) is solved numerically. We set $\dot{m}_p$ and make T_0 a known, fixed parameter value. Fixed to T_0 $\dot{Q}_{evap} = \dot{Q}_{U-tube}$ is known as well. By this we are able to calculate the value of T_{pv}, which is

$$T_{pv} = T_0 + \frac{\dot{Q}_{U-tube}}{k_{evap} \cdot A_{evap}} - \frac{\dot{Q}_{U-tube}}{2 \cdot \dot{m}_p \cdot c_p}. \quad (22)$$

Based on differential equations (23), (24) the obtained values [8], [9], [10], [11] are utilized to determine the extractable heat capacity belonging to value T_{pv} and calculated by equation (22) to the mass flow of certain primary fluids. Then, we compare this heat capacity with the heat capacity calculated during optimization, with the values of $\dot{Q}_{evap} = \dot{Q}_{U-tube}$ heat capacity utilized in equation (22). Provided that the heat capacity value of the U-tube calculated by equations (23), (24) equals to or is smaller than heat capacity values utilized in equation (22) belonging to mass flow $\dot{m}_p$, which was applied as parameter, then the given $\dot{m}_p$ is applicable. If however,

the calculated heat capacity is bigger, then the values belonging to the given $\dot{m}_p$ fall out of the optimization.

$$\dot{m}_p \cdot c_p \cdot \frac{dT_{pv}(H)}{dH} = s + \frac{\left(T_{ground}(H) - T_{pv}(H)\right)}{R_{overall}} + \dot{q}', \quad (22)$$

$$\dot{m}_p \cdot c_p \cdot \frac{dT_{pe}(H)}{dH} = s + \frac{\left(T_{ground}(H) - T_{pe}(H)\right)}{R_{overall}} + \dot{q}'. \quad (23)$$

IV. SUMMARY

With the utilization of the above described decision system theory models heating systems with U-tube installation can be optimized. By calculating transformation equations introduced at certain stages in the function of decision variables we can determine input and output values of certain stages by given consumer's heat demand.

The decision system theory scheme demonstrated in "Fig. 2" can be utilized at any operating heat pump system, besides objective functions of the system can be calculated, which is the minimization of operation costs. In case of emerging individual need the hereby described decision system theory schemes can be supplemented by further decision stages. Nevertheless, in this case supplementation has to be performed according to the laws of system theory, and the relationships between certain decision stages have to be conducted accordingly. We described the basics of this method in our earlier papers [3], [4], [5], [6].

REFERENCES

[1] G.L. Nemhauser, Introduction to dynamic programming, Wiley, New York ; London, 1966.

[2] R. Bellmann, Dynamic Programming, Princeton University Press, Princeton, 1957;

[3] L. Garbai, S. Méhes, The basic of the system theory model of heat pumps, Vykurovanie 2008. Tatranske Matliare, Slovakia, 2008 pp. 4;

[4] L. Garbai, Sz. Méhes, Hőszivattyús rendszerek komplex rendszerelméleti modellje, Magyar Épületgépészet. 2007 (2007) 5;

[5] L. Garbai, Sz. Méhes, System Theory Modell of Heat Pumps, Gépészet 2008. Budapest, Hungary, 2008 pp. 12;

[6] L. Garbai, Sz. Méhes, System Theory Models of Different Types of Heat Pumps, 2nd IASME/WSEAS International Conference on Energy and Enviroment. Portorose, Slovenia, 2007.

[7] L. Garbai, Távhőellátás, Hőszállítás, Akadémiai Kiadó, Budapest, 2006

[8] L. Garbai, Sz. Méhes, The Amount of Extractable Heat with Single U-tube in the Function of Time, Periodica Polytechnica, Mechanical Engineering. 2008/2 (2008).

[9] L. Garbai, Sz. Méhes, Modeling of the temperature change in vertical ground heat exchangers with single U-tube installation, 6th IASME/WSEAS International Conference on Heat Transfer, Thermal Engineering and Environment. Rhodes, Greece, 2008 pp. 5

[10] L. Garbai, Sz. Méhes, Heat capacity of vertical ground heat exchangers with single U-tube installation in the function of time, WSEAS Transactions on Heat and Mass transfer. 3 (2008) 9.

[11] L. Garbai, Sz. Méhes, Energy Analysis of Geothermal Heat Pumps with U-tube Installations, 3rd IEEE International Symposium on Exploitation of Renewable Energy Sources; Subotica, Serbia, 2011

[12] L. Garbai, Távhőellátás, Hőszállítás, Akadémiai Kiadó, Budapest, 2006

Importance and Value of Predictive Approach for Boiler Operating Performance Improvement

M. Kljajić*, D. Gvozdenac*, S. Vukmirović*

* University of Novi Sad, Faculty of Technical Sciences, Novi Sad, Serbia

kljajicm@uns.ac.rs; gvozden@uns.ac.rs; srdjanvu@uns.ac.rs

Abstract—Energy waste detection as a reactive approach is not proper for high demanded, complex and intensive energy systems. Efficiency forecasting by analytic modeling is essentially preventive or proactive approach which leads to avoiding inefficiency.

A comprehensive insight and added awareness, which presented approach enables, in combination with expert and soft computing assistance can locate, recommend and specify opportunities for increasing energy efficiency of boiler houses and reduce irrational energy use and related costs.

Presented analysis is led by finding possibilities how energy resources can be used wisely to secure more efficient final energy supply, to save money and limit environmental impacts. But the biggest problem and challenge are related to the stochastic nature and variety of influencing factors in energy transformation process. In that context, reliable prediction of energy output variation for expected influencing factors is very valuable.

The paper presents one method for modeling, assessing and predicting efficiency of boilers based on measured operating performance. The method implies the use of neural network approach to analyze and predict boiler efficiency. Neural network calculation reveals opportunities for efficiency enhancement and makes good insight into influencing factors onto boiler operating performance.

The analysis is based on energy surveys for randomly selected 65 boilers in the Province of Vojvodina carried out at over 50 sites covering the representative range of industrial, public and commercial users of steam and hot water. The sample formed in such a manner covers approximately 25% of all boilers in the Province of Vojvodina and provides reliability and relevance of obtained results.

Keywords: boiler efficiency; operating performance; neural nets; modeling; predicting.

I. INTRODUCTION

The consumers' area of Vojvodina can be considered as a rounded entirety. It covers the area of 21,506 km^2 on which 2,031,992 (2003) inhabitants live satisfying their energy needs for life and work by using the following primary energies: natural gas, liquid oil derivatives, coals, heating wood, and agricultural wastes, primarily from farming production.

Industrial, commercial and public companies and institutions are mostly run by old-fashioned energy technologies and energy intensive production technologies. Measuring and automation equipments are also old-fashioned and often inoperative. In the last ten years it is notable that there is a low level of investments in the energy sector. Inadequate maintenance additionally aggravates existing low energy efficiency which is expectable.

Above facts indicate that energy supplying processes are accompanied by high specific energy consumption per production/service unit and low energy efficiency. Not only is that it necessary to start again production capacities in some cases but also to reconstruct plants and installations. In order to improve energy efficiency, it is necessary to make investments which will produce benefits and energy savings on the long run. After resuming production/service capacities and essential rebuilding of plants and installations, investments in energy efficiency improvement are essential.

With right selection of plant, equipment and fuel, innovation of technology, better organization we can reduce costs and use resource and achieve higher quality in the supplying process. The next topics provide insight in such assessment.

A. Importance of energy efficiency

There are numerous reasons for the desire to improve energy efficiency in boiler operation but perhaps the most compelling one is wasted money for energy costs reflected in the balance sheet bottom line. In many cases, improvements can be made for low or no cost involving slight changes to the way a process or equipment is operated to optimize their performance rather than to purchase expensive equipment.

Saving energy has many benefits including:

– Reduced energy costs (increasing profits or releasing resources for other activities)
– Improved environmental performance due to reduced carbon dioxide emissions
– Improved competitiveness of products or services
– Enhanced public image with customers and other stakeholders
– Reduced exposure to Government drivers such as the Climate Change Levy.

II. OBJECTIVE OF ANALYSIS

Because of increasing fuel prices, industries, district heating companies and public institutions that use steam or hot water boilers for heating, process or power

generation are hard-pressed to operate at peak efficiencies. While insufficient efficiency of heat energy production and distribution contributes to overall energy costs, efficiency analysis gains significance and puts into focus the heart of energy generator - a boiler.

The creation of relevant and comprehensive performance evidence for regional boiler plants population in the region of the Province of Vojvodina provides numerous possibilities for implementing energy management approach and for critical evaluation of accepted practices in the field of energy efficiency. A comprehensive insight and added awareness, which presented approach enables, in combination with expert and soft computing assistance can locate, recommend and specify opportunities for increasing energy efficiency of boiler houses and reduce irrational energy use and related costs.

A. Analysis approach

Steam and hot water are used throughout industry, commerce and the public sector for a wide range of processes and space heating requirements, and can represent significant proportion of the organization's energy costs. It is, therefore, important for owners and operators of boilers to ensure that the plant operates as efficient as possible and consequently reduce avoidable energy costs.

All sectors, industrial, commercial and public use efficiency as the basic performance indicator. However, defining, assessing and predicting energy efficiency is not easy, primarily because it is affected by more factors than anticipated. Therefore, the basic intention of the analysis is to apply neural network approach which can create necessary preconditions and guidelines for assessing and anticipating boiler operating performance.

The approach is designed with a capability for identifying, investigating and predicting possible influence factors which should be taken into account for a reliable energy efficiency analysis. The approach uses neural network computation which reveals opportunities for efficiency enhancement and makes good insight into influence factors for efficiency.

Also, the analysis alerts to the possibility of efficiency drop in heat energy production, and timely preconditions for suggesting effective measures to ensure efficiency of power plants.

B. Model formulation

Operating performance analysis is based on computational model which uses data from energy surveys and measurements in the group of randomly selected 65 boilers. The audit has been carried out at over 50 sites covering the representative range of industrial, public and commercial users of steam and hot water. The sample covers approximately 25% of all boilers in the Province of Vojvodina which provides reliability and relevance of obtained results.

For this purpose, 65×5 experimental measurements are collected (input parameters). About 300 of those are used as training data for neural network model and the rest (25) is used for testing.

Presented approach develops a model for assessing and predicting efficiency based on real (measured) operating performance. The approach understands the use of neural network model for analyzing and identifying operational scenarios which lead to peak efficiencies.

The significance of applied method is in providing extensive possibilities for identification of inefficiencies. Proposed approach can be effectively used to assess operating performance and find optimum operational regime. The significance is more noticeable in predicting the response of a complex energy system that cannot be easily modeled mathematically.

C. Auditing methodology

The first step is selecting necessary parameters for each site and particular boiler plant. Chosen relevant information and parameters are grouped into boiler nameplate information, boiler operational performance, occupation dynamic, capacity engagement, flue gas composition and state or conditions of the plant and its subsystems.

Techniques used to carry out each audit are: metering, internal monitoring records analysis, engineering calculations and specifics based on opinions of operational staffs in energy department of each company [3]. Through measurements, direct communications and interviews with a responsible person in the energy department of each company or institution and physical audit of the plant, necessary information is collected and organized in several categories in the following way:

- Common information about the company: Activity; Sector.
- Common information for selected boiler: Basic / Optional fuel; Boiler type (steam or hot-water boiler); Exploitation time (years); Boiler purpose (technology or heating); Capacity [t/h] and [MW]; Operational parameters [oC/bar]; Plant engagement (permanent, seasonal, etc).
- Boiler operational performance: The most usual load range regarding to nominal load capacity [%]; Annual working hours [h/a]; Specific fuel consumption [m3/h, kg/h].
- Measurement parameters: Flue gas temperature [oC]; Flue gas velocity [m/s]; Load range during the measuring of flue gas composition [%].
- Calculated performances: Flue gas flow rate [m³/h]; Boiler efficiency according to GCV [%]; Boiler efficiency according to NCV [%]; Flue gas losses [%]; Annual fuel consumption [GWh/a]
- Combustion quality (flue gas composition): O_2 [%] / λ [%]; CO_2 [%]; SO_2 [ppm]; CO [ppm]; NO [ppm]; NO_X [ppm] and H_2 [ppm]; MCO [kg/h] and MNOX [kg/h].
- Monitoring and control existence: Stationary and continuity oxygen control; Measurement of heat energy delivery rate; Flow rate measurement of boiler feed water and condensate return; Combustion quality control, etc.
- Control type: Manual; Semiautomatic; Automatic.
- Reconstruction and/or revitalization record: Burners and associated equipment; Heat recovery systems (economizer); Pipes; Automatic control equipment etc.

D. Overview of existing boiler operating performance

Overview of existing boiler operating performance in the Province of Vojvodina is carried out for selected sectors: industry, district heating systems and healthcare facilities. The main reason for adopting mentioned sectors arrangement is dominant contribution rate of large and middle scale boiler plants of these three sectors in the overall energy activities in the Province of Vojvodina. Similar, selected type of input fuel is only natural gas and heavy fuel oil, because of dominant sharing rate in fuel structure. The Fig.1 presents percentage distribution according to the sector structure and activity structure for industrial sector, where companies are structured according to their activities.
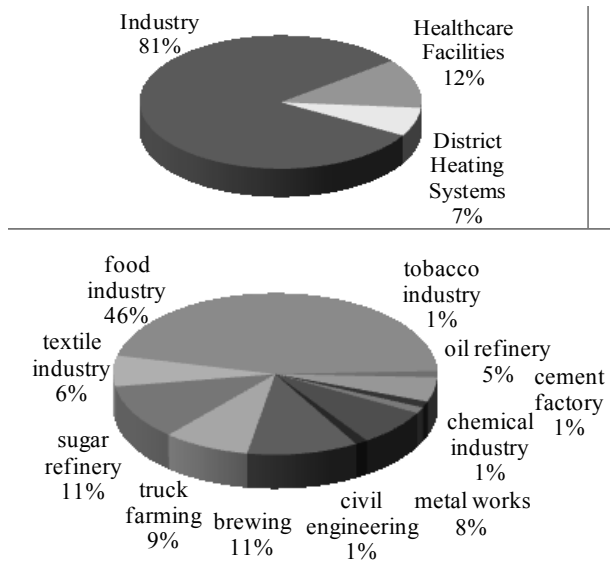

Figure 1. Distribution according to the Sector Structure and Activity Structure for Industrial Sector

Generally, in the Republic of Serbia, occupation dynamics and capacity engagement in energy departments are critical obstacles for reaching satisfactory energy efficiency [3]. By establishing reliable patterns for assessing rational use of energy, the energy audit includes information about operational character of the plant. For this purpose, for all sectors, the following categories are adopted and itemized by occupational intensity: permanent or seasonal operation, operation according to need, conserved, out of order, cut-off.

Similarly, fuel is structured for every sector and it is indicative that the dominant fuel types are natural gas and heavy fuel oil, and then sunflower shell, coal, combined sunflower shell and coal, light oil in much lower contribution rate.

Key results of measurements and calculations for the boiler population of the sample in the industrial sector, district heating systems and healthcare facilities are presented in the Table 1, structured by minimum, maximum and average values.

For configuration of input values, necessary for neural network model training, data from dominant categories in occupational intensity have been used such as: permanent or seasonal operation and operation according to need and fuel types: natural gas and heavy fuel oil.

TABLE I.
OVERVIEW OF EXISTING BOILER OPERATING PERFORMANCE

Value	Industrial Sector			District Heating Systems			Healthcare Facilities		
	Min	Av.	Max	Min	Av.	Max	Min	Av.	Max
Exploitation [years]	3	29	46	20	26	34	2	24	40
Capacity [MW]	0.4	10.5	81.6	6.8	14.0	23.0	0.5	2.6	6.7
Load range [%]	15	72	100	50	64	75	40	69	95
Oxygen content [%]	0.61	7.09	18.00	1.70	4.69	9.36	2.21	8.31	18.51
Efficiency [%]	60.1	87.8	94.0	85.5	91.3	97.6	61.1	86.0	93.4
Flue gas temp. [°C]	115.3	203.3	330.8	49.3	135.1	203.5	136.3	199.1	284.8
Operating hours [h/a]	480	4,462	8,664	1,650	3,300	4,500	1,200	4,387	8,650
Fuel energy [GWh/a]	0.57	34.02	376.2	7.51	27.43	51.59	0.44	8.45	30.40

III. NEURAL NETWORK METHODOLOGY

The biggest problem in energy efficiency analysis is related to the stochastic nature of influencing factors. In such circumstances, adequate approach understands more accurately the prediction of energy output by variation of selected inputs. Neural network methodology enables reliable prediction which consequently allows planning and carrying out the necessary measures to reach mentioned goals.

Classic methods for forecasting include regression and state space methods. The more modern methods include expert systems, fuzzy systems, evolutionary programming, artificial neural networks and various combinations of these tools. Among many existing tools, neural networks have received much attention because of their clear model, easy implementation and good performance. Neural networks have become popular in various real world applications including prediction and forecasting, function approximation, clustering, speech recognition and synthesis, pattern recognition and classification, and many others [8].

MATLAB was chosen as the technical computing language for the ANN modeling and the Neural Networks Toolbox as predefined surroundings. A model of the boiler was developed, trained, tested and used in the MATLAB interactive environment, which is highly suitable for algorithm development, data visualization, data analysis, and simulative calculations.

A. Input and output parameters selection

To learn the network, a set of input-output data is needed. To learn the network based on known data, matched input and output parameters are used. These data include a series of input data that define operational conditions with the output data that define the efficiency of energy transformation.

Input and output parameters selection is carried out in accordance with specifics of boilers in a region and identified inefficiency thorough site surveys and measurements.

An output parameter is boiler's efficiency, defined as performance indicator. Selected input parameters are: type of fuel, type of boiler, exploitation period, nominal capacity, load range and oxygen content in flue gases.

B. Learning network

In multi-layer feed forward networks, input and output vectors are used for training the network. Network will learn to associate given output vectors with input vectors by adjusting its weights which are based on output error. The weight modification algorithm is the steepest descent algorithm (often called the delta rule) to minimize a nonlinear function. The algorithm is called back error propagation or back propagation because errors are propagated back through hidden layers [7].

The weights can be learned by training the network using a training set of target states for the output for a given set of inputs. The steepest descent algorithm essentially seeks to choose weights during training. The mean square error between the target output and the actual output of the network over all training data is minimized. Thus, the weights are chosen for output neurons so that the back propagation algorithm minimizes the mean square error for N training samples.

The neural network model used in this paper has one hidden layer with ten neurons. Activation function for all layers is Logarithmic a sigmoid transfer function.

C. Neural Network architecture

Several architectures of ANN were tested with different numbers of hidden layers and different numbers of neurons in layers. The first set of experiments showed that both one and two hidden layers produce similar results, so a network with one layer was adopted. After that, a new set of experiments were conducted to establish the correct number of neurons in layer. A range of layers with the number of neurons ranging from 5 to 30 were tested. Experiments showed that a network with ten neurons in hidden layers provided the best results. Final architecture or ANN is shown in Fig. 2.
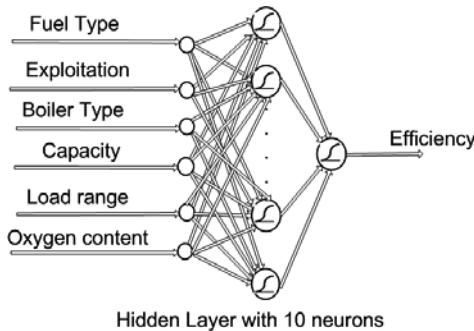
Figure 2 Architecture of proposed neural network

D. Validation process

The neural network model has been trained with 60 values in input and output values. As per recommended literature, ten percent of data have been used for validation purposes. We have limited the number of epochs to 100 but training was finished much earlier in all experiments. After few dozens of epoch errors on training, the set was less than 0.1%, which is acceptable taking into account precisions of input data. The error on verification set is less than 1 percents which suggests that trained neural network model can be used in exploration with data that are not used in training process.

The model was evaluated based on its prediction errors. The error measurement which is most commonly

employed in ANN, and which was used in the evaluation of the results presented here, is the mean absolute percentage error (MAPE), which is defined as

$$MAPE = \frac{|x_i - y_i|}{x_i} \times 100$$

Where x_i is the actual values and y_i is the predicted values at time instance i. MAPE calculated for test data is MAPE = 3.18%.

Accuracy of predictions can be enhanced by increasing the population of input parameters. In addition, as the input data can be attached to other boiler plant's data consequently increasing not only the network learning but also network accuracy. A greater number of samples have enabled better network training performance and more precise predictions of efficiency.

Larger deviations between the model results and the collected data are noticeable in ranges of operational characteristics with higher values of measured oxygen content in the flue gases or low plant load. During energy audits, data in these ranges appeared less frequently and consequently a smaller amount of data was collected and additionally these data were less useful for training the network.

IV. VALUE OF THE APPROACH

The value of the method can be assessed according to the potential for competent and reliable performance analysis and also according to the scope of method limitations. The analysis capability is described thorough following possibilities provided by the applied method:

1. Prediction of efficiency variation for different operating conditions and parameters.
2. Consideration of efficiency variation nature in accordance with any input changes.
3. Assessment of any particular previously defined input parameter onto influence potential.
4. Ranking of particular influence scaled input variable to efficiency.
5. Operating performance trend analysis.
6. Identification of reached amount of efficiency improvement for particular operate regime.

Relevance of the method is proven and confirmed by multiplicity testing process where model provided data are well matched actual data measured at the plant.

The lack of the method is a need for long and complex time-matched measurements of parameters requiring certain period of time.

Also, the method treats and covers only the most usual operating regime which creates less reliable prediction in the range of extreme variations of particular input parameters and boundary regimes. This limitation can be effectively exceed by further development of auditing procedures and spread of measurement to additional different and predefined operating regimes.

The results obtained correspond well with collected and measured results and the computational effort of the neural network method and time required in the analysis is acceptable. This achievement indicates that the neural network method can be used efficiently for predictions.

V. PREDICTION OF BOILER OPERATING PERFORMANCE

The prediction of boiler operating performance is carried out by formed neural network model and findings are arranged and structured in a form of sensitivity analysis. Operational performance examination carried out for selected variable input parameters are: nominal capacity, average operational load range and oxygen content in flue gases. Variation rate is 10% from baseline boiler performance. The fixed input parameter is exploitation period because years of exploitation do not have significance and consistent influence onto efficiency. The output parameter is efficiency.

The analysis introduces typical boiler specifications from formed sample which is used as a baseline boiler performance and characteristics. Boiler specifications include the following issues: 25 years of exploitation, capacity of 10 MW, average operational load range 69% and oxygen content in flue gases of 6.33%. Efficiencies, calculated by neural network model, for different boiler fuel and types are: efficiency of fired natural gas, which for a steam boiler is 90.20%, for natural gas and hot water boiler is 89.54%, for heavy fuel oil and steam boiler is 88.83% and for heavy fuel oil and hot water boiler is 89.74%. Fig. 3 and 4 show predicted operational performance from all studied configurations.

Figure Legend:
——————— Sensitivity of boiler efficiency on installed capacity
··············· Sensitivity of boiler efficiency on oxygen content in flue gases
– – – – – Sensitivity of boiler efficiency on operational load range
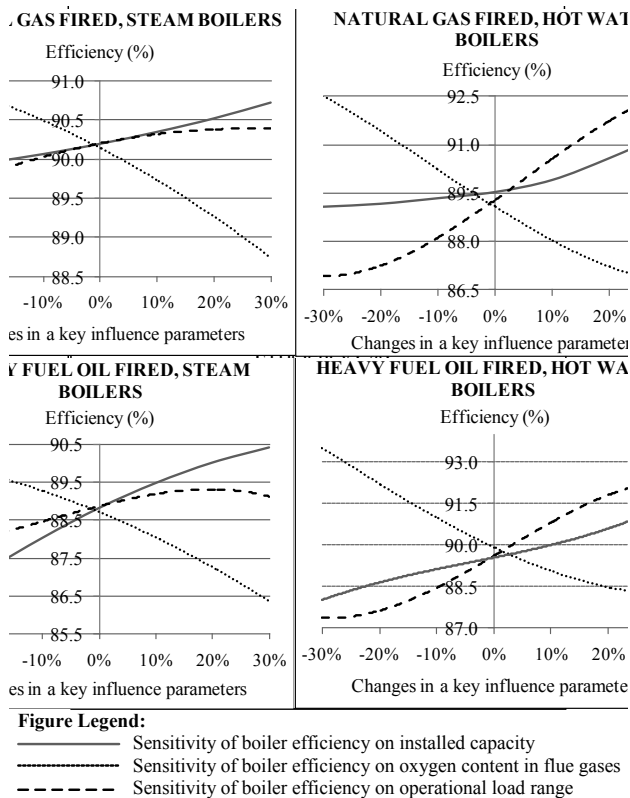
Figure 3 Natural gas fired, Steam (upper graph) and Hot water boiler (lower graph) - Sensitivity of Efficiency on Oxygen Content in Flue Gases, Installed Capacity and Operational Load Range for two Different Fuel and Types of Boilers

Figure Legend:
——————— Sensitivity of boiler efficiency on installed capacity
··············· Sensitivity of boiler efficiency on oxygen content in flue gases
– – – – – Sensitivity of boiler efficiency on operational load range
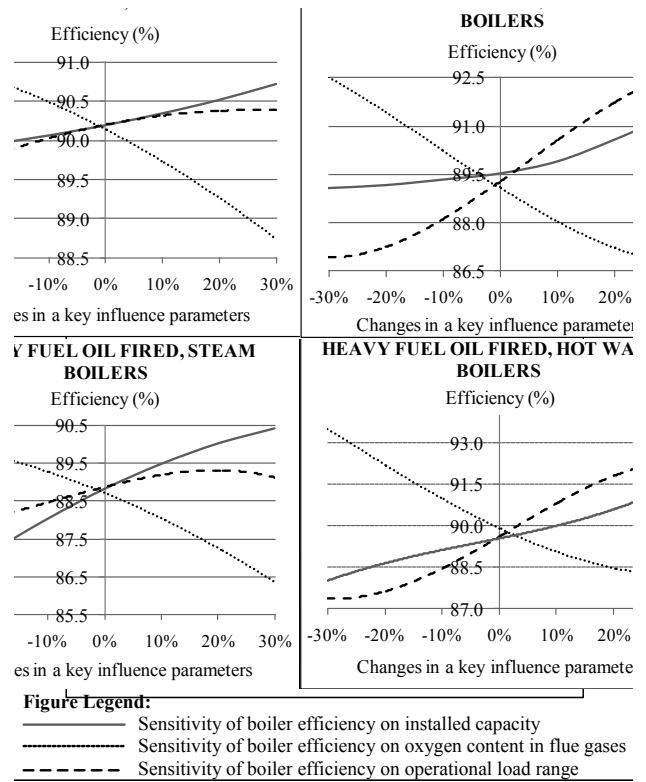
Figure 4 Heavy fuel oil fired, Steam (upper graph) and Hot water boiler (lower graph) - Sensitivity of Efficiency on Oxygen Content in Flue Gases, Installed Capacity and Operational Load Range for two Different Fuel and Types of Boilers

VI. PRACTICAL IMPLICATION

Currently, many opportunities for obtaining substantial energy efficiency improvements are not realized in the Province of Vojvodina in spite of availability of well known improvement methods and measures and necessary background data. Such a situation implicates the existence of space for implementation and valuable applications.

In terms of practicality, the ANN method can, in general, assist by indicating recommendations and guidelines for activities such as applying improved operational management and procedures, efficient use of a plant's equipment, improving maintenance of a plant's resources, establishing evidence and improved measurements, etc. Such activities can provide the preconditions for effective and systemic changes in all aspects of boiler house operations.

At the operational level, this approach raises the possibility of a more positive insight into the operational performance of a plant in circumstances where there multiple disturbances of input parameters occur simultaneously. Later on, it allows for a comprehensive analysis of resources the commitment of resources necessary for initiating and implementing systematic improvement measures and further development of operational procedures.

At a managerial level, forecasting operating performance is important for supporting the decision-making process in terms of frequent use of optional fuel as a result of fluctuations in energy prices or price parity on the open market or when certain types of fuels are periodically lacking.

At the sector level, this approach can contribute to the creation of new incentive programs at the state or provincial level, the promotion of new technological solutions, and to providing subsidies for the most urgent and effective investment, as well as many other possibilities.

Energy waste detection as a reactive approach is not proper for high demanded, complex and intensive energy systems. Efficiency forecasting by neural network method is essentially preventive or proactive approach which leads to avoiding inefficiency.

Predictive analysis with reliable and relevant obtained results can assist in recommending and specifying opportunities for reducing irrational energy use. For prediction, the neural network model can simulate wide scale of anticipated operational regimes and check efficiency for different favorable or undesirable values of input parameters.

VII. Key Considerations

In all mentioned energy sectors, systemic solutions required for improving the current situation in the Republic of Serbia and also in the Province of Vojvodina do not exist. This particularly refers to the aspect of energy efficiency related to the introduction of energy management systems, modern energy and environmentally friendly technologies and regulatory activities aimed at improving the current situation.

General recommendations are the improvement of care (through better maintenance) for plant resources, existence and observing energy procedures, establishing evidence, measures and other activities which are aimed at systemic changes and continuous care for energy and energy plants and other aspects of boiler house operations. Such systematic approach in changing the situation and attitudes towards these issues is both important and necessary. The change is equally important and indispensable not only for the community itself but also for end users of final energy [4].

In the Republic of Serbia and also in the Province of Vojvodina, investments in energy efficiency are still a great challenge for local authorities, policy makers and business leaders. Very few public or commercial companies are aware of business benefits generated by efficient energy use and how it can help to cut costs and keep them ahead of their competitors.

The neural network method can assist in mentioned regional environment by recommendations and guidelines for activities such as applying improved operational management and procedures, efficient use of plant's equipment, improving of care for plant's resources, establishing evidence and improved measurements, etc.

Such activities open preconditions for effective and systemic changes and continuous care for energy and energy plants and other aspects of boiler house operations.

References

[1] Ayhan-Sarac B, Karlık B, Bali T, Ayhan T. Neural network methodology for heat transfer enhancement data. International Journal of Numerical Methods for Heat & Fluid Flow, Vol. 17 No. 8, 2007, pp. 788-798, 0961-5539, DOI 10.1108/09615530710825774

[2] Bevilacqua M, Braglia M, Frosolini M, Montanari R. Failure rate prediction with artificial neural networks, Journal of Quality in Maintenance Engineering, Vol. 11 No. 3, 2005, pp. 279-294, 1355-2511, DOI 10.1108/13552510510616487

[3] Gvozdenac D, Kljajic M. Technical and Economical Assessments of the Energy Efficiency of Boilers Improvement in the Province of Vojvodina, PSU-UNS International Conference on Engineering and Environment - ICEE-2007, Thailand, 2007.

[4] Morvay Z, Gvozdenac D. Applied Industrial Energy and Environmental Management, John Wiley & Sons, UK, 2008.

[5] Dukelow G. S. The Control of Boilers, Instrument Society of America, USA, 1991.

[6] Carpinteiro O, Lemeb R, de Souza A, Pinheiro C, Moreira E. Long-Term Load Forecasting via a Hierarchical Neural Model with time Integrators, Electric Power Systems Research 77 (2007) 371–378

[7] Rumelhart D, Hinton G, Williams R. Learning Internal Representations by Error Propagation, Parallel Distributed Processing, Vol. 1, Chapter 8, MIT Press, pp. 318-362 1986.

[8] Masters T. Practical Neural Network Recipes in C++. London: Academic Press Inc.; 1993

[9] Good Practice Guide: Energy Efficient Operation of Boilers, the Carbon Trust, UK, 2004.

[10] Good Practice Guide: An Introductory Guide to Energy Performance Assessment – Analyzing Your Own Performance, the Carbon Trust, UK, 2005.

MATHEMATICAL MODEL AND NUMERICAL SIMULATION OF CPC-2V CONCENTRATING SOLAR COLLECTOR

Velimir P. Stefanovic Dr. Sci.[*], **Sasa R. Pavlovic** Ph.D student[**]

[*] Nis. Serbia, Faculty of Mechanical Engineering, Department for Energetics and Process technique, University in Niš, Serbia

[**] Nis. Serbia, Faculty of Mechanical Engineering, , Department for Energetics and Process technique University in Niš, Serbia

e-mail : veljas@masfak.ni.ac.rs, sasap208@yahoo.com

Abstract-- Physical and mathematical model is presented, as well as numerical procedure for predicting thermal performances of the CPC-2V solar concentrator. The CPC-2V solar collector is designed for the area of middle temperature conversion of solar radiation into heat. The collector has high efficiency and low price. Working fluid is water with laminar flow through a copper pipe surrounded by an evacuated glass layer. Based on the physical model, a mathematical model is introduced, which consists of energy balance equations for four collector components. In this paper water temperatures in flow directions are numerically predicted, as well as temperatures of relevant CPC-2V collector components for various values of input temperatures and mass flow rates of the working fluid, and also for various values of direct sunlight radiation and for different collector length.

Keywords: thermal, solar radiation, performance, model, dynamic analysis

I. INTRODUCTION

The device which is used to transform solar energy to heat is referred to as solar collector or SC. Depending on the temperatures gained by them, SC can be divided into low, middle and high temperature systems. Mid-temperature systems are applicable for refrigeration systems and industrial processes.

Numerous theoretical and experimental research of solar collectors for the mid-temperature conversion of solar radiation into heat via a liquid as a working fluid have been conducted. R. Tchinda, E. Kaptouom i D. Njomo [1] have investigated heat transfer in a CPC collector and developed model which during numerical analysis of heat transfer takes into account axial heat transfer in a CPC collector. Impact of various parameters has been investigates, such as input temperature and the value of the flow of working fluid on dynamical behavior of the collector. B. Norton, A. F. Kothdiwala i P. C. Eames [2] have developed a theoretical heat transfer model, which describes steady state heat behavior of a symmetric CPC collector and investigated the impact of the tilt angle of the collector to the CPC collector performance. R. Oommen i S. Jayaraman [3] have experimentally investigated a complex parabolic concentrator (CPC), with water as a working fluid. They have investigated efficiency of the collector for various input temperatures of water, as well as the efficiency of the collector in the conditions of steam generation. P. Gata Amaral, E. Ribeiro, R. Brites i F.

Gaspar [4] have worked on the development of solar concentrating collectors based on the shape known as complex paraboilc colector of solar energy (CPC), which allow utilization of maximal solar energy ratio. By wide area of rotation movement of a SolAgua collector, it was made possible to follow the Sun. Khaled E. Albahloul, Abdullatif S. Zgalei i Omar M. Mahgjup [5] have theoretically analyzed the use of a CPC collector with refrigeration systems. They followed the efficiency of CPC collector with refrigeration systems during the year. CPC collectors have been of different length and with different concentrating ratios.

In this paper, physical and mathematical model are given, as well as the numerical calculation of a collar collector CPC-2V. This is a solar concentrator, designed for the mid-temperature conversion [6-11] (B. Nikolic, V. Stefanovic and all). The paper gives a change of fluid temperate and collector components in the direction of the flow, as well as the influence of the input fluid temperature, radiation intensity, mass flow rate to the heating behavior and current efficiency of the collector. The change of fluid temperature was given in the direction of the fluid flow for six collectors connected in a row

II. PHYSICAL MODEL

A. Structure

In this paper, a laminar flow of the fluid (l) through the apsorber (2) is assumed. The pipe of the absorber is subjected to solar radiation. Solar rays go through the transparent cover (5) on the collector apparatus. A part of the solar radiation after going through the transparent cover of the pipe (4) and evacuated area (3), falls directly to the absorber. Another part of the solar radiation, after reflection from the reflector (6), goes through the transparent cover leyer of the pipe and falls at the pipe absorber. The look of a CPC-2V module is presented in Fig. 1. (a). Scheme of the cross section of a CPC-2V module is given in Fig. 1 (b).
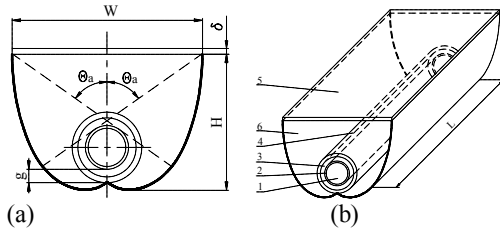
Figure 1. Functional scheme of system

The CPC module consists of a complex cylindrical-parabolic reflection surface and a copper tube with ø15 mm outside diameter used as the absorber. Cylindrical cooper absorber is surrounded by a glass surrounding layer for lowering convective loss from the collector pipe. The area between the pipe absorber and glass surrounding layer is evacuated. Conversion of solar energy into heat is conducted on the pipe collector. Pipe absorber is colored with selective color of high absorbing properties and low emissivity (ε_r). The area of the reflector has high reflection ratio (ρ_m). Between the pipe absorber and the reflector there is a gap (hole) which stops heat transfer from the collector pipe to the reflector. Water is the working fluid, with a laminar flow through the pipe of the collector. Apparatus of the collector is covered by transparent cover layer made of glass (Plexiglass) so the reflector area could be saved from wearing and to lower the value of heat loss from the assembly pipe absorber-surrounding pipe layer. The collector consists of six CPC modules which are connected parallel to the flow paths, so flow properties inside them may be considered equal.

III. MATHEMATICAL MODEL

A. Introduction

Based on the physical model represented by the CPC collector, through whose absorber pipe a laminar flow of water occurs, and which is subjected to solar radiation, a mathematical model is proposed. The mathematical model consists of the energy balance equations for four CPC module components: (1) working fluid, (2) collector pipe- absorber, (3) surrounding pipe layer, (4) transparent cover. During the set-up of mathematical model only one module of CPC collector was analyzed.

B. Basic assumption according to which the model was based

The following assumptions were introduced for the definition of mathematical model:

- The sky was treated as an absolute black object, which is the source of infrared radiation during an equivalent sky temperature

- Reflected radiation from surrounding objects was considered negligible and was not taken into account;
- Diffusive insulation on the apparatus of the cover is isotropic;
- CPC collector has permanent Sun tracking, thus Sun rays are normal to the plane of transparent cover (aperture plane);
- Radiation to the collector is unified;
- CPC module is constructed with ideal geometry, thus the concentration ratio is given by: [13]:

$$C_a = \frac{1}{sin\theta_a} = \frac{A_c}{A_r} \quad [-] \tag{1}$$

- Heat transport in the transparent cover, surrounding cover layer, collector surrounding layer, pipe absorber and the fluid is transient
- Transparent cover, transparent cover layer, collector surrounding layer, and pipe absorber are homogenous and isotropic objects;
- Heat transport by conduction in the transparent cover layer and the glass layer is negligible due to small heat conductivity of glass;
- Thermo-physical properties of the CPC collector component material (ρ^*, c, λ) as well as optic properties (ρ, τ, ε, α) of the components of CPC collector are do not depend on coordinates, temperature nor time;
- Fluid flow is steady state and it is conducted only in the axial direction, thus the velocity field is related just to the speed component w_z;
- Fluid flow shape is the same in every axial cross sections, thus the tangential velocity component w_φ does not exist;
- Radial velocity component w_r is neglected as a value of smaller order and thus the convection in radial direction is also neglected;
- Fluid flow may be considered incompressible;
- Conduction in the axial direction has a negligibly small contribution to the resulting heat transport compared to the convection.

102

C. Energy balance equation

Mathematical model consists of equations of energy balance for all of the four components of the CPC modle, relations for determining heat transfer coefficient, relations for radiation absorbed by the relevant system components. In order to gain a unified solution from the system of equations, initial and boundary conditions are defined. With a predetermined assumptions, equations of energy balance may be written as:

(1) For the working fluid

Energy balance for an elementary fluid volume of dz length in the axial direction, after sorting, may be written as:

$$\rho_f^* c_{pf} A_f^* \frac{\partial T_f}{\partial t} = -\rho_f^* c_{pf} A_f^* w_z \frac{\partial T_f}{\partial z} + U_{r/f}\left(T_r - T_f\right) 2\pi r_{r,o} \tag{2}$$

Where ρ_f^*, c_{pf} i w_z represent density, specific heat, velocity in the axial direction of the elementary fluid volume, respectively $A_f^* = r_{r,i}^2 \pi$ is the area of the cross section of the elementary fluid particle. The second term on the right hanside of the equation (2) represents heat gained from the outer side of the collector pipe

Boundary condition for this equation is:

$$\text{za } z = 0, \quad T_f = T_{in}. \tag{3}$$

(2) For the collector absorber pipe

Energy balance for elementary part of the collector of dz length in the axial direction may be written as;

$$\rho_r^* c_r A_r^* \frac{\partial T_r}{\partial t} = \frac{\partial}{\partial z}\left(\lambda_r \frac{\partial T_r}{\partial z}\right) A_r^* - \left(h_{c,r/e} + h_{r,r/e}\right)$$

$$\left(T_r - T_e\right) 2\pi r_{r,o} -$$

$$-U_{r/f}\left(T_r - T_f\right) 2\pi r_{r,o} + \left(q_{b,r} + q_{d,r}\right) 2\pi r_{r,o} \tag{4}$$

Where λ_r, ρ_r^* i c_r are head conduction coefficient, density and specific heat for elementary pipe volume, respectively. $A_r^* = \left(r_{r,o}^2 - r_{r,i}^2\right)\pi$ is the area of the cross section of elementary part of the collector pipe. The first term on the right hand side of the equation (4) represents heat transport by conduction in the axial direction of the collector, the second is the heat loss due to convention and radiation between the collector pipe and the surrounding layer of the collector pipe, the third term represents heat given to the working fluid, and the fourth represents heat gained via solar radiation

Boundary conditions for this equation are:

$$\text{za } z = 0, \quad \frac{\partial T_r}{\partial z} = 0; \tag{5}$$

$$\text{za } z = L, \quad \frac{\partial T_r}{\partial z} = 0 \tag{6}$$

(3) For the transparent cover of the pipe collector

Energy balance for the elementary part of the surrounding layer of the collector pipe of dz length is written as:

$$\rho_e^* c_e A_e^* \frac{\partial T_e}{\partial t} = \left(h_{c,r/e} + h_{r,r/e}\right)\left(T_r - T_e\right) 2\pi r_{r,o} -$$

$$-\left(h_{c,e/c} + h_{r,e/c}\right)\left(T_e - T_c\right)$$

$$2\pi r_{e,o} + \left(q_{b,e} + q_{d,e}\right) 2\pi r_{r,o} \tag{7}$$

Where ρ_e^* i c_e are density and specific heat og the surrounding layer of the collector $A_r^* = \left(r_{e,o}^2 - r_{e,i}^2\right)\pi$ is the area of the cross section of elementary part of the surraounding layer of the collector. The second term on the right hand side of the equation (7) is the heat lost due to radiation from the surrounding layer of the collector to the transparent cover

(4) For the transparent cover

Energy balance for the elementary part of the transparent cover of the concentrating collector, with dz length in the z direction and W width, may be written as:

$$\rho_c^* c_c A_c^* \frac{\partial T_c}{\partial t} = \left(h_{c,e/c} + h_{r,e/c}\right)\left(T_e - T_c\right)$$

$$2\pi r_{e,o} - h_{c,c/a}\left(T_c - T_a\right) W - h_{r,c/s}\left(T_c - T_s\right) W +$$

$$+\left(q_{b,c} + q_{d,c}\right) 2\pi r_{r,o} \tag{8}$$

$A_c^* = W \delta$ is the area of the cross section of elementary part of the transparent cover of the collector. The second term on the right hand side of the equation (8) is the heat lost due to convection from the transparent cover to the environment, the third term is the heat lost due to radiation between the transparent cover and the sky.

D. Initial conditions

It was assumed for the initial conditions that in the initial time point the temperature field in all components is equal to the environment temperature T_a, while the fluid temperature at the inlet is constant in time

$$Za \quad t = 0, \quad T_f = T_r = T_e = T_c = T_a \tag{9}$$

$$Za \quad z = 0, \quad T_f = T_{in} \tag{10}$$

F. Heat transfer coefficients

Heat transfer coefficient for convection from the cover to the environment, caused by air flow (wind) $h_{c,c/a}$ is given by the following relation je (Duffie i Beckman [12]):

$$h_{c,c/a} = \left(5.7 + 3.8v\right)\frac{A_c}{A_r} \tag{11}$$

Heat transfer coefficient for the radiation of heat between the transparent cover and the sky $h_{r,c/s}$ is calculated by :

$$h_{r,c/s} = \varepsilon_c \sigma \left(T_c^2 + T_s^2\right)\left(T_c + T_s\right)\frac{A_c}{A_r} \tag{12}$$

Convective heat transfer coefficient between the surrounding pipe layer and the transparent cover, $h_{c,e/c}$ may be calculated by [14]:

$$h_{c,e/c} = \left[3.25 + 0.0085\frac{T_e - T_c}{4r_e}\right]\frac{A_e}{A_r} \tag{13}$$

Heat transfer coefficient originating from the radiation form the surrounding pipe layer to the transparent cover $h_{r,e/c}$ is given by [14]:

$$h_{r,e/c} = \frac{\sigma\left(T_e^2 + T_c^2\right)\left(T_e + T_c\right)}{1/\varepsilon_c + A_e/A_c\left(1/\varepsilon_c - 1\right)}\frac{A_e}{A_r} \tag{14}$$

Heat transfer by convection through the evacuated area between the collector pipes and the surroundin collector layer may be neglected, so the heat transfer ceofficient by convection is $h_{c,r/e} \approx 0$.
Heat transfer coefficient for radiation from the collector pipe to the collector surrounding layer $h_{r,r/e}$, is given as:

$$h_{r,r/e} = \frac{\sigma\left(T_e^2 + T_r^2\right)\left(T_e + T_r\right)}{1/\varepsilon_r + A_r/A_e\left(1/\varepsilon_e - 1\right)} \tag{15}$$

Total heat transfer coefficient $U_{r/f}$ between the outside surface of the collector pipe and the working fluid is [14] :

$$U_{r/f} = \frac{1}{\dfrac{r_{r,o}\ln\left(r_{r,o}/r_{r,i}\right)}{\lambda_r} + \dfrac{A_{r,o}}{h_f A_{r,i}}} \tag{16}$$

Where $r_{r,o}$ i $r_{r,i}$ are outside and inside radius of the pipe of the collector , λ_r heat conduction coefficient of the collector pipe h_f coefficient of heat transfer by convection from the internal surface of the pipe of the collector to the working fluid. Coefficient of heat transfer by convection, from the internal pipe side to the fluid h_f, is given as:

$$h_f = \frac{N_{uf}\lambda_f}{d} \tag{17}$$

Where N_{uf} is the Nusselt number calculated according to Sieder and Tate relation [16, 17]:
For laminar fluid flow through the pipe Re<2300:

$$N_{uf} = 1,86\left[\frac{R_{ef}P_{rf}d}{L}\right]^{1/3}\left(\frac{\mu_f}{\mu_{fs}}\right)^{0.14} \tag{18}$$

For the valid range:

$$\left(R_{ef}P_{rf}d/L\right)^{1/3}\left(\frac{\mu_f}{\mu_{fs}}\right)^{0.14} \geq 2 , \tag{19}$$

where: $R_{ef} = \dfrac{4\dot{m}}{\mu_f \pi d}$ i $P_{rf} = \dfrac{\mu_f C_{pf}}{\lambda_f}$. the relation stands for $0.7 \leq P_{rf} \leq 16700$.

The terms for direct and diffusive radiation (reduced to a unit of absorber area) which falls on the transparent cover and is absorbed by it - $q_{b,c}$ i $q_{d,c}$, direct and diffusive radiation absorbed by the glass layer of the collector $q_{b,e}$ i $q_{d,e}$ and direct and diffusive radiation absorbed by the collector pipe - $q_{b,r}$ i $q_{d,r}$, are taken according to[14] (Hsieh).
A model set this way can be solved numerically, and for solving a complex model finite volume method was used.

IV. HEAT EFFICIENCY OF THE CPC COLLECTOR

A. Dividing the calculation area into control volumes

The numerical model is based on dividing every component of the CPC collector, with L length,on a number of control volumes, thus making each control volume surrounding a single node. Differential balance equations are integrated for every control volume of the relevant component [15]. N number of nodes in z direction is taken. Nodes 1 and N are postionoed on the system boundary.. Control volumes surrounding thiese nodes are of $\Delta z/2$ lenght, whilst control volumes surrounding internal nodes are of Δz lenght. On Fig 2. A divided working fluid with N control volumes is presented. Such division was made for other CPC collector components.
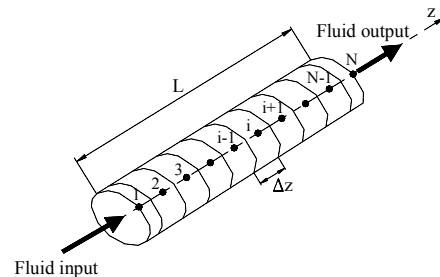

Figure 2. Grid for the working fluid of CPC collector

- *Discretization energy balance equations for the working fluid*

In order create a discretized equation for the working fluid, a control volume around a node I, is taken, as shown on Fig 3. Node i is marked by P, and the neighbouring nodes. Node i-1 i i+1 are marked by W and E, respectively. Since the time is a one way coordinate the solution is obtained by "marshcing" through time beginning with initial temperature field. Temperature T is set for the nodes in the t time step, and T values in the time step t+Δt should be found. "Old" (set) values for T in the nodes will be marked T_{fP}^0, T_{fE}^0, T_{fW}^0 and "new" (unknown) values in t+Δt timestep are marked as T_{fP}^1, T_{fE}^1, T_{fW}^1. Discretization of the diferential equations of energy balance for the working fluid is possible to conduct by its integration for the control volume as on Fig. 3.In the time interval t to t+Δt:
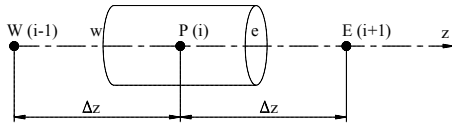

Figure 3. Grid for the working fluid of the CPC collector

$$\rho_f^* c_{pf} A_f^* \int_w^e \int_t^{t+\Delta t} \frac{\partial T_f}{\partial t} dt dz =$$

$$-c_{pf} A_f^* \int_t^{t+\Delta t} \int_w^e \rho_f^* w_z \frac{\partial T_f}{\partial z} dz dt + \qquad (20)$$

$$\int_t^{t+\Delta t} \int_w^e U_{r/f} \left(T_r - T_f \right) 2\pi r_{,o} dz dt$$

The order of the integration was chosen according the to nature of the term. For the representation of $\frac{\partial T}{\partial t}$, prevailing value for T in a node for "stepwise" scheme in the control volume. Which leaves:

$$\rho_f^* c_{pf} A_f^* \int_w^e \int_t^{t+\Delta t} \frac{\partial T_f}{\partial t} dt dz = \rho_f^* c_{pf} A_f^* \Delta z \left(T_{fP}^1 - T_{fP}^0 \right) \qquad (21)$$

For the integration of the convective term upwind scheme is used, thus the values of temperature at the mid surface is equal to the value of temperature in the node of the upwind side of the node:

$$c_{pf} A_f^* \int_t^{t+\Delta t} \int_w^e \rho_f^* w_z \frac{\partial T_f}{\partial z} dz dt =$$

$$= c_{pf} A_f^* \Delta t \begin{bmatrix} \left(T_{fP}^0 \left\| F_e, 0 \right\| - T_{fE}^0 \left\| -F_e, 0 \right\| \right) - \\ - \left(T_{fW}^0 \left\| F_w, 0 \right\| - T_{fP}^0 \left\| -F_w, 0 \right\| \right) \end{bmatrix} \qquad (22)$$

According to the assumption of the model that this is an uncompressible $\rho_{fe}^* = \rho_{we}^*$ i and $A_{fe}^* = A_{fw}^*$ we have that $w_{ze} = w_{zw}$. Further, due to more simple writing, new operator is introduced $\left\| A, B \right\|$ standing for the greater value from A and B. New sign F is introduced which stands for the convection intensity (flow): $F_e = \rho_{fe}^* w_{ze}$ i $F_w = \rho_{fw}^* w_{zw}$.

By sorting the equation (20) an equation for a node i) for the fluid in the time step (1) is, $T_{f,i}^1$:

$$T_{f,i}^1 = \frac{\Delta t}{\rho_f^* c_{pf} A_f^* \Delta z} \left[a_1 T_{f,i-1}^0 + a_2 T_{f,i}^0 + a_3 T_{f,i+1}^0 + a_4 T_{r,i}^0 \right] \qquad (23)$$

- *Discretization of the energy balance equation for collector pipe*

By integragine differential equation of the energy balance for the collector pipe for the control volume in the dime interval from t to t+Δt, and then sorting, the equation for the node (i) temperature of the pipe in the time step (1) is $T_{r,i}^1$:

$$T_{r,i}^1 = \frac{\Delta t}{\rho_r^* c_r^* A_r \Delta z} \begin{bmatrix} b_1 T_{r,i-1}^0 + b_2 T_{r,i}^0 + b_3 T_{r,i+1}^0 \\ + b_4 T_{f,i}^0 + b_5 T_{e,i}^0 + b_6 \end{bmatrix} \qquad (24)$$

Equation (29) is a general equation set for any internal control volume of the collector pipe. Boundary nodes i=1 and i=M are on adiabatic boundary. For the adiabatic boundary $\frac{\partial T}{\partial z} = 0$.

- *Discretization of the energy balance equation for the transparent cover of the collector*

In the same fashion, by integrating differential equation for the energy balance equation for transparent cover collector for the control volume in the time interval t to t+Δt, an equation for temperature of the node (i) is gained for the cover of the collector in the time step (1)

$$T_{e,i}^1 = \frac{\Delta t}{\rho_e^* c_e^* A_e \Delta z} \left[c_1 T_{e,i}^0 + c_2 T_{r,i}^0 + c_3 T_{c,i}^0 + c_4 \right] \qquad (25)$$

- *Discretization of the energy balance equation for transparent cover*

By integrating the energy balance differential equation for the tranparent cover for the control volume in the time interval t to t+Δt, an equation for

105

the temperature of the node (i) is obtained of the transparent cover for the time step (1), $T_{c,i}^1$:

$$T_{c,i}^1 = \frac{\Delta t}{\rho_c^* c_c^* A_c \Delta z}\left[d_1 T_{c,i}^0 + d_2 T_{e,i}^0 + d_3 \right] \qquad (26)$$

B. The method for solving algebraic equations

Discretization equation of energy balance components for the corresponding receiver modules CPC gets a set of coupled linear algebraic equations, with the total number of equations equals the number of nodal points in the axial direction for all four components. Since .the thermophysical properties of working fluid (water) depends on the temperature, there is a need for an iterative method of solving.

During the solving this system of algebraic equations were introduced two temperature fields, the previous time instant (0) and the next moment in time (1). Before solving each new temperature field (1), shall be converted thermophysical properties of water, the corresponding coefficient of heat transfer coefficients and equations themselves. For the initial temperature field is taken that the temperature of all components of nodal points of equal temperature environment. Nodal point i=1 for the working fluid at the entrance to the pipe receiver has a constant temperature T_{in} for the each time instant. After solving the system of algebraic equations, the new temperature field (1) now becomes the temperature field for the previous time instant (0). Solving procedure continues until the temperature difference between two successive iterations, for all nodal points are not less than the pre-ser errors ε_e. After several test, we found that the $\varepsilon_e = 10^{-5}$ (°C) i $\Delta t = 0.0005$ s

For the implementation of numerical procedures of solving the mathematical model of fluid flow ine the pipe CPC receiver, and thermal behavior of other components of the receiver in the program has been developed in FORTRAN-77, whose algoritm

TABLE I.　　CPC MODULE DATA

Dimensions
$r_{r,i} = 0.0065\,[m]$, $r_{r,o} = 0.0075\,[m]$, $r_{e,i} = 0.01\,[m]$,
$r_{e,o} = 0,012\,[m]$, $\delta = 0.005\,[m]$, $W = 0.065\,[m]$, $L = 1[m]$
$H = 0.0465[m]$
Optical properties
$\varepsilon_r = 0.05$, $\varepsilon_e = \varepsilon_c = 0.85$, $\rho_e = \rho_c = 0.05$, $\rho_r = 0.15$
$\rho_m = 0.85$, $\tau_e = \tau_c = 0.90$, $\alpha_r = 0.95$, $\alpha_e = \alpha_c = 0.05$
Thermo-physical properties
$\rho_e = \rho_c = 2700[kg/m^3]$, $d_r = 8930[kg/m^3]$,
$c_e = c_c = 840[J/kgK]$, $c_r = 383[J/kgK]$, $\lambda_r = 395[W/mK]$

is shown in Fig.7.

The procedure begins with entering the calculation of basic geometric characteristics of CPC receiver, the number of nodal point, thermophysic and optical properties of system components, working fluid inlet temperature, intensity of solar radiation, and wind velocity.

C. The results of numerical experiments

During the calculation, it was assumed that the solar rays fall normal to the aperture plane. It was assumed that all off the radiation falls to the aperture directly. In the table I. Dimensions ,thermophisical properties for the CPC module, for which the numerical simulation was conducted, is given.

During the calculations, envirponment temperature was $T_a = 28$ °C , wind speed v=2 m/s were kept constant. For direct solar radiation $I_b = 950$ W/m^2, inlet fluid temperature $T_{ul} = 32$ °C i and different flow values, the values of local temperautere of the working fluid in the direction of the flow are given in Fig. 4. (a) which shows that by increasing fluid flow rate output temperature is reduced. Fig. 4. (b) shows the change of temperature of the collector pipe, working fluid, surrounding collector pipe layer, and transparent cover in the flow direction, for the direct solar radiation $I_b = 950$ W/m^2, inlet temperature of the fluid $T_{ul} = 32$ °C and working fluid flow 0.00162 kg/s.
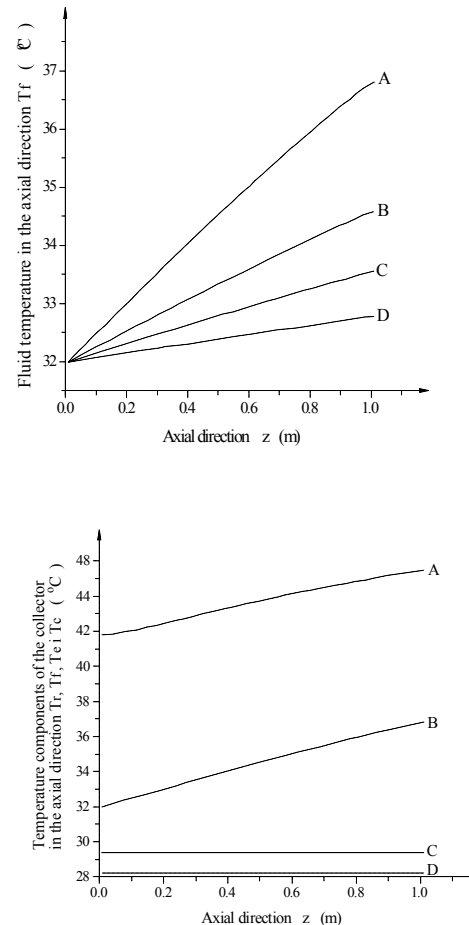

Figure 4. (a) Impact of the mass flow rate to local fluid temperature in the flow direction

T$_{ulf}$=32 ° C, A - $\dot{m}$ =0.00162 kg/s, B - $\dot{m}$ =0.003 kg/s, C - $\dot{m}$ =0.005 kg/s, D - $\dot{m}$ =0.01 kg/s;
(b) Change of local temperauter of the collector components in the flow direction: A – collector pipe , B – working fluid, C - surrounding layer of the collector, D – transparent cover

Fig 5 (a) shows the impact of the direct radiation intensity to the working temperature change in the flow direction, for the inlet fluid temperature T$_{ul}$=32 ºC and fluid flow 0.00162 kg/s. Fig 5. (b) depicts the impact of the value of local inlet temperauter of the fluid to the local fluid temperature for the flow rate of 0.00162 kg/s and direct radiation of I$_b$=950 W/m².

For the case of serial connection of six modules CPC receiver, where the output from a previous entry in folowing collector, the results are shown in Fig 6(b). Fig 6(b) shows the impact of collector length to the output fluid temperature, for the searial connection of six CPC module(overall length L=6m), I$_b$=950 W/m², input fluid temperature T$_{ul}$=32 ºC and flow rate 0.00162 kg/s where length increase compared to the collector 1 m long, a higher output temperature is achieved. Serial connection a larger number of modules CPC receiver obtained a higher outlet temperature of working fluid. In the experiment we were not able to connect the six units of CPC,but we assume that we would get significantly higher outlet temperature of working fluid, which of course opens the possibility to prove it in the future.

Figure 5. (a)Impact of the direct radiation value to the local temperature in the flow direction

A - I_b =1000 W/m², B - I_b =900 W/m², C - I_b =800 W/m², D - I_b =700 W/m²;

(b) Impact inlet fluid temperature value to the local fluid temperature in direction flow: A - T$_{ulf}$=40 ° C, B - T$_{ulf}$=32 ° C, C - T$_{ulf}$=24 ° C.

Fig 6. (a) depicts the impact of inlet fluid temperature to the current heat efficiency, for direct radiation I$_b$=950 W/m² and flow rate 0.00162 kg/s. The graphs shows that by raising inlet temperature of the fluid, heat efficiency drops. This is explained by the fact that solar fluks and environment temperature remain constant, and the diference between inlet fluid temperature is reduced, thus usefull energy is reduced.

Figure 6 . Impact of the input fluid temperature value to the current heat efficiency of the CPC collector
(b) Impact of the length to the value of the output temperature

An important feature of the program FORTRAN-77 is that it has a simple user interface that allows directinput from the keyboard of all parametersm of interest by the user. This opens wide possibilities of numericalmsimulations of real experiments and detailed numerical analysis of the impact of geometric and operating parameters on mechanism of transformation of solar energy into heat energy.

107

Start

The input parameters of the system

Calculation of the value of radiation
$q_{b,r}$, $q_{d,r}$, $q_{b,e}$, $q_{d,e}$, $q_{b,c}$, $q_{d,c}$

Do i = 1 , N

Interpolation of thermophysical
properties of water, heat transfer
coefficient calculation
and the coefficients of equation

Calculation of the temperature
$T_{f,i}^1$, $T_{r,i}^1$, $T_{e,i}^1$, $T_{c,i}^1$

$T_{f,i}^0 = T_{f,i}^1$
$T_{r,i}^0 = T_{r,i}^1$
$T_{e,i}^0 = T_{e,i}^1$
$T_{c,i}^0 = T_{c,i}^1$

If for each node
$|T_{f,i}^1 - T_{f,i}^0| < \varepsilon_e$, $|T_{r,i}^1 - T_{r,i}^0| < \varepsilon_e$,
$|T_{e,i}^1 - T_{e,i}^0| < \varepsilon_e$, $|T_{c,i}^1 - T_{c,i}^0| < \varepsilon_e$

No

Yes

Print

End

Figure 7. The Algorithm of calculation

IX.   CONCLUSION

This paper gives numerical estimated changes of temperaute in the direction of fluid flow for different flow rates, different solar radiation intensity and different inlet fluid temperatures. By fluid flow increase output temperature is reduced, whilst by solar radiation intensity increase and inlet water temperature – output temperature of water is increased. A prediction of the change of temperature of components of the CPC 2V module in the flow direction is also given. The change in efficiency is predicted with the change in input temperature of water. With the increase of the inlet water temperature current efficiency of the collector is decreased. All of the predictions are given for a 1m long module. Also, numerical estimation of the of the change of the fluid temperature in the direction of the flow for a 6m long module connected in a row, where a higher output temperature is achieved compared to the 1m long module

X.   REFERENCES

[1] R. Tchinda, E. Kaptouom, D. Njomo, Study of the C.P.C. collector thermal behaviour, *Energy Conversion and. Management* Vol. 39, (1998), No. 13, pp. 1395-1406.

[2] B. Norton, A. F. Kothdiwala and P. C. Eames, Effect of Inclination on the Performance
of CPC Solar Energy Collectors, *Renewable Energy*, Vol.5, (1994), Part I, pp. 357-367.

[3] R. Oommen, S. Jayaraman, Development and performance analysis of compound parabolic solar concentrators with reduced gap losses – oversized reflector, *Energy Conversion and Management* 42 (2001) 1379-1399.

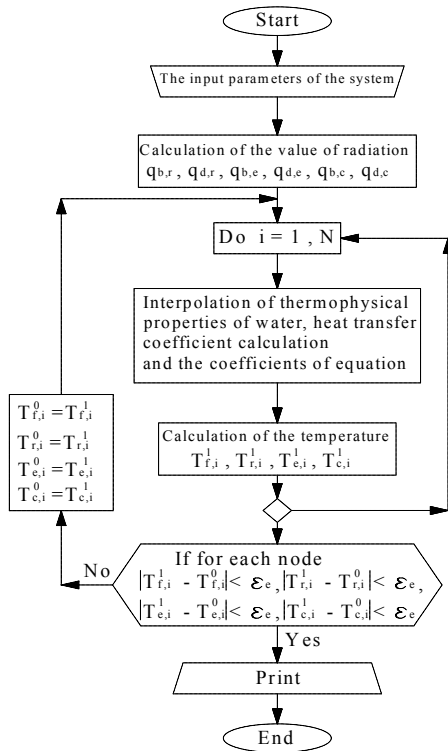[4] P. Gata Amaral, E. Ribeiro, R. Brites, F. Gaspar, SolAgua, a non static compound parabolic concentrator (CPC) for residential and service buildings.

[5] Khaled E. Albahloul, Abdullatif S. Zgalei, Omar M. Mahgjup, The Feasibility of the Compound Parabolic Concentrator For solar Cooling in Libya.

[6] Nikolić, B., Modifikovani složeni parabolični koncentrator CPC-2V. Diplomski rad, Mašinski fakultet u Nišu, Niš, Srbija, 1994.

[7] Nikolić, B., Laković, S., Stefanović, V. 1995,:Primena koncentratora sunčeve energije u oblasti srednjetemperaturne konverzije, 26th kongres o klimatizaciji, grejanju i hlađenju, Beograd, Srbija, 22-24. novembar, 1995, Vol. Sunčeva energija, nove metode, materijali i tehnologije, str. 29-40.

[8] Stefanović, V. i saradnici: Razvoj nove generacije solarnih prijemnika za oblast nisko i srednjetemperaturne konverzije sunčevog zračenja u toplotu i primena na prototipu porodične stambene zgrade sa hibridnim pasivnm i aktivnim sistemima korišćenja sunčeve energije, 2004-2005, Nacionalni projekat NPEE709300036, Mašinski fakultet u Nišu, Niš, Srbija.

[9] Stefanović, V. i saradnici. Elaborat I, II i III, Nacionalni projekat, 2004-2005,NPEE 709300036, Mašinski fakultet u Nišu, Niš, Srbija.

[10] Stefanović, V. i saradnici: Izveštaji po projektu, 2004-2005, NPEE 709300036I,Nacionalni projekat NPEE 709300036, Mašinski fakultet u Nišu, Niš, Srbija.

[11] Stefanović, V., Bojić, M.: The model of Solar receiver for middle temperature conversion of solar radiation in heat, *Thermal Science,* Vol.10, (2006), No. 4, pp. 177-187.

[12] J. A. Duffie and W. A. Beckman, Solar Engineering of Thermal Process, edited by John Wiley & Sons, Inc. 1991.

[13] J. S. Hsieh, Solar energy engineering (Englewood Cliffs, N.J :Prentice-Hall, 1986).

[14] Hsieh, C. K.,Thermal analysis of CPC collectors, Solar Energy, (1981), 27, 19.

[15] Patankar S., Numerical heat transfer and fluid flow, Hemisphere publishing Corp., 1980.

[16] Sacadura, J. F., Initiation aux transferts thermiques. Tech. et Documentation, 1982, 446 pp.

[17] Brodkey, R. S. And Hershey, H. C., Transport Phenomena. McGaw-Hill Book Company, 1988.

Comparison of Heat Pump and MicroCHP for Household Application

Dr. Péter Kádár, member of IEEE

Óbuda University, Dept. of Power Systems
Bécsi u. 94, H-1034 Budapest, Hungary
Phone: +36 209 447 241; fax: +30 1 250 0940
kadar.peter@kvk.uni-obuda.hu

Abstract — **Nowadays two new types of household heating appliances can be found in the households: the heat pumps and the microCHP (small scale Combined Heat and Power generation unit) devices. In this paper we investigate the application possibility of these devices in continental climate conditions, e.g. in Hungary. Heat pumps use electricity generated mainly from natural gas. We compare the natural gas consumptions and the CO_2 emissions, too. Natural Gas is widely used for small scale urban heating purposes in its original form, by the gas-electricity – heat pump conversion and by the microCHP-s, as well. The microCHP offers several advantages compared to the traditional gas boiler devices. We introduce also an experimental petrol/Natural Gas/Propan Butan fueled CHP unit made from a second hand car engine and a squirrel cage induction motor.**

Keywords: microCHP; induction motor; heat pump; natural gas consumption

I. DOMESTIC HEATING ALTERNATIVES

A. The usage of natural gas

In Hungary 70% of of and public heating is based on natural gas. [13] The total natural gas consumption in 2010 was over 15 billion m^3/year. 45% of it is the household consumption part [14]; it is close to 7 billion m^3/year. The average yearly household gas consumption five years ago was 2000-2200 m^3/year, it dropped to 1200-1300m^3/year (2009) [16]

In 2008 39% of the electricity was generated on natural gas base [17].The electrical efficiency of the old gas fueled plants is 36%, the most recent ones reached 59%. Nowadays the average of the gas plants' efficiency exceeds 40%.

B. The heat pump applications

The heat pump is a device that transports heat from a low temperature medium to high temperature environment with the help of external heat or mechanical energy. Heat pumps are characterized by the COP (Coefficient Of Performance) that is the quotient of the current heat output power and the current electricity power input. This value used to be between 3-4 in an average application (e.g. air/water pump). The best settings run by COP 7 (e.g. thermal water/water pump).
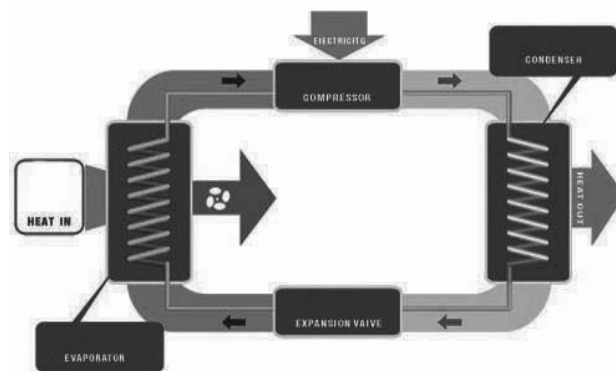
Fig. 1. The structure of the heat pump [15]

Nowadays, instead of COP rather SPF (Seasonal Power Factor) is used, it is calculated from the yearly heat energy output and electric energy input. In fig. 2 [12] we can see, that the SPF is only approx. 0,6 times the COP. In Hungary at an average application the SPF is about 2,2 – 2,3. It means, that 45% of the output heat comes from electricity.
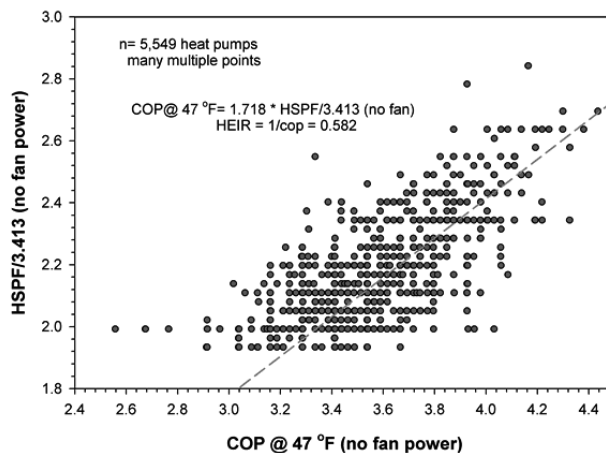

Fig. 2. The experimental relation between COP and SPF [12]

In table I. we compared how much heat can be retrieved by 1 m³ natural gas by a gas boiler with 87% efficiency and by a heat pump with SPF 2,2. We calculated with average 40 % electrical efficiency of the gas fueled power plants and 10 % loss on the electrical network.

Table I. Energy ratios of heat pump application

	used gas m³	produced/used electricity MJ	heat output MJ	waste heat MJ
Gas boiler	1		29,6	4,4
Power plant	1	13,6		20,4
Heat pump		12,24	26,93	1,36

The heat pump is far better than the clear electric heating but is worse than a local gas boiler. It has advantages in case of warm external heat sources or by applying it in summer in reverse mode (cooling). By the way, the new condensing boilers' efficiency is over 95%.

C. The micro CHP application

The microCHP (small scale Combined Heat and Power generation unit) provides electricity and heat mainly on open cycle Otto piston engine base. The heat of the exhaust gas warms the water or air through a heat exchanger.
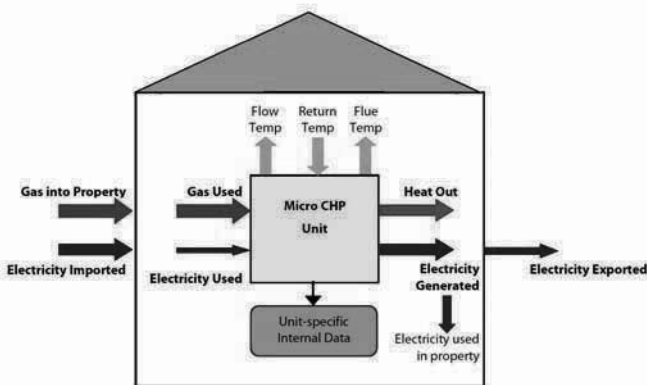
Fig. 3. The structure of the microCHP applications [applying 11]

A survey on the commercially available microCHP-s stated an average of 82% operating efficiency, taking into account both electricity consumed by the appliance and electricity generated by it. When considering thermal and electrical efficiencies independently, the average thermal efficiency for all sites is 58% and the average electrical efficiency is 24%. There was little seasonality". [11]
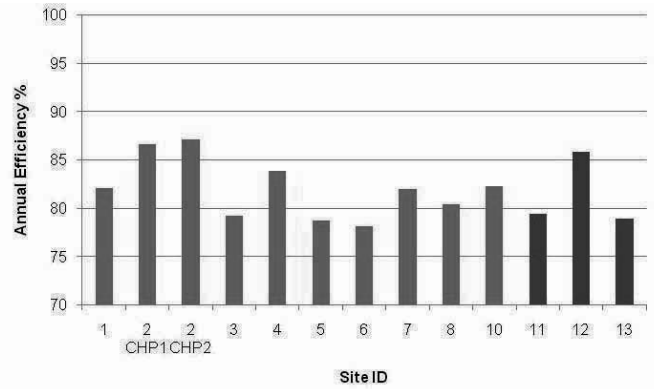
Fig. 4. Efficiencies of CHP-s [11]
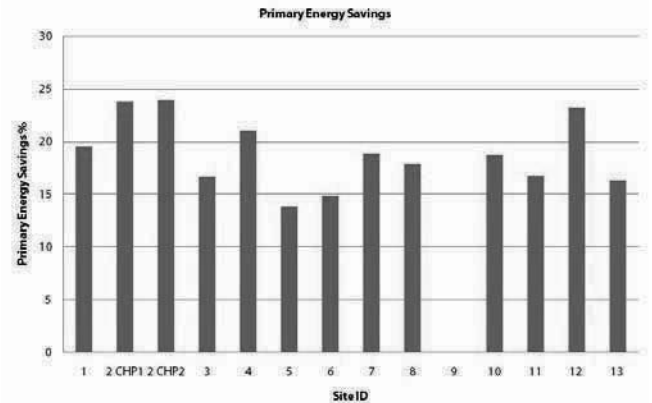
Fig. 5. Primary energy savings by usage of the waste heat [11]

If we are interested in the national energy efficiency we can investigate the alternatives, where to burn the gas. In a short calculation we compared the performance of the central electricity generation and the local heat production (gas heated boiler for heating purposes) with the distributed small CHP engines.

The up-to-date bulk Combined Cycle Gas Turbine (CCGT) power plants works with over 50% electrical efficiency.

The traditional gas boiler has 85-87% average heat efficiency. A typical microCHP has 26% electrical efficiency and 61% heat usage efficiency.

Table II. Advantage of the microCHP

	used gas m³	heat MJ	electricity MJ	waste MJ
Gas boiler	1,00	29,44		4,56
CCGT	0,42		**7,14**	7,14
MicroCHP	1,42	29,44	**12,95**	5,89

The calculation shows that the small scale co-generation produces more electricity from the same input gas by heat constraint than the simple gas boiler and the separate good efficiency CCGT. This encourages us to investigate and foster

the microCHP development. The energy performance analysis did not take into account the investment into the devices.

II. THE GREEN BALANCE

The comparison covers the effect of the national CO_2 emission, too. The following table shows the amount of the gas burned and the CO_2 emitted in case of producing the same amount of heat and electricity by different methods. We calculated with 50% efficiency of the CCGT plant, 87% of the boiler, 2.3 SPF for the heat pump and 1.73 kg CO_2 emission by 1 burning 1 m^3 natural gas.

Table III. CO_2 balance comparison

	used gas m^3	generated /used electricity MJ	heat MJ	Total CO_2 emission in kg
Gas boiler +	1		29,44	
external electricity generation in CCGT	0,761	12,95		**3,04**
Power plant for heat plant +	0,828	14,08		
Heat pump +		12,8	29,44	
external electricity generation in CCGT	0,761	12,95		**2,74**
MicroCHP	1,42	12,95	29,44	**2,45**

It's clear that the microCHP has the best CO_2 balance. The good position of the heat pump comes from the good efficiency of the CCGT.

III. THE GRID IS SMARTENING

The Smart approach infiltrates into the existing grid, more and more smart solutions and devices will perform the future's smart operations. Beside other important features all the Smart definitions mention that this grid enables
- loads and distributed resources to participate in operations [7]
- the large-scale deployment of DG (Distributed Generation) and renewable resources. [9]

There are some distributed electricity generation units that produce only electricity (PhotoVoltaics or Wind turbines), but there is a huge area where we produce a lot of heat energy waste permanently. That is the gas heating, where we produce only heat but electricity could be generated by the mechanical volume extension, too. The principle of the CHP (Combined Heat and Power generation) is
- first the electricity generation (mainly on mechanic base internal combustion engines such as the micro-gas-turbine or the Otto engine. Electricity can be

generated in fuel-cells [1], Stirling engines or Rankine cycle engines, as well. [4])
- second the usage of the heat of the exhaust gas

By this methodology operate a lot of
- bulk power plants (over 100 MW, mainly with gas turbine) a
- medium category plants (0,5-3 MW mainly with multi cylinder gas engines).

The (bulk) CHP based electricity generation ratio was over 22% in Hungary in the year 2008. [8]

IV. THE MICRO CHP TREND

The applications of CHPs have spread over also in Europe and in the last decade the small scale micro CHP (typically 1-10 kW) became commercially available. They can supply the individual households by heat and electricity, too.

In Germany 3,000 eco-power micro-CHP units have been installed, using the U.S. based Marathon Engine Systems long-life engine. [2] Furthermore over 23,000 DACHS mini-CHP units (typically 5,5 kW units) have been installed based on reciprocating engine technology. [3]

Honda's 1 kW (electrical power) system – named Ecowill – mainly is used in single-family home applications. In Japan more than 30.000 units have been installed. [5]

In Europe by the year 2020 over 10 million microCHPs are forecasted. For Central and Eastern Europe the installation potential is 700.000 units. [6] If we count an 1,5 kW average power per CHP and assume 10 million devices, it makes 15.000 MW, that is the 3,5 % of the 400 GW operational power of the European system. This huge unit number can cooperate only as controlled "virtual power plant" that will be realized by the Smart Grid philosophy.

V. THE TEST DEVICE

In the last half decade the world's yearly car production was over 50 millions [10]. Roughly, this is the number of the cars withdrawn from circulation yearly, as well. Having seen the huge amount of industrial waste, we made a trial to use an old car engine to drive a 3 phase squirrel cage induction motor. Motor (not a generator) because it operated decades in a small plant, and we looked for a second hand device. The basic approach is:
- a large number of engines are available
- they are low cost
- it is a low speed operation
- 12 V DC output is built in
- electrical efficiency is not so important for most of the heat waste is captured for heating purpose
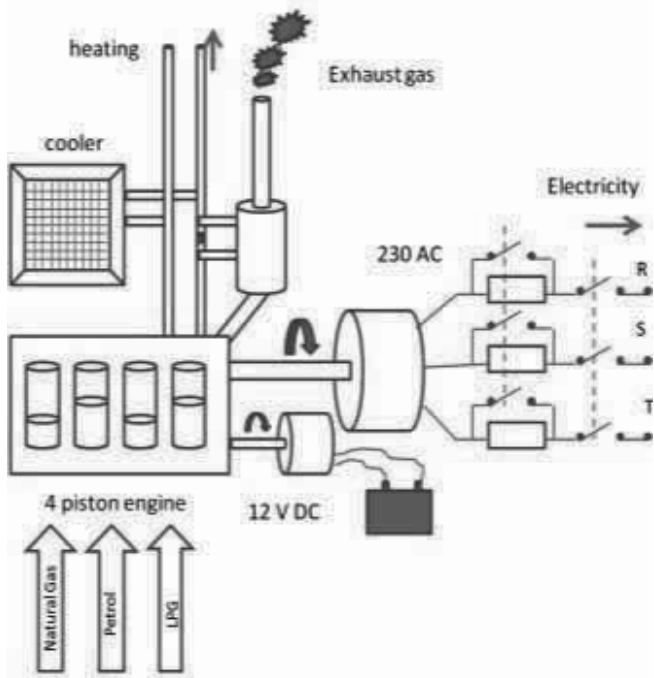
Fig. 6. The test microCHP system

We built a test microCHP with the following parameters:
- used car engine, former GDR produced Wartburg 1.3 VW-Engine, 43 kW (58 HP) for gasoline and LPG
- 7,5 kW 3 phase squirrel cage induction
- resistors for starting / synchronization
- connection to 3 phase 230/400 V AC 50 Hz utility network
- 12 V DC battery for the self start and for DC output

The material cost of the devices was approx. 2000 USD. A new device's price in the same power range is over 20 000 USD.
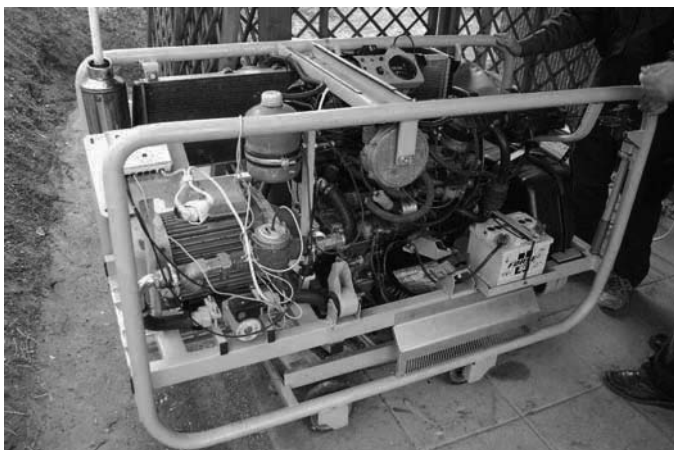
Fig. 7. The demonstrational microCHP

The first rough measurements brought the expected results. The output power is closely linear function of the speed.
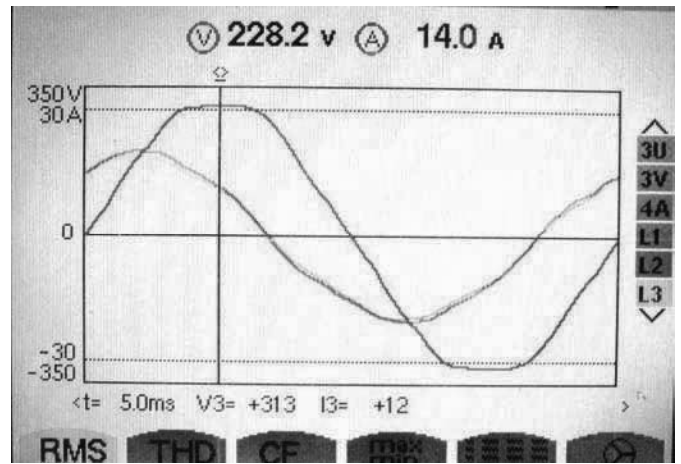
Fig. 8. Screenshot of the generator measurement
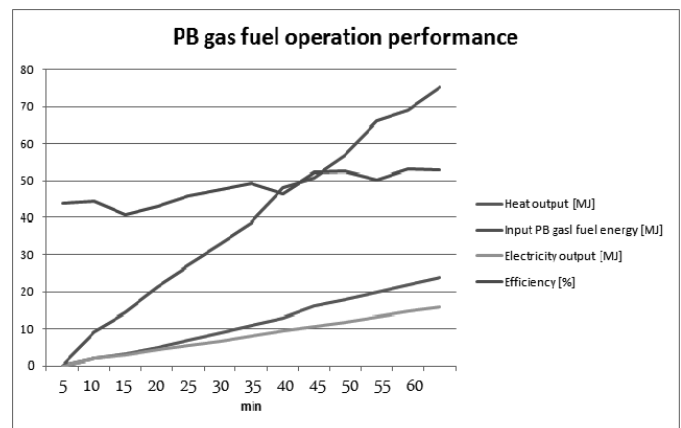
Fig. 9. Measurements of gas operation

The electrical measurements showed that an electronically not controlled "natural" induction motor consumes a lot of reactive power. In the next measurements we shall investigate the simple condenser compensation, de free run operation and the island mode start too.

The thermal data were monitored by Sontex Supercal 531 device, the energy fed back by a traditional Ferraris-wheel energy meter.

The demonstration device operates but some questions are left open:
- emission control – in the future we are going to run this device by natural gas that limits the harmful emission. The CO content must be controlled.
- lubrication oil consumption
- long term operation – we have no long-term aging experiences, but the low speed (1500 RPM) spares the car engine (peak power about at 3500 RPM)

Present development:
- Power regulation – in order to control the power output by the RPM (approx. 0-3% of over speed) a fine speed

control and stabilizer must be developed for the constant output. Also the over-speed protection functions must be solved in case of the load drop.

- Reactive power compensation – because we applied a squirrel cage induction motor, the internal voltage is over the nominal voltage so the machine's iron core can be closer to the magnetic saturation. This is one cause why our motor has relatively high reactive power consumption. The appropriate compensation method is under investigation.
- Other fuel (biogas) [18]
- Appropriate heat isolating casing – the electrical efficiency has not great importance, because the heat loss is used. The leaking heat must be caught by special coating and a cooling system.
- Remote control – the microCHP can operate as member of the virtual power plant. That is why it must be remotely controlled or at least remotely started/stopped

VI. CONCLUSION

Comparing the heat pump and the microCHP the last one has more energetic advantages. Also the CO_2 emission is favourable. It is recommendable to all gas heated household boiler positions. By spreading over these devices the manufacturing costs decrease. We demonstrated that these appliances can be built also by second hand car engine too.

REFERENCES

[1] Takahiro Kasuh, "Development strategies toward promotion and expansion of residential fuel cell micro-CHP system in Japan" http://www.igu.org/html/wgc2009/papers/docs/wgcFinal00801.pdf

[2] http://en.wikipedia.org/wiki/Micro_combined_heat_and_power, 2009

[3] Senertec GmbH http://www.triecoenergy.com/chp.html

[4] Micro-CHP: Coming to a Home Near You? http://www.esource.com/esource/getpub/public/pdf/04MicroCHPResults Flyer.pdf

[5] State-of-the-art Micro CHP systems, Final report (EIE/04/252/S07.38608), Austrian Energy Agency, Vienna, March 2006

[6] Steve Ducker: MicroCHP market report, http://www.voltimum.co.uk/news/3826/s/MicroCHP-market-report.html

[7] EPIC – SAIC: San Diego Smart Grid Study, Final Report, October 2006, http://www.ilgridplan.org/Shared%20Documents/San%20Diego%20Sm art%20Grid%20Study.pdf

[8] Energia Központ, http://www.e-villamos.hu/nyomtat.php?id=1061 Key indices of electricity sales in the framework of feed-in obligation in 2010 http://www.eh.gov.hu/gcpdocs/201009/2010_1_kat_jelentes.pdf

[9] Will McNamara & John Holt, The Utility of the Future KEMA - Perspectives and Observations http://emmos.org/prevconf/2009/Training%20A%20-%20KEMA%20UoF.pdf

[10] Cars produced in the world http://www.worldometers.info/cars/ by march 2011

[11] Commercial micro-CHP Field Trial Report, 2011 Report; Sustainable Energy Authority of Ireland; http://www.seai.ie/Publications/Your_Business_Publications/Commerci al_micro-CHP_Field_Trial_Report.pdf

[12] Philip Fairey, Danny Parker, Bruce Wilcox and Mathew Lombardi: Climate Impacts on Heating Seasonal Performance Factor (HSPF) and Seasonal Energy Efficiency Ratio (SEER) for Air Source Heat Pumps; FSEC-PF-413-04; http://www.fsec.ucf.edu/en/publications/html/FSEC-PF-413-04/

[13] ifj. Jászay Tamás, Dülk Marcell: Megtakarítási lehetőségek vizsgálata a magyar háztartások energiafelhasználásában; in Hungarian, www.e-villamos.hu portál.

[14] http://www.cylex-tudakozo.hu/ceg-info/els%C5%91-magyar-f%C3%B6ldg%C3%A1z--%C3%A9s-energiakereskedelmi-%C3%A9s-szolg%C3%A1ltat%C3%B3-kft--39610.html

[15] http://www.vencoair.com/How-Heat-Pump-work-31.htm

[16] Magyar Gázipari Vállakozók Egyesületének hírlevele,8. szám / 2010: Gondolatok a földgázról, mint energiahordozóról, valamint a földgáz elfogadottságának és presztízsének növeléséről; http://www.mgve.hu/hirlevel_8.php

[17] Statistics of the Hungarian Power System, 2008; www.mvm.hu

[18] Viktória Barbara Kovács, Attila Meggyes; Energetic Utilisation of Pyrolysis Gases in IC Engine; Acta Polytechnica Hungarica Vol. 6, No. 4, 2009, pp. 157-159

Theory of General Competitive Equilibrium and Optimization Models of the Consumption and Production

Andras Sagi, Ph.D.* and Eva Pataki, Ph.D.**

* Full Professor, The Faculty of Economics, Subotica, Novi Sad University, Serbia
** Assistant Professor at the Polytechnic Engineering College, Subotica, Serbia
peva@vts.su.ac.rs

Abstract— the work deals with the comparative and critical analysis of macroeconomic aspects of general equilibrium theory. It is about the problem of general equilibrium in production, general equilibrium in exchange and the problems of simultaneous equilibrium in production and exchange. The research of cited problems contributes to a better understanding the complete economic mechanisms. Besides, general equilibrium model represents the basis for considering welfare economics and the optimization theory of contemporary market economies.

Key words: partial equilibrium, general equilibrium, contract curves, Pareto optimum, transformation curve in production

I. INTRODUCTION

Most microeconomic models analyze equilibrium states of individual partial markets. Such market in these analyses is considered as an independent system, isolated and independent of the whole economy. This partial analysis enables perception of optimization in firm behavior and creating partial equilibria. A partial analysis, however, has necessarily its limits. It does not give satisfying answers to numerous fundamental questions. The basic shortage of partial analysis models is the same; it does not explain functions of the connected system of partial markets, i.e. the whole economy. Therefore, connecting models of analyzing partial markets and models of general economic equilibrium represent completing and connecting contemporary microeconomic analyses into a unit system.

The theory of general economic analysis, except its complexity and difficulties in practical implementation, gives invaluable benefits in the domain of analyzing efficiency and welfare in microeconomic researches and offering great support in macroeconomic modeling. The subject of this work is just the comparative and critical analysis of microeconomic aspects of fundamental questions of the general competitive equilibrium.
Introducing problems of general equilibrium into economy is connected with physiocrats. We find it in the F. Quesnay's Tableau Economique in 1758, and partly in Turgot's work. The role of market mechanisms in creating equilibrium by means of competition, i.e. the "invisible hand" of market we find in A. Smith's teachings. K. Marx brilliantly explained the effects of mechanisms of the law

of value. In his works, we find the laws of stable rate of reproduction and expanded social reproduction, which, in principle, explain the possibilities of dynamic and balanced economic growth.

Nevertheless, the first developed general equilibrium theory we find with the representatives of the Lausanne School of the Marginalist theory in the works by L. Walras and V. Pareto in the second part of the 19th century. Further contributions to development of this theory were the input-output analysis by Wassily Leontief, whose theory, according to many authors, is based on Marx's schemes of social reproduction. Kenneth Arrow, F. Hahn [8] and G. Debreu [6] founded contemporary neoclassical theory of general equilibrium on their works.
To understand better general equilibrium theory, Schumpeter's teaching are important, who, beside partial and general equilibrium, differentiates the so-called aggregate equilibrium. To his opinion, partial equilibrium is the equilibrium of economic spheres. Aggregate equilibrium is the equilibrium between selected aggregate quantities (selected in relation to the analysis, which should be done), while general equilibrium represents the equilibrium of national economy. On the other side, with A. Pigou, we find differentiated stable, neutral and unstable equilibriums.

We should get down to the analysis of general equilibrium as any other analysis in economic theory, from the row of simplified suppositions. We take the supposition of competitive market, pure exchange model, production equilibrium, and then simultaneous equilibrium is considered.

II. GENERAL EXCHANGE EQUILIBRIUM

In the analysis of general equilibrium, theoreticians Pareto, Edgeworth, Walras and others start from researching the so-called general exchange equilibrium, i.e. in the this analysis, they firstly abstract money, i.e. commodity prices. Equilibrium conditions are explained starting from the so-called "Edgeworth box" or Edgeworth diagram. At the beginning, they usually take two people who exchange two goods. Take A and B, and goods to be exchanged are X and Y.

In Figure 1, in relation to the ordinate OA several curves of indifference (line of equal utility) of participants in exchange are taken. All the points of the curve of indifference represents such alternative combinations of goods X and Y for an individual A giving him the same level of utility. The slope of determined indifference curve expresses the so-called MRS (Marginal Rate of Substitution), i.e. marginal rate of goods exchange in a determined point of indifference curve, where the utility level of actor A remains unchanged. If some curve of indifference is further from the origo, the utility level representing mutual indifferent combinations, presented on it, is bigger. For that, the relation can express utility values represented by indifference curves of the individual A: A3 > A2 > A1.
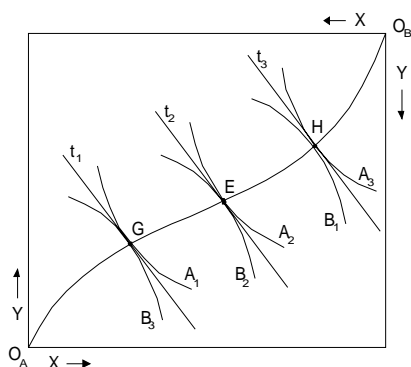

Figure 1.

The origo B is in the opposite northeast angle of the Edgeworth closed diagram, and in relation to it, the indifference curve of Participant B in exchange, i. e. the curves B3 > B2 > B1. Every of them represent numerous mutually equivalent or indifferent combinations of goods X and Y for the individual B. The slope of indifference curve is now MRS but for the trader B.

The exchange of goods for individuals is useful, until they are not on indifference curves, which have not points of contact. The marginal rates of goods substitution X and Y for exchangers become equal in points of contact of their indifference curves. As MRS of consumption goods are appropriate to the relations of their indifference curves, it results that exchange is done until marginal utilities of these goods X and Y become equal for A and B. The row of these points represents the general equilibrium of exchange for A and B in the observed model. The geometric set of equilibrium points gives the so-called Edgeworth contract curve, which connects OA with OB. When participants of exchange are in this curve, they reach the so-called Pareto-optimality in exchange. It is said that the "distribution is optimal in the Pareto sense if it is such that every improvement of the situation causes the aggravation of other situations." In other words, some distribution is Pareto optimal only if there is no possibility of such change, which could improve the situation of one not damaging others. Therefore, every point in the contract curve represents the Pareto optimality, and this curve is the geometric place in Pareto optimality. The Pareto optimality was dome in 1896 in the work Cours d'economie politique. When the ordinary understanding of utility was defined (i.e. not the absolute but the relative

value or the level of utility providing comparative combinations of properties) his work Manuale d'economica, the policy in 1906, reached its real importance. In this work, namely, for the first time, the attitude was defined that maximization of aggregate social utility can be reached with the relations of exchange, when no individual utility can be increased without decreasing the of somebody else's utility.

In Figure 1, along the Edgeworth contract curve, there are numerous alternative equilibrium combinations of exchange. To make the choice between them, it is necessary to define the so-called Social Welfare Function (SWF). To define this function is a very complex task. We should start from the evaluation of values of some situations, evaluation of preferences of social subjects, especially those who create economic policy, and so on. However, this task can be solved with some exactness. Knowing social welfare functions, the Pareto criterion enables eliminating non-optimal combination in exchange.

Now, look at Figure 2. Suppose that the initial distribution X and Y between A and B is at point N, where the curves of utility and indifference A2 and B cut, it is easy to understand that all points for participants in exchange in the shaded surface represent better combinations than the ratio of exchange expressed by point N. The shaded area in Diagram is called the "region of mutual advantages", and the interval of Edgwort contract curve between points G and H is called the "core or pith of economy" [Stojanovic, 1944].
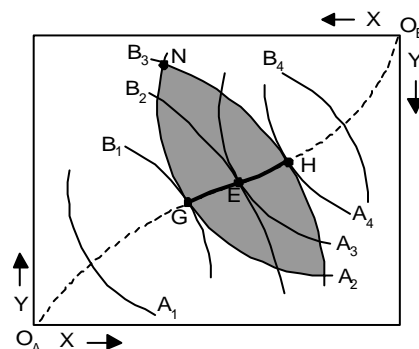
Figure 2.

Correct definition of the position of SWF enables the choice between optimal exchange combinations in the line between points G and H.

Completing general equilibrium in exchange requires the introduction of relative prices of properties and incomes of consumers. Namely, it is generally accepted that consumers or households as traders try to optimize their economic position, or, in other words, to maximize their consumption utility, starting from the following factors:

1. Preference consumers' system expressed by indifference functions;

2. Amount of money income of consumers;

3. Prices of individual goods and services, P (price), as the indicator of the level of social utility of goods and services.

In the two-dimensional model of consumers' choice limits or the so-called budget consumption limitation are expressed by the so-called line or consumption limit. In case that the variables of money income of traders A and B are equal in exchange, i.e. IA = IB, and prices of properties X and Y which come in exchange between them Px and Py, the budget limitation of consumption for both exchangers can be expressed by the relation:

$$I_{A,B} = X \cdot P_X + Y \cdot P_Y \quad \text{whence} \tag{1}$$

$$X = \frac{I}{P_X} - \frac{P_X}{P_X} \cdot Y \tag{2}$$

$$Y = \frac{I}{P_Y} - \frac{P_X}{P_Y} \cdot X \tag{3}$$

Under the above supposition, the identical budget line can present the limits of consumers' choice for traders A and B. With unchanged prices of goods and amount of money income, the position of budget line remains unchanged, and its slope expresses the relation of property prices, i.e. Px and Py. Look now at Figure 3, the possibilities of general equilibrium in exchange, taking into consideration the amount of money income and prices of exchanged goods
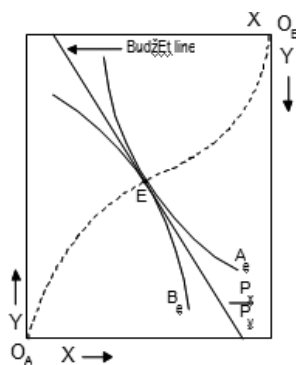
Figure 3.

In Figure 3, general exchange equilibrium between A and B is at point E on the Egdeworth contract curve. At this point, namely, we have matching up the slopes of indifference curves of trader A, on the curve Ae and the slope of indifference curve B, the other trader in exchange. In this point (as in all other points of the contract curve), we have matching up of marginal substitution rates of X and Y for traders A and B. However, contrary to other points on the contract curve, in E, the slope of their marginal substitution slope, i. e. MRS (it is in fact the slope of tangent in some point) is matching up with the slope of their budget line. The slope of budget line expresses relative prices, in other words, the relation of prices of goods in exchange, i.e. X and Y. At the equilibrium point E, the following equalities are valid:

$$MRS_{A(X,Y)} = MRS_{B(X,Y)} = \frac{P_X}{P_Y} = \frac{MU_X}{MU_Y} \tag{4}$$

(MU – Marginal Utility)

At point E, equilibrium goods prices have the same mutual relations in marginal rate of goods substitution, i.e. MRS is equal for both traders in exchange, and at the

same time, it is appropriate to relations of marginal utility of exchanged goods. It means that the equilibrium point E is suitable for relation of the proportion where supply and demand of exchanged goods become equal.
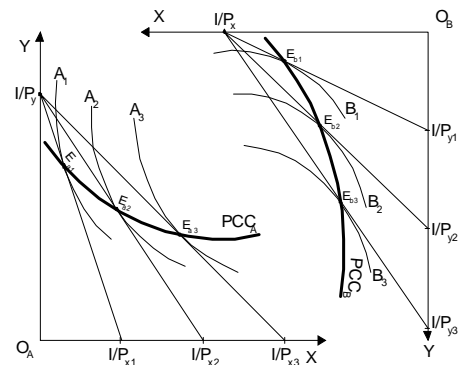
Figure 4.

By the combination of indifference curves and budget lines we obtain the so-called PCC (Price Consumption Curve), which show the structure of optimal consumer baskets in case of price changes of some goods (supposing that prices of other goods, the level of money incomes of consumers and their preference system are steady). In Figure 4, we presented the curves of relations of prices and consumption for individuals A and B, supposing that the product price X changes for trader A; for trader B, the product price Y is changeable. All other relations and conditions remain unchangeable.

The curve of relations of price and consumption of trader A, i.e. curve PCCA shows that, starting from the combination of goods in point Ea1, which is located along with the starting position of budget line, the trader A is ready to offer increasing quantity of product X for increasing less quantity of product Y. It is done by gradually price reduction of product X presented by budget lines I/Px2 and I/Px3. This trader tries to optimize his consumer utility in the conditions of changed prices. Contrary to trader A, in northeast angle of Diagram, considering PCCB, i.e. the curve of relations of price and consumptions of trader B, we see that the latter trader is ready to exchange more product Y whose price reduces for increasingly less quantity of product X, in view of maximization of his consumer utility.

In fact, the curve of relations of prices and consumption of the trader A, i. e. PCCA, represents the curve of offer A, i.e. its readiness to change goods X for Y in exchange. On the other side PCCB, i.e. the curve of relations of prices and consumption of trader B, presents the curve of offer B, i.e. acceptable relation of goods exchange X and Y for Individual B, depending on price change of product Y.

Traders of exchange A and B along their offer curves, starting from points Ea1 and Eb1 to points Ea3 and Eb3 get to indifference curves which become more distant from the origos, i.e. which express an increasing level of utility for them.

Present, finally, in Figure 5, the curve of relations of prices and consumption of both traders, i.e. PCCA and PCCB, inside of the so-called "region of mutual advantages", limited by their starting indifference curves Ae and Be.

Figure 5.

Figure 6.

We can see the point of section of supply curves of observed traders of exchange is on Edgeworth contract curve and inside of the core of exchange in the interval of points G and H in point E. It expresses the relations of exchange where the product offer of the individual A (i.e. his demand for product Y) and product offer by trader B (i.e. his demand for product X). The general exchange equilibrium is established in point E – of course, in the simplified model with two traders and two products. However, this model enables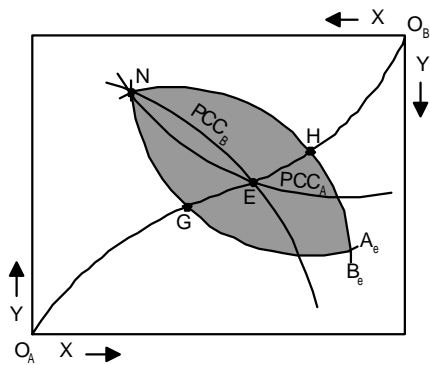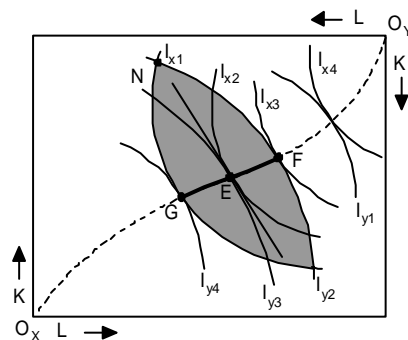 to define the general law on equilibrium of exchange in the following sense: general exchange equilibrium is established with equality of marginal substitution rates of traders along with equality of supply and demand that they present.

The analysis of general equilibrium mechanism is needed to continue by researching the mechanism of general production equilibrium.

III. GENERAL PRODUCTION EQUILIBRIUM

In analyzing of general production equilibrium, we can take the simplified production model analog to the model used in the analysis of general exchange equilibrium. In the model, we suppose that a producer makes two products X and Y, with combination of only two inputs, labor and capital, i.e. by means of L (Labor) and C (Capital). The general production equilibrium is established when marginal technical rate of factor substitution equalize, i.e. MRTS (Marginal Rate of Technical Substitution) for both products. Equilibrium can be established on the so-called Edgeworth closed production box [Kopanyi, 2003], i.e. in Figure 6. The curves IX1, IX2, IX3 and IX4 represent isoquants or the so-called curves of equal product of production of product X. Therefore, isoquants IY1, IY2, IY3 and IY4 show the curves of equal products for product Y. If the starting point is point N in the section of isoquants IX1 and IY3, it is visible that production maximization X and Y is not realized here, therefore, nor general production equilibrium. The producer can increase both production X and production Y, i.e. reaches isoquants at the higher position (i.e. further than the origo) reducing capital consumption for production X on behalf of production Y and conversely, increasing labor consumption in production X, on behalf of consumed labor in production Y.

With these relations and limitations, production maximization of both products is reached in the tangential point of production isoquants X and Y, i.e. at point E. In point E, the curve slopes of equal products X and Y, i.e. Ix2 and Iy3 are equal, i.e. the marginal technical rates of substitution in their production are equalized. Thence, these relations are valid:

$$MRTS_{L,K(X)} = MRTS_{L,K(Y)} \quad \text{Then} \tag{5}$$

$$MRTS_{L,K} = \frac{MP_L}{MP_K} \quad \text{(MP=Marginal Product)} \tag{6}$$

It means that production equilibrium criterion is realized with the condition

$$\left(\frac{MP_L}{MP_K}\right)_X = \left(\frac{MP_L}{MP_K}\right)_Y \tag{7}$$

The point of equilibrium is on the so-called Edgewort contract production curve, which connects origo Ox and origo Oy. When production of goods is on this curve, it is not possible any more to increase production of one material product without decreasing production of the other product. On the contract production curve, there are such combinations of production of goods, which realize the so-called Pareto production equilibrium [Pareto, 1971]. In the above analysis of production equilibrium, two marginal rates of technical substitution and marginal products of observed are taken into consideration, but not using the price factor.

In further analysis, suppose that the sum of engaged resources (or TC – total costs) is the constant for production of goods X and Y. Then, suppose that, with ceteris paribus, labor price, i.e. PL1 < PL2 < PL3 in production of product X decreases gradually. So, we obtain isocost lines (lines of equal costs) in different positions for production of product X. Connecting tangential points of appropriate isoquants and isocost lines with different labor prices, we obtain the production curve of product X, which expresses the optimal combination of input under cited conditions, i.e. the curve Tx.
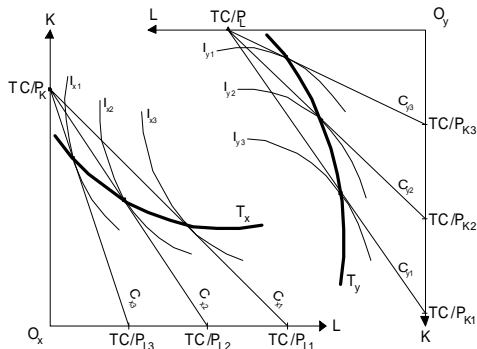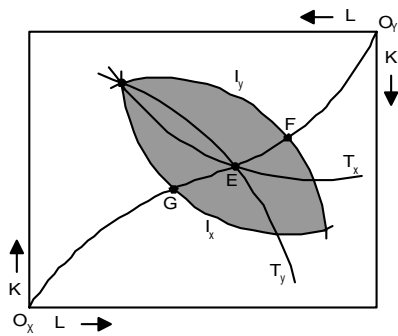
117

Figure 7.

Figure 8.

In production of product Y, we gradually reduce the price of capital use (PK1 < PK2 < PK3) and analog to logic in production optimization X, we obtain the curve of production T whose points show the optimal combination of input with different capital prices, i.e. the function Ty. production function Tx and Ty are presented in Figure 7. Curves Tx and Ty cut inside the so-called "region of mutual production advantages" limited by isoquants Ix and Iy. the curve Tx , on the one side, represents the factor demand curve (L, K) used for production of product X, and at the same time, it is the product supply curve X, on the other side. Therefore, the curve Ty represents the factor demand curve for production of goods Y, but also the supply curve Y.

The slopes of isoquants, i.e. the curve of equal product MRTS, express the technical substitution possibilities of input factors in the given isoquant point (in fact, the slope of tangent along with this point) and with the condition that the volume of production remains the same. The slopes of isocost lines (line of equal costs) express the relations of prices used and combined factors in production, i.e. the relation Pk/Pl. That means that isoquants and isocost lines of marginal substitution rates of production factors in the points of tangents are appropriate to the relations of current prices of these factors. It is, together, the criterion of optimal factor combination. Thus, this relation is valid:

$$MRTS_{L,K} = \frac{MP_L}{MP_K} = \frac{P_L}{P_K}$$

(8)

Hence, it gives the following equality on the contract production curve:

$$\left(\frac{MP_L}{MP_K}\right)_X = \left(\frac{MP_L}{MP_K}\right)_Y = \frac{P_L}{P_K}$$

(9)

These equalities "must exist even when more goods are made and more production factors are used – more than two" [Stojanovic, 1994].

After all these considerations, we can start to define general production equilibrium in the sense of the Pareto optimum. In Figure 9, we again draw the amounts of products X and Y.
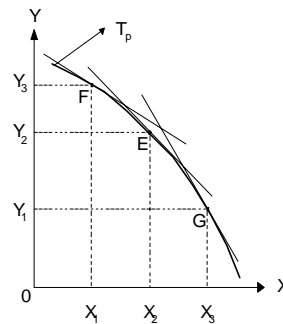
Figure 9.

The contract curves of production transferred from previous diagrams (Figure 6 and 8), change into the function of production possibilities or the curve of production transformation. The slope of transformation curve expresses the marginal rates of product transformation X and Y, i.e. MRT (Marginal Rate of Transformation). Marginal transformation curves with coordinate axes express extreme cases, i.e. when only one or only other kind of product is produced. Individual points of production transformation curves express different alternatives combinations of final products X and Y, which can be maximally produced by full employment of available inputs R and K with available technology. It means that all the combinations along the transformation production curve satisfy the criteria of Pareto optimum, i.e. general production equilibrium. In the area under the curve of alternative production possibilities there are differently realizable possibilities X and Y with suboptimal use of resource use, and combinations in the area of alternative production possibilities out or above the curve of production transformation are unrealizable based on available possibilities.

After the differentiated analysis of conditions and suppositions of general equilibrium of production and exchange, we can analyze the general economic equilibrium in the economy, i.e. the equilibrium of production and exchange.

IV. GENERAL EQUILIBRIUM OF PRODUCTION AND EXCHANGE

The cited conditions of general exchange equilibrium and general production equilibrium must unite in order to make the simultaneous equilibrium of production and

exchange, as in reality, economies where only production or exchange of goods do not exist [Stojanovic, 1994].

In Figure 10, the curve of transformation TP(X,Y) represents the combinations of goods X and Y. The curve OAOB represents the so-called contract consumption curve – exchange. The simultaneous or general equilibrium of production and exchange, or the so-called Pareto optimal equilibrium is realized with the condition:

$$MRT_{X/Y} = (MRS_{X,Y})_A = (MRS_{X,Y})_B \qquad (10)$$

where exchangers of goods X and Y are participants A and B.

The general production equilibrium is realized at point M (or OB) which provides production per 10 units X and Y. The curve tangent of production possibilities Tp(x,y) at point M expresses the marginal transformation rate X in Y, i.e.   MRTX,Y.The tangent along the curve Tr(X,Y) expresses the marginal rate of substitution of cited goods in production, i.e. MRSX,Y. At points M and E there is pararellism of the cited tangents. They provide general production equilibrium at point M and general exchange production at point E. Point E shows also the distribution of made equilibrium amount of goods X and Y between A and B in the sense: A gets six pieces of X and five units of Y, while B will obtain four pieces X and five pieces Y.
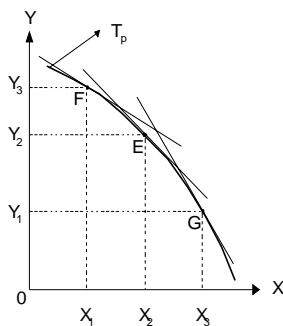
Figure 10.

The criterion of simultaneous   equilibrium of production and exchange in the sense of equalizing marginal transformation rates and marginal substitution rates can be generalized , of course, in case of the existence of more kinds of goods, i.e. more producers and consumers. It makes the economic analysis more complete and near its reality.

MRT, i.e. marginal rate of transformation of goods in equilibrium reflect the relations of their marginal production costs, and MRS, i.e. the marginal rate of substitution of goods at the equilibrium level equalize marginal utility goods (and these reflect the relations of their equilibrium prices).   Thus, the criterion of simultaneous general equilibrium in production and exchange can be expressed in the following way:

$$\frac{MC_X}{MC_Y} = \left(\frac{MU_X}{MU_Y}\right)_A = \left(\frac{MU_X}{MU_Y}\right)_B \qquad (11)$$

The above relation is valid, of course, also in the model with a large number of goods and services in case of many producers and consumers.

The presented (and simplified) analysis of general equilibrium of exchange and production, besides completing the knowledge of functioning connected and complex system of market mechanisms has a broader importance. The conditions and criteria of general competitive equilibrium are applied in the analysis of a very important and current subject matter of economic theory to the so-called welfare economics and the theory of optimum (efficiency) of contemporary market economy. However, this will be the subject of researching in the next work.

REFERENCES

[1] Schuman J., "Grundzuge der mikrookonomischen Therie", JATEPress Szeged 1988

[2] Suvakov T., Sagi A., "Mikroekonomija", Ekonomski fakultet, Subotica 2011

[3] Trivic N., Sagi A., "Savremeni mikroekonomski modeli", Ekonomski fakultet, Subotica 2008

[4] Kopány M. et. all, "Mikroökonómia", Közgazdasági és Jogi Könyvkiadó, Budapest 2008

[5] Samuelson P., Nordhaus, "Economics", Mc-Graw Hill, 2006

[6] Debreu G., "Theorie of Value", John Wiley & Sons, New York 1959

[7] Pareto V., " Manual of Political Economie", August M. Kelley, New York 1971

[8] Arrov K. J., "The organization of economic activity: Issues pertinent to the choice market versus nonmarket allocation. In:US Joint Economic Committee, The analysis and evaluation of public expenditure: The PBB system, vol. I., pp. 59-73 Washington.

Renewable Energy Resources and Energy Efficiency – Imperative or Choice?

S.Tomić*, D.Šećerov**

*Faculty of Economics/Department of Management, Subotica, Serbia
** Faculty of Economics/Department of Management, Subotica, Serbia
tomics@ef.uns.ac.rs, dsecerov@ef.un.ac.rs

Abstract: **A new management strategy (or even philosophy), has been developed with a view to create bigger value with fewer negative impact on the living environment. The concept of eco-efficiency, based, among other things, on energy efficiency and renewable energy resources connects ecological performances and economic (financial) benefits. As economic efficiency is realized through the principle of maximal results with minimal inputs, therefore, energy efficiency in the context of enterprise economic efficiency would mean the realization of maximal results (volume of production and services provided) with minimal energy inputs. The topic of this paper is the question whether the realization of above mentioned principles is imperative or choice for companies.**

I. INTRODUCTION

Energy efficiency includes the efforts to reduce the amount of energy required to provide products and services. Improvements in energy efficiency are most often achieved by adopting a more efficient technology or production process. Energy efficiency and renewable energy resources are twin pillars of sustainable energy policy. At the same time, energy efficiency improvements and usage of renewable energy resources pave the cleaner energy path.

Energy efficiency can be used to reduce the level of energy consumption and may slow down the rate at which energy resources are depleted. The idea of meeting energy needs by increasing efficiency instead of increasing energy production is realized through negawatt power - a theoretical unit of power representing an amount of energy (measured in watts) saved. The energy saved is a direct result of energy conservation or increased efficiency.

Energy efficiency used to be known as "the fifth fuel"[1]. It can help to satisfy growing demand for energy just as surely as coal, gas, oil or uranium can and could get the world halfway towards the goal of keeping the concentration of greenhouse gases in the atmosphere below 550 parts per million. Unlike most other schemes to reduce emissions, a global energy-efficiency drive would be profitable.

Nowadays, rational energy use, energy efficiency improvements and renewable energy resources are the key elements of energy policy, and crucial factors of the sustainable development and fight against climate change. The Intergovernmental Panel on Climate Change, a group of scientists advising the United Nations on global warming, believes that profitable energy efficiency investments and renewable energy resources would allow countries such as Greece to cut its emissions by a quarter and Britain by more than a fifth.

Investments in energy efficiency would more than pay for themselves, and fairly fast within 3 to 5 years or, in case of, complex projects within 10 years[2]. But, there are still unfulfilled but potentially profitable opportunities in energy efficiency available to companies. The problem is a series of distortions and market failures that discourage investment in efficiency. Financing energy-efficiency investments can be difficult, especially in the developing world where capital can be scarce. Also, businesses still tend to put greater emphasis on increasing revenues than on cutting costs. One of the key driver for energy efficiency will be the price of the energy. As energy prices rise and more countries adopt limits on greenhouse-gas emissions, banks and consultancies are beginning to sniff an opportunity.

There are three key factors that affects company's response to environmental protection challenges: 1. national and international regulations (laws, standards, policies, different environmental protection instruments), 2. stakeholders pressure (consumers, business partners, investors, insurances companies i local communities) and 3. need for economic, environmental and energy efficiency.

II. ENERGY EFFICIENCY AND RENEWABLE ENERGY RESOURCES – IMPERATIVE?

The companies whose technologies represent the most serious polluters of the human environment and environmental degradation usually resist the requirements of significant ecological investments. The conflict can be characterized as simultaneous aspiration to profit maximization on the one side, and the avoidance to bear

---

[1]http://www.economist.com/specialreports/displaystory.cfm?story_id=115 65685

[2] http://www.mie.gov.rs/sektori/sektor-za-odrzivu-energetiku-obnovljive-izvore-energije-i-stratesko-planiranje/?lang=lat

responsibilities for consequences, on the other side. There is a question now if companies are ready to finance ecological investments. First, their obligation to obey laws passed by the state, and more important, how governmental agencies can control putting the law into effect and apply sanctions for violating it.

Ratifying the Energy Community Treaty in 2006, Serbia has accepted the obligation to apply the European directives in the field of energy to increase share of renewable energy sources and energy efficiency. Serbia is obliged to the Energy Community of South-East Europe and EU countries to increase energy efficiency for 9% from 2011 to 2020, i.e. for 1.5% in 2012 relating to 2011[3].

The Law on Rational Energy Use should enable and stimulate responsible, rational and the long-term sustainable energy use in households, industry, local communities, traffic, civil engineering, and so on. This Law will force obligations of rational energy use on organizations, but it will also include stimulating mechanisms for energy efficiency projects and the use of renewable energy sources. The application of the Law would decrease energy consumption, i.e. it would advance energy efficiency, which, broadly speaking, would bring to economic efficiency. Although energy consumption per capita in Serbia is lower relating to some developed countries, three to four times more energy per product unit is spent in Serbia than in Europe. This Law would force enterprises to establish energy management. Without it, laws and strategies would be a dead letter. Besides, it is very important to inform and educate companies about advantages and benefits of applying the measures of energy efficiency, i.e. applying the 'Dutch model motto': talk, talk, talk. Therefore, it is not enough to pass the laws; we should inform the public because something cannot be applied if nobody knows about it.

Besides the law on Rational Energy Use, an important document in this field is the Strategy of Energy Development in Serbia until 2015, where, except energy efficiency, the importance of renewable energy use for stabile, sustainable economic development of the country is emphasized[4].

United Nations Environment Programme (UNEP) and United Nations Industrial Development Organization (UNIDO) have partnered together to promote Cleaner Production. According to UNEP Cleaner Production means the continuous application of an integrated preventive environmental strategy to processes and products to reduce risks to humans and the environment. For production processes, cleaner production includes conserving raw materials and energy, eliminating toxic raw materials, and reducing the quantity and toxicity of all emissions and wastes before they leave a process. For products, the strategy focuses on reducing impacts along the entire life cycle of the product, from raw material extraction to the ultimate disposal of the product. The goal of cleaner production is to avoid generating waste in the first place, and to minimize the use of raw materials and energy.[5] In 2007, Clener Production Center is established in Serbia with the aim to help companies to minimize waste and emissions and maximize product output.

TABLE I.
CLEANER PRODUCTION FRAMEWORK

Processes
– Raw material, energy, water savings
– Emission reduction
– Assesment of different technological options
– Risks and costs reduction
Products
– Waste reduction with better product design
– Waste usage for new products
Services
– Efficient environmental management within service providing

III. ENERGY EFFICIENCY AND RENEWABLE ENERGY – THE ANSWER TO THE CHALLENGES OF CONTEMPORARY BUSINESS?

Expectations of the companies increasingly grow, not only in relation to profit realization but also for environmental protection, corporative management and human rights. Human activities, including economic competition, too, exert pressure largely on natural functions of the Earth that the capabilities of the Planet ecosystem to 'endure' the future generations cannot be understood. Ecosystem degradation does not threaten only to decrease the life quality of humankind, but it deeply exerts influence on entrepreneurial business.

The Millennium Ecosystem Assessment underlines it as an imperative that business communities, especially companies as dominant institutions, should take the leading role in creating a sustainable society6. The duty of corporations is to do business in the way, which means sustainable development and social responsibility. The role of companies is to maximize profit legally, but also to include the long-term social price of natural resources use and the environmental protection. The Director of the DuPont Company emphasized that there would not be business success if the state of global ecosystems would continue to aggravate.

Preservation and advancement of the environment should become the structural part of almost all business activities.

[3] [3] http://www.mie.gov.rs/sektori/sektor-za-odrzivu-energetiku-obnovljive-izvore-energije-i-strasko-planiranje/?lang=lat
[4] http://www.tent.rs/images/stories/TENTA/strategija_energetika_lat.pdf

[5] http://www.cleanproduction.org/Steps.Process.UN.php
[6] http://millenniumassessment.org/documents/document.356.aspx.pdf

The important number of multinational companies usually has bigger financial power and influence than some countries relating to preservation, restoration and advancement of the living environment. Today, multinational companies have become an important factor of economic and social development.

Within the framework of the corporative development strategy, an increasing number of companies 'give' answers to sustainable development because they are under pressure of responsibility imposed by the public opinion, reacting on some environmental problems which companies themselves create through production and other business activities.

In the future, only those company management strategies will survive, i.e. those companies that simultaneously increase economic efficiency and decrease (or eliminate largely) the negative influence on the living environment, i. e. they increase eco-efficiency. Basically, eco-efficiency means an efficient production process and the production of better products and rendering services with a simultaneous decrease of resource use (energy, among others), waste creation and pollution in the whole chain of values.

The concept of eco-efficiency, as well as energy efficiency connects ecological performances and economic (financial) benefits. A new management strategy (or even philosophy), based on this concept, has been developed with a view to create bigger value with fewer negative influence on the living environment. As economic efficiency is realized through the principle of maximal results with minimal inputs, therefore, energy efficiency in the enterprise economic efficiency would mean the realization of maximal results (volume of production and rendered services) with minimal energy inputs.

IV. ENERGY EFFICIENCY AND RENEWABLE ENERGY RESOURCES – CHOICE?

Making businesses more efficient, through energy efficiency and usage of renewable resources, is seen as a largely untapped solution to addressing the problems of pollution, global warming, energy security, and fossil fuel depletion. Companies recognize the effects that a changing climate could potentially have on the sustainability of business operations and supply chain. Threats to water availability, increased energy prices and regulation could cause additional costs and reduce ability to manufacture and distribute products. Therefore, companies strive to minimize climate impact by reducing emissions, increasing efficiency and changing the way they use energy as well as sources of energy. In this context, definition of company's goals and principles, as well as indicators of business performances have changed. Both include and reflect consideration for the environment protection.

The following selected examples presents how companies and public authorities can reduce costs and improve economic efficiency through energy efficiency and usage of renewable resources.

A. Coca-Cola Enterprise Inc

Company is committed to reduce overall carbon footprint of business operations (manufacturing, distribution and product cooling) by an absolute 15% by 2020 as compared to 2007 baseline. In 2010, Coca-Cola Enterprise Inc invested $10.4 million of capital expenditures on carbon project reduction [7].

Manufacturing operations make up 22% of company's core business emissions and around 80% of this comes from energy used at manufacturing and distribution sites. In 2010, company used nearly 2% less energy in manufacturing operations than in 2009 – a total of 494,000 megawatt hours (MWH), down from 504,000 MWH – while increasing production volume. This reduction is achieved through monitoring energy use, planning and training, energy efficient technologies, and investing in renewable energy. Company placed energy meters on production lines and energy intensive equipment such as bottle blowers, compressors and chillers in order to discover where energy is being used and how efficiently the equipment is working. Coca-Cola also invests in new, energy efficient technologies - new lighting, compressed air and heat recovery. In facility in Sidcup, Great Britain, company have invested $125,000 to replace standard fluorescent light tubes with new Light Emitting Diode (LED) technology. Each new LED uses a quarter of the energy of a fluorescent tube, so the company will save 416 MWH of energy per year, (one percent of Sidcup's total usage) and around 197 tonnes of CO2e. As LEDs last longer, it will also make annual maintenance savings of around $6,000. Company is exploring the most suitable renewable and low-carbon energy solution at each site, depending on geography and location (water turbine, wind turbines, solar panels, combined heat and power).

Transporting products currently accounts for 16% of core business emissions. In the Netherlands, company has introduced five new 'Eco-Combi' trucks. This improve the carbon efficiency of company's deliveries by transporting 38 rather than 26 pallets at once, reducing CO_2 emissions by 20 percent per pallet. In Great Britain, company is trialing biogas-powered vehicles and in Belgium, piloting hybrid vehicles.

Cold drinks equipment makes up the greatest proportion (62 %) of core business emissions. At the end of 2010

----

[7] http://www.corporateregister.com/a10723/39362-11Co-10627740Y4906158404N-Eu.pdf

Coca-Cola Enterprise Inc had approximately 490,000 coolers, vendors and fountain machines in the marketplace (not including Norway and Sweden). Coca-Cola have approximately 21,000 open-fronted coolers across Europe. By fitting doors, energy use can be reduced by up to 50 percent. By replacing standard fluorescent lighting with long-life LEDs which can be up to 80 percent more efficient. Company has installed energy management devices which recognize patterns of use and responds by shutting off lights and adjusting temperatures when the cooler is not being opened regularly. In this way it can reduce energy consumption by up to 35 percent per cooler.

B. Air France & KLM

KLM has voluntarily committed to improve its energy efficiency by on average 2% per year between 2012 and 2020. Since 2009, the reduction achieved has reached 4.8% - by installing curtains that keep cold air inside saved 365,000 kWh/year, changing washing methods for trolleys saved 156,000 m^3 of gas per year and 136,000 kWh per year was saved on cooling computer rooms[8].

In September 2010, Air France also committed to improving energy efficiency by signing the World Business Council for Sustainable Development (WBCSD) Manifesto for energy efficiency in offices. At the end of 2010, 45% of Air France's ground equipment fleet was electrically powered, in line with targets for 2020. For the purchase of new material, electrically powered equipment has priority.

At KLM's Engineering & Maintenance division, a pilot has been launched together with Philips, the Dutch lighting company, with LED lights in the hangars. This reduces energy usage and energy costs, improves the workplace comfort of employees and increases the total amount of light covering the planes that are undergoing maintenance. At the end of 2010, KLM started to replace all cabin lights – tubular lighting – in its F70s by LED lights that use around 20% less energy, have a longer life span, create less heat and are also 8 kilos lighter, thus saving fuel and CO2 emissions. By 2011 all 26 F70s should have their lighting replaced with LED cabin lights.

C. Boutiquehotel Stadthalle

Boutiquehotel Stadthalle in Vienna is world's first city hotel with a zero energy-balance. It means that in the course of a year hotel creates the same amount of energy that is used to run it. For this, renewable energy sources like solar and photovoltaic panels, ground water heat pumps and even three wind turbines are used[9]. Rain water is used to tend plants and flowers and hotel rooms are provided with hot

water heated by the solar power. Construction costs for this type of hotels are about 10% higher than for conventional ones. It has been estimated that additional investments would pay off within 8 years, even less if the energy price is about to grow. In order to promote environmental consciousness, each guest that arrive at the hotel by train or by bike, get 10% discount.

D. Green Public Procurement

Green Public Procurement (GPP) is defined as a process whereby public authorities seek to procure goods, services and works with a reduced environmental impact throughout their life cycle when compared to goods, services and works with the same primary function that would otherwise be procured. Public authorities are major consumers in Europe: they spend approximately 2 trillion euros annually, equivalent to some 19% of the EU's gross domestic product. By using their purchasing power to choose goods and services with lower impacts on the environment, they can make an important contribution to sustainable consumption and production[10]. Local and state governments may obtain significant reduction in energy bills by changing purchasing policies to, for example, specify Energy star qualified products. The table below presents a basket of Energy Star products – computers, vending machines, compact fluorescent lamps, and water coolers – applicable to state and local governments.

TABLE II.
SAVINGS ACHIEVED WITH ENERGY STAR PRODUCTS

Action	Annual Energy&Maintenance Savings ($)	Net Life-Cycle Savings ($)
Use Energy Star power management to enable low-power mode on 5.000 computers	13.900	50.300
Replace 50 conventional vending machines with energy star versions	10.600	112.200
Replace 300 incandescent lamps with CFLs	7.800	23.500
Replace 100 water coolers with Energy star versions	3.400	27.900
Totals	35.700	213.900

According to this example, these products combination can save about $214.000 in electricity costs (based on an electricity rate $ 0.095 kWh) and prevent 2.000 tons of

---

[8] http://www.corporateregister.com/a10723/39677-11Su-10038281K4288964669B-Gl.pdf
[9] http://www.hotelstadthalle.at/hotel-vienna

[10] http://ec.europa.eu/environment/gpp/what_en.htm

carbon dioxide emissions over their lifetime compared to conventional products[11].

V. Conclusion

Factors that affects company's response to environmental protection challenges are mainly national and international regulation and stakeholders pressure. In the giving context, energy efficiency and renewable energy resources are the imperative for companies. But, nowadays, energy efficiency improvements and renewable energy resources have become the key elements of company's business strategy because more and more companies, in order to achieve economic efficiency, consider energy efficiency and renewable energy resources i.e. energy management as a chance and choice.

References

[1] Field C.B., Field K.M., *Environmental Economics: an introduction*, McGrawHill, 2006.

[2] Goodstein E.S.,*Economics and Environment*, John Wiley& Sons, 2007.

[3] Wetherly P., Otter D., *The Business Environment*, Oxford University press, 2008.

[4] Kew J., Stredwick J., *Business Environment: Managing in a strategic context,* CIPD, 2008.

---

[11] http://www.energystar.gov/

Flow Pattern Map for In Tube Evaporation and Condensation

László Garbai Dr.[*], **Róbert Sánta** [**]

[*] Budapest University of Technology and Economics, Hungary
[**]College of Applied Sciences – Subotica Tech, Serbia

Abstract - The aim of the article is the review of two phase flow pattern maps for horizontal tubes. The flow pattern in evaporation and condensation section in a small tube has been analyzed in this article. The two-phase flow pattern map for evaporation is proposed by Wojtan et al. while the condensation section is proposed by Thome and El Hajal. The simulation was in MathCAD and the results are presented in diagrams. In the simulation refrigerant R134a was used.

Nomenclature

d	diameter (m)
x	vapor quality (-)
G	mass velocity (kg/sm^2)
$\dot{m}$	mass flow rate (kg/s^2)
p	pressure (Pa)
Q	heat flux (W/m^2)
T	temperature (K)
f	friction factor (-)
A	area of tube (m^2)

Greeks

α	heat transfer coefficient (W/m^2K)
λ	thermal conductivity (W/mK)
ε	void fraction (-)
η	dynamic viscosity (Ns/m^2)
σ	surface tension (-)
ρ	density (m^3/kg)

Index

l	liqued
v	vapor
tp	two phase

I. INTRODUCTION

For two-phase flows, the respective distribution of the liquid and vapor phases in the flow channel is an important aspect of their description. Their respective distributions take on some commonly observed flow structures, which are defined as two-phase flow patterns that have particular identifying characteristics. Heat transfer coefficients and pressure drops are closely related to the local two-phase flow structure of the fluid, and thus two-phase flow pattern prediction is an important aspect of modeling evaporation and condensation. In fact, recent heat transfer models for predicting in tube boiling and condensation are based on the local flow pattern and hence, by necessity, require reliable flow pattern map to identify what type of flow pattern exists at the local flow conditions.

Flow patterns have an important influence on prediction of flow boiling and convective condensation heat transfer coefficients, and two-phase pressure drops. For horizontal tubes, the methods of Taitel and Dukler [1] (1976) and Baker [2] (1954), Hashizume [3], Steiner [4], are widely used. The more recent flow pattern map of Kattan, Thome and Favrat (1998) and its more subsequent improvements, which was develop specifically for small diameter tubes typical of shell-and-tube heat exchangers for both adiabatic and evaporating flows. Another version of their map also been proposed by El.Hajal, Thome and Cavalinni [6] (2003) for in tube condensation.

II. FLOW REGIMES IN HORIZONTAL PIPES

When a vapor and a liquid are forced to flow together inside a pipe, there are at least seven different geometrical configurations, or flow regimes, that are observed to occur. The regime depends on the fluid properties, the size of the conduit and the flow rates of each of the phases.

Vapor and liquid phases flow in horizontal tubes according to several topological configurations, called flow patterns or flow regimes that are determined by the interfacial structure between the two phases.

Two-phase flow patterns in horizontal tubes are similar to those in vertical flows but the distribution of the liquid is influenced by gravity that acts to stratify the liquid to the bottom of the tube and the vapor to the top. Flow patterns for co-current flow of vapor and liquid in a

horizontal tube are show in Figure 1. and are categorized as follows.

- Bubbly flow – the gas bubbles are dispersed in the liquid with a high concentration of bubbles in the upper half of the tube due to their buoyancy. When shear forces are dominant, the bubbles tend to disperse uniformly in the tube. In horizontal flows, the regime typically only occurs at high mass flow rates.
- Stratified flow – At low liquid and gas velocities, complete separation of the two phases occurs. The gas goes to the top and the liquid to the bottom of the tube, separated by an undisturbed horizontal interface. Hence the liquid and gas are fully stratified in this regime.
- Stratified-wavy flow – Increasing the gas velocity in a stratified flow, waves is formed on the interface and travel in the direction of flow. The waves climb up the sides of the tube, leaving thin films of liquid on the wall after the passage of the wave.
- Intermittent flow – Further increasing the gas velocity, these interfacial waves become large enough to wash the top of the tube. Large amplitude waves often contain entrained bubbles. The top wall is nearly continuously wetted by the large amplitude waves and the thin liquid films left behind. Intermittent flow is also a composite of the plug and slug flow regimes. These subcategories are characterized as follows:
  - o Plug flow. This flow regime has liquid plugs that are separated by elongated gas bubbles. The diameters of the elongated bubbles are smaller than the tube such that the liquid phase is continuous along the bottom of the tube below the elongated bubbles. Plug flow is also sometimes referred to as elongated bubble flow.
  - o Slug flow. At higher vapor velocities, the diameters of elongated bubbles become similar in size to channel height. The liquid slugs separating such elongated bubbles can also be described as large amplitude waves.

- Annular flow - At high gas flow rates, the liquid forms a continuous annular film around the perimeter of the tube, similar to that in vertical flow but the liquid film is thicker at the bottom than the top. The interface between the liquid annulus and the vapor core is disturbed by small amplitude waves and droplets may be dispersed in the gas core.
- Mist flow – Similar to vertical flow, at very high gas velocities, all the liquid may be stripped from the wall and entrained as small droplets in the now continuous vapor phase.
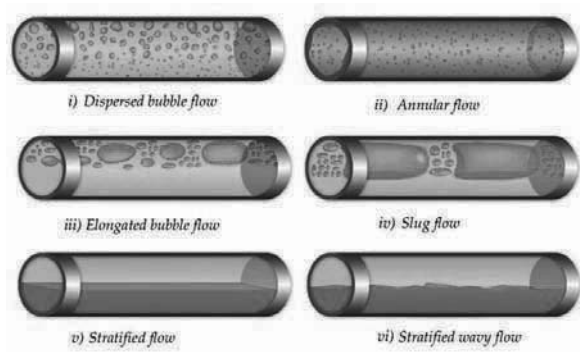
Figure 1. Flow regimes in horizontal pipes [11]

III. FLOW REGIME MAPS

To predict the local flow pattern in a tube, a flow pattern map is used. It is a diagram that displays the transitions boundaries between the flow patterns and is typically plotted on log-log axes using dimensionless parameters to represent the liquid and gas velocities.

Flow regime maps of the sort shown in figure 2. are useful when we want to gain insight into the mechanisms creating the flow regimes. Along the horizontal axis the superficial gas velocity has been plotted. Along the vertical axis we have plotted the superficial liquid velocity.
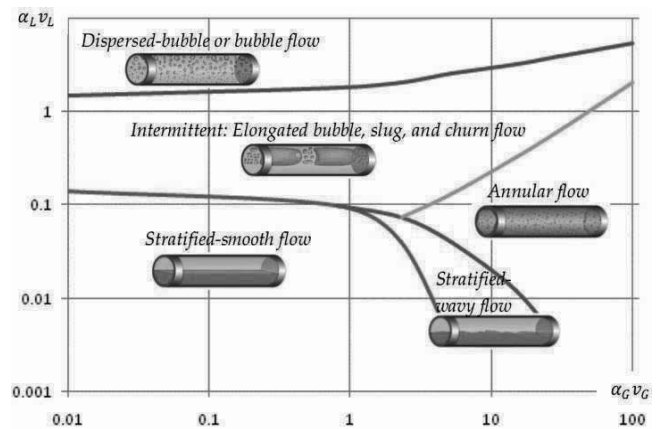
Figure 2. Example of steady-state flow regime map for a horizontal pipe

- If the superficial gas and liquid velocities is very low the flow is stratified.
- If increase the gas velocity, waves start forming on the liquid surface. Due to the friction between gas and liquid, increasing the gas flow will also affect the liquid by dragging it faster towards the outlet and thereby reducing the liquid level.
- If continue to increase the gas flow further, the gas turbulence intensifies until it rips liquid from the liquid surface so droplets become entrained in the gas stream, while the previously horizontal surface bends around the inside of the pipe until it covers the whole

circumference with a liquid film. The droplets are carried by the gas until they occasionally hit the pipe wall and are deposited back into the liquid film on the wall.

- If the liquid flow is very high, the turbulence will be strong, and any gas tends to be mixed into the liquid as fine bubbles. For somewhat lower liquid flows, the bubbles float towards the top-side of the pipe. The appropriate mix of gas and liquid can then form Taylor-bubbles, which is the name we sometimes use for the large gas bubbles separating liquid slugs.

- If the gas flow is constantly kept high enough, slugs will not form because the gas transports the liquid out so rapidly the liquid fraction stays low throughout the entire pipe.

IV. FLOW PATTERN MAP FOR EVAPORATION IN HORIZONTAL TUBES

The two-phase flow pattern map and heat transfer model for evaporation proposed Wojtan et al.[7] (2005), is a slightly modified version of Kattan, Thome and Favrat [5] map for evaporation flows in small diameter horizontal tubes.

The six principal flow patterns encountered during evaporation inside horizontal tubes are:

- Stratified flow(**S**),
- Stratified-wavy flow (**SW**),
  - Slug flow zone,
  - Slug/Stratified-Wavy zone
  - Stratified-Wavy zone.
- Intermittent flow (**I**),
- Annular flow (**A**),
- Dryout (**D**),
- Mist flow (**MF**)

A. FLOW PATTERN MAP OF WOJTAN ET AL. (2005)

- The transition boundary curve between stratified flows to stratified-wavy flow is:

$$G_{strat} = \left(\frac{226.2 \cdot A_{ld}^2 \cdot A_{vd}^2 \cdot \rho_v \cdot (\rho_l - \rho_v) \cdot \mu_l \cdot g \cdot \cos\varphi}{x^2 \cdot (1-x) \cdot \pi^3} \right)^{1/3} \quad (1)$$

- The transition boundary curve between annular and intermittent flows to stratified-wavy flow is:

$$G_{wavy} = \left(\frac{16 \cdot A_{vd}^3 \cdot g \cdot D \cdot \rho_l \cdot \rho_v}{x^2 \cdot \pi^2 \cdot \left(1 - (2 \cdot \alpha_{ld} - 1)^2\right)^{0.5}} \cdot \left[\frac{\pi^2}{25 \cdot \alpha_{ld}^2} \cdot (1-x)^{-F_1} \cdot \left(\frac{We}{Fr} \right)^{-F_2} + 1 \right] \right)^{0.5} + 50 \quad (2)$$

- Threshold line of the intermittent to annular flow transition at X_{IA} is:

$$X_{IA} = \left[\left(0.34^{1/0.875} \cdot \left(\frac{\rho_v}{\rho_l} \right)^{-1/1.75} \cdot \left(\frac{\mu_v}{\mu_l} \right)^{-1/7} \right) + 1 \right]^{-1} \quad (3)$$

- The stratified-wavy region is then subdivided into three zones as follows:
  - $G \rangle G_{wavy}(X_{IA})$ gives the slug flow zone,
  - $G_{strat} \langle G \langle G_{wavy}(X_{IA})$ and $0 \langle x \langle X_{IA}$ give the Slug/Stratified-Wavy zone
  - $1 \rangle x \rangle X_{IA}$ gives the Stratified-Wavy zone.

- The transition boundary curve between annular flows to dryout flow is:

$$G_{dryout} = \left[\frac{1}{0.235} \cdot \left(\ln\left(\frac{0.58}{x} \right) + 0.52 \right) \cdot \left(\frac{d_i}{\rho_g \cdot \sigma} \right)^{-0.17} \cdot \left(\frac{1}{\rho_g \cdot (\rho_l - \rho_v) \cdot g \cdot d_i} \right)^{-0.37} \cdot \left(\frac{\rho_g}{\rho_l} \right)^{-0.25} \cdot \left(\frac{q}{q_{DNB}} \right)^{-0.7} \right]^{0.926} \quad (4)$$

- The transition boundary curve between dryout flows to mist flow is:

$$G_{mist} = \left[\frac{1}{0.0058} \cdot \left(\ln\left(\frac{0.61}{x} \right) + 0.57 \right) \cdot \left(\frac{d_i}{\rho_g \cdot \sigma} \right)^{-0.38} \cdot \left(\frac{1}{\rho_g \cdot (\rho_l - \rho_v) \cdot g \cdot d_i} \right)^{-0.15} \cdot \left(\frac{\rho_g}{\rho_l} \right)^{0.09} \cdot \left(\frac{q}{q_{DNB}} \right)^{-0.27} \right]^{0.943} \quad (5)$$

V. FLOW PATTERN MAP FOR CONDENSATION IN HORIZONTAL TUBES

The two-phase flow pattern map for condensation proposed by El Hajal, Thome and Cavallini [6] is a slightly modified version of Kattan, Thome and Favrat [5] map for evaporation and adiabatic flows in small diameter horizontal tubes. Thome and El Hajal have simplified implementation of that map by bringing a void fraction equation into the method to eliminate its iterative solution scheme.

The five principal flow patterns encountered during condensation inside horizontal tubes are:

- Annular flow (often referred to as sheared-controlled regime) (**A**),
- Intermittent flow (heat transfer modeled like annular flow), (**I**),
- Mist flow (annular flow heat transfer model assumed for this regime) (**MF**)
- Stratified-wavy flow (**SW**),
- Stratified flow (**S**),

Intermittent flow refers to both the plug and slug flow regimes (it is essentially a stratified-wavy flow pattern with large amplitude waves that wash the top of the tube). Also, stratified-wavy flow is often referred to in the literature as simply wavy flow.

A. FLOW PATTERN MAP OF THOME AND EL HAJAL (2003)

This model can be easily applied and gives the void fraction as a function of total mass flux. Hence it makes sense to use the same void fraction model in both the flow pattern map and the flow boiling heat transfer model for which the Rouhani-Axelson [8] model is a better choice as a general method.

The sectional area of the tube **A** and after calculating ε, the values and are directly determined by:

$$A_{ld} = \frac{A \cdot (1-\varepsilon)}{D^2}, \qquad A_{vd} = \frac{A \cdot \varepsilon}{D^2} \qquad (6)$$

The stratified angle can be calculated from an expression evaluated in terms of void fraction proposed by Biberg [9]

$$P_D = \sin\left(\frac{2\pi - \theta_{strat}}{2}\right)$$

- The transition boundary curve between Stratified flows to Stratified-wavy flow is:

$$G_{strat} = \left(\frac{226.2 \cdot A^2_{vd} \cdot A^2_{vd} \cdot \rho_v \cdot (\rho_l - \rho_v) \cdot \mu_l \cdot g \cdot \cos\varphi}{x^2 \cdot (1-x) \cdot \pi^3}\right)^{\frac{1}{3}} \qquad (7)$$

- The transition boundary curve between Stratified flows to Intermittent/Annular flow is:

$$G_{wavy} = \left(\frac{16 \cdot A^3_{vd} \cdot g \cdot D \cdot \rho_l \cdot \rho_v}{x^2 \cdot \pi^2 \cdot \left(1-(2 \cdot \alpha_{ld}-1)^2\right)^{0.5}} \cdot \left[\frac{\pi^2}{25 \cdot \alpha^2_{ld}} \cdot (1-x)^{-F_1} \cdot \left(\frac{We}{Fr}\right)^{-F_2} + \frac{1}{\cos\varphi}\right]\right)^{0.5} + 50 \qquad (8)$$

- The transition boundary curve between Annular flows to Mist flow is:

$$G_{mist} = \left(\frac{7680 \cdot A^2_{vd} \cdot g \cdot D \cdot \rho_v \cdot \rho_l}{x^2 \cdot \zeta_{ph} \cdot \pi^2} \cdot \left(\frac{We}{Fr}\right)_l\right)^{0.5} \qquad (9)$$

- The transition boundary curve between Annular flows to Intermittent flow is:

$$X_{IA} = \left[\left(0.34^{1/0.875} \cdot \left(\frac{\rho_v}{\rho_l}\right)^{-1/1.75} \cdot \left(\frac{\mu_v}{\mu_l}\right)^{-1/7}\right) + 1\right]^{-1} \qquad (10)$$

V. SIMULATION OF MATHEMATICAL MODEL

Mathematical models are simulated by the use of the software tool MathCAD. The solution of the deterministic mathematical models of the flow pattern and heat transfer coefficients is complex. The applied numerical simulation model for each variable is discretized. The input data and initial conditions in the deterministic mathematical model clearly define the value of flow pattern and heat transfer coefficient i.e. is the output of the model.

The initial condition and values for the simulation:

- Refrigerant: R134a
- Mass velocity: $G = 100 \quad \left\lfloor\frac{kg}{m^2 s}\right\rfloor$
- Vapor quality ranged: $x = 0 - 1 \; [\,-\,]$

- Tube diameter: $\qquad d = 6 \quad [\text{mm}]$

- Heat flux: $\qquad q = 3000 \quad \left[\dfrac{\text{W}}{\text{m}^2}\right]$

- Temperature of evaporation: $\quad t_o = 5 \; [°\text{C}]$

- Temperature of condensation: $\quad t_c = 40 \; [°\text{C}]$

Graphs are drawn for the considered evaporation and condensation heat transfer coefficients and flow pattern in function of different quality.

VI. RESULTS AND DISCUSES

The motivation for the composition of this article was to investigate the flow pattern map and heat transfer coefficients in the horizontal tube of the condenser and the evaporator.

The flow pattern is of crucial definition. With the change of flow pattern, the change of mass velocity of refrigerant occurs. The value of the two-phase heat transfer coefficient is determined by the mass velocity.

The discrete value of the two-phase heat transfer coefficient is a function of the refrigerant mass velocity, the vapor quality, the refrigerant condensing or evaporation temperature and the inner diameter of tube.

$$\alpha = f\left(\dot{m}, x, T, d\right)$$

Besides the heat transfer coefficients, accuracy of the pressure drop and the void fraction value is determined by the heat pump system of the accurate mathematical model.

The flow pattern map for boiling and flow boiling heat transfer model for refrigerant R134a on the inside of horizontal tubes are proposed of Wojtan et al. (2005).

The flow pattern for condensation of refrigerant R134a on the inside of horizontal tubes are suggested by Thome and El Hajal (2003). The condensation heat transfer model was used of Shah [10] correlation (1979).

The existence of a particular flow regime depends on a variety of parameters, including the thermo physical properties of the fluid, the tube diameter, orientation and geometry, force field, mass flux, heat flux and vapor quality.

On the flow pattern maps, the value change of the heat transfer coefficients of evaporation and condensation can be seen. It can be seen that the added input values, the annular flow is predominantly formed in the evaporating

section. (Figure 3.) On the contrary, in the condensing section of the annular flow pattern the image did not even appear. In the condensing sections the flow regime is stratified wavy. (Figure 4.) In practice, however, this is not completely the case. If the cross section of wall is considered, the condenser tube wall is the coldest, hence the vapor of the two-phase refrigerant is condensed in the wall, so there a degree of annular flow develops.
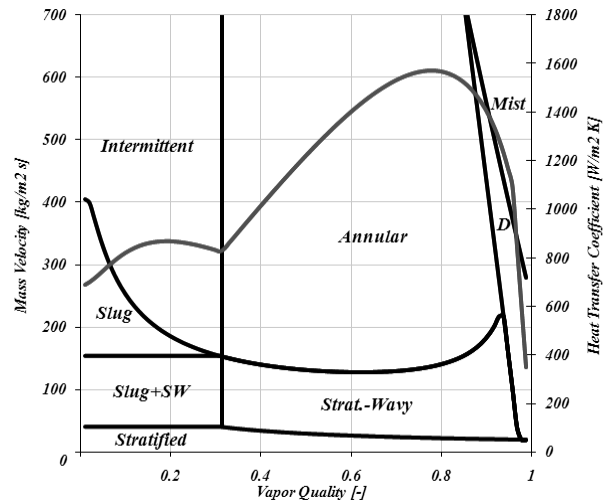

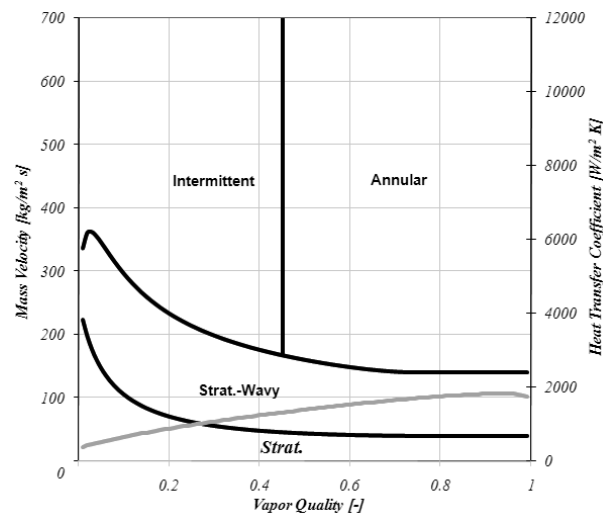Figure 3. Flow Pattern map and Heat Transfer model for in tube boiling

Figure 4. Flow Pattern map and Heat Transfer model for in tube Condensation

Flow patterns that occur during condensation inside horizontal tubes are similar to those for evaporation, with the following exceptions:

- The process begins without any entrainment of liquid.
- There is no dryout.

- During condensation, the condensate formed coats the tube perimeter with a liquid film.
- During condensation in stratified flow regimes, the top of the tube is wetted by the condensate film while in evaporating flows the top perimeter is dry.

REFERENCES

[1] Y.Taitel and A.E. Dukler, A model for predicting low regime transitions in horizontal and near horizontal gas-liquid flow, AICHE Journal 13. no.2, 43-69

[2] O. Baker, Design of pipe lines for simultaneous flow of oil and gas, Oil and gas journal (1954), 185-190

[3] K. Hashizume, Flow pattern and void fraction of refrigerant two-phase flow in a horizontal pipe, Bulletin of JSME26, no.219, 1597-1602

[4] Verein Deutscher Ingenieure VDI-Warmeatlas (VDI Heat Atlas), Chapter HBB, VDI-Gessellschaft Verfahrenstechnik und Chemieingenieurwsen (GVC), Düsseldorf, 1993

[5] Kattan, N., Thome, J. R., and Favrat, D. (1998). Flow Boiling in Horizontal Tubes. Part 1: Development of a Diabatic Two-Phase Flow Pattern Map, *J. Heat Transfer*, 120, 140-147.

[6] El Hajal, J., Thome, J.R., and Cavallini, A. (2003). Condensation in Horizontal Tubes, Part 1: Two-Phase Flow Pattern Map, *Int. J. Heat Mass Transfer*, vol. 46, 3349-3363.

[7] L Wojtan, T Ursenbacher, J Thome, Investigation of flow boiling in horizontal tubes: Part I: A new diabatic two-phase flow pattern map, International Journal of Heat and Mass Transfer (2005)

[8] Rouhani, S. Z., and Axelsson, E., Calculation of Void Volume Fraction in the Subcooled and Quality Boiling Regions. *International Journal of Heat and Mass Transfer*, vol. 13, no. 2, pp. 383–393, 1970.

[9] D. Biberg, An explicit approximation for the wetted angle in two-phase stratified pipe flow, Canadian J. Chemical Engineering (1999), 1221-1224

[10] Shah MM. A general correlation for heat transfer during film condensation inside pipes. Int. J Heat & Mass Transfer 1979; 22: 547–56

[11] Dr. Ove Bratland: The Flow Assurance, Bergen Area, Norway, Oil & Energy

Realization of Concurrent Programming in Embedded Systems

Anita Sabo*, Bojan Kuljić**, Tibor Szakáll***, Andor Sagi****

Subotica Tech, Subotica, Serbia

* saboanita@gmail.com ** bojan.kuljic@gmail.com *** szakall.tibor@gmail.com   **** peva@vts.su.ac.rs

Abstract — **The task of programming concurrent systems is substantially more difficult than the task of programming sequential systems with respect to both correctness and efficiency. Nowadays multi core processors are common. The tendency in development of embedded hardware and processors are shifting to multi core and multiprocessor setups as well. This means that the problem of easy concurrency is an important problem for embedded systems as well. There are numerous solutions for the problem of concurrency, but not with embedded systems in mind. Due to the constrains of embedded hardware and use cases of embedded systems, specific concurrency solutions are required. In this paper we present a solution which is targeted for embedded systems and builds on existing concurrency algorithms and solutions. The presented method emphasizes on the development and design of concurrent software. In the design of the presented method human factor was taken into consideration as the major influential fact in the successful development of concurrent applications.**

Keywords – concurrent systems, embedded systems, parallel algorithms

I. INTRODUCTION

Concurrent computing is the concurrent (simultaneous) execution of multiple interacting computational tasks. These tasks may be implemented as separate programs, or as a set of processes or threads created by a single program. The tasks may also be executing on a single processor, several processors in close proximity, or distributed across a network. Concurrent computing is related to parallel computing, but focuses more on the interactions between tasks. Correct sequencing of the interactions or communications between different tasks, and the coordination of access to resources that are shared between tasks, are key concerns during the design of concurrent computing systems. In some concurrent computing systems communication between the concurrent components is hidden from the programmer, while in others it must be handled explicitly. Explicit communication can be divided into two classes:

A. Shared memory communication

Concurrent components communicate by altering the contents of shared memory location. This style of concurrent programming usually requires the application of some form of locking (e.g., mutexes (meaning(s) mutual exclusion), semaphores, or monitors) to coordinate between threads. Shared memory communication can be achieved with the use of Software Transactional Memory (STM) [1][2][3]. Software Transactional Memory (STM) is an abstraction for concurrent communication mechanism analogous to database transactions for controlling access to shared memory. The main benefits of STM are composability and modularity. That is, by using STM one can write concurrent abstractions that can be easily composed with any other abstraction built using STM, without exposing the details of how the abstraction ensures safety.

B. Message Passing Communication

Concurrent components communicate by exchanging messages. The exchange of messages may be carried out asynchronously (sometimes referred to as "send and pray"), or one may use a rendezvous style in which the sender blocks until the message is received. Message-passing concurrency tends to be far easier to reason about than shared-memory concurrency, and is typically considered a more robust, although slower, form of concurrent programming. The most basic feature of concurrent programming is illustrated in Figure 1. The numbered nodes present instructions that need to be performed and as seen in the figure certain nodes must be executed simultaneously. Since most of the time intermediate results from the node operations are part of the same calculus this presents great challenge for practical systems. A wide variety of mathematical theories for understanding and analyzing message-passing systems are available, including the Actor model [4]. In computer science, the Actor model is a mathematical model of concurrent computation that treats "actors" as the universal primitives of concurrent digital computation: in response to a message that it receives, an actor can make local decisions, create more actors, send more messages,
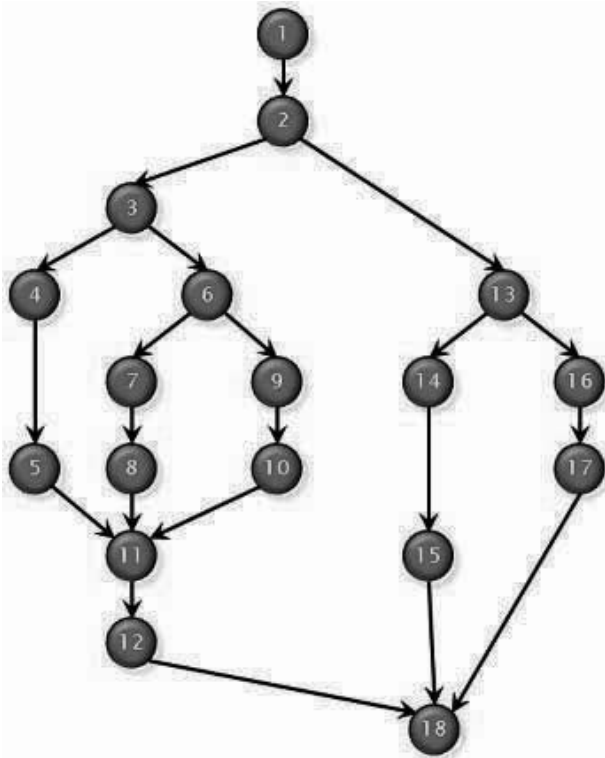
Figure 1. The data flow of a software

and determine how to respond to the next message received. Figure 1 demonstrates the most basic but essential problem in the concurrent programming. Each number represents one process or one operation to be performed. The main goal is not to find the resource for parallel computing but to find the way to pass intermediate results between the numbered nodes.

C. Advantages

Increased application throughput - the number of tasks done in certain time period will increase. High responsiveness for input/output - input/output intensive applications mostly wait for input or output operations to complete. Concurrent programming allows the time that would be spent waiting to be used for another task. It can be stated that there are more appropriate program structures - some problems and problem domains are well-suited to representation as concurrent tasks or processes.

II. COMMUNICATION

In case of distributed systems the performance of parallelization largely depends on the performance of the communication between the peers of the system. Two peers communicate by sending data to each other, therefore the performance of the peers depends on the processing of the data sent and received. The communication data contains the application data as well as the transfer layer data. It is important for the transfer layer to operate with small overhead and provide fast processing. Embedded systems have specific requirements. It is important that the communication meets these requirements.

The design of the presented method is focused around the possibility to support and execute high level optimizations and abstractions on the whole program. The graph-based software layout of the method provides the

possibility to execute graph algorithms on the software architecture itself. The graph algorithms operate on the software's logical graph not the execution graph. This provides the possibility for higher level optimizations (super optimization). The architecture is designed to be easily modelable with a domain specific language. This domain specific language eases the development of the software, but its primary purpose is to provide information for higher level optimizations. It can be viewed as the logical description, documentation of the software. Based on the description language it is possible to generate the low level execution of the software, this means that it is not necessary to work at a low level during the development of the software. The development is concentrated around the logic of the application. It focuses on what is to be achieved instead of the small steps that need to be taken in order to get there.

III. REALIZATION IN EMBEDDED SYSTEMS

The architecture of modern embedded systems is based on multi-core or multi-processor setups. This makes concurrent computing an important problem in the case of these systems, as well. The existing algorithms and solutions for concurrency were not designed for embedded systems with resource constraints. In the case of real-time embedded systems it is necessary to meet time and resource constraints. It is important to create algorithms which prioritize these requirements. Also, it is vital to take human factor into consideration and simplify the development of concurrent applications as much as possible and help the transition from the sequential world to the parallel world. It is also important to have the possibility to trace and verify the created concurrent applications. The traditional methods used for parallel programming are not suitable for embedded systems because of the possibility of dead-locks. Dead-locks pose a serious problem for embedded systems [5], because they can cause huge losses. The methods presented in [6] (Actor model and STM), which do not have dead-locks, have increased memory and processing requirements, this also means that achieving real-time execution becomes harder due to the use of garbage collection. Using these methods and taking into account the requirements of embedded systems one can create a method which is easier to use than low-level threading and the resource requirements are negligible. In the development of concurrent software the primary affecting factor is not the method used for parallelization, but the possibility to parallelize the algorithms and the software itself. To create an efficient method for parallel programming, it is important to ease the process of parallelizing software and algorithms. To achieve this, the used method must force the user to a correct, concurrent approach of developing software. This has its drawbacks as well, since the user has to follow the rules set by the method. The presented method has a steep learning curve, due to its requirements toward its usage (software architecture, algorithm implementations, data structures, resource management). On the other hand, these strict rules provide advantages to the users as well, both in correctness of the application and the speed of development. The created applications can be checked by verification algorithms and the integration of parts, created by other users is provided by the method itself. The requirements of the method provide a solid base for the users. In the case of sequential

applications the development, optimization and management is easier than in the case of concurrent applications. Imperative applications when executed have a state. This state can be viewed as the context of the application. The results produced by imperative applications are context-dependent. Imperative applications can produce different results for the same input because of different contexts. Sequential applications execute one action at a given moment with a given context. In the case of concurrent applications, at a given moment, one or more actions are executed with in one or more contexts, where the contexts may affect each other. Concurrent applications can be decomposed into sequential applications which communicate with each other through their input, but their contexts are independent. This is the simplest and cleanest form of concurrent programming.

IV. MAIN PROBLEMS

Embedded systems are designed to execute specific tasks in a specific field. The tasks can range from processing to peripheral control. In the case of peripheral control, concurrent execution is not as important, in most cases the use of event-driven asynchronous execution or collective IO is a better solution [7]. In the case of data- and signal processing systems the parallelization of processing tasks and algorithms is important. It provides a significant advantage in scaling and increasing processing capabilities of the system. The importance of peripheral and resource management is present in data processing systems as well. The processing of the data and peripheral management needs to be synchronized. If we fail to synchronize the data acquisition with data processing the processing will be blocked until the necessary data are acquired, this means that the available resources are not being used effectively. The idea of the presented method is to separate the execution, data management and resource handling parts of the application. The presented method emphasizes on data processing and is made up of separate modules. Every module has a specific task and can only communicate with one other module. These modules are peripheral/resource management module, data management module and the execution module. The execution module is a light weight thread, it does not have its own stack or heap. This is a requirement due to the resource constrains of embedded systems. If required, the stack or heap can be added into the components of the execution thread with to the possibility of extending the components of the execution thread with user-defined data structures. The main advantage of light weight threads is that they have small resource requirements and fast task switching capabilities [8][9]. The execution module interacts with the data manager module which converts raw data to a specific data type and provides input for the execution module. The connection between the data manager and the execution module is based on the Actor model [10] which can be optimally implemented in this case, due to the restrictions put on the execution module which can only read and create new data (types) and cannot modify it. The execution module can be monolithic or modular. The modular composition is required for complex threads were processing is coupled with actions (IO). The execution threads can be built up from two kinds of components, processing and execution/action components. The component used in the execution
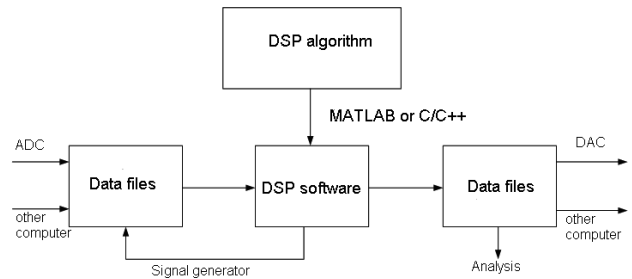

Figure 2. The software development process

module is a type which for a given input type 'a' creates a given type 'b'. This operation will always give the same result for the same input.

The processing component is referentially transparent, meaning it does not support destructive actions [11]. The type variables 'a' and 'b' can have the same types. The action component is similar to the processing component, it is usable in case where one needs to support destructive actions. These components request the execution of specific actions which are received and executed by a transactional unit. The design of the transactional mechanism is based on transactions, just as in software transactional memory. The threads in the execution module are not connected to each other. It is possible to achieve interaction between the threads. One or more execution threads can be joined with the use of the reduce component. The reduce component iterates through the values of the given threads, merging them into one component or value. The merging algorithm is specified by the user, as well as the order of the merging. The joining of the threads follows the MapReduce model, where the map functions correspond to the threads and the reduce function corresponds to the merging algorithm provided by the user [12]. The method introduced in this paper is usable for concurrent programming in real-time embedded systems as well. The complexities of the algorithms used in the method are linear in the worst case. The priority of threads can be specified, this mean that the order of execution can be predetermined. It is possible to calculate the amount of time required to execute a specific action. This way the created systems can be deterministic.

Threads can be separated into two parts. The two parts create a client server architecture, where the server is the data manager and the client is the actions/steps of the thread. The job of the server (producer) is to provide the client (consumer) with data. The server part sends the data to the client part. The server part protects the system form possible collisions due to concurrent access or request to resources. The client part has a simple design it is made up of processing steps and actions.

The job of the asynchronous resource manager is to provide safe access to resources for the server part of the threads. The resource manager does not check the integrity of data, its only job is to provide the execution threads server part with raw data. Parallelization of software is not trivial in most cases. The method presented in the paper takes this fact into consideration. It is an important that the parallelizable and sequential parts of the software can be easily synchronizable. The presented view of software (as seen in Figure 2) is easily implementable into the model of the presented method. Based on the data

flow of the software, it is possible to implement it into the model of the presented method for concurrency.

V. CONCLUSION

Concurrent programming is complex and hard to achieve. In most cases the parallelization of software is not a straightforward and easy task. The realized concurrent programs usually have safety and performance issues. For embedded systems the existing parallelization algorithms and solutions are not optimal due to resource requirements and safety issues. The goal is to realize such a solution for concurrent programming, which is optimal for embedded systems and helps and simplifies the development of concurrent programs. The key to successful development of parallel programs is in the realization of tools which take into consideration the human factors and aspects of parallel development.

The model presented in this paper builds on the advantages of existing parallelization algorithms with human factor as its primary deciding factor. In the development of a concurrent applications, the used parallelization algorithms and solutions are important, but the most important factor is the developer/user itself. To achieve the best possible results, to achieve efficient software, we must concentrate on the most important factor of development, the human (developer).

The presented parallelization model is best applicable if the problem we would like to solve is not trivially parallelizable, which is true for the great number of algorithms and software.

REFERENCES

[1] Tim Harris, Simon Marlow, Simon Peyton Jones, Maurice Herlihy, "Composable memory transactions," Proceedings of the tenth ACM SIGPLAN symposium on Principles and practice of parallel programming, pp. 48–60, 2005.

[2] Anthony Discolo, Tim Harris, Simon Marlow, Simon Peyton Jones, Satnam Singh, "Lock -Free Data Structures using STMs in Haskell," Functional and Logic Programming,pp.65–80, 2006.

[3] Tim Harris and Simon Peyton Jones, "Transactional memory with data invariants," ACM SIGPLAN Workshop on Transactional Computing, 2006.

[4] Paul Baran, "On Distributed Communications Networks," IEEE Transactions on Communications Systems, vol. 12, issue 1., pp 1-9, 1964.

[5] César Sanchez, "Deadlock Avoidance for Distributed Real-Time and Embedded", Dissertation, Department of Computer Science of Stanford University, 2007 May.

[6] Y. Yorozu, M. Hirano, K. Oka, and Y. Tagawa, "MTIO. A multithreaded parallel I/O system," Parallel Processing Symposium,. Proceedings, 11th International, pp. 368-373, 1997.

[7] Girija J. Narlikar, Guy E. Blelloch, "Space-efficient scheduling of nested parallelism," ACM Transactions on Programming Languages and Systems, pp. 138-173, 1999.

[8] Girija J. Narlikar, Guy E. Blelloch, "Space-efficient implementation of nested parallelism," Proceedings of the Sixth ACM SIGPLAN Symposium on Principles and Practice of Parallel Programming, 1997.

[9] Bondavalli, A.; Simoncini, L., "Functional paradigm for designing dependable large-scale parallel computing systems," Autonomous Decentralized Systems, 1993. Proceedings. ISADS 93, International Symposium on Volume, Issue, 1993, pp. 108 – 114.

[10] Jeffrey Dean and Sanjay Ghemawat, "MapReduce: Simplified Data Processing on Large Clusters," OSDI'04: Sixth Symposium on Operating System Design and Implementation, 2004.

[11] *Gene Amdahl, "Validity of the Single Processor Approach to Achieving Large-Scale Computing Capabilities," AFIPS Conference Proceedings, (30), pp. 483-485, 1967.*

[12] Rodgers, David P., "Improvements in multiprocessor system design," ACM SIGARCH Computer Architecture News archive Volume 13, Issue 3, pp. 225-231, 1985

Renewable energy sources in automobility

Zoltán J. Pék MScME*, Jozsef M. Nyers Dr. Sci**

*Technical School Ivan Sarić/Mechanical Department, Subotica, Serbia
**Subotica Tech. Serbia , University Obuda Budapest, Hungary
e-mail: pekzoli@tippnet.rs
e-mail : jnyers@vts.su.ac.rs

Abstract—**This article gives a instruction into the basic guidelines for preparing an automobile for application of the renewable energy sources. The energy source is a sunlight uses the photovoltaic elements. In paper describe the history and materials of photovoltaic elements.**

Index Terms – **renewable energy sources, solar power, solar energy, electromobil, photon energy, electrical, photovoltaic elements, materials, solar cell efficiency.**

I. Introduction

A solar cell (also called photovoltaic cell or photoelectric cell) is a solid state electrical device that converts the energy of light directly into electricity by the photovoltaic effect. What powers the electric motor and solar energy?

The idea that the drive uses a motor vehicle is not new. A charge of electric current through the battery, we get by using solar cells, the question is quite recent past, present and especially future. Large electric motors started back in the early nineties 20th century, unfortunately without much success. The electric motor is most efficient in city driving, where over 90% of the mileage driven at low speeds. Some of the first cars ever built were powered by electricity. These first-fueled cars electric appeared as early as the late 19th century (actually 1880), a step which the vehicle is driven on gasoline are held until the early 20th century, when oil was due to the increasing exploitation has become significantly cheaper and has developed infrastructure for its distribution. Today is the time that this technology back in a big way, because it offers many advantages, especially when it comes to ecology. In addition to ecology, electric range offers even more advantages as a fuel for vehicles. This is its excellent mechanical simplicity, eliminating the need for a complex currency exchange and transmission assembly makes this car extremely reliable. The electric motor has the advantage of being reversible, except that the energy transferred into kinetic energy, is able to transform kinetic energy into electricity to supplement the battery. Modern electric motors are much more advanced today were the direct switch to AC power, and electronic engine control was significantly improved, and from these aggregates can be drawn significantly better performance without increasing in size. Before the mass introduction of electric motor drives for passenger cars must be resolved some issues and concerns mainly energy driven by the electric motor. Current technology offers a couple of complete and several intermediate solutions that work in practice. The complete solution is still in development phase. Here it comes to batteries and fuel cells, while the transitional arrangements, or hybrids, largely in the sale and are available to customers. When charging the battery and fuel cell applications of solar energy has its own solutions, although the pilot testing phase.

A. History of solar cells

The term "photovoltaic" comes from the Greek φῶς (*phōs*) meaning "light", and "voltaic", from the name of the Italian physicist Volta, after whom a unit of electro-motive force, the volt, is named. The term "photo-voltaic" has been in use in English since 1849.[1]

The photovoltaic effect was first recognized in 1839 by French physicist A. E. Becquerel. However, it was not until 1883 that the first photovoltaic cell was built, by Charles Fritts, who coated the semiconductor selenium with an extremely thin layer of gold to form the junctions. The device was only around 1% efficient. In 1888 Russian physicist Aleksandr Stoletov built the first photoelectric cell based on the outer photoelectric effect discovered by Heinrich Hertz earlier in 1887.

Albert Einstein explained the photoelectric effect in 1905 for which he received the Nobel prize in Physics in 1921.[2] Russell Ohl patented the modern junction semiconductor solar cell in 1946, [3] which was discovered while working on the series of advances that would lead to the transistor.

B. Solar energy

Assemblies of solar *cells* are used to make solar modules which are used to capture energy from sunlight. When multiple modules are assembled together (such as prior to installation on a pole-mounted tracker system), the resulting integrated group of modules all oriented in one plane is referred to in the solar industry as a *solar panel*. The general public and some casual writers often refer to solar modules incorrectly as solar panels; technically this is not the correct usage of terminology. Nevertheless, both designations are seen in regular use, in reference to what are actually solar modules. The distinction between a module and a panel is that a module cannot be disassembled into smaller re-usable components in the field, whereas a solar panel is assembled from, and can be disassembled back into, a stack of solar modules. The electrical energy generated from solar modules, referred to as *solar power*, is an example of *solar energy*.

C. Photovoltaic

Photovoltaics is the field of technology and research related to the practical application of photovoltaic cells in producing electricity from light, though it is often used specifically to refer to the generation of electricity from sunlight.

Cells are described as *photovoltaic cells* when the light source is not necessarily sunlight. These are used for detecting light or other electromagnetic radiation near the visible range, for example infrared detectors, or measurement of light intensity.

D. Bell produces the first practical cell

The modern photovoltaic cell was developed in 1954 at Bell Laboratories.[4] The highly efficient solar cell was first developed by Daryl Chapin, Calvin Souther Fuller and Gerald Pearson in 1954 using a diffused silicon p-n junction.[5] At first, cells were developed for toys and other minor uses, as the cost of the electricity they produced was very high; in relative terms, a cell that produced 1 watt of electrical power in bright sunlight cost about $250, comparing to $2 to $3 for a coal plant.

Solar cells were rescued from obscurity by the suggestion to add them to the Vanguard I satellite, launched in 1958. In the original plans, the satellite would be powered only by battery, and last a short time while this ran down. By adding cells to the outside of the body, the mission time could be extended with no major changes to the spacecraft or its power systems. There was some scepticism at first, but in practice the cells proved to be a huge success, and solar cells were quickly designed into many new satellites, notably Bell's own Telstar.

Improvements were slow over the next two decades, and the only widespread use was in space applications where their *power-to-weight ratio* was higher than any competing technology. However, this success was also the reason for slow progress; space users were willing to pay anything for the best possible cells, there was no reason to invest in lower-cost solutions if this would reduce efficiency. Instead, the price of cells was determined largely by the semiconductor industry; their move to integrated circuits in the 1960s led to the availability of larger boules at lower relative prices. As their price fell, the price of the resulting cells did as well. However these effects were limited, and by 1971 cell costs were estimated to be $100 per watt.[6]

E. Berman's price reductions

In the late 1960s, Elliot Berman was investigating a new method for producing the silicon feedstock in a ribbon process. However, he found little interest in the project and was unable to gain the funding needed to develop it. In a chance encounter, he was later introduced to a team at Exxon who were looking for projects 30 years in the future. The group had concluded that electrical power would be much more expensive by 2000, and felt that this increase in price would make new alternative energy sources more attractive, and solar was the most interesting among these. In 1969, Berman joined the Linden, New Jersey Exxon lab, Solar Power Corporation (SPC).[7]

His first major effort was to canvas the potential market to see what possible uses for a new product were, and they quickly found that if the price per watt were reduced from then-current $100/watt to about $20/watt there would be significant demand. Knowing that his ribbon concept would take years to develop, the team started looking for ways to hit the $20 price point using existing materials.[7]

The first improvement was the realization that the existing cells were based on standard semiconductor manufacturing process, even though that was not ideal. This started with the boule, cutting it into disks called wafers, polishing the wafers, and then, for cell use, coating them with an anti-reflective layer. Berman noted that the rough-sawn wafers already had a perfectly suitable anti-reflective front surface, and by printing the electrodes directly on this surface, two major steps in the

cell processing were eliminated. The team also explored ways to improve the mounting of the cells into arrays, eliminating the expensive materials and hand wiring used in space applications. Their solution was to use a printed circuit board on the back, acrylic plastic on the front, and silicone glue between the two, potting the cells. The largest improvement in price point was Berman's realization that existing silicon was effectively "too good" for solar cell use; the minor imperfections that would ruin a boule (or individual wafer) for electronics would have little effect in the solar application.[8] Solar cells could be made using cast-off material from the electronics market.

Putting all of these changes into practice, the company started buying up "reject" silicon from existing manufacturers at very low cost. By using the largest wafers available, thereby reducing the amount of wiring for a given panel area, and packaging them into panels using their new methods, by 1973 SPC was producing panels at $10 per watt and selling them at $20 per watt, a fivefold decrease in prices in two years.

F. Navigation market

SPC approached companies making navigational buoys as a natural market for their products, but found a curious situation. The primary company in the business was Automatic Power, a battery manufacturer. Realizing that solar cells might eat into their battery profits, Automatic had purchased a solar navigation aid prototype from Hoffman Electronics and shelved it.[9] Seeing there was no interest at Automatic Power, SPC turned to Tideland Signal, another battery company formed by ex-Automatic managers. Tideland introduced a solar-powered buoy and was soon ruining Automatic's business.

The timing could not be better; the rapid increase in the number of offshore oil platforms and loading facilities produced an enormous market among the oil companies. As Tideland's fortunes improved, Automatic Power started looking for their own supply of solar panels. They found Bill Yerks of Solar Power International (SPI) in California, who was looking for a market. SPI was soon bought out by one of its largest customers, the ARCO oil giant, forming ARCO Solar. ARCO Solar's factory in Camarillo, California was the first dedicated to building solar panels, and has been in continual operation from its purchase by ARCO in 1977 to 2011 when it was closed by SolarWorld.

This market, combined with the 1973 oil crisis, led to a curious situation. Oil companies were now cash-flush due to their huge profits during the crisis, but were also acutely aware that their future success would depend on some other form of power. Over the next few years, major oil companies started a number of solar firms, and were for decades the largest producers of solar panels. Exxon, ARCO, Shell, Amoco (later purchased by BP) and Mobil all had major solar divisions during the 1970s and 1980s. Technology companies also had some investment, including General Electric, Motorola, IBM, Tyco and RCA.[10]

G. Further improvements

In the time since Berman's work, improvements have brought production costs down under $1 a watt, with wholesale costs well under $2. "Balance of system" costs are now more than the panels themselves. Large

commercial arrays can be built at below $3.40 a watt,[11] [12] fully commissioned.

As the semiconductor industry moved to ever-larger boules, older equipment became available at fire-sale prices. Cells have grown in size as older equipment became available on the surplus market; ARCO Solar's original panels used cells with 2 to 4 inch (51 to 100 mm) diameter. Panels in the 1990s and early 2000s generally used 5 inch (125 mm) wafers, and since 2008 almost all new panels use 6 inch (150 mm) cells. Another major change was the move to polycrystalline silicon. This material has less efficiency, but is less expensive to produce in bulk. The widespread introduction of flat screen televisions in the late 1990s and early 2000s led to the wide availability of large sheets of high-quality glass, used on the front of the panels.

H. Current events

Other technologies have tried to enter the market. First Solar was briefly the largest panel manufacturer in 2009, in terms of yearly power produced, using a thin-film cell sandwiched between two layers of glass. Since then Silicon panels reasserted their dominant position both in terms of lower prices and the rapid rise of Chinese manufacturing, resulting in the top producers being Chinese. By late 2011, efficient production in China, coupled with a drop in European demand due to budgetary turmoil had dropped prices for crystalline solar-based modules further, to about $1.09[12] per watt in October 2011, down sharply from the price per watt in 2010.

I. Applications, photovoltaic system

Solar cells are often electrically connected and encapsulated as a *module*. Photovoltaic modules often have a sheet of glass on the front (sun up) side, allowing light to pass while protecting the semiconductor wafers from abrasion and impact due to wind-driven debris, rain, hail, etc. Solar cells are also usually connected in *series* in modules, creating an additive *voltage*. Connecting cells in parallel will yield a higher current; however, very significant problems exist with parallel connections. For example, shadow effects can shut down the weaker (less illuminated) parallel string (a number of series connected cells) causing substantial power loss and even damaging excessive reverse bias applied to the shadowed cells by their illuminated partners. As far as possible, strings of series cells should be handled independently and not connected in parallel, save using special paralleling circuits. Although modules can be interconnected in series and/or parallel to create an *array* with the desired peak DC voltage and loading current capacity, using independent MPPTs (maximum power point trackers) provides a better solution. In the absence of paralleling circuits, shunt diodes can be used to reduce the power loss due to shadowing in arrays with series/parallel connected cells.

To make practical use of the solar-generated energy, the electricity is most often fed into the electricity grid using inverters (grid-connected photovoltaic systems); in stand-alone systems, batteries are used to store the energy that is not needed immediately. Solar panels can be used to *power or recharge* portable devices.

II. THEORY OF SOLAR CELLS

The solar cell works in three steps:

1.Photons in sunlight hit the solar panel and are absorbed by semiconducting materials, such as silicon.

2.Electrons (negatively charged) are knocked loose from their atoms, causing an electric potential difference. Current starts flowing through the material to cancel the potential and this electricity is captured. Due to the special composition of solar cells, the electrons are only allowed to move in a single direction.

3.An array of solar cells converts solar energy into a usable amount of direct current (DC) electricity.

III. SOLAR CELL EFFICIENCY

Solar panels on the International Space Station absorb light from both sides. These Bifacial cells are more efficient and operate at lower temperature than single sided equivalents.

The efficiency of a solar cell may be broken down into reflectance efficiency, thermodynamic efficiency, charge carrier separation efficiency and conductive efficiency. The overall efficiency is the product of each of these individual efficiencies.

Due to the difficulty in measuring these parameters directly, other parameters are measured instead: thermodynamic efficiency, quantum efficiency, integrated quantum efficiency, V_{OC} ratio, and fill factor. Reflectance losses are a portion of the quantum efficiency under "external quantum efficiency". Recombination losses make up a portion of the quantum efficiency, V_{OC} ratio, and fill factor. Resistive losses are predominantly categorized under fill factor, but also make up minor portions of the quantum efficiency, V_{OC} ratio.

The *fill factor* is defined as the ratio of the actual maximum obtainable power, to the product of the open circuit voltage and short circuit current. This is a key parameter in evaluating the performance of solar cells. Typical commercial solar cells have a fill factor > 0.70. Grade B cells have a fill factor usually between 0.4 to 0.7. The fill factor is, besides efficiency, one of the most significant parameters for the energy yield of a photovoltaic cell.[13] Cells with a high fill factor have a low equivalent series resistance and a high equivalent shunt resistance, so less of the current produced by light is dissipated in internal losses.

Single p-n junction crystalline silicon devices are now approaching the theoretical limiting efficiency of 37.7%, noted as the Shockley–Queisser limit in 1961. However multiple layer solar cells have a theoretical limit of 86%.

In October 2010, triple junction metamorphic cell reached a record high of 42.3%.[14] This technology is currently being utilized in the Mars Exploration Rover missions, which have run far past their 90 day design life.

The Dutch Radboud University Nijmegen set the record for thin film solar cell efficiency using a single junction GaAs to 25.8% in August 2008 using only 4 μm thick GaAs layer which can be transferred from a wafer base to glass or plastic film.[15]
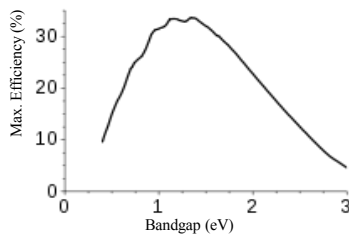
IV. Materials

Different materials display different efficiencies and have different costs. Materials for efficient solar cells must have characteristics matched to the spectrum of available light. Some cells are designed to efficiently convert wavelengths of solar light that reach the Earth surface. However, some solar cells are optimized for light absorption beyond Earth's atmosphere as well. Light absorbing materials can often be used in *multiple physical configurations* to take advantage of different light absorption and charge separation mechanisms.

Materials presently used for photovoltaic solar cells include monocrystalline silicon, polycrystalline silicon, amorphous silicon, cadmium telluride, and copper indium selenide/sulfide.[16]

"Picture 1." The Shockley-Queisser limit for the theoretical maximum efficiency of a solar cell. Semiconductors with band gap between 1 and 1.5eV, or near-infrared light, have the greatest potential to form an efficient cell. (The efficiency "limit" shown here can be exceeded by multijunction solar cells.) Many currently available solar cells are made from bulk materials that are cut into wafers between 180 to 240 micrometers thick that are then processed like other semiconductors.

Other materials are made as thin-films layers, organic dyes, and organic polymers that are deposited on supporting substrates. A third group are made from nanocrystals and used as quantum dots (electron-confined nanoparticles). Silicon remains the only material that is well-researched in both *bulk* and *thin-film* forms.

Picture 1. Shockley - Queisser full curve

A. Crystalline silicon

By far, the most prevalent *bulk* material for solar cells is crystalline silicon (abbreviated as a group as *c-Si*), also known as "solar grade silicon". Bulk silicon is separated into multiple categories according to crystallinity and crystal size in the resulting ingot, ribbon, or wafer.
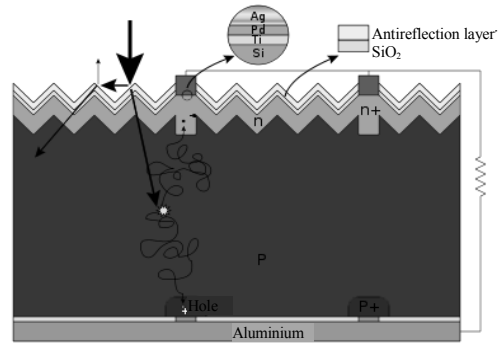
"Picture 2." show basic structure of a silicon based solar cell and its working mechanism.

1) Monocrystalline silicon (c-Si)

Often made using the Czochralski process. Single-crystal wafer cells tend to be expensive, and because they are cut from cylindrical ingots, do not completely cover a square solar cell module without a substantial waste of refined silicon. Hence most *c-Si* panels have uncovered gaps at the four corners of the cells.

2) Polycrystalline silicon, or multicrystalline silicon, (poly-Si or mc-Si)

Made from cast square ingots — large blocks of molten silicon carefully cooled and solidified. Poly-Si cells are less expensive to produce than single crystal silicon

Picture 2. Basic structure of a silicon based solar cell and its working mechanism.

cells, but are less efficient. United States Department of Energy data show that there were a higher number of polycrystalline sales than monocrystalline silicon sales.

3) Ribbon silicon

Is a type of polycrystalline silicon: it is formed by drawing flat thin films from molten silicon and results in a polycrystalline structure. These cells have lower efficiencies than poly-Si, but save on production costs due to a great reduction in silicon waste, as this approach does not require sawing from ingots.[17]

B. Thin films

In 2010 the market share of thin film declined by 30% as thin film technology was displaced by more efficient crystalline silicon solar panels (the light and dark blue bars).

Cadmium telluride (CdTe), copper indium gallium selenide (CIGS) and amorphous silicon (A-Si) are three thin-film technologies often used as outdoor photovoltaic solar power production. CdTe technology is most cost competitive among them.[18] CdTe technology costs about 30% less than CIGS technology and 40% less than A-Si technology in 2011.

1) Cadmium telluride solar cell

A cadmium telluride solar cell uses a cadmium telluride (CdTe) thin film, a semiconductor layer to absorb and convert sunlight into electricity. The cadmium present in the cells would be toxic if released. However, release is impossible during normal operation of the cells and is unlikely during fires in residential roofs.[19] A square meter of CdTe contains approximately the same amount of Cd as a single C cell Nickel-cadmium battery, in a more stable and less soluble form.[19]

2) Copper indium gallium selenide

Copper indium gallium selenide (CIGS) is a direct band gap material. It has the highest efficiency (~20%) among thin film materials (see CIGS solar cell). Traditional methods of fabrication involve vacuum processes including co-evaporation and sputtering. Recent developments at IBM and Nanosolar attempt to lower the cost by using non-vacuum solution processes.

3) Gallium arsenide multijunction

High-efficiency multijunction cells were originally developed for special applications such as satellites and space exploration, but at present, their use in terrestrial concentrators might be the lowest cost alternative in terms of \$/kWh and \$/W.[20] These multijunction cells consist

of multiple thin films produced using metalorganic vapour phase epitaxy. A triple-junction cell, for example, may consist of the semiconductors: GaAs, Ge, and GaInP$_2$.[21]

Each type of semiconductor will have a characteristic band gap energy which, loosely speaking, causes it to absorb light most efficiently at a certain color, or more precisely, to absorb electromagnetic radiation over a portion of the spectrum. The semiconductors are carefully chosen to absorb nearly all of the solar spectrum, thus generating electricity from as much of the solar energy as possible.

GaAs based multijunction devices are the most efficient solar cells to date.

Tandem solar cells based on monolithic, series connected, gallium indium phosphide (GaInP), gallium arsenide GaAs, and germanium Ge p-n junctions, are seeing demand rapidly rise.

4) Light-absorbing dyes (DSSC)

Dye-sensitized solar cells (DSSCs) are made of low-cost materials and do not need elaborate equipment to manufacture, so they can be made in a DIY fashion, possibly allowing players to produce more of this type of solar cell than others. In bulk it should be significantly less expensive than older solid-state cell designs. DSSC's can be engineered into flexible sheets, and although its conversion efficiency is less than the best thin film cells, its price/performance ratio should be high enough to allow them to compete with fossil fuel electrical generation. The DSSC has been developed by Prof. Michael Grätzel in 1991 at the Swiss Federal Institute of Technology (EPFL) in Lausanne (CH).

Typically a ruthenium metalorganic dye (Ru-centered) is used as a monolayer of light-absorbing material. The dye-sensitized solar cell depends on a mesoporous layer of nanoparticulate titanium dioxide to greatly amplify the surface area (200–300 m^2/g TiO$_2$, as compared to approximately 10 m^2/g of flat single crystal). The photogenerated electrons from the *light absorbing dye* are passed on to the *n-type* TiO$_2$, and the holes are absorbed by an electrolyte on the other side of the dye. The circuit is completed by a redox couple in the electrolyte, which can be liquid or solid. This type of cell allows a more flexible use of materials, and is typically manufactured by screen printing and/or use of Ultrasonic Nozzles, with the potential for lower processing costs than those used for *bulk* solar cells. However, the dyes in these cells also suffer from degradation under heat and UV light, and the cell casing is difficult to seal due to the solvents used in assembly. In spite of the above, this is a popular emerging technology with some commercial impact forecast within this decade. The first commercial shipment of DSSC solar modules occurred in July 2009 from G24i Innovations. [22]

5) Organic/polymer solar cells

Organic solar cells are a relatively novel technology, yet hold the promise of a substantial price reduction (over thin-film silicon) and a faster return on investment. These cells can be processed from solution, hence the possibility of a simple roll-to-roll printing process, leading to inexpensive, large scale production.

Organic solar cells and polymer solar cells are built from thin films (typically 100 nm) of organic semiconductors including polymers, such as polyphenylene vinylene and small-molecule compounds like copper phthalocyanine (a blue or green organic pigment) and carbon fullerenes and fullerene derivatives such as PCBM. Energy conversion efficiencies achieved to date using conductive polymers are low compared to inorganic materials.

In addition, these cells could be beneficial for some applications where mechanical flexibility and disposability are important.

These devices differ from inorganic semiconductor solar cells in that they do not rely on the large built-in electric field of a PN junction to separate the electrons and holes created when photons are absorbed. The active region of an organic device consists of two materials, one which acts as an electron donor and the other as an acceptor. When a photon is converted into an electron hole pair, typically in the donor material, the charges tend to remain bound in the form of an exciton, and are separated when the exciton diffuses to the donor-acceptor interface. The short exciton diffusion lengths of most polymer systems tend to limit the efficiency of such devices. Nanostructured interfaces, sometimes in the form of bulk heterojunctions, can improve performance.[23]

6) Silicon thin films

Silicon thin-film cells are mainly deposited by chemical vapor deposition (typically plasma-enhanced, PE-CVD) from silane gas and hydrogen gas. Depending on the deposition parameters, this can yield:[24]

a) Amorphous silicon (a-Si or a-Si:H)

An amorphous silicon (a-Si) solar cell is made of amorphous or microcrystalline silicon and its basic electronic structure is the p-i-n junction. A-Si is attractive as a solar cell material because it is abundant and non-toxic (unlike its CdTe counterpart) and requires a low processing temperature, enabling production of devices to occur on flexible and low-cost substrates. As the amorphous structure has a higher absorption rate of light than crystalline cells, the complete light spectrum can be absorbed with a very thin layer of photo-electrically active material. A film only 1 micron thick can absorb 90% of the usable solar energy.[25]

Amorphous silicon has a higher bandgap (1.7 eV) than crystalline silicon (c-Si) (1.1 eV), which means it absorbs the visible part of the solar spectrum more strongly than the infrared portion of the spectrum. As nc-Si has about the same bandgap as c-Si, the nc-Si and a-Si can advantageously be combined in thin layers, creating a layered cell called a tandem cell. The top cell in a-Si absorbs the visible light and leaves the infrared part of the spectrum for the bottom cell in nc-Si.

b) Protocrystalline silicon or Nanocrystalline silicon (nc-Si or nc-Si:H), also called microcrystalline silicon.

It has been found that protocrystalline silicon with a low volume fraction of nanocrystalline silicon is optimal for high open circuit voltage.[26] These types of silicon present dangling and twisted bonds, which results in deep defects (energy levels in the bandgap) as well as deformation of the valence and conduction bands (band tails). The solar cells made from these materials tend to have lower *energy conversion efficiency* than *bulk* silicon, but are also less expensive to produce. The quantum efficiency of thin film solar cells is also lower due to

reduced number of collected charge carriers per incident photon.

V. Conclusion

Analysts have predicted that prices of polycrystalline silicon will drop as companies build additional polysilicon capacity quicker than the industry's projected demand. On the other hand, the cost of producing upgraded metallurgical-grade silicon, also known as UMG Si, can potentially be one-sixth that of making polysilicon.[27]

Manufacturers of wafer-based cells have responded to high silicon prices in 2004-2008 prices with rapid reductions in silicon consumption. According to Jef Poortmans, director of IMEC's organic and solar department, current cells use between eight and nine grams of silicon per watt of power generation, with wafer thicknesses in the neighborhood of 0.200 mm. At 2008 spring's IEEE Photovoltaic Specialists' Conference (PVS'08), John Wohlgemuth, staff scientist at BP Solar, reported that his company has qualified modules based on 0.180 mm thick wafers and is testing processes for 0.16 mm wafers cut with 0.1 mm wire. IMEC's road map, presented at the organization's recent annual research review meeting, envisions use of 0.08 mm wafers by 2015.[28]

Thin-film technologies reduce the amount of material required in creating the active material of solar cell. Most thin film solar cells are sandwiched between two panes of glass to make a module. Since silicon solar panels only use one pane of glass, thin film panels are approximately twice as heavy as crystalline silicon panels. The majority of film panels have significantly lower conversion efficiencies, lagging silicon by two to three percentage points.[29] Thin-film solar technologies have enjoyed large investment due to the success of First Solar and the largely unfulfilled promise of lower cost and flexibility compared to wafer silicon cells, but they have not become mainstream solar products due to their lower efficiency and corresponding larger area consumption per watt production.

VI. References

[1] Alfred Smee (1849). *Elements of electro-biology,: or the voltaic mechanism of man; of electro-pathology, especially of the nervous system; and of electro-therapeutics*. London: Longman, Brown, Green, and Longmans. p. 15.

[2] *"The Nobel Prize in Physics 1921: Albert Einstein"*, Nobel Price official page

[3] "Light sensitive device" *U.S. Patent 2,402,662* Issue date: June 1946

[4] K. A. Tsokos, "Physics for the IB Diploma", Fifth edition, Cambridge University Press, Cambridge, 2008, ISBN 0521708206

[5] Perlin, John (2004). "The Silicon Solar Cell Turns 50". National Renewable EnergyLaboratory. Retrieved 5 October 2010.

[6] John Perlin, "From Space to Earth: The Story of Solar Electricity", Harvard University Press, 2002, pg. 50

[7] Perlin, John. *From Space to Earth: The Story of Solar Electricity.* Harvard University Press, 2002, pg. 53

[8] John Perlin, "From Space to Earth: The Story of Solar Electricity", Harvard University Press, 2002, pg. 54

[9] http://books.google.com/books?id=IlQyronardUC&lpg=PA19&vq=&pg=PA60

[10] "The multinational connections-who does what where" , *New Scientist*, 18 October 1979, pg. 177

[11] $1/W Photovoltaic Systems DOE whitepaper August 2010

[12] http://247wallst.com/2011/10/06/solar-stocks-does-the-punishment-fit-the-crime-fslr-spwra-stp-jaso-tsl-ldk-tan/

[13] "T.Bazouni: What is the Fill Factor of a Solar Panel". Retrieved 2009-02-17.

[14] Spire pushes solar cell record to 42.3%. Optics.org. Retrieved on 2011-01-19.

[15] http://www.ru.nl/home/nieuws/imm/nieuw_wereldrecord

[16] Mark Z. Jacobson (2009). Review of Solutions to Global Warming, Air Pollution, and Energy Security p. 4.

[17] "String ribbon silicon solar cells with 17.8% efficiency".

[18] "Thin-Film Cost Reports". *pvinsights.com.* 2011 [last update]. Retrieved June 19, 2011.

[19] Fthenakis, Vasilis M. (August 2004). "Life cycle impact analysis of cadmium in CdTe PV production" (PDF). *Renewable and Sustainable Energy Reviews* **8** (4): 303–334. doi:10.1016/j.rser.2003.12.001.

[20] Swanson, R. M. (2000). "The Promise of Concentrators". *Progress in Photovoltaics: Res. Appl.* **8** (1): 93–111. doi:10.1002/(SICI)1099-159X(200001/02)8:1<93::AID-PIP303>3.0.CO;2-S.

[21] Triple-Junction Terrestrial Concentrator Solar Cells, http://www.spectrolab.com/DataSheets/TerCel/tercell.pdf

[22] http://www.g24i.com/

[23] Mayer, A et al. (2007). "Polymer-based solar cells". *Materials Today* **10** (11): 28. doi:10.1016/S1369-7021(07)70276-6.

[24] Collins, R (2003). "Evolution of microstructure and phase in amorphous, protocrystalline, and microcrystalline silicon studied by real time spectroscopic ellipsometry". *Solar Energy Materials and Solar Cells* **78** (1-4): 143. doi:10.1016/S0927-0248(02)00436-1.

[25] Photovoltaics. Engineering.Com (2007-07-09). Retrieved on 2011-01-19.

[26] J. M. Pearce, N. Podraza, R. W. Collins, M.M. Al-Jassim, K.M. Jones, J. Deng, and C. R. Wronski (2007). "Optimization of Open-Circuit Voltage in Amorphous Silicon Solar Cells with Mixed Phase (Amorphous + Nanocrystalline) p-Type Contacts of Low Nanocrystalline Content". *Journal of Applied Physics* **101**: 114301. doi:10.1063/1.2714507.

[27] Charting a Path to Low-Cost Solar. Greentech Media (2008-07-16). Retrieved on 2011-01-19.

[28] Katherine Derbyshire (January 9, 2009). "Wafer-based Solar Cells Aren't Done Yet".

[29] Datasheets of the market leaders: *First Solar* for thin film, *Suntech* and *SunPower* for crystalline silicon

EXPRES 2012
4th International Symposium on Exploitation of Renewable Energy Sources

---

In technical co-sponsors

- **Subotica Tech**, Subotica

- **Óbuda University**, Hungary

- **Tera Term** doo, Subotica,

In technical co-operation with

- **Government** of Subotica
- **Faculty of Economics**, Subotica
- **Inter** Mol Srbija
- **Cim-Gas**, Subotica
- **ELZETT**, Subotica
- **Selma,** Subotica
- **Bane,** Subotica
- **Đantar,** B.Topola
- **Fornetti,** Subotica